Torben Schiffner

Refocusing Antibody Responses by Chemical Modification of Vaccine Antigens

The Sir William Dunn School of Pathology and

'The College of the Blessed Mary and All Saints', Lincoln, in the

University of Oxford

A thesis submitted for the degree of Doctor of Philosophy at the University of

Oxford, Trinity term 2014

Abstract

Torben Schiffner
Lincoln College

Submitted for the degree of Doctor of Philosophy
Michaelmas Term 2014

Refocusing Antibody Responses by Chemical Modification of Vaccine Antigens

The envelope glycoprotein (Env) of Human Immunodeficiency Virus 1 (HIV-1) has developed several immune-evasion mechanisms to avoid the induction of neutralising antibodies, including immunodominant non-neutralising epitopes, conformational flexibility of conserved epitopes, and spontaneous subunit dissociation, thus impeding vaccine development. Here, chemical modification of Env-based vaccine antigens is explored to overcome these obstacles.

Firstly, covalent fixation of Env by chemical cross-linking was used to stabilise the conformationally flexible structure and prevent subunit dissociation. Cross-linked Env constructs showed reduced binding of many non-neutralising antibodies whilst largely maintaining antibody recognition by broadly neutralising antibodies. Compared to unmodified material, immunisation with some of these cross-linked proteins led to the induction of significantly increased antibody titres targeting the conserved CD4 binding site of Env despite similar overall antibody titres. These refocused antibody responses resulted in increased serum neutralising titres compared to animals receiving unmodified protein.

Secondly, an epitope masking strategy was developed to reduce or eliminate the immunogenicity of neutralisation-irrelevant surfaces. This was achieved using site-selective addition of theoretically immunosilent glycoconjugates to lysine residues. Masking of model protein hen egg lysozyme (HEL) led to site-selective loss of antibody binding to the modification sites *in vitro*, which translated into refocusing of antibody responses from masked to unmasked epitopes *in vivo*. Mutant HIV-1 and influenza virus surface glycoproteins were designed that had lysine residues removed from close proximity to the respective broadly neutralising epitopes, but added throughout the remaining surface. Masking of these mutant proteins with second-generation glycoconjugates led to predictable perturbations of antibody binding *in vitro*. However, administration of these modified glycoproteins revealed unexpectedly that the masking glycans were highly immunogenic *in vivo*. Thus, this strategy may well prove useful if truly non-immunogenic glycoconjugates can be identified.

Taken together, these chemical modifications of vaccine antigens may allow focused targeting of specific antigenic regions for increased B cell recognition, and may thus be a valuable tool for vaccine antigen design.

Acknowledgements

I would like to express my gratitude to everyone who helped me during my studies. In particular, I would like to thank my supervisor Professor Quentin J. Sattentau for his guidance and support. Further great thanks go to Professor Benjamin G. Davis who co-supervised my work on the glycan masking project. This project was a close collaboration in which first-generation glycans were developed by Heiko Schuster and SiaLac-IME reagents by Regis Saliba and Karolis Leonavicus.

I would also like to thank all members of the Sattentau lab in particular Chris Duncan for performing epitope mapping neutralisation assays and Amy E. Baxter and Adjoa R. Smalls-Mantey for reading this thesis as well as Leopold Kong, Rebecca A. Moore, Frank Wegmann, Gemma A. Needham, Kate H. Gartlan, Amin Moghaddam, Thao Do and William Hillson for their support and helpful discussions. I'd also like to thank my students Florian Brod, Raffael de Leon and Imafidon Oboh for their contributions to my work.

Additional thanks go to my many collaborators who have contributed data or materials to the work presented in this thesis. In particular, neutralisation assays were performed in David C. Montefiori's and Michael S. Seaman's laboratories, peptide arrays were performed by Jaap W. Back and guinea pig immunisations were performed by Rachel P.J. Lai in Johnathan L. Heeney's lab. Helen Kim and Travis Nieusma from Andrew Ward's lab performed Cryo-EM experiments. Leanne Minall and Sonia De Munari provided further support with chemical experiments. Sophie Fleurdepine provided assistance with molecular cloning. I would also like to thank everyone who contributed reagents as listed in the materials and methods section.

I gratefully acknowledge the support of the EP Abrahams trust which financed my studies.

Finally, special thanks go to my parents for their continued support throughout my studies.

Table of contents

Expanded table of contents

List of abbreviations

ADCC	antibody dependent cellular cytotoxicity
AIDS	acquired immunodeficiency syndrome
AUC	area under curve
BCR	B-cell receptor
bNAbs	broadly neutralising antibodies (polyclonal)
bNmAb	broadly neutralising monoclonal antibody
CCR5	C-C chemokine receptor type 5
CD	cluster of differentiation
CD4bs	CD4 binding site
CD4i	CD4 inducible
CDR	complementarity determining region
CHAPS	3-[(3-Cholamidopropyl)dimethylammonio]-1-propanesulfonate
CHO	Chinese hamster ovary
CMC	critical micelle concentration
CoRbs	coreceptor binding site
CST-II	Campylobacter *jejuni* sialyl transferase II
CT	cytoplasmic tale
CXCR4	C-X-C chemokine receptor type 4
DMEM	Dulbecco's modified eagle's medium
DNA	deoxyribonucleic acid
DSG	disuccinimidyl glutarate
DSS	disuccinimidyl suberate
EC_{50}	50% effective dose
EDC	1-Ethyl-3-(3-dimethylaminopropyl) carbodiimide
EDTA	ethylenediaminetetraacetic acid
ELISA	enzyme-linked immunosorbent assay
EM	electron microscopy
Env	envelope protein
eOD	engineered outer domain
ESI	electron spray ionisation
F_{AB}	antigen binding fragment
FACS	fluorescence-activated cell sorting
F_C	crystallisable fragment
F_CR	F_c receptor
FCS	foetal calf serum
fDC	follicular dendritic cells
GnT	N-acetylglucosaminyltransferase
gp	glycoprotein
HAART	highly active antiretroviral therapy
HBS	HEPES buffered saline
HEK	human embryonic kidney
HEL	hen egg lysozyme
HEPES	(4-(2-hydroxyethyl)-1-piperazineethanesulfonic acid
HIV-1	human immunodeficiency virus 1

HR	heptad repeat
HRP	horse-radish peroxidase
IC_{50}	50% inhibitory concentration
IME	imidate
kDa	kilo dalton
KCM buffer	potassium, calcium, magnesium buffer
KM	lysine mutant
LCT	liquid chromatography time-of flight
LTR	long terminal repeat
mAb	monoclonal antibody
MBS	mes buffered saline
MPER	membrane proximal extracellular region
MS	mass spectrometry
MW	molecular weight
NAbs	neutralising antibodies
NHP	non-human primate
OD	optical density
ON	overnight
PEI	polyethylenimine
PST	polysialyl transferase
RNA	ribonucleic acid
RSC3	resurfaced core 3
RT	room temperature
RU	response unit
SiaLac	Sialyllactose
SHIV	simian human immunodeficiency virus
SIV	simian immunodeficiency virus
SNHS	Sulfo-NHS
SP	signal peptide
SPR	surface plasmon resonance
TAE buffer	Tris, acetic acid, EDTA buffer
TE buffer	Tris, EDTA buffer
T/F virus	transmitted/founder virus
TBS	tris buffered saline
TLC	thin layer chromatography
TMD	trans-membrane domain
UV	ultraviolet

Chapter 1: Introduction

1.1 Chapter overview

In 2012, an estimated 35.3 million people were infected with the human immunodeficiency virus 1 (HIV-1) (UNAIDS, 2013) leading to 1.6 million deaths related to acquired immunodeficiency syndrome (AIDS). In the same year, approximately 2.3 million people were newly infected with HIV-1 (UNAIDS, 2013). The highly active antiretroviral treatment (HAART) available in many countries today is able to reduce or halt disease progression if taken regularly, but for the majority of infected people in the developing world therapeutic treatment of HIV-1 is currently not possible. Thus, a prophylactic vaccine able to prevent infection would be the most cost-effective approach to end the HIV-1 pandemic. Most vaccines licenced to date work by inducing antibodies, soluble glycoprotein molecules of the adaptive immune response which specifically bind and neutralise pathogens, but HIV-1 has developed a number of countermeasures allowing it to avoid the induction of neutralising antibody (NAb) responses. Consequentially, all attempts to develop a prophylactic vaccine able to induce such protective antibody responses have failed to date. In this thesis, mechanisms are explored to use chemical modification of vaccine antigens to improve immunogenicity, which might help in the development of an antibody-based HIV-1 vaccine.

This chapter gives a brief overview of HIV-1 followed by more detailed descriptions of the topics specific to the work presented in this thesis, including the structure and function of the envelope glycoproteins (Env) and the nature of antibody responses elicited to HIV-1.

1.2 Human immunodeficiency virus type 1

1.2.1 HIV-1 life cycle

HIV-1 is an enveloped retrovirus that infects cells expressing the receptor cluster of differentiation 4 (CD4), which are generally cells of the immune system such as $CD4^+$ T cells, but also dendritic cells and macrophages (Fields et al., 2007). HIV-1 virions contain two positive strand copies of an RNA genome, which are bound to a polymerase and an integrase in a capsid structure that is enveloped in a viral lipid membrane derived from the plasma membrane of the infected cell (Fig. 1.1).

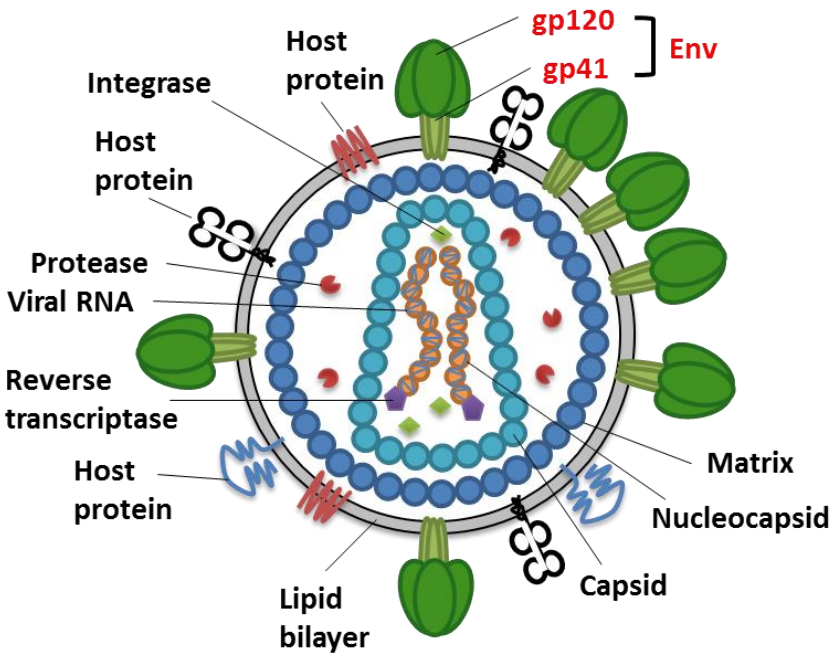

Fig. 1.1: Schematic of an HIV-1 virion. 2 copies of the RNA genome, including attached integrase and reverse transcriptase proteins are packaged in a cone-shaped capsid. The virion is surrounded by a lipid envelope containing the surface glycoprotein Env composed of three copies of gp120 and gp41 each in non-covalently linked heterotrimers. Figure prepared by A.E. Baxter and adapted with permission.

To enter target cells, the surface glycoprotein gp120, anchored to the HIV-1 virion envelope by the transmembrane glycoprotein gp41, associates with CD4 on the surface of $CD4^+$ cells (Dalgleish et al., 1984; Klatzmann et al., 1984; Blumenthal et al., 2012). The binding results in conformational changes in Env (described in more detail in section 1.3.1), which allow

the engagement of the co-receptor, usually C-C chemokine receptor type 5 (CCR5) or C-X-C chemokine receptor type 4 (CXCR4), and subsequent fusion of the viral membrane with the host cell membrane (see section 1.3.1 below) (Deng et al., 1996; Dragic et al., 1996). Early during an infection, the coreceptor is usually CCR5 and individuals with a mutation in this receptor are almost completely resistant to infection (Liu et al., 1996). Viruses using CCR5 as their coreceptor are thus called R5 viruses. Later during infection, coreceptor usage changes to utilise CXCR4 (X4 viruses) or both CCR5 and CXCR4 (R5X4 viruses) in ~50% of patients (Tersmette et al., 1989; Connor and Ho, 1994; Richman and Bozzette, 1994).

After fusion, the viral capsid enters the cytoplasm where reverse transcription occurs. The RNA-dependent DNA polymerase (reverse transcriptase) reverse transcribes the RNA, and at the same time degrades the transcribed RNA strand. Subsequently, the DNA genome is imported into the nucleus and integrated into the host DNA by the integrase (reviewed by Lever and Jaeng (2006)).

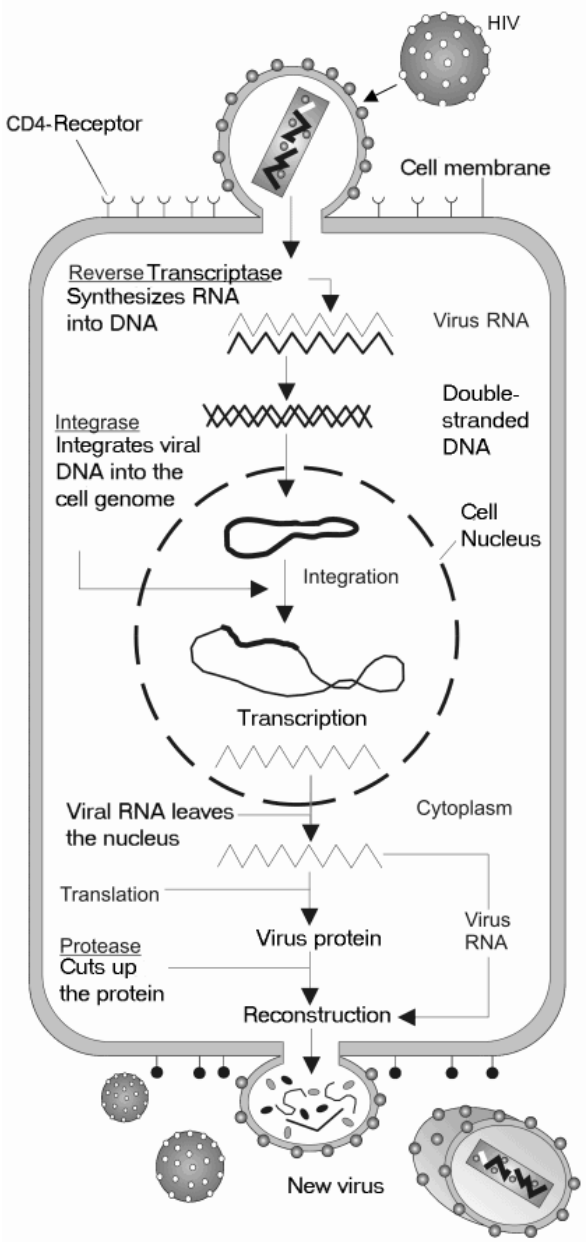

Fig. 1.2: Schematic of the HIV-1 life-cycle. HIV enters $CD4^+$ target cells and releases its core including the RNA into the cytoplasm where reverse transcription into double-stranded DNA occurs. The DNA is imported into the nucleus and integrated into the host genome by the viral integrase protein. Transcription and nuclear export lead to formation of viral proteins and new viral RNA genomes. New virions bud from the plasma membrane. Image based on (Fields et al., 2007) and reproduced from (Wikipedia, 2014) under Creative Commons CC0 1.0 Universal Public Domain Dedication.

After integration, transcription of viral genes by host RNA polymerase II commences, driven by the promoter activity of the 5'-long terminal repeat (LTR). Different splice variants are formed which allow the expression of 15 proteins. Initially, transcription and nuclear export of unspliced or singly spliced viral genomes is very inefficient (Lever and Jeang, 2006).

Expression of regulatory proteins Tat and Ref from fully spliced mRNAs leads to an increased efficiency of these steps respectively (Lever and Jeang, 2006). Later in the viral life-cycle, accumulation of viral proteins and efficient expression of full-length viral genomes leads to the formation of budding sites at the plasma membrane where new viruses can be released (Sierra et al., 2005). After release, protease-induced processing of the immature virions occurs by cleavage of Gag (Sierra et al., 2005). This process leads to the formation of the characteristic cone-shaped capsids found inside HIV-1 virions. Apart from cell-free infection by free virions, HIV-1 can directly spread from cell-to-cell. This alternative route has been shown to be more efficient *in vitro* and might be a mechanism to restrict the exposure of the virion to antibodies (reviewed by Schiffner et al. (2013c)) and reverse transcriptase inhibitors (Sigal et al., 2011; Duncan et al., 2013; Titanji et al., 2013).

1.2.2 HIV-1 transmission and pathogenesis

HIV-1 is transmitted mainly via vaginal or anal sexual intercourse as well as direct contact with contaminated blood, for example by sharing needles amongst intravenous drug users. Further routes of transmission include mother-to-child transmission at birth or during breast feeding, and rare oral transmissions (Rothenberg et al., 1998). Depending on the prevalence, heterosexual transmission is the most common form of HIV-1 acquisition in sub-Saharan Africa whereas in Europe and North America homosexual transmission is more common (Kilmarx, 2009).

Heterosexual transmission of HIV-1 is very inefficient with an estimated 1:200 – 1:10,000 coital acts resulting in infection (Shattock and Moore, 2003), whereas male-to-male

homosexual transmission is estimated to be slightly more efficient (1:10 – 1:1,600 instances resulting in transmission) (Vittinghoff et al., 1999; Gray et al., 2001). Thus, often only a single so-called transmitted/founder (T/F) virus is transmitted. One reason for the low rate of infection is the inefficient transfer of HIV-1 virions across epithelial barriers (Bobardt et al., 2007), although it has been suggested that micro-abrasions and other disruptions of epithelial integrity can increase transmission efficiency (Pope and Haase, 2003). Crossing the epithelium and the underlying lamina propria has been proposed to be facilitated by intra-epithelial cells such as Langerhans cells and CD4+ T cells (reviewed by Shattock and Moore, 2003). After crossing the epithelium, HIV-1 replicates locally to form a focus of infection within the lamina propria (Haase, 2011). HIV-1 is subsequently trafficked to local draining lymph nodes and further to systemic lymphoid tissues, in particular the gut-associated lymphoid tissue (Miller et al., 2005). After infection, HIV-1 very quickly (< 3 days in macaques challenged with the simian immunodeficiency virus (SIV) model) establishes a long-lived viral reservoir that is preserved even after prolonged treatment with antiretroviral drugs (Whitney et al., 2014). These long-lived reservoirs hamper efforts to eradicate the virus from infected patients.

Following infection, HIV-1 replicates quickly to high levels, causing the rapid decline of CD4+ T cells. However, infection levels peak after ~3 weeks and subsequently decline due to adaptive immune responses and/or target cell depletion (Phillips et al., 1991; Borrow et al., 1994; Huber et al., 2006). Following this acute phase of infection, CD4+ T-cell counts partially recover, although the virus keeps replicating at low levels during the chronic phase of the natural infection (Fig. 1.3). CD4+ T-cell counts progressively decline over the course of several years until the immune system is no longer able to protect against infection of

otherwise non-lethal diseases caused by opportunistic infections and cancers unusual in people with healthy immune systems (Gorry et al., 2002), leading to AIDS.

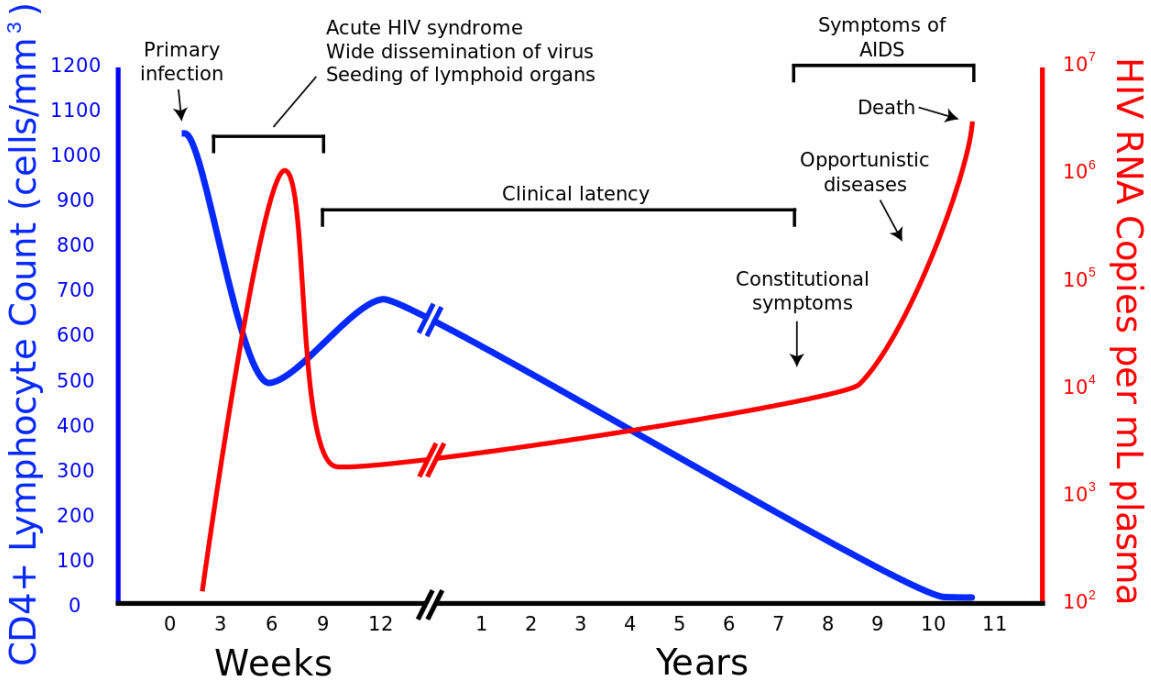

Fig. 1.3: Viral loads and CD4+ T-cell counts during HIV infection. Image similar to (Paiardini et al., 2009) and reproduced from (Wikipedia, 2014) under Creative Commons CC0 1.0 Universal Public Domain Dedication (http://upload.wikimedia.org/wikipedia/commons/thumb/0/0e/Hiv-timecourse_copy.svg/1280px-Hiv-timecourse_copy.svg.png).

1.3 Env structure and function

HIV-1 contains a single species of viral Env spike on its surface, made up of three copies of each of the glycoproteins gp120 and gp41. Thus, Env is the only target available for functional antibody recognition, placing it at the centre of any attempt of antibody-based vaccine design. Hence, detailed knowledge of the molecular and atomic structure, general functional properties, and immune evasion mechanisms of this glycoprotein are of primary importance for immunogen development.

1.3.1 **Function of Env**

Entry of HIV-1 into the target cell is facilitated by Env-mediated fusion of the viral membrane with the target cell membrane (Fig. 1.4). In its native conformation, Env forms compact trimeric spikes (described in more detail in section 1.3.2). Binding to CD4 triggers conformational rearrangements in Env that lead to an opening of the compact quaternary conformation by rotation of the gp120 subunits (Liu et al., 2008; White et al., 2010; Harris et al., 2011). In this more open structure, the coreceptor binding site (CoRbs) is exposed thus allowing coreceptor binding (Fig. 1.4). In addition, the N-terminal portion of gp41, which contains a lipophilic region called the fusion peptide, inserts into the target cell membrane (Blumenthal et al., 2012) and gp120 probably dissociates from gp41 (Moore et al., 1990). Further rearrangements in gp41 lead to the formation of a six-helix bundle via leucine zippers formed by portions of the gp41 subunit termed heptad repeat (HR) (Brasseur et al., 1990; Dubay et al., 1992). The formation of this six-helix bundle draws the membranes closer together until fusion occurs (Blumenthal et al., 2012).

Initial studies suggested that a single Env spike would be sufficient to achieve membrane fusion (Yang et al., 2005; Yang et al., 2006). This hypothesis was based on experiments in which defective Env mutants were mixed with functional Env spikes at different ratios and modelling the resulting infectivity under those conditions. However, subsequent studies analysing the same dataset came to the conclusion that five to eight Env complexes are required for fusion to occur (Klasse, 2007; Magnus et al., 2009).

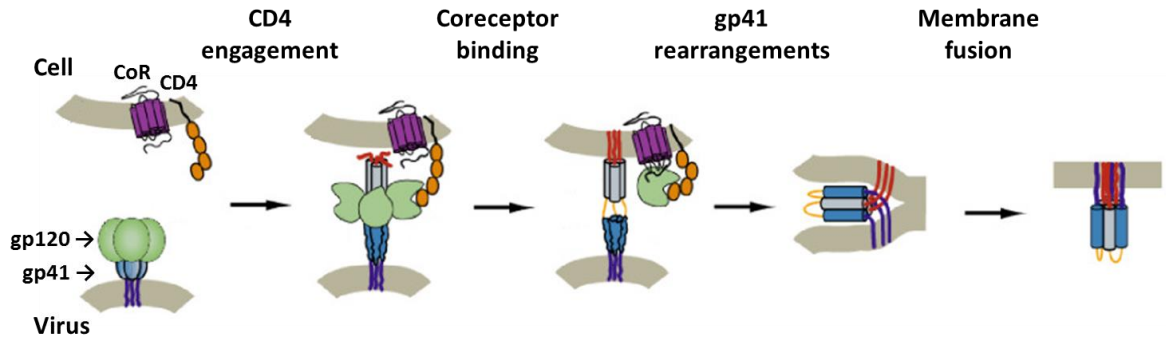

Fig. 1.4: Env-mediated membrane fusion. CD4 binding induces structural rearrangements in Env that lead to an opening of the compact structure and the exposure of the CoRbs. Upon coreceptor binding, the fusion peptide of gp41 is inserted into the target membrane, triggering conformational rearrangements that draw the two membranes closer together ultimately leading to membrane fusion. Adapted from (Lederman et al., 2008).

1.3.2 Structure of Env

Current strategies to develop B-cell vaccines include so-called structure-guided vaccine design, in which immunogens are rationally designed based on a detailed knowledge of broadly neutralising epitopes and their recognition by bNmAbs (Kulp and Schief, 2013; McLellan et al., 2013; Correia et al., 2014). At the core of every attempt of structure-guided vaccine design is therefore detailed knowledge of the structure of the target protein, which should resemble the surface protein found on native virions as closely as possible (Kulp and Schief, 2013). During most of the course of this PhD project, no such structure was available for the entire HIV-1 Env glycoprotein although x-ray crystallographic studies had solved the atomic structure of truncated elements of gp120 and gp41.

In the absence of a crystal structure of the native Env trimer, a lot of *in vitro* characterisations were performed on Env. According to these studies, the trimeric gp160 precursor is cleaved by furin in the Golgi apparatus into gp120 and gp41, which remain non-covalently attached to each other as a trimer of heterodimers, and migrate to the

plasma membrane via a poorly defined secretory pathway (Hallenberger et al., 1992; Jolly et al., 2011). The sequence of gp120 is segmented into 5 relatively conserved regions (named C1-C5) intersected by 5 highly variable sections (V1-V5, Fig. 1.5). In addition, an N-terminal signal peptide is included, that leads to the expression of the protein into the endoplasmatic reticulum and is cleaved off during expression. The tertiary structure of gp120 is stabilised by highly conserved disulfide bridges (Leonard et al., 1990). gp41 contains the fusion peptide, which is inserted into the target membrane, and the two heptad repeats which drive the formation of the six-helix bundle (Fig. 1.5) (Brasseur et al., 1990; Dubay et al., 1992; Blumenthal et al., 2012). Further elements of gp41 include the membrane-proximal extracellular region (MPER), the transmembrane domain (TMD) and the cytoplasmic tail (CT).

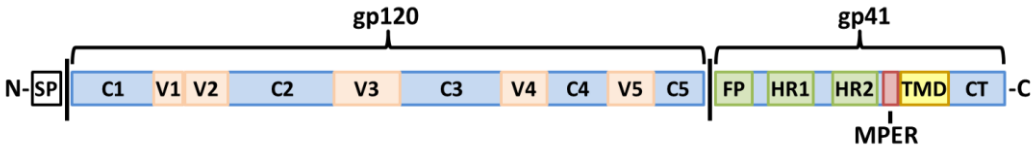

Fig. 1.5: Linear representation of gp160. SP: signal peptide; C1-C5: constant regions; V1-V5: variable regions; FP: fusion peptide; HR1-2: heptad repeat 1-2; MPER: membrane-proximal extracellular region; TMD: transmembrane domain; CT: cytoplasmic tail.

To gain insight into the three-dimensional structure of Env, x-ray crystallographic experiments have been performed, but due to difficulties in the crystallisation process, most studies used a truncated, deglycosylated core of the surface protein gp120, which has the N- and C- terminus as well as most of the variable loops deleted (Kwong et al., 1998; Wyatt et al., 1998). Furthermore, structures of gp120 were generally solved in complex with soluble CD4 and/or an anti-gp120 antibody that stabilised the structure but might have induced a conformation different from the native unliganded trimeric Env spike (Kwong et al., 1998; Huang et al., 2005; Chen et al., 2009a; Pancera et al., 2010).

According to such crystal structures, core gp120 consists of three domains: the inner domain which contains both the N- end the C-termini which form contacts with the gp41 subunit, the outer domain which contains most of the CD4 binding site (CD4bs), and the bridging sheet mini-domain which is formed when the two other domains come together (Fig. 1.6) (Kwong et al., 1998). The co-receptor binding site, as probed by the monoclonal antibody 17b, is formed by this bridging sheet (Kwong et al., 1998).

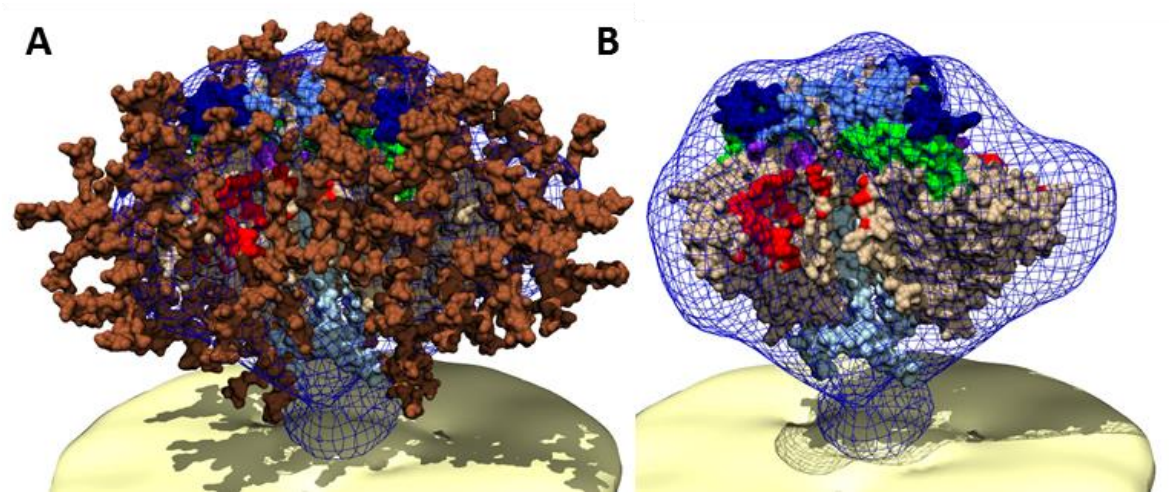

Fig. 1.6: Molecular model of Env with (A) and without (B) glycans. Brown: glycans; blue mesh: gp160 (EM); fawn: gp120; cyan: gp41; cream: membrane; red: CD4bs; purple: CoRbs; blue: V1V2; green V3. The image was created in UCSF chimera by superimposing PDB# 3J5M (Lyumkis et al., 2013), 4NCO (Julien et al., 2013a), 3TYG (Pejchal et al., 2011), 3U4E (McLellan et al., 2011), EMD# 5019 and 5022 (Liu et al., 2008). gp140 is derived from 3JPM, glycans are combined from crystal structures 4NCO, 3TYG, 3U4E. The remaining glycans are computational predictions derived from (Kong et al., 2010). Electron density maps 5019 and 5022 were used for the membrane and the overall structure of gp160, respectively.

Another approach to solve the structure of Env uses cryo electron tomography (EM), which can be applied to obtain the molecular structure of native spikes on the surface of viruses, although the resolution of this approach was until recently restricted to about 20 Å. These low-resolution models of native Env showed it as a trimeric mushroom-like structure, in which the gp41 forms a compact stalk (Zanetti et al., 2006; Liu et al., 2008; Hu et al., 2010; White et al., 2010). Initially, the gp120 subunits seemed to form a water-filled cavity by contacting the gp41 stalk at the bottom and the individual V1V2 loops forming contacts at

the apex of the trimer, although the existence of such a cavity has recently been questioned (Liu et al., 2008; Hu et al., 2010; White et al., 2010).

In the past year, substantial progress has been made towards solving a high-resolution structure of Env. Major improvements were made possible due to the recent development of relatively stable soluble mimics of Env termed SOSIP gp140s (described in section 1.3.4 below). These constructs for the first time allowed the crystallisation of a trimeric Env mimic at modest resolution (Julien et al., 2013a). At the same time, progress in the field of cryo-EM, such as feature-enhancement by F_{AB} binding and sub-frame alignment of "movies" of the sample (Campbell et al., 2012; Wu et al., 2012), allowed visualisation of similar constructs at resolutions of < 6 Å (Bartesaghi et al., 2013; Lyumkis et al., 2013; Mao et al., 2013). Most of these structures agree that the water-filled cavity seen in earlier structures was actually an artefact from the low-resolution techniques utilised in previous studies (Bartesaghi et al., 2013; Julien et al., 2013a; Lyumkis et al., 2013). The improved accuracy of these new structures show that trimer contacts at the trimer apex are formed by the V1V2 loops (Fig. 1.7). At the same time, the V3 loop seems to be 'tucked under' the adjacent gp120 monomer before CD4 engagement (Julien et al., 2013a; Lyumkis et al., 2013). Further interesting insights provided by these structures includes mechanisms of immune evasion, which are discussed in section 1.3.3 .

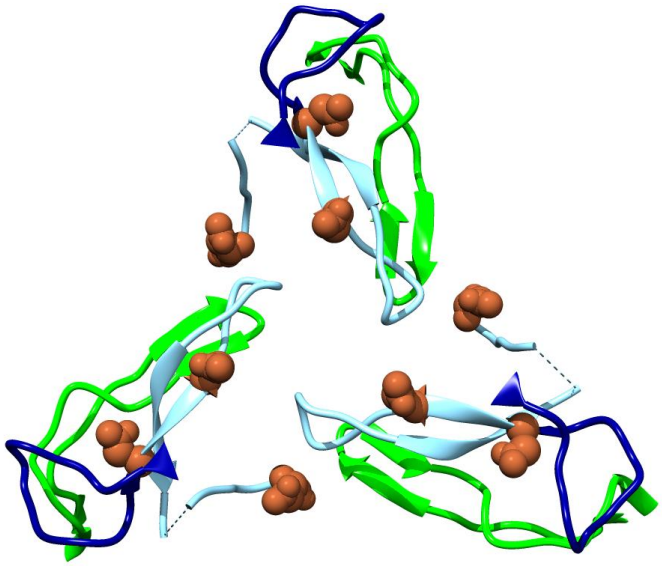

Fig. 1.7: Trimer contacts at the apex of Env spikes. Dark blue: V1 loop; light blue: V2; green: V3; brown: N-linked glycosylation sites involved in broadly neutralising epitopes (see below). Image was created from PDB# 3J5M (Lyumkis et al., 2013) using UCSF Chimera.

An additional problem in the search for the structure of native Env is its extensive glycosylation (Fig. 1.6A). The structure of the carbohydrates is often heterogeneous and relatively flexible unless stabilised by antibody binding and thus deglycosylation is usually required for x-ray crystallography. Whilst cryo-EM is capable of solving structures of glycosylated proteins, the flexible glycans are predominantly averaged out during image processing. Therefore, only computer models of the structure of the glycans exist so far (Kong et al., 2010).

Overall, the latest progress in the determination of the overall structure of Env allows new insights into the molecular mechanisms of immune evasion and antibody engagement and might facilitate structure-guided vaccine design.

1.3.3 Immune evasion mechanisms

Infection with HIV-1, as well as immunisation with HIV-1 Env subunits, usually gives rise to high titres of binding antibodies. However, these antibodies predominantly fail to neutralise HIV-1 since Env has evolved to evade antibody-mediated neutralisation.

One mechanism of immune evasion is that >50% of the mass of gp120 is made up by glycans, which are normally recognised as 'self' by the immune system and thus this 'glycan shield' protects a major proportion of the envelope trimer from antibody recognition (Fig. 1.6) (Wyatt et al., 1998; Wei et al., 2003). In addition to being generally immunosilent, glycans are also very flexible therefore posing an energetic barrier to antibody binding due to entropic effects. The glycan shield in particularly protects the so-called 'silent face` of gp120, which makes up the majority of the outward facing surface of functional Env trimers on the virion surface (Fig. 1.6A) (Wyatt et al., 1998). As discussed in more detail in section 1.4.6 , the glycan shield has some unusual features which distinguish it from normal mammalian glycosylation thus allowing the induction of neutralising antibodies to these unusual glycan structures in some cases.

In contrast to the 'silent face', the so-called 'non-neutralising face' is a highly immunogenic surface but this surface is usually occluded within the trimer interface of Env (Moore and Sodroski, 1996; Wyatt et al., 1998; Richman et al., 2003; Julien et al., 2013a; Lyumkis et al., 2013). These immunodominant surfaces of the trimer interface are only accessible if gp120 has been shed from the trimer, but are occluded in intact membrane-associated Env (Moore and Sodroski, 1996; Richman et al., 2003). Thus, these mAbs are negative in neutralisation assays such as the TZM-bl assay, in which artificial pseudoviruses, capable of

a single round of infection, are used to infect reporter cell lines in the presence or absence of antibodies (Li et al., 2005; Schiffner et al., 2013a; Sarzotti-Kelsoe et al., 2014). In such assays, neutralising antibodies (NAbs) are able to prevent infection, thus inhibiting the expression of the reporter gene in the target cells.

Similar to the non-neutralising epitopes on the 'non-neutralising face', strong antibody responses are also usually generated against the variable loops of gp120, which mutate rapidly, thus generally avoiding antibody-mediated neutralisation (Richman et al., 2003; Frost et al., 2005).

The conserved regions of the receptor and co-receptor binding sites have evolved other mechanisms of antibody evasion. The co-receptor binding site is only exposed upon CD4 engagement, protecting it from recognition by antibodies until the virus has bound to the cell surface (Labrijn et al., 2003). The receptor binding site, which makes up the majority of the 'neutralising face', is protected by an inherent flexibility called 'conformational masking' which imposes an entropic barrier upon antibody recognition (Kwong et al., 2002; Yuan et al., 2006). In addition, the angle at which an antibody approaches this vulnerable site has to be very precisely tuned, since on intact trimers the CD4bs is recessed within the trimer (Fig. 1.6) with each gp120 subunit shielding the CD4bs of the adjacent subunit (Chen et al., 2009a; Schief et al., 2009; Julien et al., 2013a; Lyumkis et al., 2013). Further shielding of the CD4bs is provided by the surrounding glycans which limit access to this site (Kong et al., 2010). Theses steric restrictions impede antibody access without obstructing CD4 due to the larger size of the former (two immunoglobulin domains at the antigen binding site compared to a single immunoglobulin at the tip of CD4). Similarly to the immunodominant

surfaces of the trimer interface, antibodies that are raised against the CD4bs on shed gp120 are generally not able to bind and neutralise intact Env trimers due to these conformational restrictions.

Taken together, Env has evolved to utilise a large array of counter-measures which impede the development of NAbs.

1.3.4 **Env constructs for vaccine design**

Most current antibody-based HIV-1 vaccination strategies use some form of the target protein as the immunogen. It is generally believed that antibodies binding to functional Env will in most cases lead to neutralisation of the virus and therefore immunisation with proteins identical to or closely resembling native Env complexes might lead to the induction of NAb responses. However, in many cases (including HIV-1) the target protein is a membrane-anchored protein which can be challenging to express and formulate in a vaccine setting.

Even native Env when expressed in a cell membrane does not exclusively form functional Env spikes but also displays monomeric gp160, uncleaved gp160 and gp41 'stumps' which can arise by shedding of gp120 (Fig. 1.8A) (Moore et al., 1990; Moore et al., 2006; Crooks et al., 2011). Mutants of Env have been designed which aim to stabilise the correctly folded trimers. These include a set of mutations termed SOSIP which includes the introduction of a disulfide bond between gp120 and gp41 (SOS) and the destabilisation of the post-fusion conformation (mutation I559P) the latter of which is supposed to preserve the pre-fusion (native) conformation as well as increase trimer stability (Fig. 1.8B) (Sanders et al., 2002b;

Schulke et al., 2002). Nevertheless, these mutations do not completely prevent the formation of monomeric uncleaved gp160s, which display immunodominant, neutralisation-irrelevant epitopes. One way to produce pure native trimer is to exploit the relative protease resistance of the native Env trimers compared to aberrant forms (Fig. 1.8C) (Crooks et al., 2011; Tong et al., 2012). However, the large-scale production of selectively protease-digested virus-like particles is difficult and work with membrane-bound proteins is challenging.

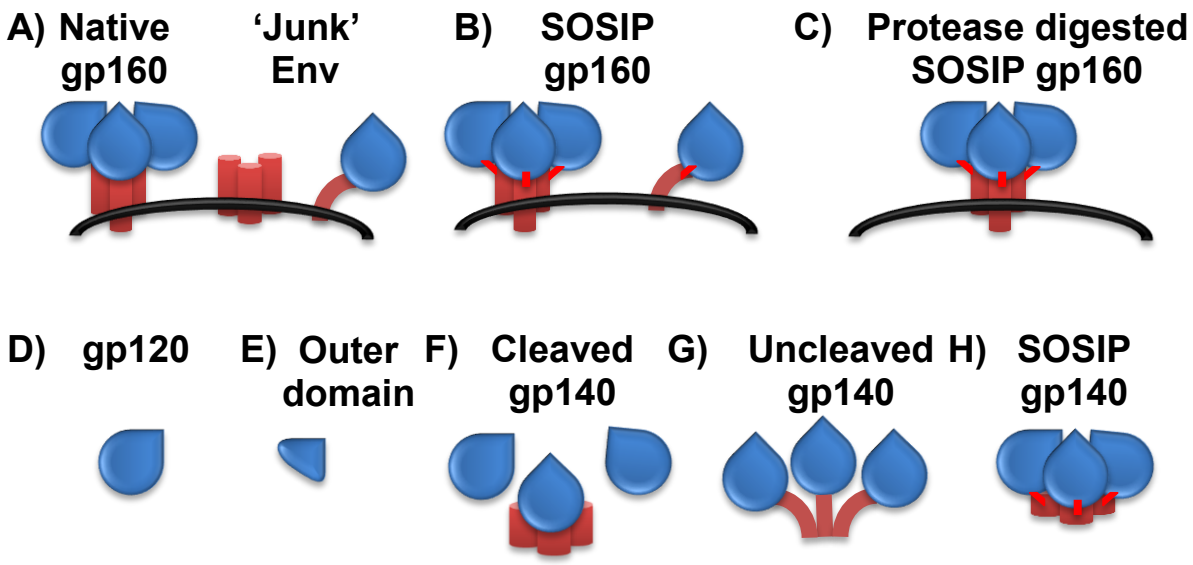

Fig. 1.8: Env constructs. A) Native Env expressed in a membrane forms compact trimers which bury non-neutralising epitopes. At the same time 'junk' molecules are displayed to confound the immune system. These include gp41 stumps, monomeric and uncleaved gp160s. **B)** Introduction of SOSIP stabilising mutations prevent gp120 dissociation from gp41 but monomeric gp160s still expose non-neutralising epitopes. **C)** Mild protease digestion cleaves non-functional gp160 but leaves the more compact native Env trimers intact. **D)** Soluble gp120 is monomeric and displays the 'non-neutralising face' usually hidden in the trimer interface. **E)** subunit constructs composed of only the outer domain have fewer non-neutralising epitopes **F)** gp140, consisting of gp120 plus the extracellular portion of gp41, form trimeric stalks but gp120 dissociates. **G)** Mutation of the cleavage site of gp140 leads to trimeric glycoproteins but the monomers do not for the compact native conformation found in functional membrane trimers. **H)** Cleaved stabilised SOSIP.664 gp140 forms 'native-like' compact trimers. Adapted from Sattentau (2014).

To overcome problems with membrane-bound proteins, a range of different soluble Env constructs has been developed and analysed in the context of vaccine development. The simplest variant is to only express the extracellular glycoprotein gp120 without the transmembrane protein gp41 (Fig. 1.8D). However, gp120 fails to trimerise in the absence of gp41 and consequentially the non-neutralising face and the variable loops are exposed, thus displaying immunodominant non-neutralising epitopes to the immune system. The presence of non-neutralising epitopes can be reduced by generating subunit constructs such as stable outer domain constructs including engineered outer domain (eOD) and others (Joyce et al., 2013; Qin et al., 2014).

Since Env trimerisation is dependent on gp41, other constructs have been designed which contain the extracellular portion of gp41 in addition to gp120. However, these constructs are generally very unstable and gp120 dissociates from the gp41 trimers (Ringe et al., 2013). To prevent dissociation, the cleavage site between gp120 and the extracellular portion of gp41 can be removed (mutating the REKR cleavage site to SEKS) creating so-called gp140 molecules (Fig. 1.8F). These gp140 molecules are often trimeric and together with gp120 are the most commonly used constructs utilised in antibody-based vaccine design to date, including many experiments in this thesis. However, gp140 does not form properly folded native-like trimers, as shown by probing with quaternary-specific mAbs, which selectively bind to the correct quaternary structure of Env, and cryo-EM studies (Walker et al., 2009; Walker et al., 2011a; Klein et al., 2012a; Ringe et al., 2013). Instead, uncleaved gp140 molecules consist of a trimeric gp41 ‘stalk’ to which three gp120 molecules are attached without interacting with each other (Ringe et al., 2013).

Recently, a strain (BG505, clade A) was discovered which, when combined with the SOSIP mutations and an additional truncation of the MPER, forms native-like trimers in solution (Fig. 1.8G) (Julien et al., 2013a; Klasse et al., 2013; Lyumkis et al., 2013; Ringe et al., 2013; Sanders et al., 2013). X-ray crystallography, cryo-EM as well as probing with quaternary-specific mAbs have shown this protein (BG505 SOSIP.664) to be almost identical to functional envelope glycoprotein of the same strain (Julien et al., 2013a; Lyumkis et al., 2013; Sanders et al., 2013). Furthermore, with the exception of some V3-loop specific mAbs, binding of mAbs to these trimers was strongly correlated with neutralisation of the corresponding pseudovirus showing that non-neutralising epitopes were mostly buried in this construct (Sanders et al., 2013).

Therefore, the recent development of natively folded soluble gp140 constructs for the first time allows the almost exclusive display of neutralising epitopes to the immune system and might be a major step forward in HIV vaccine design.

1.4 Antibody responses

1.4.1 **Structure and formation of antibodies**

Antibodies bind and either directly neutralise, or assist Fc receptor (F_cR)-expressing innate immune cells, to eliminate pathogens and pathogen-infected cells. To this end, a huge diversity of antibodies is generated to respond to virtually any invading pathogen which can be further modified for increased affinity in a process called affinity maturation (Victora and Nussenzweig, 2012). Antibodies are composed of four subunits, two so-called heavy chains of ~50 kDa and two light chains of ~25 kDa which are connected via disulfide bonds (Fig. 1.1). Whereas the general structure of most antibodies is similar, a region at the interface of the heavy and light chain shows a huge sequence and structural variability and

is generally the site of antigen recognition (also called the paratope) (Berg, 2012). The variability is mostly (though not exclusively) concentrated in variable regions termed complementarity determining regions (CDRs). Antibodies can be subdivided into the antigen binding domain (F_{AB}), which contains the paratope and is linked via a flexible hinge region to a more conserved domain, the crystallisable fragment (F_c), which is recognised by a number of innate immune cell surface receptors as described above and are responsible for effector functions (Berg, 2012). The F_c domain can be one of several different subtypes, which determines its effector functions and in some cases promotes oligomerisation of the antibody.

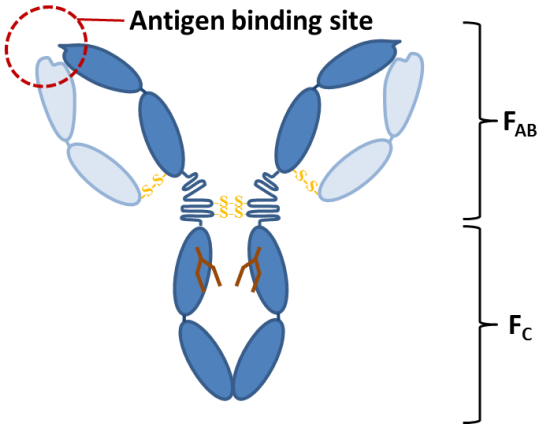

Fig. 1.9: Schematic structure of an antibody. Heavy chains are shown in dark blue, light chains in light blue, disulfide bonds in yellow, glycans in brown and the approximate position of the antigen binding site (paratope) is circled in red.

Antibodies are produced by B cells, immune cells that develop in the bone marrow, with each B cell expressing a specific antibody. Diversity is generated by splitting the genetic material of each antibody chain in multiple segments each present in multiple variants in the genome (Jung et al., 2006). For instance, the heavy chain is composed of the variable (V), diversity (D) and joining (J) segments which are present in the human genome in 44, 27 and 6 diverse copies respectively (Jung et al., 2006). By somatically joining a randomly chosen copy of each of these segments, a large number of combinations can be generated

(Jung et al., 2006). Similarly, joining of one copy out of 40 V and 5 J segments is required to form the light chain (which does not contain D segments). Further, diversity is generated by random pairing of light and heavy chains and imprecise merging of the V, D and J segments leading to frame-shift mutations (Berg, 2012). To avoid the induction of auto-antibodies, these steps are tightly controlled and self-reactive cells are eliminated in a process termed immunological tolerance (Jung et al., 2006).

Initially, antibodies are membrane bound (called the B-cell receptor; BCR) on so-called naïve B cells and each B cell expresses a specific B-cell receptor. Upon engagement of an antigen, the B cells can be activated leading to affinity maturation (explained below) of the antibody and expansion of the B-cell clone (Victora and Nussenzweig, 2012). The F_c portion of the antibody is initially of the IgM isotype but upon activation of the B cell, the subtype can be switched leading to the production of secreted forms including IgG and IgA, which bind to the pathogen and recruit specific immune cells depending on their isotype. Concomitantly, the B cell can differentiate into antibody secreting plasma cells, or memory B cells which are very long-lived and can quickly be activated if at a later stage the same antigen is encountered again.

1.4.2 **Antibody affinity maturation**

In addition to the diversity produced by V(D)J recombination, further diversity of antibodies is generated by affinity maturation, a process that leads to dramatic increases in affinity of the BCR for its antigen (Victora and Nussenzweig, 2012). Affinity maturation takes place in specialised compartments termed germinal centres in a Darwinian-like process in which

diversity is generated by high mutation rates of the BCR coupled with high levels of cell division and B cells carrying affinity-enhancing mutations are then selected for.

The two processes, diversification and selection, are spatially separated into two sub-compartments of the germinal centre, the light zone and the dark zone (Victora and Nussenzweig, 2012). In the light zone B cells interact with T cells and antigen presenting cells such as follicular dendritic cells (fDCs) (Victora and Nussenzweig, 2012). Antigen captured by the B cell is then presented to follicular helper T (T_{FH}) cells which trigger the migration of the B cell to the dark zone where cell division and somatic hypermutation of the B-cell receptor occur (Shih et al., 2002; Victora et al., 2010; Gitlin et al., 2014). Recent data suggest that the number of cell divisions in the dark zone depends on the amount of T-cell help provided to the B cell during the light zone selection (Gitlin et al., 2014). Following amplification and diversification, B cells can then migrate back to the light zone for additional rounds of selection (Victora et al., 2010). Without any positive selection B cells are prone to undergo apoptosis thus eliminating low-affinity BCR bearing cells (Liu et al., 1989). Therefore, competition between B cells exists at multiple levels including antigen uptake and T-cell help (Victora et al., 2010; Natkanski et al., 2013; Gitlin et al., 2014). In summary, high-affinity antibodies are generated by cycles of diversification, amplification and clonal selection.

1.4.3 **Non-neutralising antibody responses to HIV-1 and the RV144 clinical trial**

During natural infection with HIV-1 and during the vaccination strategies tested to date, large numbers of antibody specificities are raised against Env but usually these antibodies

are not able to neutralise a broad range of isolates. However, the nature of these non-neutralising responses may be important for vaccine design.

Most of the antibody responses generated are non-neutralising and target epitopes in the V3 and C5 regions of gp120 and the N-terminal regions of gp41, although one has to bear in mind that such analyses are often restricted to linear epitopes (Gottardo et al., 2013). Vaccination often leads to the induction of antibody responses targeting the same regions as well as epitopes in the C1 and V1V2 regions (Gottardo et al., 2013). As described above, antibodies to the C1 and C5 regions such as A32 (a list of anti-HIV-1 Env mAbs used in this thesis can be found in the appendix, Table A. 1) are often non-neutralising since these regions are occluded within the trimer interface on intact virions (Wu et al., 1996). On the other hand, antibodies to the variable loops (e.g. HGP68, HR10, HGN194, 447-52D…) can be neutralising but due to the high sequence variability these antibodies often have a very narrow breadth and during infection escape occurs quickly (Richman et al., 2003; Frost et al., 2005; Corti et al., 2010a).

Non-neutralising antibodies targeting conformation dependent epitopes include F105, b6 and 15e, which bind to regions within the conserved CD4bs. In contrast to broadly neutralising monoclonal antibodies (bNmAbs) targeting the same region (described below), these antibodies only bind to aberrant forms of Env since their angle-of-approach does not allow the binding of native Env spikes due to shielding of the CD4bs from the adjacent monomer (Chen et al., 2009b; Lyumkis et al., 2013).

Another target of conformation specific antibodies is the CD4 inducible (CD4i) epitope. This epitope, targeted by mAbs such as 17b or X5, is only formed after receptor engagement due to CD4 induced structural rearrangements in gp120 (Thali et al., 1993; Moulard et al., 2002). However, in the context of cell-surface anchored receptor and co-receptors, the close proximity of the cellular membrane restricts access of full-length antibodies to the CD4i epitope, in particular for primary HIV isolates (Labrijn et al., 2003). Therefore, CD4i mAbs are generally weakly or non-neutralising unless the CD4i state of Env is induced by synthetic soluble CD4 constructs (Sullivan et al., 1998; Labrijn et al., 2003).

Although non-neutralising antibodies are by definition not able to neutralise HIV-1 virions, they are not necessarily irrelevant in a vaccine setting since even non-neutralising antibodies can mark infected cells for clearance by a number of different immune cells. One such mechanism is antibody-dependent cell-mediated cytotoxicity (ADCC) (Madhavi et al., 2012). ADCC is mediated by natural killer (NK) cells, monocytes and neutrophils (Smalls-Mantey et al., 2013) which recognise antibodies bound to viral proteins expressed on the surface of an infected the target cell and kill the infected cell (Baum et al., 1996; Chung et al., 2011; Smalls-Mantey et al., 2012; Guan et al., 2013). Even with neutralising mAbs, effector functions can play a role as demonstrated in a study that used passive transfer of the bNmAb b12 to non-human primates (Hessell et al., 2007; Hessell et al., 2009b). When challenged with chimeric simian-human immunodeficiency virus (SHIV), the animals were better protected by wild-type bNmAb than with a mutant that lacked effector functions (Hessell et al., 2007; Hessell et al., 2009b; Bournazos et al., 2014). Similarly, even non-neutralising mAbs showed some protective effect in a number of different mouse

models of HIV-1 infection if effector functions were increased by mutations in the Fc portion of the mAbs (Bournazos et al., 2014).

Further evidence for the importance of non-neutralising antibodies came from a large clinical trial in Thailand, the RV144 trial. In this phase 3 clinical trial, over 16,000 participants were immunised with either a placebo or a canarypox vector vaccine (ALVAC-HIV) as well as two booster injections with a gp120 subunit vaccine (Rerks-Ngarm et al., 2009). In contrast to all other phase 3 trials completed so far, a modest transient protection of the vaccine was found (Rerks-Ngarm et al., 2009). In the modified intention to treat analysis after 2 years the number of HIV-infected subjects group was found to be significantly reduced by 31.2 % (Rerks-Ngarm et al., 2009). Despite the modest and only transient effect, the study raised the hope that the development of a protective vaccine was possible.

Follow-up studies found that non-neutralising antibody responses targeted to the gp120 V2 loop correlated with decreased infection in this trial (Haynes et al., 2012b). In contrast, no correlation with NAb responses was found (Haynes et al., 2012b). Interestingly, ADCC correlated with reduced risk of infection in vaccinees that displayed low anti-gp120 IgA titres (Haynes et al., 2012b). In another follow up study it was shown that high levels of plasma IgA, which does not exhibit ADCC, could block IgG-mediated ADCC in the RV144 patients thus providing a potential explanation for the lack of protection in the presence of high IgA levels (Tomaras et al., 2013). Thus, antibody-mediated innate immune responses such as ADCC might be part of a protective vaccine, even in the absence of broadly neutralising antibodies (bNAbs).

Taken together, strong non-neutralising antibody responses are generated by both natural infection and immunisation with Env based experimental vaccines. Although these non-neutralising antibody responses can achieve some level of protection due to antibody effector functions, the immunodominance of the non-neutralising responses might impede the induction of bNAbs by competition of B cells for antigen and for T-cell help.

1.4.4 Development of neutralising antibody responses against HIV-1

For a long time it was unclear whether it would be possible for a high percentage of people to develop bNAbs. More recent studies showed that cross-clade neutralising antibodies are elicited in 10-30 % of infected humans 3-4 years after infection (Doria-Rose et al., 2009; Piantadosi et al., 2009; van Gils et al., 2009; Euler et al., 2010) although the most comprehensive study looking at the prevalence of NAbs in chronically infected patients found a continuum of responses rather than a discrete subset of neutralising responses (Hraber et al., 2014). The induction of bNAbs could be correlated with a high viral RNA load at set point (Piantadosi et al., 2009; Sather et al., 2009; van Gils et al., 2009), a low CD4+ T-cell count (van Gils et al., 2009; Euler et al., 2010) and a greater variability of Env early in infection (Piantadosi et al., 2009).

However, only very few patients, so-called elite neutralisers, generate extremely potent and broadly neutralising antibody responses (Simek et al., 2009). There might be a number of reasons why bNAbs are so infrequently made. First of all, it has been shown that B cells with antibodies displaying auto-reactivity induce immunological tolerance and are arrested before they become immature B cells (Haynes et al., 2005; Verkoczy et al., 2010). Furthermore, most bNmAbs found to date feature uncommon properties such as domain

exchange, long complementary determining regions or a high amount of somatic hypermutation (Calarese et al., 2003; Haynes et al., 2005; Walker et al., 2009; Doores et al., 2010c; Wu et al., 2010; Walker et al., 2011a).

In addition, until recently it was unclear whether the elicitation of antibody towards glycans or glycan-containing epitopes was possible in a high proportion of people. However, glycan specific bNAbs were found in a number of elite neutralisers (see detailed explanation in section 1.4.6) (Lavine et al., 2012). In addition, the development of broadly neutralising glycan-directed antibodies was detected in an SIV-infected Macaque that developed such antibodies about 9 months after infection (Walker et al., 2011c). These antibodies conferred cross-clade neutralising ability to the infected macaque, and drove the virus of this animal towards resistant escape mutants (Walker et al., 2011c). Attempts have been made to raise similar glycan-specific antibodies by immunisation. A range of studies achieved the induction of glycan-specific antibodies, but most of them did not bind glycans on the surface of gp120 (Astronomo et al., 2008; Astronomo et al., 2010; Doores et al., 2010b; Dunlop et al., 2010), or despite binding to gp120 were unable to neutralise the virus (Luallen et al., 2008; Agrawal-Gamse et al., 2011). However, these results in combination with the broad and potent neutralisation potential of several glycan specific mAbs have drawn a lot more attention to the glycan shield as a possible vaccine target.

In the past few years, a number of very potently neutralising mAbs have been discovered (described in detail below). Computational analysis of these bNmAbs allows prediction of the germline combination of V, D and J genes that was initially selected for the B cell that was then affinity maturated into the bNmAb. Interestingly, it was found that none of these

inferred unmutated ancestor antibodies were able to bind Env (Xiao et al., 2009; Wu et al., 2010; Bonsignori et al., 2011; Hoot et al., 2013). However, in a few cases longitudinal samples were available from patients who later went on to develop bNAbs (Liao et al., 2013a; Doria-Rose et al., 2014). In these few patients it was found that the initial T/F virus had unusual properties which allowed it to be recognised by the unmutated germline precursor of a bNmAb. Thus, one of the reasons that bNAbs are so rarely induced might be that the precursors of bNAbs do not bind or only bind weakly to Env and are therefore not selected for, or are outcompeted by non-neutralising antibodies during affinity maturation (Xiao et al., 2009). A strategy currently explored for the elicitation of broadly neutralising antibodies by immunisation is the subsequent immunisation with different immunogens which have been optimised to select germline B cells and direct them towards the maturation into broadly neutralising antibodies (Jardine et al., 2013; Liao et al., 2013a; McGuire et al., 2013).

In conclusion it has now been shown that NAbs can develop in HIV-1 infected patients over many years, although large hurdles have still to be overcome to elicit such responses by vaccination.

1.4.5 **Broadly neutralising antibodies and their epitopes**

The array of counter-measures of HIV-1 that confounds and evades the immune system has made it difficult to isolate bNAbs and in fact until recently, only few examples had been characterised. Furthermore, all of them featured uncommon properties that made it uncertain whether it would be possible to elicit similar antibodies in a significant proportion of humans. However, during the last four years, a range of broadly and potently

neutralising antibodies has been isolated from infected people (Fig. 1.10). This progress has mainly been due to improved methods of mAb isolation.

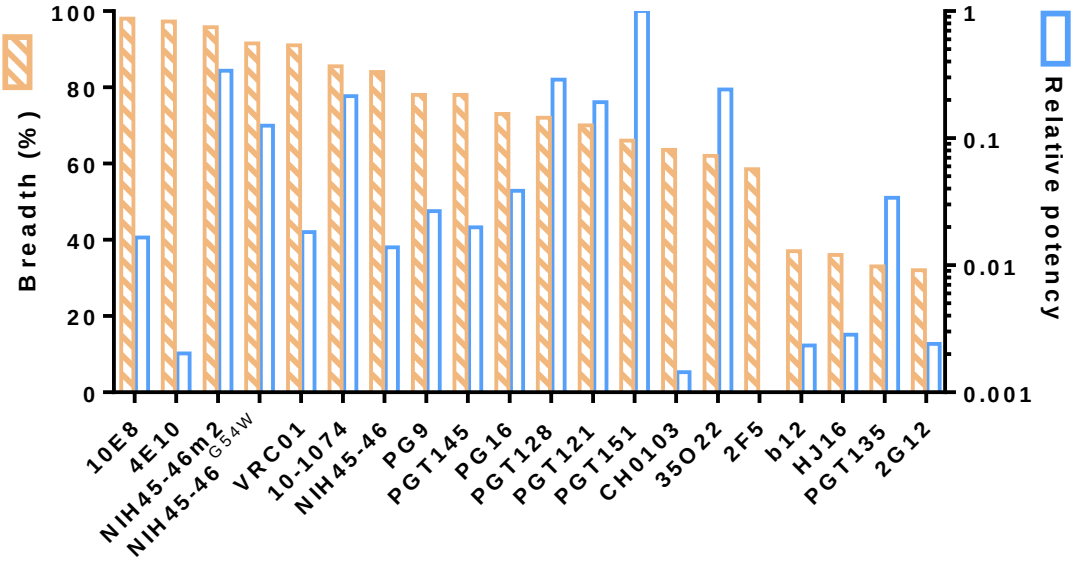

Fig. 1.10: Breadth and potency of published bNAbs. Breadth is defined as the percentage of viruses neutralised at a 50% inhibitory concentration (IC_{50}) < 50 µg/ml. Relative potency shows the normalised (to PGT151) median IC_{50} of all viruses neutralised with an IC_{50} < 50 µg/ml.

Early attempts to discover bNmAbs mainly used gp120-binding as a method to isolate HIV-specific antibodies. However, the majority of antibodies binding to soluble gp120 are not able to neutralise HIV-1. Recent studies that managed to isolate bNmAbs utilised high throughput neutralisation assays to first identify so-called elite neutralisers, HIV-1 infected patients capable of extraordinarily broad and potent neutralisation (Simek et al., 2009). Blood samples from the most potent neutralising patients were then used to isolate antibodies from single B cells (Walker et al., 2009; Walker et al., 2011a), again using high throughput neutralisation assays rather than gp120 binding as the isolation criterion. Another study used a gp120-based probe that had been engineered to bind preferentially to a known bNmAb with all other exposed surfaces altered by structure-guided mutagenesis, known as resurfaced core 3 (RSC3) (Wu et al., 2010).

1.4.6 Env bNAb epitopes and neutralisation

The CD4 binding site

One of the neutralising surfaces of Env is the well-conserved CD4bs (Fig. 1.11). The prototypic antibody targeting this site is b12 (Burton et al., 1994), which neutralises approximately 35 % of circulating HIV-1 isolates (Walker et al., 2009). As b12 was isolated from a phage display library (Burton et al., 1994), it was feared that it might be a unique antibody and that it might not be possible to elicit similar antibodies *in vivo*. In 2009, a second broadly neutralising antibody (HJ16) with similar breadth and potency was discovered by screening immortalised memory B cells from a broadly neutralising HIV-1 infected donor that were subjected to multiple parallel binding assays (Corti et al., 2010a).

Shortly thereafter, VRC01 and the closely related antibodies VRC02 and VRC03 were isolated by probing B cells from an infected individual using RSC3 as bait to select for B cells expressing a binding B cell receptor (RSC3; Wu et al., 2010). All three antibodies target the CD4-binding site and showed a much larger breadth of neutralisation than previous CD4bs antibodies, with VRC01 neutralising 91% of a panel of 192 pseudoviruses (Wu et al., 2010). Subsequently, antibodies closely related to VRC01 were discovered in different patients and a consensus motif was identified that seems to be required for the breadth and potency of this class of antibodies (Scheid et al., 2011). Analysis of the crystal-structure of such an antibody (NIH45-46) in complex with gp120 and comparison with the CD4 binding mode led to the structure-based enhancement of the breadth of this antibody, giving rise to improved antibodies (such as NIH45-46^{G54W} and NIH45-46m2) which neutralise 98% of the tested strains with very high potency (Diskin et al., 2011; Diskin et al., 2013). Another study isolated a single-chain antibody (Vhh) from llamas immunised with gp140, which was

able to neutralise ~96 % of a diverse panel of pseudoviruses (McCoy et al., 2012). Thus, antibodies targeting the CD4bs are able to potently neutralise the majority of HIV-1 strains at concentrations that might be achievable by immunisation (Walker et al., 2011b).

The gp41 membrane-proximal external region

A second class of bNmAb targets the MPER of gp41 (Fig. 1.11). These types of bNmAbs, the classical members of this group being 2F5, 4E10 and Z13, typically show a high breadth of neutralisation of up to 98% but they neutralise most strains only at very high concentrations (Binley et al., 2004; Walker et al., 2009; Walker et al., 2011a). Furthermore, their epitope is partially embedded in the membrane (Sun et al., 2008) and these antibodies typically show reactivity to membrane-lipids (Haynes et al., 2005). In 2012, a new MPER antibody was discovered which shows similar breadth but much higher potency than the classic antibodies (Huang et al., 2012). Furthermore, it has substantially lower autoreactivity compared to the other members of this class despite targeting an overlapping epitope that is embedded in the viral membrane (Huang et al., 2012).

Glycan-dependent epitopes centred on glycan N332

Another broadly neutralising surface is located on the glycan shield of gp120 (Fig. 1.6 and Fig. 1.11). This glycan shield is normally a mechanism by which gp120 protects itself against recognition by antibodies, since such glycans are generally recognised as ‘self’ by the immune system. However, some differences exist between normal mammalian glycans and those found on Env (Doores et al., 2010a). After correct folding of a glycoprotein (and concomitant removal of three glucose residues), glycans attached to asparagine residues of a protein (called N-linked glycans) are generally composed of di-N-acetylglucosamine

residues followed by nine mannose residues in a specific branched pattern called $Man_9GlcNAc_2$ (Man-9) (Moremen et al., 2012). In the endoplasmatic reticulum and subsequently in the Golgi apparatus, some of these mannose are successively removed until only five remain (forming Man-5) (Moremen et al., 2012). Due to the high number of mannose residues, Man-5, Man-9, and the intermediate glycoforms are collectively referred to as "high-mannose" glycans (Moremen et al., 2012). In normal human glycoproteins, additional glycans moieties are subsequently attached to this Man-5 cluster in the Golgi apparatus, almost always starting with the addition of glucosamine by N-acetylglucosaminyltransferase I (GnT-I) (Moremen et al., 2012). A variety of different glycoforms can be generated (collectively referred to as complex glycans), many of which terminate in sialic acid residues. Most glycoproteins that reach the cell surface are not of the high-mannose type (An et al., 2012). In contrast, N-linked glycans on Env are frequently partially processed high-mannose glycans, thus distinguishing them from typical cellular glycoforms (Doores et al., 2010a).

The prototype glycan specific anti-Env bNmAb 2G12 binds to a cluster of such high-mannose glycans on gp120 (Buchacher et al., 1994; Sanders et al., 2002a; Scanlan et al., 2002), exploiting the unusual glycosylation of this protein (Doores et al., 2010a). 2G12 neutralises about 31 % of circulating isolates (Binley et al., 2004; Walker et al., 2009; Walker et al., 2011a). However, both its glycan-binding nature (Sanders et al., 2002a; Scanlan et al., 2002) and its unique domain-swapped architecture (Calarese et al., 2003) casted doubt on whether it would be possible to elicit similar antibodies by immunisation.

Another study identified a range of glycan-specific bNmAbs some of which have a much higher potency than other bNmAbs (Walker et al., 2011a). The majority of these mAbs target previously unidentified epitopes involving glycans, in particular glycan N332 (Pejchal et al., 2011; Walker et al., 2011a; Kong et al., 2013b). These N332 specific antibodies can further be subdivided into PGT121-, PGT128-, and PGT135-like mAbs which differ in their precise epitopes and inferred germline ontology. The epitope of PGT128 and its somatically related relatives target an epitope in the V3 loop (Pejchal et al., 2011). Interactions require 2 out of 3 closely spaced glycosylation sites but in contrast to 2G12, binding also relies on interaction of the antibody with relatively sequence-independent atoms in the gp120 protein backbone (Pejchal et al., 2011).

Quaternary specific epitopes on gp120

In 2009, the somatically related antibodies PG9 and PG16 were discovered (Walker et al., 2009). These antibodies recognise an epitope in the V2 loop, which includes 2 glycans (Walker et al., 2009; McLellan et al., 2011) and neutralise about 79% of viruses. This broad reactivity of an antibody targeting one of the highly variable loops can be explained by the mode of recognition of gp120 by PG9 (McLellan et al., 2011). The antibody makes extensive contacts with the peptide backbone of gp120 with only minimal contacts of the side-chains. Furthermore, different glycans can be accommodated in the binding site on PG9 (McLellan et al., 2011). Interestingly, PG9 and PG16, as well as the later identified CH01-CH04 and PGT145 antibodies (McLellan et al., 2011; Walker et al., 2011b), are able to bind to trimeric membrane-bound Env in the correct quaternary conformation, but fail to recognise most monomeric gp120 and soluble engineered trimeric gp140 constructs (Walker et al., 2009). Additional quaternary specific mAbs (3BC176 and 3BC315) were discovered but these are

distinct from the PG9 group and their precise epitope has not been identified yet (Klein et al., 2012a).

bNAb epitopes spanning gp41 and gp120

Very recently, three separate broadly neutralising epitopes were discovered that each span both gp41 and gp120 (Fig. 1.11) (Blattner et al., 2014; Falkowska et al., 2014; Huang et al., 2014; Scharf et al., 2014). bNmAb 8ANC195 was actually isolated in 2011 (Scheid et al., 2011) but it was only very recently shown to bind to a surface of gp120 in proximity to the CD4bs as well as some glycans on gp41 (Scharf et al., 2014). Antibodies PGT151 and 35O22 both recognise glycan-dependent quaternary epitopes (Blattner et al., 2014; Falkowska et al., 2014; Huang et al., 2014). In addition, PGT151 has been shown to preferentially recognise cleaved Env (Blattner et al., 2014; Falkowska et al., 2014) although it is thought that uncleaved Env does not fold properly (Ringe et al., 2013) thus making it difficult to distinguish between cleavage and quaternary dependency.

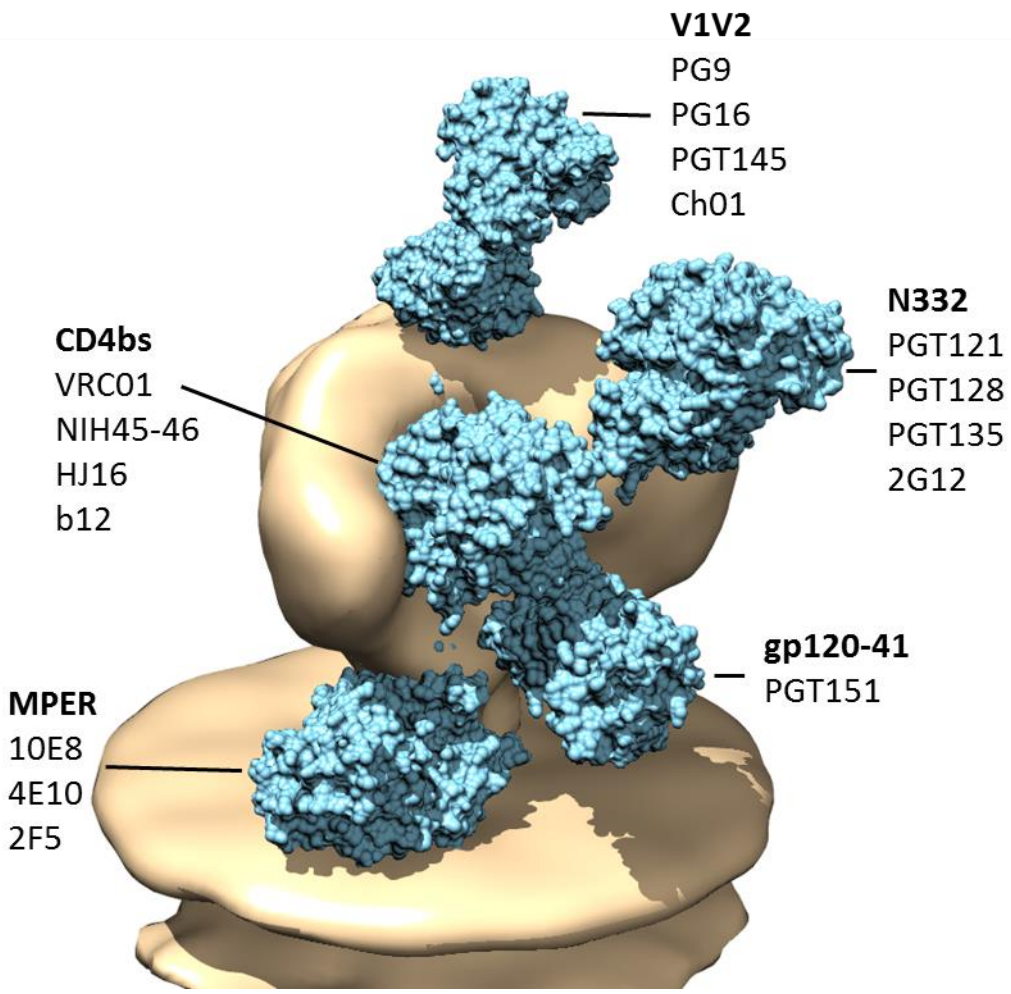

Fig. 1.11: bNmAb epitopes on Env. The approximate position of F_{Ab}s of bNmAbs (blue) on Env (fawn) is indicated. The image was created by superpositioning PDB# 3NGB (Zhou et al., 2010), 3TYG (Pejchal et al., 2011), 3U2S (McLellan et al., 2011), 4NUG (Blattner et al., 2014), EMD# 5019 and 5022 (Liu et al., 2008) in UCSF Chimera.

Taken together, a number of epitopes of broadly and potently neutralising antibodies has been described, including the CD4bs, the MPER, glycan-dependent epitopes at the N332 super-site, the trimer apex and the gp41-gp120 interface.

1.4.7 **Action of broadly neutralising antibodies**

Patients with very potent bNAb responses have now been identified including several elite neutralisers. In these patients it was found that the appearance of bNAbs does not delay disease progression and NAb titres were not different in long-term non-progressors

compared to progressors (Piantadosi et al., 2009; van Gils et al., 2009; Euler et al., 2010). This can be explained by the immune evasion of HIV-1 by rapid mutation of Env (Kepler et al., 2014) which leads to an escape of the contemporary isolates from NAbs (Liao et al., 2013a; Wibmer et al., 2013; Doria-Rose et al., 2014). This suggests that even if a vaccine would be able to induce bNAbs, it would not exert a therapeutic effect. However, infusion of combinations of bNmAbs are able to suppress viraemia in animal models (Klein et al., 2012b; Barouch et al., 2013; Horwitz et al., 2013; Shingai et al., 2013). Furthermore, in humanised mice single antibodies are able to prevent HIV-1 rebound if treatment is started during HAART thus preventing the development of escape mutations (Horwitz et al., 2013). Therefore, the possibility of an antibody based therapeutic vaccine cannot be completely ruled out.

Whereas the feasibility of a therapeutic vaccine is still uncertain, a lot of data has been generated concerning the prophylactic potential of bNmAbs. In challenge studies in macaques or humanised mice, bNmAbs have consistently provided sterilising immunity (Mascola et al., 2000; Hessell et al., 2009a; Hessell et al., 2009c; Hessell et al., 2010; Burton et al., 2011; Moldt et al., 2012; Shingai et al., 2014). Recent data have also highlighted that relatively low concentrations of mAbs suffice to protect from SHIV challenge in the case of very potent bNmAbs such as PGT121 (Shingai et al., 2014) or VRC07 (a more potent variant of VRC01 (Rudicell et al., 2014)), in particular if mutations are introduced that increase serum half-life (Rudicell et al., 2014) or F_c-mediated effector functions (Bournazos et al., 2014). By contrast, non-neutralising mAbs showed no or limited protection in the SHIV model (Burton et al., 2011) and increasing the potency of neutralisation of a bNmAb by

mutagenesis increased its ability to protect animals from SHIV challenge (Rudicell et al., 2014).

Therefore, bNmAbs are able to provide sterilising immunity and might even be used in future treatment settings.

1.5 Cross-linking of vaccine antigens

Chemical cross-linking of vaccine antigens has been used since 1954 when Jonas E. Salk and colleagues developed the inactivated polio vaccine, which uses formaldehyde (FA) cross-linking to inactivate polio virions (Salk et al., 1954). Since then, cross-linking has been used as a method of inactivation in a number of vaccines and thus extensive data have been gathered proving its safety in human use (Melnick, 1978; Rappuoli, 1994). To date, formaldehyde (GLA, Fig. 1.12A) is the only cross-linker used for vaccine purposes, but the safety of other cross-linkers such as glutaraldehyde (GLA, Fig. 1.12B) have been shown to be safe and well tolerated in human trials on allergy immunotherapy (Garcia-Selles et al., 2003; Riechelmann et al., 2010; DuBuske et al., 2011).

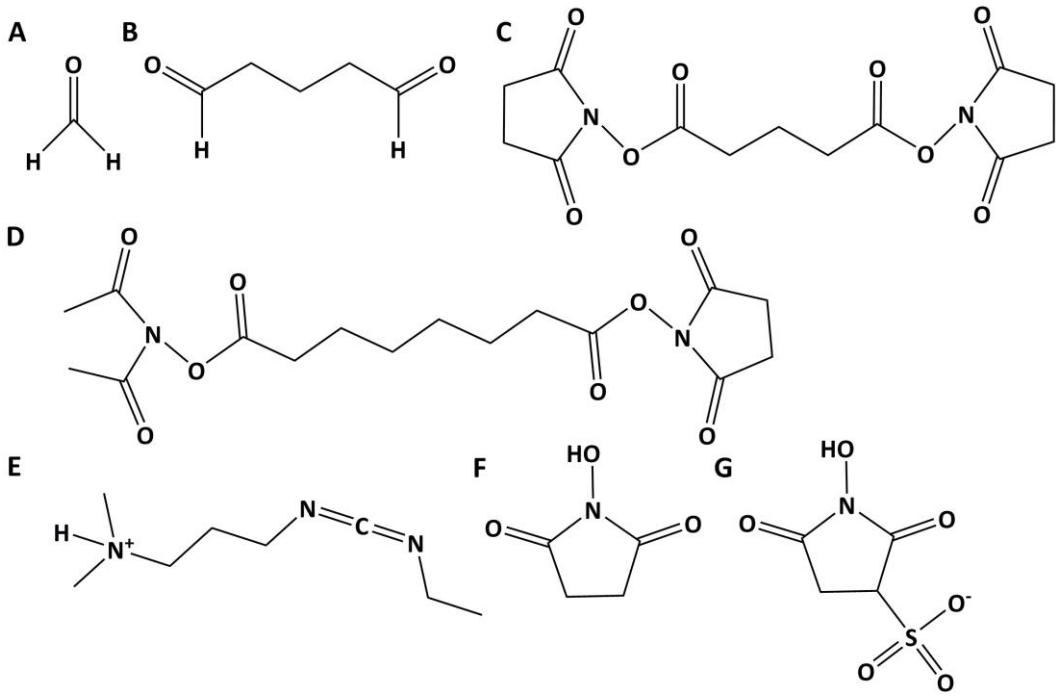

Fig. 1.12: Chemical structure of cross-linkers used in this thesis. A: Formaldehyde (FA); **B:** Glutaraldehyde (GLA); **C:** disuccinimidyl glutarate (DSG); **D:** disuccinimidyl suberate (DSS); **E:** 1-Ethyl-3-(3-dimethylaminopropyl) carbodiimide (EDC); **F:** N-hydroxysuccinimide (NHS); **G:** N-hydroxysulfosuccinimide (Sulfo-NHS).

GLA is a homobifunctional cross-linker consisting of two aldehyde groups separated by a three atom spacer. Despite its simple chemical structure, GLA forms a complex mixture of different monomeric and oligomeric forms in aqueous solution, depending on concentration, pH and temperature (Fig. 1.13) (Hopwood et al., 1970; Kawahara et al., 1992; Migneault et al., 2004). Due to the complexity of GLA in solution, controversy exists concerning the reaction of GLA with proteins. A number of possible reactions has recently been reviewed by Migneault et al. (2004). However, it is generally agreed that primary amines, in particular those found on the Ɛ-group of lysine residues, are the primary target sites for GLA on proteins (Hopwood et al., 1970; Kawahara et al., 1992; Migneault et al., 2004). Nevertheless, other amino acids, including tyrosine, tryptophan, phenylalanine, histidine, cysteine, proline, serine, glycine, and arginine, can also be modified by GLA with varying efficiencies (Hopwood et al., 1970; Migneault et al., 2004).

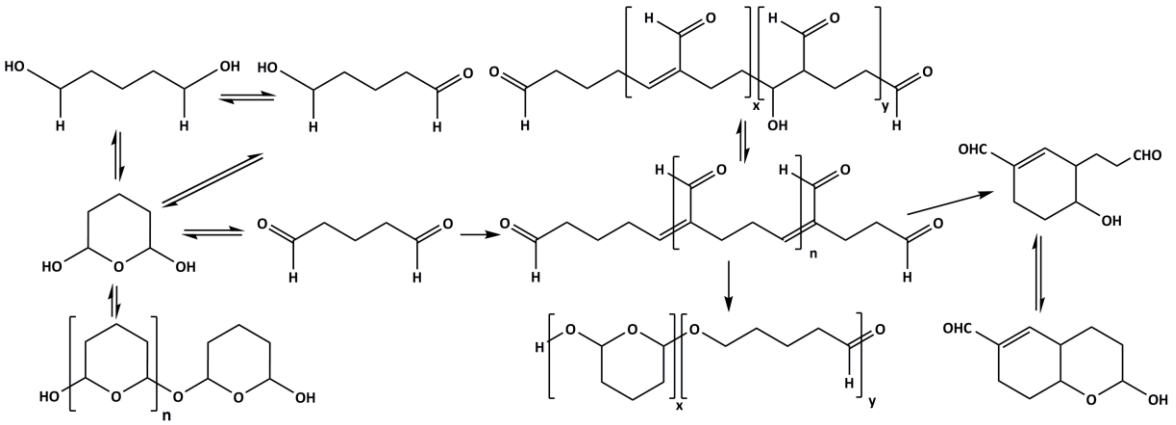

Fig. 1.13: Forms of GLA in aqueous solutions. Adapted from (Migneault et al., 2004).

Since glutaraldehyde forms ill-defined cross-linking products, alternatives such as N-hydroxysuccinimide (NHS) esters, including disuccinimidyl glutarate (DSG, Fig. 1.12C) and disuccinimidyl suberate (DSG, Fig. 1.12D), can be used instead. These are more specific for primary amines, and result in well-defined linkers which can be tailored to different lengths (Mattson et al., 1993). However, since such linkers could in principle be immunogenic, it might be beneficial to use a so-called zero-length cross-linker such as the combination of 1-Ethyl-3-[3-dimethylamino-propyl]carbodiimide hydrochloride (EDC, GLA, Fig. 1.12D) and N-hydroxysuccinimide (NHS, GLA, Fig. 1.12E) or the alternative N-hydroxysulfosuccinimide (Sulfo-NHS, Fig. 1.12F) which is better soluble in aqueous solutions (Mattson et al., 1993; Nakajima and Ikada, 1995). These cross-linkers form a peptide bond between carboxy groups and primary amines but no atom from the cross-linkers is retained on the protein after the reaction is completed (Mattson et al., 1993; Nakajima and Ikada, 1995). The reaction is initiated by EDC reacting with a carboxy group on the protein (Fig. 1.14), forming an unstable intermediate that can then be stabilised by either NHS or Sulfo-NHS (Mattson et al., 1993; Nakajima and Ikada, 1995). Either of these intermediates can then react with a primary amine such as the Ɛ-group of lysine residues, forming a peptide bond, or the intermediate can hydrolyse, thus restoring the initial carboxy group (Mattson et al., 1993;

Nakajima and Ikada, 1995). No clinical trials of EDC/NHS cross-linking have been conducted to date, but the low cytotoxicity and the fact that it is a zero-length cross-linker that does not remain on the target protein suggest that these reagents might be safe to use as well (Park et al., 2002).

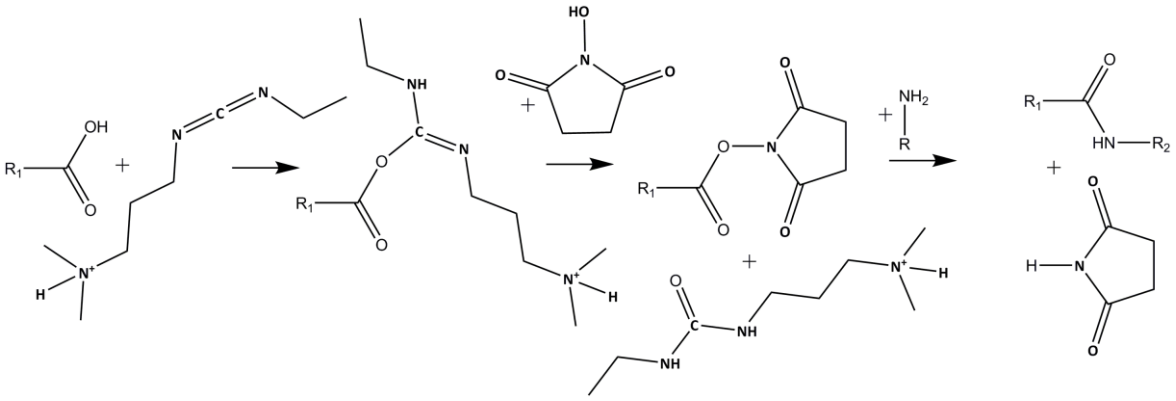

Fig. 1.14: Reaction of EDC and NHS with carboxy and priamry amine groups. Adapted from (Fischer, 2010).

Thus, a number of cross-linkers with a range of different properties exist that can be used to fix protein conformations and cross-linking strategies can be optimized to meet specific requirements such as linker lengths and target site utilisation.

1.6 Scope of thesis

Current evidence suggests that bNAbs might be able to protect from HIV-1 acquisition, but the elaborate defence mechanisms of Env such as amino acid variation and immunodominance of non-neutralising epitopes have so far prevented the induction of such responses by vaccination. These problems could in principle be overcome by retargeting antibody responses away from immunodominant non-neutralising epitopes towards conserved broadly neutralising but normally immunorecessive epitopes. In this thesis, the feasibility of using chemical modification of vaccine antigens to refocus antibody responses is explored. In chapter three, four and five, chemical cross-linking is used to

modify first-generation soluble Env, membrane-expressed Env and next-generation soluble Env respectively, and the effects of cross-linking on antigenicity and immunogenicity are investigated. In chapters six and seven, a strategy is devised to predictively refocus antibody responses by 'masking' of immunodominant epitopes with glycans. This strategy might in principle be used to develop immunogens against a number of pathogens, including influenza and hepatitis C virus, which escape the induction of bNmAbs by displaying immunodominant non-neutralising epitopes. Taken together, in this thesis proof of principle of refocusing of antibody responses using chemical modification of vaccine antigens is provided and further improvements required to apply this strategy to vaccines against a number of diseases are highlighted.

Chapter 2: Materials and methods

2.1 Materials

2.1.1 **Proteins**

Hen egg lysozyme (HEL): Lysozyme from chicken egg white, Sigma-Aldrich, St. Louis, USA.

CN54 gp140 (uncleaved, SEKS, Chinese hamster ovary (CHO) cell expressed): Polymun Scientific, Klosterneuburg, Austria. This protein was further prepared by depletion of contaminating IgG via protein A beads followed by buffer-exchange into PBS as described below.

UG37 gp140 (uncleaved, SEKS, human embryonic kidney (HEK) strain 293T (HEK-293T) or CHO cell expressed): Kind donation from J.L. Heeney (HEK-293T) or purchased from Polymun Scientific (CHO) and processed similar to CN54 gp140.

JRFL gp140 (uncleaved, SEKS, HEK-293T cell expressed): Kind donation from G.E. Stewart-Jones.

YU2 gp140 (uncleaved, SEKS, HEK-293T cell expressed): Kind donation from G.E. Stewart-Jones.

BG505 SOSIP.664 gp140 (cleaved by RRRRRR enhanced furin cleavage site + SOSIP set of mutations, HEK-293T or CHO cell expressed): Kind donation from R.W. Sanders, A.B. Ward or J.P. Moore or recombinantly expressed and purified from HEK-293T as described below. In addition to the untagged trimer, a protein with a C-terminal flexible linker followed by a D7324 tag (GSAPTKAKRRVVQREKR) was provided by J.P. Moore. A constructs with a C-terminal His-tag was expressed and purified as described below.

2.1.2 Antibodies

Monoclonal anti-HIV-1 Env antibodies, their respective sources as well as their epitopes including relevant references are listed in Table A. 1 in the appendix. gp120 capture mAb was purchased from Aalto Bio Reagents Ltd (cat# D7324; Dublin, Ireland). Streptavidin-biotinylated horseradish peroxidase (HRP) was purchased from Fisher scientific (cat# 10470705). Secondary antibodies are listed in Table 2-1.

Table 2-1: List of secondary antibodies

Target	Raised in	Enzyme/ fluorophore	Working concentration	Comment	Cat#	Company
human IgG	goat	HRP	1:10,000		109-035-098	Jackson ImmunoResearch, West Grove, USA.
human IgG	goat	HRP	1:10,000	cross-adsorbed	109-035-088	Jackson ImmunoResearch
mouse IgG	goat	HRP	1:10,000		STAR120P	AbD Serotec, Kidlington, UK
mouse IgM	rat	HRP	1:10,000	monoclonal	550588	BD Biosciences, New Jersey, USA
rabbit IgG	goat	HRP	1:10,000		10004301	Cayman Chemical Group, Ann Arbor, USA
human IgG	goat	R-phyco-erythrin	1:100		109-116-088	Jackson ImmunoResearch
human IgG	goat	DyLight 800	1:1,000		072-07-10-06	Insight Biotechnology, Wembley, UK

2.1.3 Buffers

Phosphate buffered saline (PBS): Sigma-Aldrich.

10x PBS: Fisher Scientific.

PBST: PBS + 0.005% Tween-20.

PBSC: PBS + 1.6 mM 3-[(3-Cholamidopropyl)dimethylammonio]-1-propanesulfonate (CHAPS, Sigma-Aldrich).

Blocking buffer: PBST + 2% BSA.

Fluorescence activated cell sorting (FACS) buffer: 2% foetal calf serum (FCS; Sigma) in PBS.

Mes buffered saline (MBS): 150 mM NaCl in 50 mM Mes pH 6.0.

Tris buffered saline (TBS): 150 mM NaCl in 50 mM Tris pH 7.6.

TAE buffer: 40 mM Tris, 20mM acetic acid, 1 mM Ethylenediaminetetraacetic acid (EDTA, Sigma).

TE buffer: 10 mM Tris, 1mM EDTA, pH 8.0.

KCM buffer (5X): 0.5 M KCl, 0.15 M $CaCl_2$, 0.25 M $MgCl_2$, sterile filtered.

HBS buffer (2X): 280 mM NaCl, 10 mM KCl, 1.5 mM Na_2HPO_4, 12 mM Glucose, 50 mM (4-(2-hydroxyethyl)-1-piperazineethanesulfonic acid (HEPES, Sigma), pH 7.05-7.12, sterile filtered.

CELISA wash buffer: 1.8 mM $CaCl_2$, 1 mM $MgCl_2$, 140 mM $NaCl_2$, 20 mM HEPES, pH 7.4

Western blot transfer buffer: 10% Methanol, 25 mM Bicine, 25 mM Bis-Tris, 1 mM EDTA, pH 7.2

2.1.4 Growth media

Complete Dulbecco's modified eagle's medium (DMEM): 500 ml DMEM (Sigma-Aldrich, D6429) + 50 ml FCS + 5 ml Pen/Strep (Invitrogen).

Suspension medium: Freestyle 293 expression medium, Life Technologies.

LB medium: Purchased from the Sir William Dunn School of Pathology.

Suspension DMEM: 500 mL calcium-free DMEM (Life technologies, 21068028) + 50 mL FCS + 5 mL Penicillin/Streptomycin + 5 mL Pluronic F-68 (MP Biomedicals, Santa Ana, USA), 0.15 g Primatone (Sigma-Aldrich).

2.1.5 Commercial kits

Gel extraction: QIAquick Gel Extraction Kit, Qiagen, Hilden, Germany.

Miniprep: QIAprep Spin Miniprep Kit, Qiagen.

Maxiprep: GenElute HP Maxiprep Kit, Sigma-Aldrich.

Gigaprep: PureLink HiPure Plasmid Gigaprep Kit, Life Technologies.

HEL activity assay: EnzChek Lysozyme Assay Kit, Life Technologies.

2.2 Methods

2.2.1 Modelling

Sequences of circulating strains of HIV-1, influenza virus and Hepatitis C envelope proteins were downloaded from the HIV sequence database (http://www.hiv.lanl.gov/content/sequence/HIV/mainpage.html), influenza virus resource (http://www.ncbi.nlm.nih.gov/genomes/FLU/FLU.html) and the Hepatitis C Virus Databases (http://hcv.lanl.gov/content/sequence/HCV/ToolsOutline.html) respectively. Alignments were built using MAFFT (version 6.903; Katoh et al., 2009). Based on naturally-occurring variants, suitable mutations were searched for in UCSF Chimera to cover the whole surface with lysines spaced less than 20 Å apart which should not allow a whole antibody to bind in between. The only exception was the broadly neutralising epitope where all lysines within a 10 Å radius were mutated to arginine or the appropriate most common amino acid at the respective position. Where no suitable mutations were found for a particular surface, molecular modelling was performed in PyRosetta (Chaudhury et al., 2010). Crystal structures were mutated to match the wildtype protein and a comprehensive pre-built relax of the structure was performed. Based on this structure, side-chain repacking was performed to further relax the structure and the lowest energy conformation out of 1000 repeats was chosen as the energy of this structure. This process was repeated 10 times to give 10 values for each structure. Mutations were introduced and

the mutations were accepted if the 10 energies were not statistically significantly higher than those of the wildtype protein.

2.2.2 **Cloning**

Genes for gp120 and eOD constructs were codon optimised for improved expression in human cells and ordered from GeneArt (Regensburg, Germany). Genes were then subcloned into expression vector pHLSec (Aricescu et al., 2006) using standard molecular biology methods. Briefly, genes and vector were digested with the appropriate restriction enzymes (purchased from New England Biolabs, Massachusetts, USA or Roche Applied Science, Penzberg, Germany) according to manufacturer's instructions. 0.5-2% agarose (Sigma Aldrich, St. Louis, USA) was melted in TE buffer, supplemented with sybrsafe DNA stain (Invitrogen, Carlsbad, USA) and poured into a gel casting tank including a comb to induce the appropriate number of wells. After the gel had solidified, the gel was placed in the running cartridge and covered in TE buffer. DNA samples were mixed with loading dye and loaded into the wells. DNA ladder (Sigma D-7058) was added in a separate lane. Separation was achieved by applying 80V until the dye front showed sufficient migration in the gel (40-60 min). Gel slices containing the DNA fragments of interest were cut on a Safe Imager 2.0 Blue Light Transilluminator (Invitrogen) and purified using a gel extraction kit according to manufacturer's instructions. Inserts were ligated into the vector backbone using a T4 DNA ligase (Invitrogen) according to manufacturer's instructions. Ligation products were then transformed into E.coli as described below. Positive colonies were picked, grown overnight (ON) in 2 mL LB medium containing the appropriate antibiotic (ampicillin in case of pHLSec) and DNA was purified using a miniprep kit. Successful cloning was confirmed by Sanger sequencing (Source BioScience, Nottingham, UK)

2.2.3 Site-directed mutagenesis

Primers were designed by inducing the appropriate mutation flanked by 15 perfectly annealing nucleotides on both sides. This primer, as well as its reverse complement, were then ordered from Invitrogen, mixed with the plasmid containing the gene of interest in the following reaction mix:

Table 2-2: Site-directed mutagenesis reaction mix

Plasmid (1-15 ng/µl)	1 µL
10X Turbo Pfu Buffer	5 µL
Forward oligo (10 nM)	1.25 µL
Reverse oligo (10 nM)	1.25 µL
dNTPs (10 mM each)	1 µL
Turbo Pfu	1 µL
H_2O	39.5 µL

The mix was heated to 95°C for 1 min, followed by 18 cycles of 50 seconds denaturation at 95°C, 50 seconds annealing at 55°C and 9 min extension at 68°C. The final extension after the last cycle was elongated by an additional 7 minutes. Plasmids were then digested with DpnI (1 µl, New England Biolabs) for 1h at 37°C, and 10 µl of the mix were transformed into E.coli as described below. Colonies were picked and amplified and DNA was prepped and sequenced as described above.

2.2.4 Transformation of *E. coli*

DNA was mixed with 20 µl KCM buffer and topped up to a final volume of H_2O. After briefly chilling on ice, the DNA mix was transferred to a tube containing 100 µl competent cells. After 30 min incubation on ice, samples were heated to 42°C for 60 sec and immediately chilled down on ice again. After 3 min, 700 µl LB medium were added and cells were shaken

for 60 min at 37°C. Afterwards, 400 µl were spread out on agar plates supplemented with the appropriate antibiotic for selection of positive colonies.

2.2.5 Cell culture

Adherent cell lines (HEK-293T, HEK-293A and HEK-293S GnT-I$^{-/-}$ (Reeves et al., 2002)) were maintained in appropriate tissue culture vessels (Corning, New York, USA) at 37°C in 5% CO_2 in complete DMEM. When confluency was reached, cells were washed with PBS and lifted with trypsin/EDTA (Life technologies) for 4 min at 37°C. The reaction was stopped by adding complete medium and cells were reseeded in fresh medium as required.

Suspension cells (Freestyle 293F as well as adapted HEK-293S GnT$^{-/-}$ cells) were cultured according to manufacturer's instructions (Life technologies). Briefly, cells were cultured for 2-3 days in suspension medium at 37°C and 5-8% CO_2 under orbital shaking at 115 rpm. When reaching high density, an aliquot of the cells was mixed 1:1 with trypan blue (Sigma-Aldrich) and cells were counted in a haemocytometer (Philip Harris, Hyde, UK). Cells were reseeded at 0.3X10^6 cells/mL in fresh medium.

2.2.6 Glycoprotein expression in human cells

DNA was produced by maxiprep or gigaprep following the manufacturer's instructions and freeze-thawed at -80°C. Three different approaches were optimised and used for the experiments performed in this thesis as described below.

Expression in adherent HEK-293 cells in 15 cm dishes

The day before transfection, HEK-293 (HEK-293T or HEK-293S GnT-I$^{-/-}$ as required) cells were seeded in 15 cm dishes (Corning) in complete DMEM to reach 50% confluency the following day. After 24 h, medium was exchanged and cells returned to the incubator for 1 h. In the meantime, per plate to be transfected, 15 µg DNA were topped up to 450 µl with sterile H_2O and 50 µl of a sterile 2.5 M $CaCl_2$ solution were added. After 30 min, 500 µl HBS were added in a drop-wise fashion and after ~12 min, the mixture was added to the cells drop by drop. After briefly tilting of the plates, the cells were returned to the incubator overnight. Next day, plates were washed three times with pre-warmed PBS or in case of loosely adherent cells with DMEM. Medium was replaced with 18 mL DMEM supplemented with 4 mM valproic acid (Sigma-Aldrich). Proteins were harvested after 4-7 days depending on their resistance to protease released from dying cells. Culture supernatants containing secreted protein were centrifuged for 30 min at 4°C followed by filtration using a 0.22µl stericup filter (Millipore, Billerica, USA).

Expression in adherent HEK-293A cells in roller bottles

Strongly adherent cells such as HEK-293A cells could be grown in roller bottles. Cells from a confluent T175 flask were lifted and seeded in a roller bottle (Greiner Bio-One, Kremsmünster, Austria) in 250 mL complete DMEM. After rolling for 3 days at 37°C at 0.5 rounds per min, medium was exchanged for 200 mL DMEM + 2 % FCS (no antibiotic) and cells returned to the roller rack. For each bottle, 0.5 mg DNA were mixed with 25 mL DMEM. Separately, 25 mL DMEM were mixed with 875 µL of a 1 mg/ml polyethylenimine (PEI) solution (Polyethylenimine "Max", molecular weight (MW) 40,000, High Potency Linear PEI, Polysciences, Warrington, USA). PEI and DNA solutions were mixed and, after 10 min incubation at RT, added to the cells. Cells were incubated rolling at 37°C and after 24h valproic acid was added up to a concentration of 3.75 mM. Secreted glycoproteins were harvested after 5-7 days as described above.

Expression in serum-free suspension cultures

Cells were grown to ~2X10^6 cells/mL in half the desired volume and one day before transfection were split down to 1X10^6 cells/mL in approximately the final desired volume. On the day of transfection, cells were counted and spun down followed by resuspension in fresh medium at 2.5-3X10^6 cells/mL in half the final volume required. 3 mg/L DNA were added to the cells and flasks returned to the shaking incubator for ~5 min. PEI was diluted 1:1 in suspension medium and 9 mL per litre culture added to the flask. Next morning, cultures were diluted 1:1 with pre-warmed suspension medium and in the evening valproic acid was added to a final concentration of 3.75 mM. After 4-7 days supernatants were harvested as described above.

2.2.7 Protein purification

A number of different purification strategies were used in this thesis. mAbs were purified by protein A affinity chromatography, and his-tagged proteins by immobilised metal affinity chromatography. Untagged next-generation gp140 were purified by immuno-affinity chromatography. In case of oligomeric proteins (haemagglutinin (HA) and gp140) or proteins for *in vivo* immunisation experiments, size exclusion chromatography was used as a second purification step.

Protein A affinity chromatography

Supernatants were slowly passed over a protein A agarose column (Fisher Scientific, Hampton, USA) by gravity flow. The column was washed with PBS until no protein was washed off anymore (optical density (OD) at 280 nm < 0.01) and proteins were eluted with 100 mM glycine, pH 3.0. The eluate was immediately neutralised by adding an appropriate amount of 1M Tris pH 9.0.

Immobilised metal affinity chromatography

Cobalt- or nickel-affinity chromatography was performed using HisPur columns (Fisher scientific) according to manufacturer's instructions. Briefly, supernatants were passed over affinity columns and washed with PBS (cobalt beads) or PBS + 10 mM imidazole (nickel beads). Proteins were eluted with PBS + 250 mM imidazole and columns regenerated as per manufacturer's instructions (including stripping of beads with EDTA and reloading with fresh ions).

Immunoaffinity chromatography

Antibody columns (2G12 or PGT145) were prepared on AminoLink Plus resin (Fisher Scientific) according to manufacturer's instructions. Supernatants were passed over beads by gravity flow and washed with PBS. Proteins were eluted with 3M $MgCl_2$ and immediately buffer-exchanged into fresh PBS.

Size exclusion chromatography

Size exclusion chromatography was performed on an endotoxin-free Superdex 200 16/60 column (GE Healthcare, Little Chalfont, UK) on an Äkta purifier (various models, GE Healthcare) that was extensively cleaned prior to use to remove endotoxin from the system. Samples were injected and separated by floating over the column at 1 mL/min in degassed PBS. Fractions containing the desired protein species were identified by SDS-PAGE and pooled and concentrated in spin filters (Millipore).

2.2.8 Protein quantitation

Proteins were generally quantified by OD_{280} UV spectroscopy on a nanodrop 2000c (Fisher Scientific) using appropriate correction factors calculated by ProtParam (Expasy server, http://web.expasy.org/protparam/ (Wilkins et al., 1999)). For applications requiring precise protein concentrations (surface plasmon resonance (SPR) and *in vivo* experiments), bicinchoninic acid protein assays (Fisher Scientific) were performed according to manufacturer's instructions. All concentrations stated in this thesis are referring to the protein concentration only, without reflecting any glycan contributions.

2.2.9 **Cross-linking**

A large number of cross-linking conditions were tested and analysed in this thesis. Thus, conditions are indicated in the relevant results sections. Selected standard conditions are described below.

Standard glutaraldehyde (GLA) cross-linking was performed by mixing gp140 (1 mg/ml) with an equal volume of 15 mM GLA at RT (final GLA concentration: 7.5 mM). After 5 min, 1 M tris (pH 7.4) was added to a final concentration of 75 mM and the reaction was quenched for 10 min. Proteins were then either buffer-exchanged into fresh PBS or simply diluted ~200-fold in PBS for ELISA analysis.Re-optimised glutaraldehyde cross-linking was performed by cross-linking for 60 seconds with 500 mM GLA followed by quenching by 20-fold dilution in 3 M tris buffer (pH 7.4).

Cross-linking with a combination of the cross-linkers EDC and NHS was performed by pre-mixing 2 M EDC with 20 mM NHS in mes buffered saline (pH 6.0, MBS) followed by addition of the cross-linker (EDC/NHS) to an equal volume of protein (in PBS) for 30 min after which the reaction was quenched with an equal volume of 1 M glycine (pH 7.4).

Analytical cross-linking for SDS-PAGE was performed by mixing the protein with GLA (final concentration 15 mM) for 30 min prior to SDS-PAGE analysis.

2.2.10 **Protein gel electrophoresis and Western blot**

For SDS-PAGE, Proteins were supplemented with 1X LDS loading buffer (Life technologies; with or without reducing agent as required) and denatured at 95°C for 5 min. Denatured

proteins were loaded onto the appropriate gel (12% bis/tris for small proteins including HEL, 4-12% bis/tris for intermediate sizes including gp120 and eOD and 3-8% tris-acetate for large complexes including trimeric gp140, gp160 and HA; all purchased from Life Technologies). Molecular weight markers (Novex Sharp or HiMark Prestained Protein markers, Life Technologies) were included. Proteins were separated at 150 V until the dye front reached the bottom of the gel. Proteins were stained with a SilverQuest staining kit (Life Technologies) or InstantBlue protein stain (Expedeon, San Diego, USA) according to manufacturer's instructions or processed for Western blotting.

Western blotting was performed by soaking the gel in NuPAGE transfer buffer (life technologies) supplemented with 10% methanol for 10 min. Hybond-LFP membrane (Fisher Scientific) was cut to the appropriate size, activated for 30 sec in methanol and soaked in transfer buffer. The gel was placed on the membrane, sandwiched by Whatman paper and transfer cushions and the assembly was placed in the transfer tank. An ice-pack was added and the buffer filled to cover the gel. The transfer was performed at 100 V for 1h at 4°C. Membranes were blocked for 1h with 5% milk in WB buffer (PBS + 0.05% tween-20, Sigma-Aldrich) or superblock (Sigma-Aldrich) at room temperature (RT). Proteins were stained with the appropriate antibody ON at 4°C. Membranes were washed 3X with WB buffer and detected with the matching fluorophore-conjugated secondary mAb in WB buffer + 0.001% SDS. Membranes were washed 3x with WB buffer and membranes read on an Odyssey SA reader (Li-cor Biosciences, Lincoln, USA). Data were analysed in Image Studio for Odyssey SA (Li-cor Biosciences).

To analyse the oligomerisation of proteins, analytical cross-linking was performed by incubating proteins for 30 min with 15 mM GLA prior to mixing with loading dye. Alternatively, blue native PAGE was performed using Life Technologies reagents according to manufacturer's instruction.

2.2.11 Synthesis and purification of SiaLac

Lactose containing the precursor for the 2-imido-2-methoxy-ethyl (IME) linker (Lactose S-cyanomethyl glycoside, LacSCM) was provided by K. Leonavicus, R. Saliba or S. De Munari from the Davis lab. Sialic acid was enzymatically attached by incubation of the following mix for 30 min at 37°C:

Table 2-3: Reaction mix to create SiaLacSCM

LacSCM	1.5 mM
Sialic acid	2 mM
Cytidine triphosphate	2 mM
Sodium carbonate	100 mM
$Mg(OAc)_2$	25 mM
***Neisseria meningitides* CMP-sialic acid synthetase**	4.1 mg/L
***Pasteurella multocida* Sialyltransferase**	5.4 mg/L
pH	8.5

SiaLacSCM was purified by SiO_2 (Biotage-SNAP Flash column, Biotage, Uppsala, Sweden) chromatography using a 5% to 15% water in acetone gradient over 15 column volumes. Fractions containing the SiaLacSCM were identified by thin layer chromatography (TLC, 10% water in 90% acetone), pooled and liquid evaporated (40°C, 7mbar) followed by resuspension in 5 mL H_2O and subsequent freeze-drying.

2.2.12 Activation of IME reagents and coupling to target proteins

Imidate (IME) reagents SiaLacIME or LacIME were produced from SiaLacSCM or LacSCM by resuspending the glycans in methanol and adding 0.4 equivalents methoxide. After 2h, pH was neutralised with glacial acetic acid and products precipitated by adding an equal volume of diethylether. Glycans were spun down and supernatants removed followed by vacuum drying of the pellet.

Proteins were modified with activated IME reagents by dissolving 75 equivalents per lysine residue of the appropriate activated carbohydrates directly in the protein solution in PBS at a protein concentration of 1 mg/mL. Additional sugar (75 equivalents per lysine residue) was added twice after incubating for 1h at RT or ON at 4°C. Following coupling, the buffer of the protein was exchanged to fresh PBS thus removing unreacted sugar. Successful coupling was confirmed by mass spectroscopy and SDS-PAGE or Western blot as described below. Removal of N-linked glycans was performed prior to gel analysis of glycoproteins containing native N-linked glycosylation sites in which case Western blotting was used instead of gel staining to avoid confounding bands from the deglycosylation mix.

2.2.13 Mass spectrometry

Mass spectrometry (MS) was performed on an LCT Premier XE liquid chromatography time of flight (LCT) electron spray ionisation (ESI) mass spectrometer (Waters Corporation, Milford, USA) in positive mode. Data were analysed in MassLynxx (v4.1, Waters Corporation). Further MS was performed by Heiko Schuster in Benjamin G. Davis lab at the University of Oxford.

2.2.14 **Deglycosylation**

PNGase F (New England Biolabs) was used for deglycosylation of N-linked glycans. Proteins were diluted to 0.4 mg/ml in denaturation buffer and heated to 97°C for 10 min. Subsequently, 1X NP-40, 1X G7 buffer and 1X BSA as well as 12 µl H_2O and 0,15 µl PNGase per µg target protein were added and deglycosylation was performed for 4h at 37°C.

2.2.15 **ELISA**

Direct ELISA

Enzyme-linked immuno-sorbent assays (ELISAs) were performed by coating proteins onto ELISA plates (Greiner Bio-One) at 4°C ON at 2.0 or 0.5 µg/mL in 50 µl PBS per well for assays detecting monoclonal and polyclonal antibodies respectively. Wells were washed 3X with PBST in an Ultrawash Plus plate washer (Dynex Technologies, Chantilly, USA) and blocked with 200 µl blocking buffer (PBST + 2% BSA) for >30 min at RT. Plates were washed 1X and 50 µl of dilution series of primary mAbs or sera in PBST + 1% BSA were added for 2h. Starting concentrations for mAbs were determined empirically and 3-fold dilution series were used. For end-point titres, sera were diluted 100-fold for the highest concentration followed by a 5-fold titration series.

Plates were washed 3X or 5X for purified mAbs and sera respectively and 50 µl HRP-coupled secondary antibodies were added at 1:10,000 in PBST + 1% BSA. After 1h, plates were washed 3X and 50 µl 1-Step Ultra TMB (Fisher Scientific) substrate was added. After 10 min (for end-point titres) or after the required intensity had been reached, 50 µl 0.5 M H_2SO_4 were added to stop the reaction and absorption was read at 450 and 570 nm on a spectramax M3 or M5 plate reader (Molecular Devices, Sunnyvale, USA). Background

subtraction was performed by subtracting the 570 nm value from the corresponding 450 nm value. Subsequently, the average of blank control wells was subtracted from the values of each cell.

Data were further analysed in Prism (v6; GraphPad Software, La Jolla, USA). For endpoint titres, curves were fitted to the data and endpoint titres were defined as the concentration that corresponded to a value of 0.01, which was always greater than 3 standard deviations (SD) above background levels. If sera from the same experiment were analysed on multiple days, control sera were run on each day and the threshold of 0.01 was adjusted to give equivalent titres. Reproducibility of end-point titres was found to be very good with R^2=0.99, slope 0.98 ± 0.03, X=0.008 at Y=0 between experiments performed 2 months apart. 50% effective doses (EC_{50}) were defined as the concentration at which half the maximum signal was reached, according to a "one-site specific binding" model.

Capture ELISA

For capture ELISAs, capture antibodies were coated onto the plates at 4 µg/ml. After blocking, antigens were captured at RT for 2h. Subsequent staining, detection and data processing were identical to direct ELISAs except for using highly cross-adsorbed secondary antibodies or, when isotypes of capture and detection mAb were identical, using biotinylated detection mAbs and streptavidin-HRP for staining.

Competition ELISA

Competition ELISAs were performed similar to direct ELISAs except that after addition of 25 µl of a titration series of serum (starting with 15-fold and diluting down 2-fold) or glycans (starting at 250 mM and diluting down 2-fold), 25 µl of a mAb (at its EC_{50}) was added. Highly

cross-absorbed secondary antibodies were used to prevent detection of the serum. In addition, data analysis included normalising the data by dividing the final value of each well by the value of positive-control wells without serum. Cross-competition IC_{50} values were generated by fitting data to a "dose response – inhibition" curve in prism and interpolating the serum concentration at which binding of the mAb was inhibited by 50%.

2.2.16 **Cell-based ELISA**

HEK-293A cells were seeded into 15 cm dishes and transfected by calcium-phosphate precipitation as described above. 24h after transfection, cells were lifted with 10 mM EDTA in PBS and reseeded into 96-well plates at 100,000 cells per well. Next day, cells were washed 3X with CELISA wash buffer by flicking off the medium and submerging plates in blocking buffer. After the final wash, residual liquid was removed by tapping plates onto tissues. Half the wells were cross-linked by adding 7.5 mM in CELISA wash buffer for 5 min at RT followed by quenching by adding 1 M tris (pH 7.5) up to a final concentration of 75 mM. Cells were washed 3x in CELISA wash buffer and cells were re-blocked in complete DMEM and dilution series of primary mAb was added for 1.5 h in 50 µL complete DMEM. Wells were washed as before and 50 µl secondary mAb in complete DMEM were added to each well. After 1h plates were washed. For each plate, substrate was individually mixed (200 µl 3M NaCl, 1.9 mL Oxidiser, 1.9 mL Luminol; Western-Lightning Plus-ECL, Perkin-Elmer, Waltham, USA) and 35 µl added to each well. Luminescence was read on a spectramax M5 for 1000ms. Data analysis was performed similar to ELISA assays.

2.2.17 Surface plasmon resonance

SPR analysis was performed at 37°C on a Biacore 3000 system (GE Healthcare). Proteins were immobilised on CM5 chips (GE Healthcare) via standard amine coupling. Briefly, chips were cleaned with a 30s injection (10 µl/min) of 1M NaOH followed by activation with 70 µl EDC/NHS (GE Healthcare), mixed 1:1 directly before the injection. Proteins were injected over activated surfaces for 7 min in low-pH acetate buffer as required (pH 4.0-4.5, 1-5 µg/mL). Surfaces were quenched by injecting 1M ethanolamine for one minute. Most experiment were performed by immobilising rabbit anti-human IgG antibodies (Jackson ImmunoResearch) on the surface and capturing mAbs for each cycle as described below. For kinetic analysis ~700 response units (RUs) of mAbs were immobilised. However, some mAbs were inactivated by direct immobilisation. In those cases, streptavidin was immobilised followed by capturing of ~700 RUs of biotinylated mAbs. Unreacted sites were then quenched with biotin.

Kinetic assays

For kinetic assays, fast flow rates of 50 µl/min were used. Dilution series of antigens were floated over mAbs covalently immobilised on the surface. After 5 min, the injection was stopped and dissociation of antigens followed for 5 min. In case of very slow off-rates, extended dissociation periods of up to 1h were used for the highest concentration only. Chips were regenerated by two 30 sec injections of 10 mM glycine, pH 2.0. Data were analysed by performing double referencing (subtraction of signal from a control flow cell followed by subtraction of a buffer injection) and fitted to a 1:1 Langmuir model in the BIA evaluation software (version 4.0.1, GE healthcare).

Binding analysis

For more complex binding events such as 3:2 binding of trimeric gp140 to mAbs, flow rates of 30 µL/min were used. In each cycle, mAbs were captured onto the chip surface via immobilised anti-human IgG. Antigens were passed over the chip for 4 min followed by a 4 min dissociation period. Flow cells were regenerated by two 30 sec injections of 10 mM glycine, pH 2.0. Data were analysed by double referencing followed by determining the area under the curve (AUC).

2.2.18 Peptide array

Peptide arrays were performed by Pepscan Therapeutics as described elsewhere (Schiffner et al., 2013a). Briefly, reactivity of sera (n=4 per group, including 3 randomly chosen animals plus the highest responder from each group) to immobilised 15-mer peptides covering homologous CN54 gp140 were measured. Coloured substrate was quantified with a charge-coupled device camera and an image processing system. Statistical analysis was performed by averaging the responses to 8 regions for each animal and performing a one-way analysis of variance (ANOVA) with Bonferroni's post-test.

2.2.19 Neutralisation assays

Neutralising titres were measured in fully standardised TZM-bl or A3R5 cells in D. Montefiori or M. Seaman labs as described previously (Li et al., 2005; Schiffner et al., 2013a; Sarzotti-Kelsoe et al., 2014). Briefly, pseudovirus (TZM-bl assay) or replication-competent luciferase reporter viruses (A3R5 assay) were incubated with serial dilutions of sera and added to their respective target cells. After 2 days (TZM-bl) or 4 days (A3R5), luciferase expression was measured and IC_{50} values were determined as the serum concentration

that reduced the background-subtracted relative light units by 50% compared to virus-only control wells. For V3 inhibition assays, sera were pre-incubated with an excess of V3 peptide (TRPNNNTRKSIRIGPGQTFYATGDIIGNIRQAH), scrambled control peptide, or PBS only. RSC3 inhibition assays were performed by C. Duncan in TZM-bl cells as described above with HIV-1 clade C clone NL-LucR.T2A-MW965.ecto under single-cycle conditions. Serum dilutions were pre-incubated with 10 µg/ml circularised CN54 V3 loop (CTRPGNNTRKSIRIGPGQTFYATGDIIGDIRQAHCGC) plus either 20 µg/ml RSC or ΔRSC3. Statistical analysis of neutralising titres was performed using a one-way ANOVA of log-transformed data with Bonferroni's post-test. Statistical analysis of overall differences was performed using a Mantel-Cox log-rank test on magnitude-breadth curves. Comparison of RSC3 neutralisation curves was performed by an F-test of pooled curves from all animals of each group. Fold inhibition was calculated as IC_{50} (no V3 loop)/IC_{50} (V3 loop) for the V3 loop and IC_{50} (V3 + ΔRSC3)/IC_{50} (V3 + RSC3) for the CD4bs.

2.2.20 **Flow cytometry**

HEK-293T cells were transfected with Env or negative control protein coding plasmids as described above. On the day of the experiment, cells were lifted with 10 mM EDTA. For cross-linking, cells were washed three times with PBS and resuspended in formaldehyde-containing solutions as required. After 30 min shaking at 4°C, cells were quenched with tris and buffer exchanged into FACS buffer. Both cross-linked and unmodified cells were then incubated with primary antibodies or sera for 1h at 4°C. Cells were washed 3 times and stained with the appropriate fluorophore-conjugated secondary antibodies. After 30 min, cells were washed 3 times followed by measuring cells on a FACSCalibur flow cytometer (Beckton Dickinson, New Jersey, USA)). Mean fluorescence intensities of single live cells

were determined in FlowJo (VX.0.6, Ashland, USA) and data were analysed similar to procedures for ELISA assays described above.

2.2.21 Establishing stably transfected cell lines

DNA constructs for full length gp160 Envs AC10 (AC10.0, clone 29, Genbank no AY835446) and Du156 (Du156.12, #DQ411852) expressing plasmids were obtained from the NIH AIDS reagent program. gp160ΔCT mutants were created by introducing a stop-codon directly after the trans-membrane domain replacing tyrosine Y712 (Hxbc2 numbering) via site-directed mutagenesis. The cleavage site remained unchanged. HEK-293S GnT-I$^{-/-}$ cells were transfected via lipofectamine (Life technologies) transfection according to manufacturer's instructions and 24h after transfection, cells were split into new 10cm dishes at a range of different dilutions. Next day the medium was replaced with complete DMEM containing 1 mg/ml geneticin (Life technologies). Medium was replaced every 2 days. After 2 weeks, cells were stained for fluorescence-activated cell sorting (FACS) similar to methods described for flow cytometry above. The ~2% highest-staining cells were selected by FACS and grown up to form the stably transfected cell-line. Colony picking to achieve a more homogenous population was attempted in parallel but the heterogeneous population obtained from FACS showed higher expression levels of Env.

2.2.22 Extraction and purification of membrane-expressed Env

Stable cell lines were grown adherently until confluency was reached in five T175 flasks. Cells were then lifted and further cultured in stirred spinner flasks (Techne, Staffordshire, UK) under calcium-withdrawal in suspension DMEM which prevents overt-clumping of cells and thus allows short-term suspension cultures of normally adherent cells without a

weaning period (Chaudhary et al., 2012). When Cells reached the required volume and density, 3.75 mM valproic acid was added and next day cells were harvested by centrifugation. After washing 5X with PBS, cells were frozen at -80°C until further processing.

Membrane-proteins were extracted by resuspending the thawed pellet in PBS supplemented with 16 mM CHAPS as well as protease inhibitors (Roche). After rotating for 4h at 4°C cells were pelleted at 1700 rpm followed by high-speed centrifugation of the supernatants at 15,000xg for 30 min. Finally, supernatants were clarified by 0.22µl filtration. Supernatants were applied to a Galanthus nivalis lectin (GNL) column (Vector labs, Burlingame, USA), which recognises (α-1,3) mannose residues, and washed with PBS + 1.6 mM CHAPS (PBSC). Bound glycoproteins were eluted with 1M α-methylmannoside in PBSC and buffer-exchanged into fresh PBSC. Standard GLA cross-linking was performed as described above and proteins were applied to a PGT145 immunoaffinity column. After washing with PBSC, proteins were eluted in 3M $MgCl_2$ + 1.6 mM CHAPS, and buffer exchanged into TBS + 1.6 mM CHAPS.

2.2.23 **Immunoprecipitation**

Immunoprecipitation of extracted Env was performed by extracting protein from membranes and clarifying the supernatants as described above, followed by GLA cross-linking. Supernatants were then buffer-exchange into PBSC, 5 µg mAb (PG09, HIVIG or negative control anti human IgG CD8) were added to 500 µl supernatant and tubes rotated for 4h at 4°C. 900 µl protein A beads were washed 3X with PBSC and 50 µl beads were added to each tube. After rotating ON at 4°C, beads were washed 3X with PBSC followed

by directly resuspending the beads in 2X SDS-PAGE loading buffer. Subsequently, Western blotting was performed as described above.

2.2.24 **Electron microscopy**

Negtative-stain cryo-EM microscopy was performed by T. Nieusma and H. Kim from the Andrew Ward's lab at Scripps research institute as described previously (Ringe et al., 2013). Briefly, ~5,000 individual trimers were imaged and reference-free class averages were built. "Correctly" folded classes were manually selected, and the number of proteins contributing to these classes was expressed as the percentage of overall protein complexes imaged.

2.2.25 **Animal experiments**

Mouse immunisations were performed in-house at The Sir William Dunn School of Pathology, Oxford University under the appropriate personal, project and establishment licenses in accordance with the UK Animals (Scientific Procedures) Act 1986 and were authorised by the UK Home Office and the Oxford local institutional ethical review board. Typically, female BALB/c mice were immunised subcutaneously with 10 µg protein in a total volume of 100 µl at weeks 0, 3 and 7. Proteins were formulated in various adjuvants as described in the respective experiments. If necessary, additional immunisations were administered in 4 week intervals. Blood was collected from tail veins before the first as well as 2 weeks after each immunisation. Blood samples were left to clot for at least 1h at RT or at 4°C ON. Clotted samples were centrifuged at 6000 xg for 10 min and serum was extracted from the top layer of the pelleted samples. Sera were stored at - 80°C until analysis.

Guinea pig immunisations were performed by Rachel Pei-Jen Lai from the Heeney group in Cambridge. 20 µg cross-linked or unmodified UG37 gp140 in Carbopol 974p + MF59 (Lai et al., 2012) were administered intramuscularly at weeks 0, 4 and 8. Sera were collected two weeks after each immunisation and animals were terminally bled at week 15.

Rabbit immunisations were performed by Covance Inc. (USA). 20 µg cross-linked or unmodified CN54 gp140 were administered to 8 New Zealand white rabbits per group intramuscularly at weeks 0, 6, 12 and 22 and serum collected 2 weeks following each immunisation. Proteins were formulated in 1 % Carbopol 971p for the first two immunisations and PEI (25 kDa; branched; 1 mg/ml; 1 ml) for the following immunisations.

Chapter 3: Chemical cross-linking of first-generation soluble gp140

3.1 Introduction

HIV-1 vaccine studies published to date have shown that soluble monomeric or trimeric Env-based immunogens can induce strong binding antibody responses against Env but NAb responses induced by such immunisations are typically restricted to laboratory adapted neutralisation-sensitive tier 1 isolates (Schiffner et al., 2013b). The inability to induce NAbs by these immunogens is probably due to the array of counter-mechanisms employed by HIV-1 to avoid antibody-mediated neutralisation (discussed in detail in chapter 1). One of these mechanisms is the so-called 'conformational masking' of the CD4bs. According to this theory proposed by Kwong, Sodroski and colleagues (Kwong et al., 2002; Yuan et al., 2006) the CD4bs can fluctuate between a number of different conformations. Moreover, non-neutralising antibodies only recognise one specific conformation of the CD4bs whereas bNAbs can bind to most or all conformations (Kwong et al., 2002; Yuan et al., 2006). This hypothesis is based on the finding that in contrast to bNmAbs, the binding of non-neutralising mAbs induces a large decrease in entropy. Further evidence supporting this hypothesis is based on earlier experiments in the Sattentau lab, and a follow-up study from the Sodroski lab, in which it was shown that chemical fixation of Env results in a loss of binding of non-neutralising CD4bs mAbs with smaller effects on the binding on the first-generation CD4bs bNmAbs available at the time (Sattentau, 1995; Yuan et al., 2006). Another immune-evasion mechanism of HIV-1 is the instability of Env which leads to the 'opening' of the trimer and, at the extreme end of the spectrum, the shedding of gp120, leading to the exposure of immunodominant epitopes that are occluded within the trimer interface on functional Env spikes and hence induce non-neutralising antibody responses.

These findings led to the hypothesis that cross-linked Env constructs might enhance the display of broadly neutralising epitopes by preventing conformational changes necessary for the binding of non-neutralising CD4bs mAbs. Such fixation could also prevent the disassembly of Env required to expose immunodominant epitopes within the trimer interface. Therefore, soluble cross-linked gp140 might be able to preferentially present neutralising epitopes to the immune system, leading to the induction of a more potent antibody response. Here, mild aldehyde cross-linking is optimised *in vitro* and the antigenicity of cross-linked gp140 trimers is analysed using a panel of mAbs including recently isolated potent bNmAbs. Subsequently, the effect of cross-linking on immunogenicity of gp140 is tested in two different *in vivo* models.

3.2 Results

3.2.1 *In vitro* optimisation of GLA cross-linking of gp140

Before testing the effects of chemical cross-linking on immunogenicity, cross-linking conditions were optimised *in vitro*. Primarily, the GLA concentration was optimised since this was expected to have the greatest impact on antigenicity. First-generation gp140 (strain CN54, clade C) was cross-linked with a titration series of GLA and analysed by denaturing SDS-PAGE. As expected, unmodified gp140 migrated as a single band of approximately 140 kDa (Fig. 3.1). Cross-linking with increasing GLA concentrations led to covalent stabilisation of trimeric gp140 with no monomer apparent at concentrations of approximately 5-10 mM (Fig. 3.1 and data not shown).

To test the effects of cross-linking on antibody recognition, direct ELISA analysis was performed analysing the binding of selected mAbs to cross-linked gp140. As reported

previously (Yuan et al., 2006), binding of non-neutralising CD4bs mAb F105 was reduced with increasing GLA concentrations in a dose-dependent manner, plateauing at 10 mM (Fig. 3.1 and data not shown). Similarly, the 17b mAb, which binds a CD4i epitope (Sullivan et al., 1998), was reduced by increasing GLA treatment and also levelled off around the same concentration. By contrast, binding of CD4bs bNmAbs HJ16 and b12 was relatively unaffected by cross-linking. Based on these data and additional experiments (data not shown), 7.5 mM GLA was chosen as the optimal concentration for further GLA cross-linking experiments.

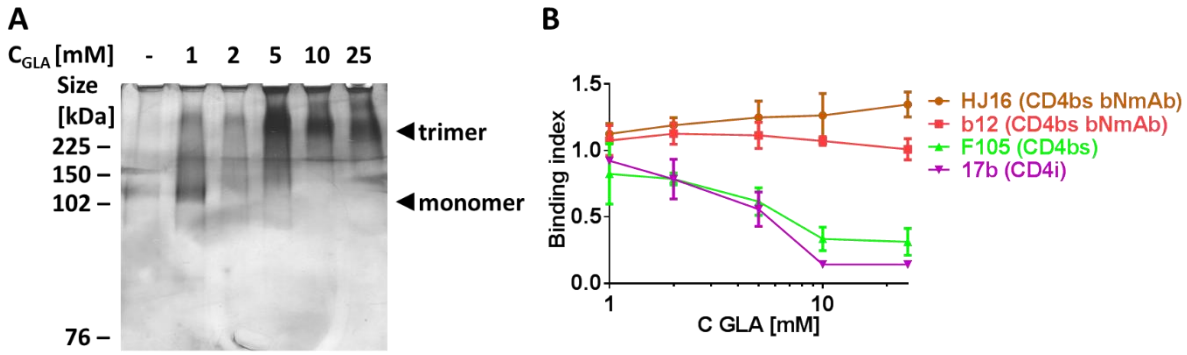

Fig. 3.1: Titration of GLA concentration. CN54 gp140 was cross-linked with the indicated concentrations of GLA and analysed by SDS-PAGE (**A**) and ELISA (**B**). **A:** Covalent trimer stabilisation was achieved by 5-10 mM GLA. **B:** Binding of non-neutralising CD4bs mAb F105 and CD4i mAb 17b was reduced by cross-linking and levelled off at concentrations of ~10 mM whereas binding of CD4bs bNmAbs HJ16 and b12 was not affected. Data are representative of 3 independent repeats. Error bars represent SD of replicate wells.

Apart from trimeric gp140, some higher molecular weight aggregates were apparent in the SDS-PAGE (Fig. 3.1 and data not shown). To minimise the formation of these aggregates, cross-linking at lower protein concentrations was investigated. A titration series of CN54 gp140 was cross-linked with 7.5 mM GLA and analysed as before (Fig. 3.2). No significant protein concentration dependency of cross-linking effects was detected in either the SDS-PAGE or ELISA analysis (Fig. 3.2).

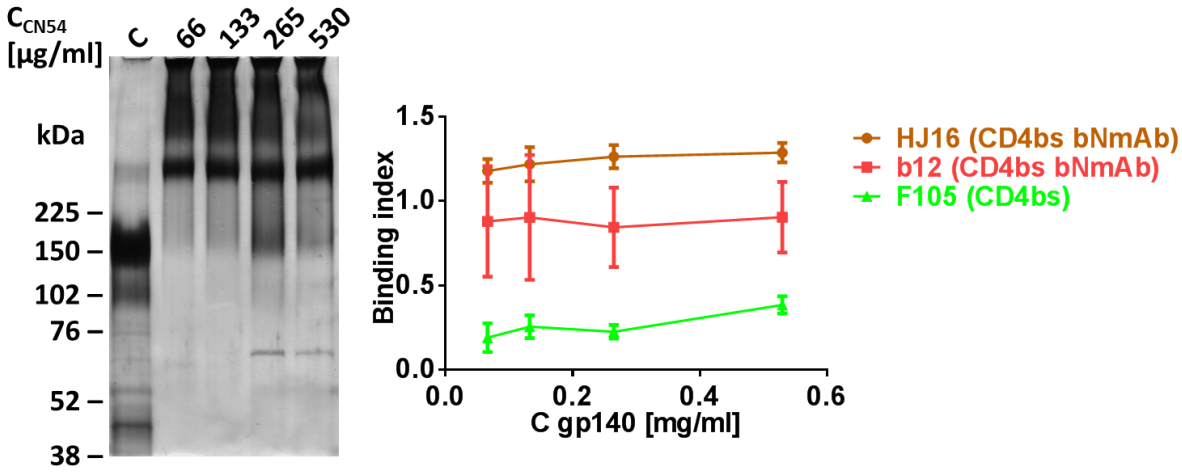

Fig. 3.2: Protein concentration dependency of cross-linking effects. CN54 gp140 was cross-linked with 7.5 mM GLA at the indicated protein concentrations and analysed by SDS-PAGE (**A**) and ELISA (**B**). C: unmodified control protein. Epitopes are indicated in parentheses.

Another possible cause of the aggregation might be a very high transient localised GLA concentration upon addition of the GLA before the liquids are properly mixed. To rule out the involvement of such effects, cross-linking of CN54 gp140 by the usual 250 mM GLA stock was compared to cross-linking with a 15 mM GLA stock pre-diluted in PBS (Fig. 3.3). Antibody binding to gp140 showed no significant differences between these two conditions for antibodies VRC01, HJ16, F105 and HIVIG by a curve-comparison F-test (Fig. 3.3). By contrast, binding of mAb 17b was significantly different ($p = 0.005$). However, binding of this mAb was barely detectable with a maximum OD_{450} of < 0.01 despite extended development time and the minor difference might be due to decreased data quality.

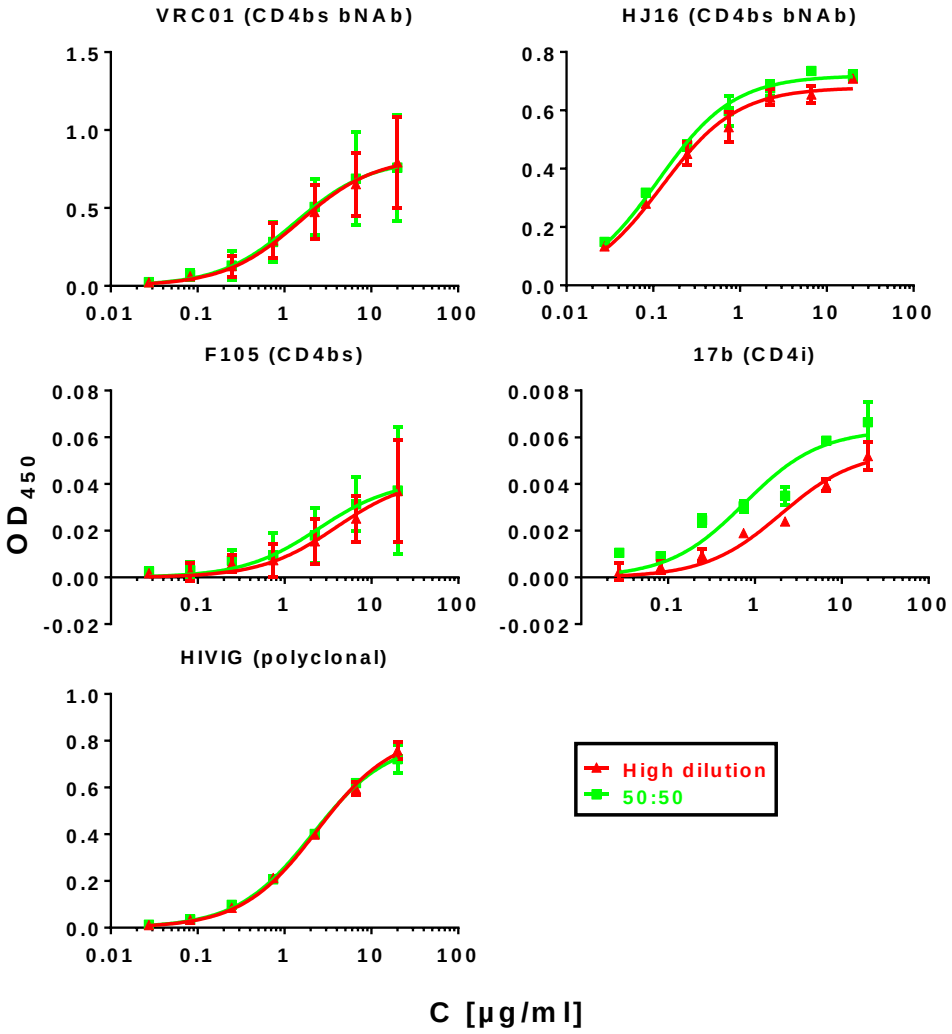

Fig. 3.3: GLA dilution dependency of cross-linking effects. CN54 gp140 was cross-linked with a final concentration of 7.5 mM GLA from either a 250 mM (high dilution) or a 15 mM (50:50) GLA stock and analysed by ELISA using the indicated mAbs. Curves indicate results of a nonlinear fit. Epitopes are indicated in parenthesis.

Finally, the effect of the glycoprotein preparation on aggregate formation during cross-linking was investigated. To examine this, 2 different preparations of the same glycoprotein (UG37 gp140), one kindly provided by J.L. Heeney, the other purchased from Polymun Scientific, were cross-linked with GLA and subjected to SDS-PAGE analysis (Fig. 3.4). The two preparations showed remarkable differences in oligomer composition. The protein from J.L. Heeney (University of Cambridge) migrated as monomeric, dimeric and trimeric fractions with only very low levels of oligomer apparent (Fig. 3.4). By contrast, the material

from Polymun Scientific showed only small amounts of monomer and dimer but larger amounts of aggregate compared to the other preparation (Fig. 3.4). Therefore, the oligomer formation seems to be predominantly preparation dependent rather than induced by the cross-linking procedure.

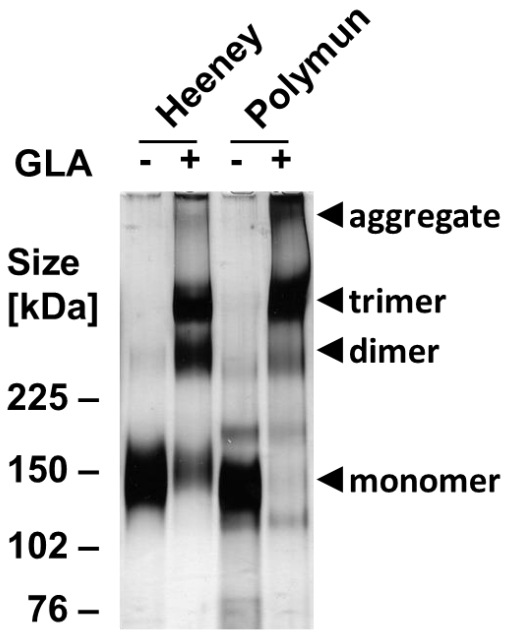

Fig. 3.4: Protein preparation influence on aggregate formation during cross-linking. UG37 gp140 from two independent sources (provided by J.L. Heeney and Polymun Scientific respectively) were cross-linked with GLA and analysed by SDS-PAGE.

Based on the results of the optimisation of cross-linking conditions, cross-linking with 7.5 mM GLA by diluting a 1 mg/ml (maximum) protein stock 2-fold in 15 mM GLA was chosen as the standard treatment for subsequent cross-linking experiments.

3.2.2 *In vitro* characterisation of cross-linked gp140

Once optimised conditions of cross-linking were found, a more comprehensive analysis of the effects of cross-linking was conducted. First, oligomer formation was analysed for two different strains under both native and denaturing conditions. Under native conditions, UG37 gp140 migrated as trimers, dimers and monomers, whereas CN54 gp140 was pre-

dominantly in a trimeric state with some higher molecular weight aggregates present (Fig. 3.5). In line with the results presented in section 5.2.1 , cross-linking led to a covalent fixation of the respective oligomers as confirmed by a denaturing SDS-PAGE (Fig. 3.5).

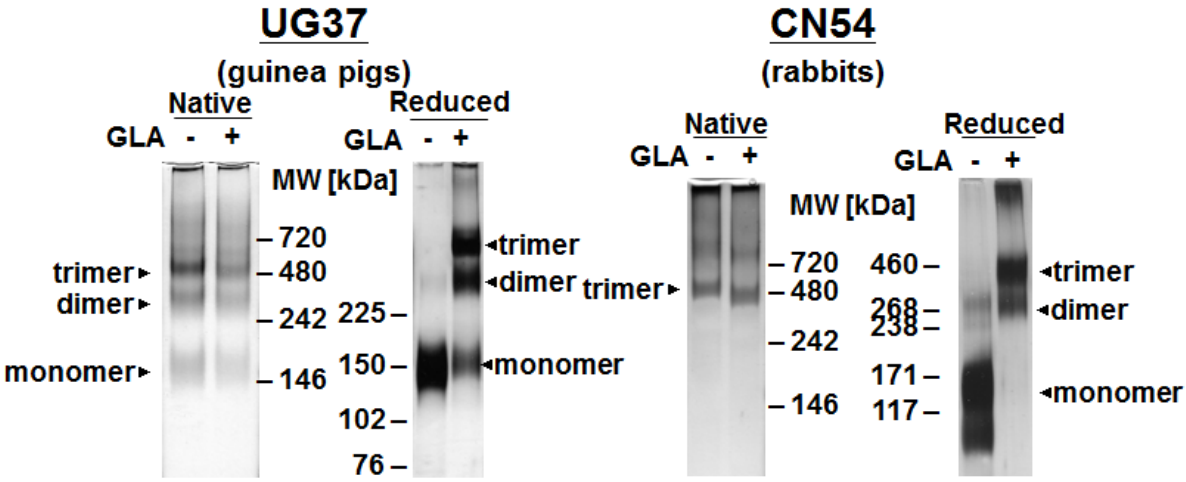

Fig. 3.5: Native and denaturing PAGE analysis of cross-linked gp140 from two different viral strains. UG37 gp140 and CN54 gp140 were cross-linked with GLA and analysed by blue native PAGE and reducing denaturing SDS-PAGE as indicated. Animal species in brackets refer to the *in vivo* experiments conducted subsequently (sections 3.2.3 and 0).

To get a more comprehensive overview of the changes in antigenicity upon cross-linking, an extended panel of mAbs was titrated onto cross-linked CN54 gp140 in an ELISA analysis (representative titration curves in Fig. 3.6 and summary of the full dataset in Fig. 3.7). Overall antigenicity of cross-linked gp140, as probed by polyclonal Ab HIVIG, was unaffected by cross-linking. Similarly, recognition of gp41 (probed by HR1-specific mAb 5F3) was unchanged. Binding of V2 and V3 loop mAbs HGP68 and HR10 was slightly though significantly reduced ($p=0.02$) or unchanged respectively. By contrast, binding of a soluble sCD4-IgG fusion protein (CD4-IgG2) to CN54 was significantly ($p<0.0001$) reduced after cross-linking, consistent with the inhibition of structural rearrangements in gp120 required for high affinity CD4 binding (Kwong et al., 2002; Yuan et al., 2006). In line with the results presented above, mAb 17b which binds a CD4-induced (CD4i) epitope (Sullivan et al., 1998) showed dramatically reduced binding to GLA cross-linked gp140 ($p<0.0001$). The binding of

non- or weakly neutralising CD4bs mAbs 15e and F105 was substantially reduced (p=0.02 and p<0.0001 respectively). This can be explained by the previous finding that, similar to CD4, these mAbs require conformational rearrangement of gp120 for tight binding (Kwong et al., 2002). This may also explain the partial reduction in IgG1b12 binding after GLA treatment (Fig. 3.7). By contrast, binding of the CD4bs bNmAbs VRC01 and HJ16 was unaffected by gp140 cross-linking, confirming a predicted lack of requirement for gp120 conformational change during binding. Additional mAbs tested include the glycopeptide specific bNmAbs PGT121, PGT122, PGT123, PGT128 and PGT135. None of these bNmAbs showed any significant difference in binding to GLA-treated and untreated gp140 (Fig. 3.6 and Fig. 3.7).

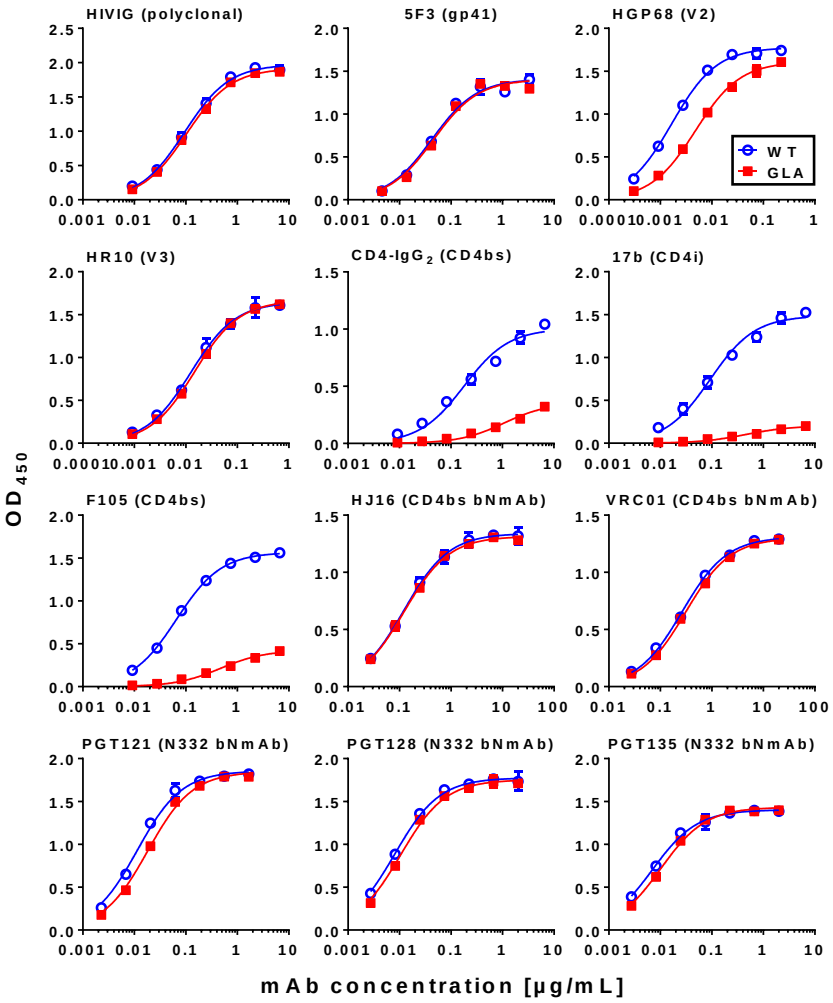

Fig. 3.6: Antigenicity of GLA cross-linked CN54 gp140. Antibody binding to unmodified (WT) or cross-linked (GLA) gp140 was analysed by ELISA. Representative titration series against CN54 gp140 using mAbs covering tested epitopes (indicated in parentheses) show selective decreases of binding of non-neutralising CD4bs antibody and CD4i antibodies. Curves indicate results of the nonlinear fit. Error bars represent SD of replicate wells.

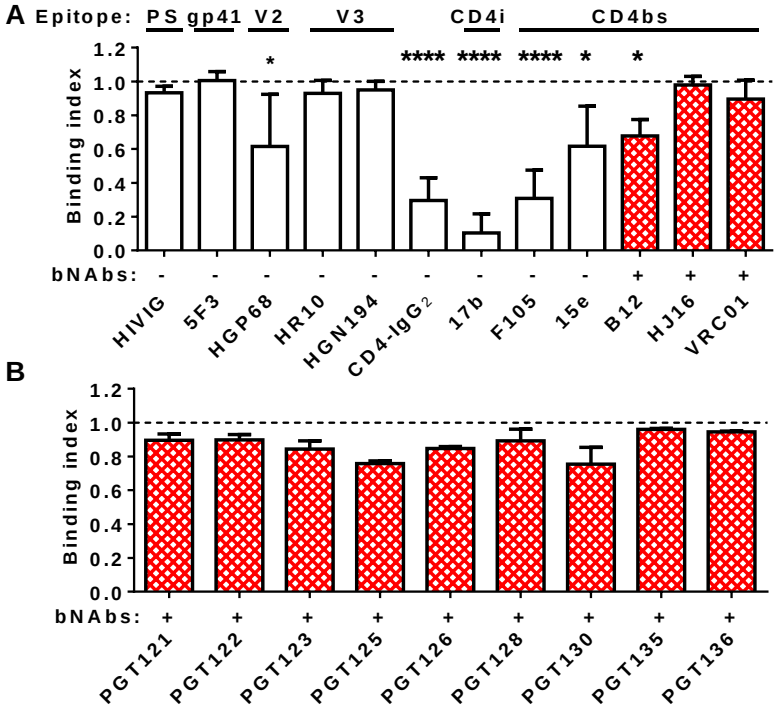

Fig. 3.7: Antigenicity of cross-linked CN54 gp140. The binding index (cross-linked/unmodified) is shown for all antibodies tested, with glycan-dependent antibodies presented in panel B. Values lower than 1.0 indicate reduced binding. Epitopes of mAbs are indicated above the bars. Error bars indicate SD from at least five (A) or two (B) independent experiments. PS, polyclonal serum; *, $p < 0.05$; ****, $p < 0.0001$ according to a Kruskal-Wallis test.

To further investigate the effects of cross-linking upon antigenicity, SPR analysis was performed. Using this more sensitive technique, the same trends as in ELISA were detected although all changes were more pronounced than in ELISA (Fig. 3.8). In addition, a modest reduction in binding of CD4bs bNmAb VRC01 was detected in this assay, but the effect was far less pronounced than with the non-neutralising CD4bs F105 or CD4i mAb 17b (Fig. 3.8).

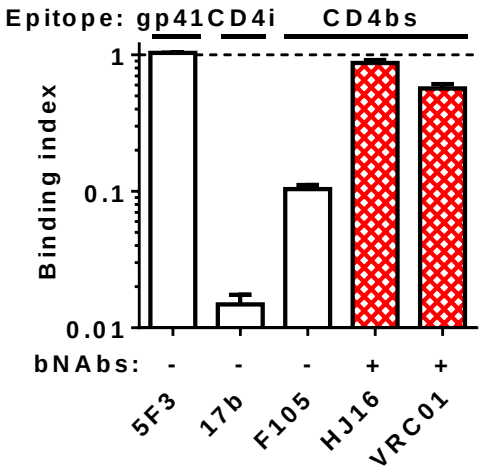

Fig. 3.8: SPR analysis of cross-linking induced changes of antibody recognition of gp140. The indicated mAbs were captured onto the sensor chip surface using immobilised anti-human IgG. Unmodified or cross-linked gp140 were floated over the captured mAbs and binding indices were calculated by dividing the AUC from cross-linked material by the corresponding value from unmodified protein. Error bars indicate SD of technical repeats. Epitopes are indicated on top of the graphs.

To rule out that the observed effects were HIV-1 strain-specific, 3 more gp140s from different clades were cross-linked and analysed by ELISA similar to the data described above (Fig. 3.9). In general, similar trends as described for strain CN54 were observed with other strains tested although a statistically significant reduction of binding was only seen for CD4i mAb 17b ($p = 0.01$). However, in line with the data presented for CN54, a trend towards reduced F105 binding was seen in this cross-strain analysis, although it did not reach statistical significance ($p = 0.09$) (Fig. 3.9). One additional control included in this experiment was mAb 2G12, which was not used before since it does not recognise strain CN54 used in the previous experiments (data not shown). This bNmAb binds to oligo-mannose glycans on gp120, without a peptide-binding component (Scanlan et al., 2002; Calarese et al., 2003). Since cross-linking does not influence glycan conformation and flexibility, binding of this mAb should not be influenced by cross-linking and serves as a

loading control in this assay. Indeed, binding indices for this mAb are around 1 (mean = 1.01) showing equal loading of modified and unmodified protein.

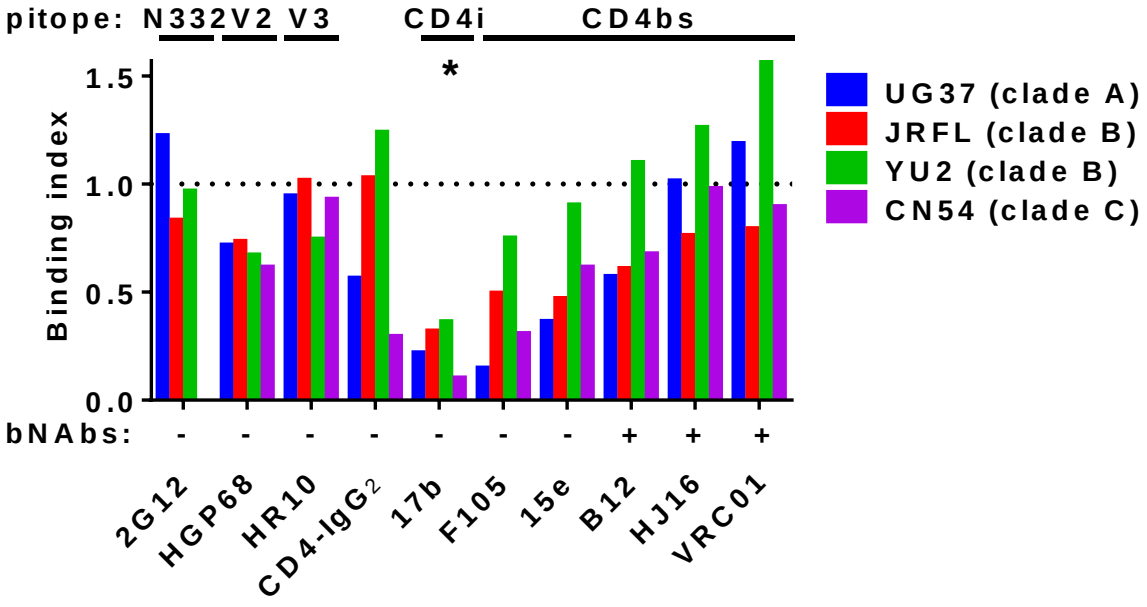

Fig. 3.9: ELISA analysis of cross-linked gp140s from multiple strains. The indicated gp140 proteins were cross-linked and binding of a panel of mAbs was analysed by ELISA. Epitopes are indicated above the bars. mAb 2G12 does not bind to isolate CN54 and no binding index could be determined. * $p < 0.05$ in a Kruskal Wallis test.

One possible explanation of the differential effects of mAb recognition of different epitopes might be steric hindrance of binding of mAbs to modification sites. To investigate this, an analysis of the distribution of lysine residues, which are the primary modification sites (Hopwood et al., 1970), was conducted. Crystal structures of a few of the mAbs tested here are available. Mapping of CN54 lysines onto these structures showed no obvious correlation of lysine residues located within epitopes and reduced mAb binding (Fig. 3.10). By contrast, bNmAb VRC01 forms direct contacts with two lysine residues and still shows no reduced binding in ELISA (Fig. 3.10). On the other hand, CD4 itself as well as CD4i mAb 17b and CD4bs mAb F105 contact only one lysine residue yet they show dramatically

reduced binding to cross-linked gp140 (Fig. 3.10). Thus, cross-linking effects cannot be explained by the positioning of modification sites.

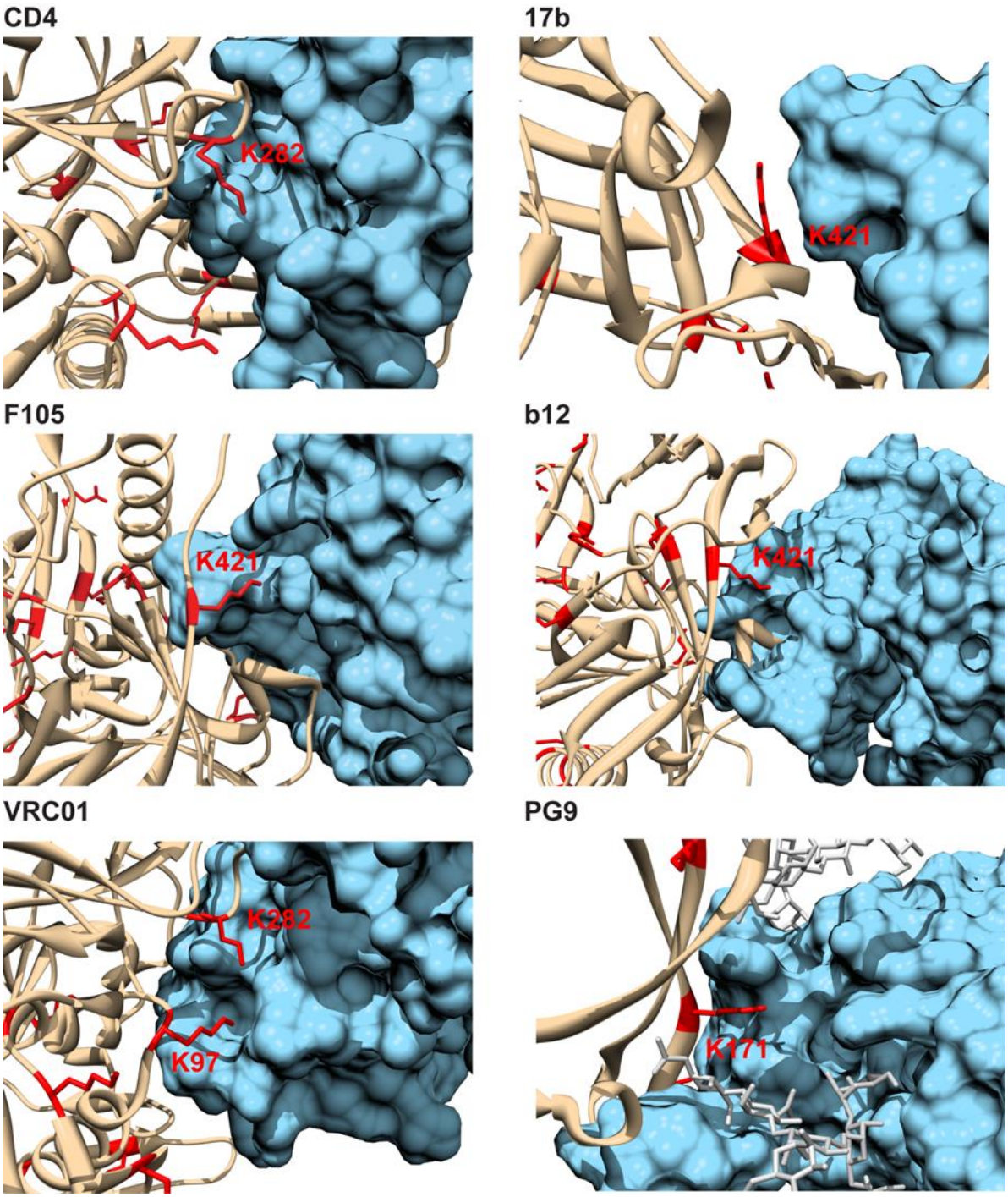

Fig. 3.10: Modification sites within mAb epitopes. Ribbon representations of published crystal structures of gp120 or gp120 fragments (fawn) are displayed in complex with surface representations of CD4 or mAbs as indicated (blue). Lysine residues are highlighted in red and residue numbers of lysine residues interacting with mAbs are labelled according to HXB2 numbering. PG9 interacts with a second lysine of UG37 (K168), which is shielded from view by PG9 in this orientation. This figure was first published in the Journal of Virology (Schiffner et al., 2013a).

To further investigate the cause of the observed selective reductions of antigenicity upon cross-linking, gp140 was cross-linked before or after incubation with soluble CD4. Subsequently, binding of CD4i mAb 17b was analysed by SPR (Fig. 3.11). Whereas binding of 17b was undetectable if cross-linking was performed in absence of sCD4, binding was partially restored if the gp140 was pre-complexed with sCD4 before cross-linking (Fig. 3.11), suggesting that effects of cross-linking were at least in part caused by inhibition of conformational changes. Taken together, these data suggest that differential alterations in antigenicity upon cross-linking are caused by conformational restrictions rather than steric hindrance.

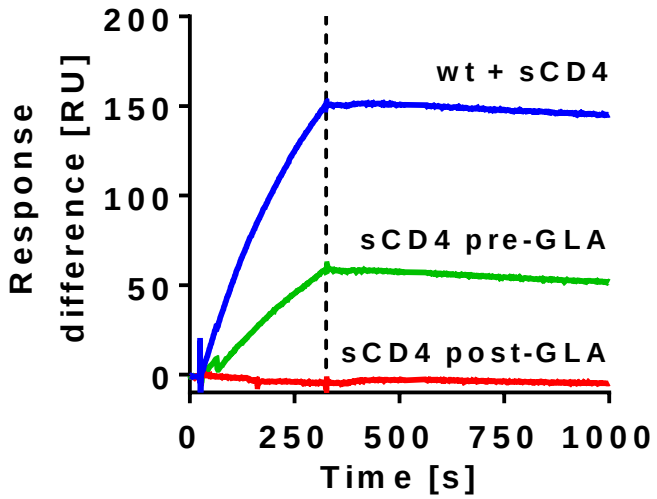

Fig. 3.11: Antigenicity of the CD4i epitope upon cross-linking in presence or absence of sCD4. sCD4 was added to CN54 gp140 either before (pre-GLA) or after (post-GLA) cross-linking as indicated. SPR traces are shown for unmodified or cross-linked CN54 gp140 binding to the CD4i MAb 17b. The dotted vertical line indicates the end of the injection.

In summary, cross-linking leads to the covalent preservation of the target proteins' oligomeric state and leads to selective loss of binding of non-neutralising CD4bs antibodies whilst preserving binding of bNmAbs.

3.2.3 Immunogenicity of GLA cross-linked UG37 gp140 in guinea pigs

The selective loss of binding of non-neutralising antibodies described above raises the possibility that immunisation with cross-linked gp140 might induce more potent neutralising antibody responses compared to unmodified glycoprotein since competition from non-neutralising antibody responses will be reduced. To test this hypothesis, guinea pigs (n=4 per group) were immunised with a preparation of unmodified or cross-linked UG37 gp140 characterised above (Fig. 3.5 and Fig. 3.9). This glycoprotein was a mixture of monomeric, dimeric and trimeric gp140s with a typical reduction of binding of non-neutralising CD4bs mAbs upon cross-linking (Fig. 3.5 and Fig. 3.9).

Three immunisations of unmodified or cross-linked glycoprotein were administered at 4 week intervals using a combination of the adjuvants carbopol (1%) and MF59 (Lai et al., 2012). Both groups developed very strong binding IgG antibody responses (> 10^6; Fig. 3.12). No significant differences between the groups immunised with unmodified or cross-linked gp140 were detected. However, sera from both groups showed stronger binding to unmodified gp140 than GLA treated gp140 (both $p < 0.001$). Thus, even sera from animals immunised with GLA-modified gp140 were better able to recognise unmodified protein.

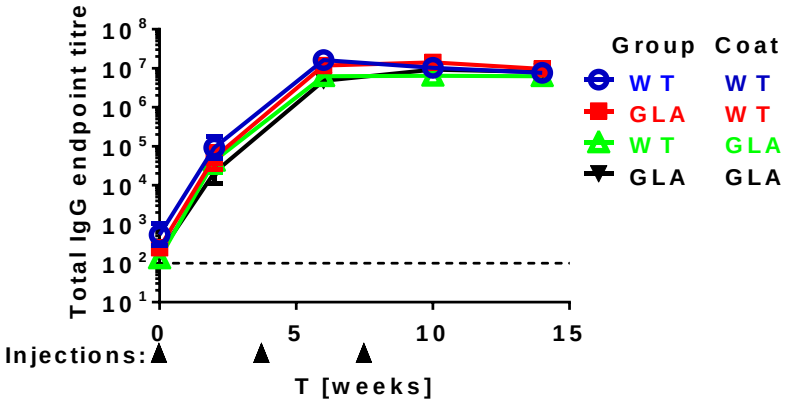

Fig. 3.12: Binding antibody responses of guinea pigs immunised with cross-linked gp140. Animals (n=4 per group) were immunised with unmodified (WT) or cross-linked (GLA) UG37

gp140. Total IgG endpoint titres were determined by ELISA coating with either unmodified (WT) or cross-linked (GLA) material as indicated. Error bards indicate SD of tested animals.

Next, epitope mapping was performed by cross-competition with a panel of well-characterised mAbs covering the major epitopes of Env. Strong cross-competition was detected against epitopes around the CD4bs, the V3 loop and regions of gp41 (Fig. 3.13). Only weak responses against the V2 loop, the N332 glycan-dependent epitope and the CD4i epitopes were detected. Epitope mapping showed no statistically significant differences between animals immunised with unmodified or cross-linked material although a trend towards reduced gp41-specific responses was apparent (p=0.097). However, it should be noted that with only 4 animals per group this study was relatively weakly powered.

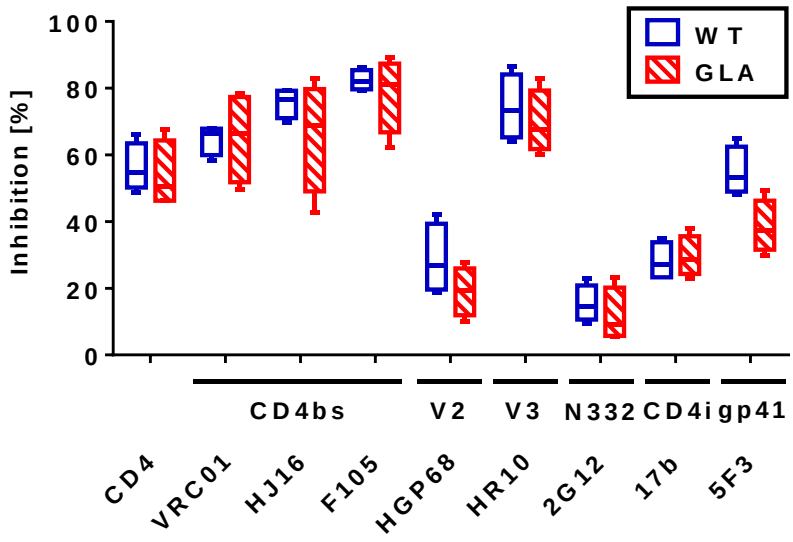

Fig. 3.13: Epitope mapping of antibody responses induced by cross-linked UG37 gp140. Sera from guinea pigs immunised with unmodified (WT) or cross-linked (GLA) animals were analysed by cross-competition ELISA with indicated mAbs. No statistically significant differences between the two groups were found in a 2-way ANOVA.

A number of studies have shown that binding antibodies are not necessarily able to neutralise the virus (discussed in the introduction chapter). Thus, pseudovirus neutralisation assays can be performed which have been shown to better correlate with

the ability of antibodies to prevent infection in the SHIV model (Burton et al., 2011). The guinea pig sera were subjected to the standardised TZM-bl assay as well as the more sensitive A3R5 assay (Fig. 3.14). All sera were able to neutralise sensitive tier 1 isolates from different clades as well as the homologous UG37 pseudo-virus in the TZM-bl assay (Fig. 3.14 A). In addition, neutralisation of partially neutralisation-resistant (tier 2) viruses was detected in the more sensitive A3R5 assay (Fig. 3.14 B). However, no difference in neutralisation potency was detected between the two groups for any virus nor in the magnitude-breadth analysis (Huang et al., 2009) of pooled data.

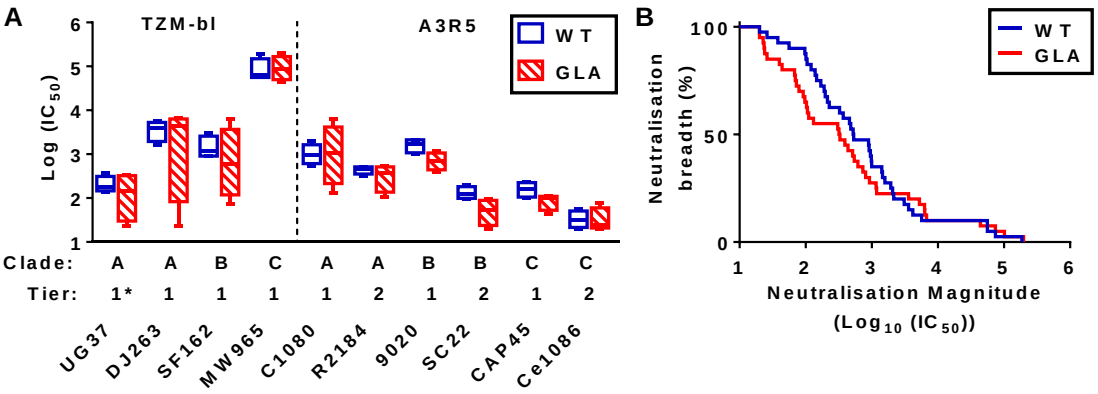

Fig. 3.14: Neutralisation breadth and potency of animals immunised with cross-linked UG37 gp140. A: Sera from guinea pigs immunised with unmodified (WT) or cross-linked (GLA) UG37 gp140 were analysed for their neutralisation potency in the TZM-bl or A3R5 assay as indicated. The general neutralisation sensitivity (tier) and clade of the (pseudo-) viruses are indicated underneath the graph. **B:** Pooled data are displayed as a magnitude-breadth curve. * Isolate UG37 is classified as tier 1 here as it is homologous to the immunogen.

In summary, both unmodified and cross-linked UG37 gp140 induced strong binding responses in guinea pigs and sera were able to neutralise sensitive (tier 1) pseudoviruses. However, no functional differences between the two groups were detected in binding antibody titres, epitope utilisation or neutralisation activity.

3.2.4 **Immunogenicity of GLA cross-linked CN54 gp140 in rabbits**

To further investigate the immunogenicity of cross-linked gp140, rabbits (n=8 per group) were immunised with unmodified or GLA-treated CN54 gp140. In contrast to the UG37 gp140, this glycoprotein was largely trimeric with minor amounts of dimer as well as aggregate apparent in PAGE analysis (Fig. 3.5). This protein was already extensively characterised above (Fig. 3.6, Fig. 3.7, Fig. 3.8, Fig. 3.9 and Fig. 3.11) and upon cross-linking showed typical reduction in antigenicity of non-neutralising CD4bs mAbs, CD4i mAbs as well as some V2 mAbs.

Unmodified or cross-linked gp140 were administered in an extended schedule with immunisations at week 0, 6, 12 and 22 formulated in either 1% carbopol (week 0 and 6) or 1 mg PEI (week 12 and 22). Overall binding antibody responses against CN54 gp140 were indistinguishable between the two groups at any time point (Fig. 3.15A). To further analyse overall binding antibody responses, binding to cell-surface expressed Env was tested by FACS. At the final time-point (week 24), animals immunised with GLA-treated gp140 showed significantly increased ($p < 0.01$) binding to heterologous ZM54 gp150 in this assay (Fig. 3.15B). No increased binding was detected in pre-immune sera (data not shown).

To examine whether GLA-specific responses were induced, an unrelated protein (HEL) was cross-linked and residual binding to this protein was examined by ELISA. No difference in binding between the two groups was detected ($p=0.91$, Fig. 3.15C) indicating the absence of anti GLA-responses.

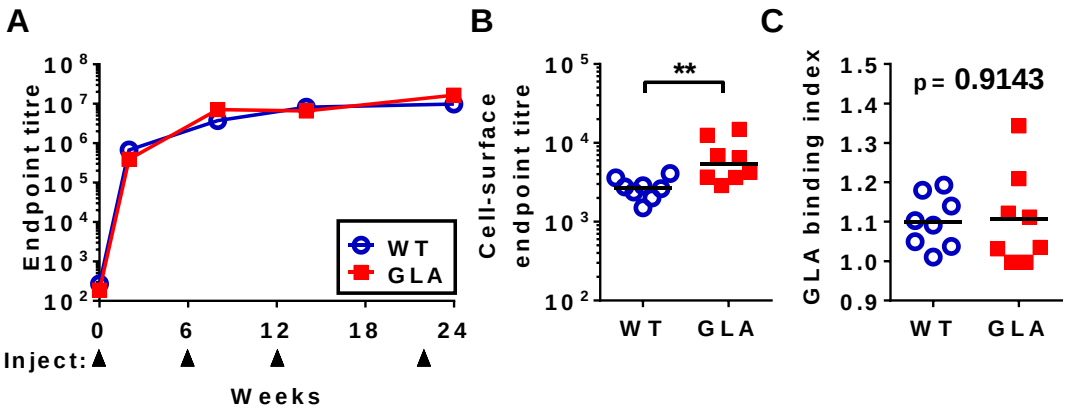

Fig. 3.15: Binding antibody responses induced by cross-linked CN54 gp140. Total IgG endpoint titres of sera from New Zealand White rabbits (n=8 per group) immunised with unmodified (WT) or GLA cross-linked (GLA) were detected by ELISA (**A, C**) or cell-based ELISA (**B**). **A:** CN54 gp140-specific total IgG endpoint titres showed no significant differences at any time point (one-way ANOVA of log-transformed data with Bonferroni's post-test). Time points of immunisations are indicated underneath the graph. **B:** Binding of week 24 sera to cell surface expressed heterologous ZM53 Env was analysed by FACS. ** P<0.01 according to a t test of log-transformed data. **C:** Binding of sera to a GLA cross-linked or unmodified irrelevant protein (HEL) was analysed for week 24 sera, and results are expressed as an index of binding to GLA-treated/untreated HEL. Student's t test was performed for statistical analysis.

To analyse the epitope utilisation in these animals, peptide array analysis (Pepscan) was performed. In this assay, binding of sera to 15-mer overlapping (by 14 AA) CN54 peptides covering the whole length of gp140 were analysed for 3 randomly selected sera plus the highest binder from each group. All sera showed strong responses to the V3 region in this assay, although responses in the GLA group were slightly stronger (p= 0.0045; Fig. 3.16). Large differences in antibody recognition were detected in the C1 and V1V2 regions where animals from the GLA group showed significantly stronger responses (p = 0.0005 and P = 0.0293 respectively). By contrast, cross-linking reduced the responses directed towards linear epitopes in the immunodominant region of gp41 (p = 0.0169). Similar results were

obtained when sera were tested against peptides from a range of heterologous strains (data not shown).

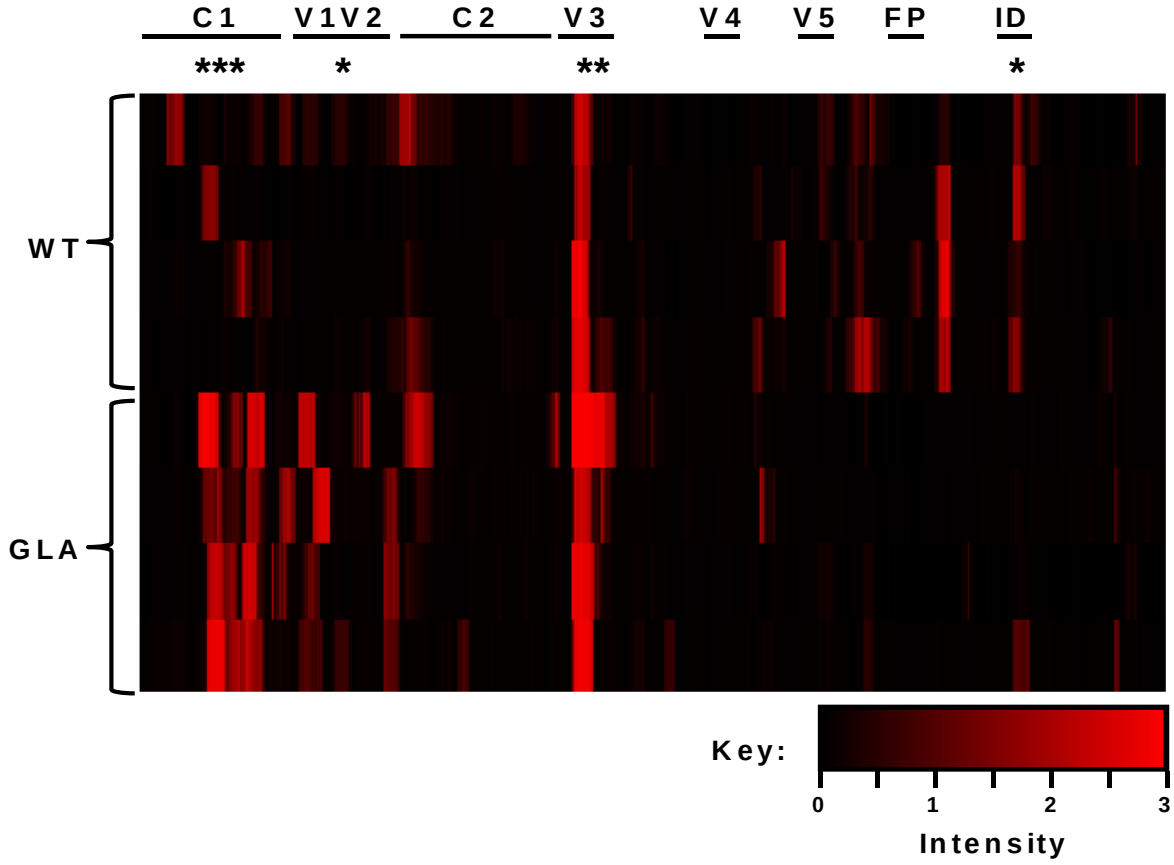

Fig. 3.16: Peptide array analysis of week 24 sera from rabbits immunised with GLA-treated or unmodified CN54 gp140. The binding intensity is plotted in arbitrary units. Pre-defined regions of gp140 are marked at the top. Statistical analysis for individual regions was performed by one-way ANOVA with Bonferroni's post-test. * $p < 0.05$; ** $p < 0.01$; *** $p < 0.001$.

Since peptide arrays are only able to detect responses towards linear epitopes, antibody cross-competition analysis was performed to analyse conformation-dependent epitopes. In this assay, sera from animals immunised with cross-linked gp140 competed significantly stronger with soluble CD4 (CD4-IgG2) and CD4bs bNmAb VRC01 ($p = 0.0006$ and $p = 0.012$ respectively) compared to sera from the WT group (Fig. 3.17A). By contrast, responses to the HR1 regions of gp41 were significantly reduced in the GLA group, in line with the results from the peptide array (Fig. 3.16) as well as the (non-significant) trend seen in the guinea pigs immunised with UG37 gp140 (Fig. 3.13).

To confirm the induction of increased antibody titres targeting the CD4bs in the GLA group, three more assays were conducted. First, binding of sera to gp120 carrying a point mutation (D368R) that abolishes binding of many CD4bs mAbs was compared to binding to the wildtype protein (Fig. 3.17B). Significantly increased sensitivity to this mutation was found in the GLA group compared to the WT group ($p = 0.0011$). Second, binding to an engineered outer domain of gp120 was analysed which lacks the inner domain, bridging sheet and the V3 loop and therefore almost exclusively displays the CD4bs (Pejchal et al., 2011; Jardine et al., 2013). Binding to this probe was significantly ($p = 0.021$) higher in the GLA group (Fig. 3.17C). Finally, an RSC3 CD4bs assay was performed in which binding to a core gp120 which is resurfaced with SIV residues is measured after pre-incubation with and in presence of a mutant glycoprotein carrying knockout mutations in the CD4bs (Wu et al., 2010). In this assay, the GLA group showed on average 3-fold increased CD4bs reactivity although this trend did not reach statistical significance (Fig. 3.17D).

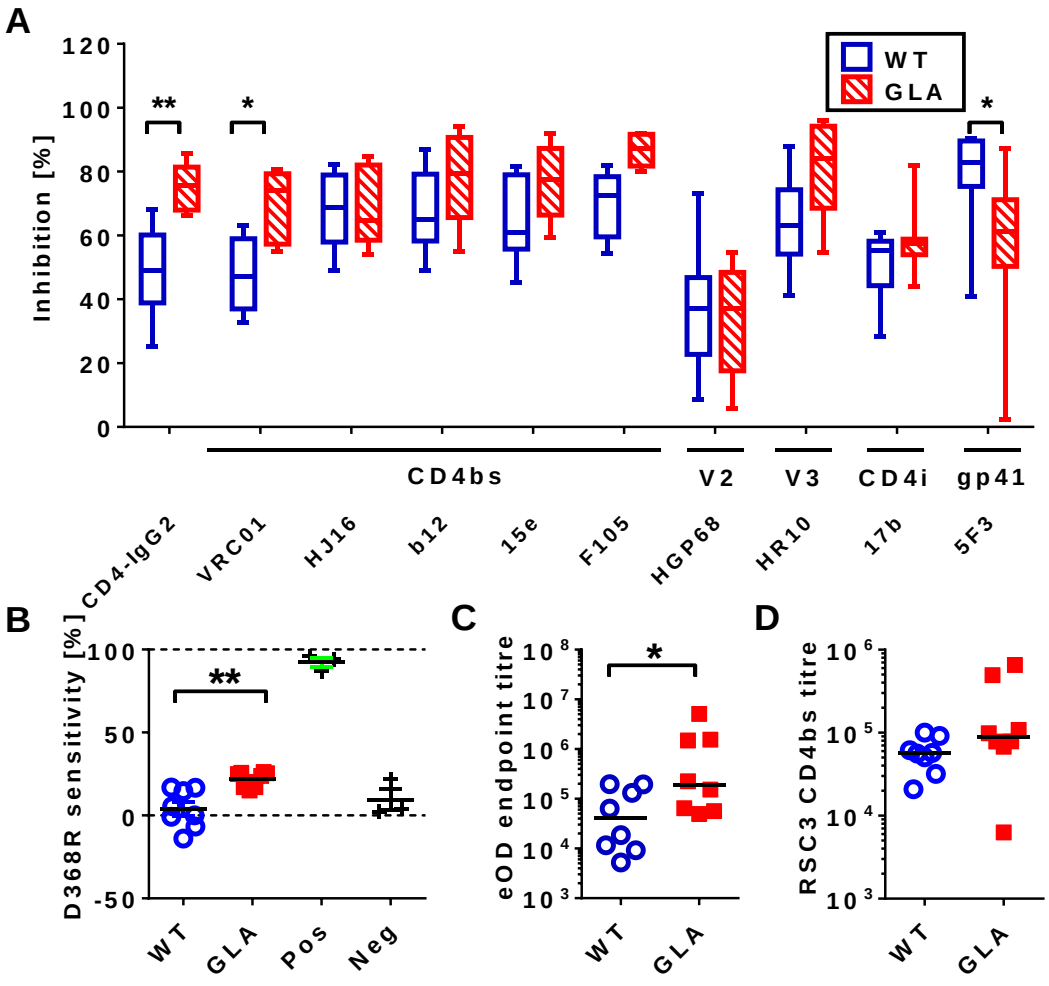

Fig. 3.17: Mapping of antibody responses towards conformational epitopes in week 24 sera from rabbits immunised with GLA-treated or unmodified CN54 gp140. A: Cross-competition ELISA of sera against a panel of human mAbs against Env. **B:** Sensitivity of sera to a CD4bs knockout mutation (D368R) as measured by ELISA. Pos, panel of CD4bs mAbs; Neg, panel of non-CD4bs MAbs. **C:** Endpoint titres against an engineered variable-loop deleted outer domain of Env. **D:** Binding of sera to the CD4bs probe RSC3 was measured after pre-incubation of sera with an excess of competing RSC3 Δ371I/P363N CD4bs knockout protein. A one-way ANOVA with Bonferroni's post-test (**A**), a Student's t test (**B**), and a Student's t test of log-transformed data (**C** and **D**) were used for statistical analysis. * $p < 0.05$; ** $p < 0.01$; *** $p < 0.001$.

To test how these changes in epitope recognition affect the neutralisation activity of the sera, neutralisation assays were performed as before. Neutralisation of sensitive tier 1 but not tier 2 isolates was detected in the TZM-bl assay (Fig. 3.18 and data not shown). Sera from animals immunised with cross-linked gp140 showed significantly increased neutralisation of a number of isolates in this assay (Fig. 3.18A). In the more sensitive A3R5

assay, neutralisation of more neutralisation resistant tier 2 isolates was observed. In this assay differences between the two groups were generally smaller and only reached statistical significance for one tier 1 isolate (Fig. 3.18A). Taking all data from this time-point together in a single magnitude-breadth analysis, animals immunised with cross-linked CN54 gp140 showed significantly ($p = 0.0016$) increased neutralising activity compared to the control group (Fig. 3.18B) at week 24. It should be noted though that at week 14, no difference in neutralisation was detected between the two groups for any viral isolate tested (data not shown) nor in the over-all magnitude-breadth analysis (Fig. 3.18B). Therefore, extended immunisation regimens may be required to bring out the observed differences in immunogenicity.

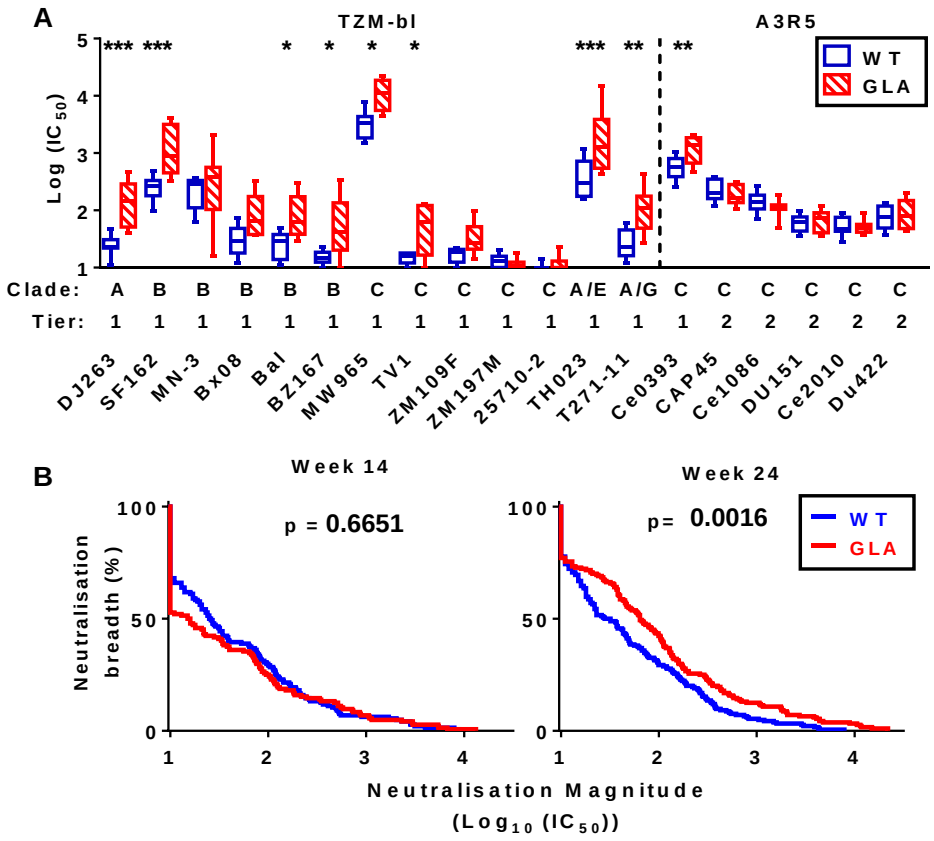

Fig. 3.18: Neutralising activity induced by cross-linked CN54 gp140. A: Neutralisation of sera from animals immunised with unmodified (WT) or cross-linked (GLA) gp140 was tested in the TZM-bl assay against tier 1 viruses (left) and in the more sensitive A3R5 assay against tier 2 viruses (right). **B:** Magnitude-breadth curves are shown for pooled data from all animal sera from both assays for the indicated time-points. A two-way ANOVA of log-transformed data with

Sidak's post-test (**A**) and a Mantel-Cox log-rank test (**B**) were used for statistical analysis. * $p < 0.05$; ** $p < 0.01$; *** $p < 0.001$.

Neutralisation of tier 1 viruses by polyclonal sera is often due to their sensitivity to V3-loop directed antibodies. To investigate whether the increased neutralisation potency shown above was due to the stronger V3-loop responses seen in the peptide array, additional neutralisation assays were performed with sera pre-incubated in the presence of an excess of V3 loop peptide. Compared to scrambled peptide or PBS only, neutralising responses were substantially reduced under V3-loop adsorbing conditions (Fig. 3.19 A and C). However, the GLA group still showed significantly enhanced responses even under V3-loop adsorbing conditions, indicating that the difference between groups was not due to V3-loop directed antibody responses (Fig. 3.19 A). Similarly, the loss-of-binding upon V3-loop depletion was not significantly different between the two groups (Fig. 3.19 C).

To investigate whether the difference in binding was due to CD4bs-directed antibody responses, a neutralisation assay was performed in which CD4bs directed responses were depleted with the CD4bs probe RSC3 or the matching negative-control ΔRSC3. To increase the signal-to-noise ratio, V3-peptide depletion was included in all conditions. Under CD4bs depleting conditions, no significant difference ($p= 0.73$) was detected between the two groups (Fig. 3.19 B). By contrast, neutralisation in the GLA group was significantly ($p = 0.022$) increased in the negative control reaction using ΔRSC3. In line with these results, the inhibition of RSC3 depletion compared with ΔRSC3 was significantly ($p = 0.0076$) increased in the GLA group. Thus, the increased neutralising activity induced by immunisation with cross-linked gp140 seems to be mediated, at least in part, by CD4bs specific antibodies.

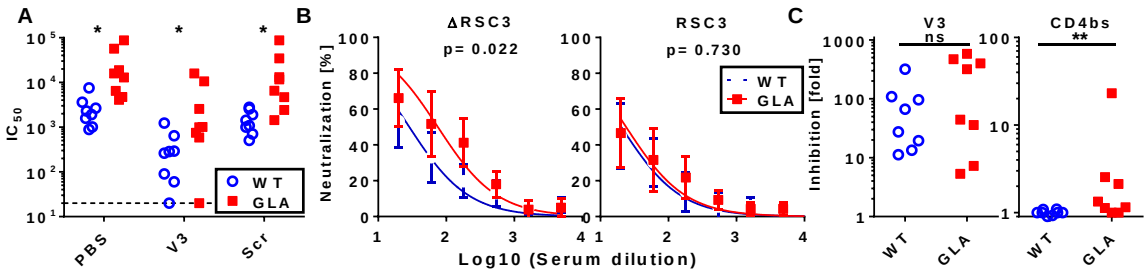

Fig. 3.19: Mapping of week 24 neutralising responses. A: Neutralisation of strain MW965 pseudovirus was measure after pre-incubation with and in the presence of V3 peptide (V3), scrambled peptide control (Scr), or PBS alone in TZM-bl cells. **B:** Neutralisation curves of MW965 in the presence of V3 peptide plus either the CD4bs probe RSC3 or the corresponding negative control, ΔRSC3. Curves show averages of all animals from the two groups. **C:** Inhibition of neutralising activity is shown as the ratio IC_{50} (no inhibitor)/IC_{50} (inhibitor). A curve-comparison F test (**B**) and a Mann-Whitney test **(C)** were used for statistical analysis. ** $p < 0.01$.

In conclusion, cross-linking of gp140 leads to a selective loss of binding of non-neutralising antibodies, in particular those targeting the CD4bs. Immunisation with trimeric cross-linked CN54 gp140 leads to the induction of more potent neutralising responses in rabbits which are at least in part due to CD4bs-specific antibodies.

3.3 Discussion

The GLA-mediated chemical cross-linking optimised here mediated covalent fixation of trimeric gp140 constructs. The conditions chosen (7.5 mM GLA for 5 min at RT) led to selective reduction in binding of some non-neutralising mAbs whilst maintaining binding of all bNmAbs tested. Aggregate accumulation was detected but further analysis showed that cross-linking did not induce the formation of such aggregates but rather covalently fixed the oligomeric state of the source material. It should be noted though, that under the chosen conditions covalent trimer fixation was not complete (see Fig. 3.5). Instead the

chosen conditions offered optimal knock-down of binding of non-neutralising CD4bs mAbs such as F105 with minimal impact on binding of CD4bs bNmAbs.

The data presented here confirm earlier reports on the effects of Env cross-linking on antibody recognition and extend it to include newly discovered CD4bs bNmAbs VRC01 and HJ16. An explanation for the differential behaviour of non-neutralising vs. neutralising CD4bs mAbs might lie in the 'conformational masking' of this epitope. According to the theory proposed by Kwong et al. (2002), the CD4bs epitope can exist in a range of different conformations. Broadly neutralising antibodies targeting this epitope are able to recognise most or all conformations whereas non-neutralising antibodies only bind to a small subset of these conformations (Kwong et al., 2002). The data presented in this chapter support this theory as the newly identified broad and potent CD4bs bNmAbs are generally unaffected by cross-linking whereas a number of non-neutralising CD4bs mAbs are unable to bind the GLA-treated material efficiently. Potential steric hindrance imposed by cross-linking adducts cannot fully account for the differential effects since primary modification sites can be found with the epitopes of both neutralising and non-neutralising antibodies. On the other hand, experiments in which sCD4 was added to gp140 before or after cross-linking showed increased binding of CD4i mAb 17b if cross-linking was performed in presence of sCD4, suggesting an involvement of conformational effects (Fig. 3.11).

The selective changes of antigenicity induced by cross-linking led to the hypothesis that cross-linked gp140 might be able to preferentially present neutralising epitopes to the immune system which might lead to the induction of more broadly and/or potently neutralising responses. In addition, covalent preservation of the trimeric state might induce

positive avidity effects and the presentation of immunodominant epitopes within the trimer interface might be reduced. Furthermore, in the setting of human immunisation, scavenging by CD4-expressing cells as well as the exposure of CD4-induced epitopes might be reduced. However, due to the lack of compatible CD4, the animal models used here would be predicted to be unsuitable to investigate the latter two effects.

Immunisation of guinea pigs with modified UG37 gp140 showed no differences in immunogenicity between unmodified or GLA-treated material in any of the assays conducted. By contrast, GLA-treated CN54 gp140 induced remarkably different antibody responses in rabbits compared to unmodified protein. In the rabbits, the overall magnitude of antibody responses was indistinguishable between the two groups, indicating a redirection of antibody responses rather than increased responses of the same type (Fig. 3.15). This hypothesis is supported by data from the peptide array, which showed remarkable differences in recognition of linear epitopes with increased responses in the GLA group towards N-terminal regions such as C1 and V1V2 but decreased responses to C-terminal regions including the immunodominant region of gp41 (Fig. 3.16). Furthermore, epitope mapping by cross-competition showed increased responses to the CD4bs in the GLA group whereas gp41-specific responses were reduced (Fig. 3.17). Taken together these data strongly support the hypothesis of a redirection of antibody responses.

The increased responses directed to the V1V2 loop which were detected in the peptide array might be of particular interest in light of the results from the RV144 clinical trial (Haynes et al., 2012b; Tomaras et al., 2013). In this trial, reduced risk of infection was correlated with binding antibody responses towards the V1V2 loop and although the

causality of this effect is still under investigation, induction of higher titres of V1V2-directed responses might be a beneficial effect of an HIV-1 vaccine (Haynes et al., 2012a; Karasavvas et al., 2012; Rolland et al., 2012; Zolla-Pazner et al., 2013; Yates et al., 2014).

Increased cross-competition with a soluble CD4 construct and CD4bs bNmAb VRC01 was detected in rabbits immunised with GLA-treated CN54 gp140 during the epitope mapping analysis (Fig. 3.17). A number of other CD4bs mAbs (b12, 15e and F105) showed similar trends but did not reach statistical significance. However, cross-competition data on its own should not be considered definitive, since this assay only examines whether the mAb probe and its competitor are able to bind the target protein simultaneously. Therefore, cross-competition with a CD4bs bNmAb such as VRC01 does not indicate that the competing probe must contain VRC01-like antibodies. In fact, the probe and the competitor do not even have to target the same epitope, as cross-competition can occur as long as any part of the antibodies clashes, but this does not necessarily have to be at the 'footprint' of the mAb. For example, it is known that CD4bs mAbs can compete with C1 directed mAbs (Moore and Sodroski, 1996). Therefore, in this study, 3 additional assays measuring CD4bs specific responses were performed to confirm the results from the cross-competition analysis (Fig. 3.17). All assays showed a trend towards increased CD4bs responses although this trend did not reach statistical significance in one of the assays. Nevertheless, taken together these data strongly indicate increased CD4bs specific antibody responses in the GLA group.

CD4bs directed antibodies are amongst the most broadly and potently neutralising responses discovered to date (Fig. 1.10). However, as described in Chapter 1, not all CD4bs

directed antibodies are neutralising. Thus, neutralising assays as well as epitope mapping of neutralising responses were conducted with the sera from rabbits immunised with GLA-treated or unmodified gp140. At the final time point, neutralising responses, in particular against tier 1 viruses, were significantly higher in the GLA group. Although strong responses could be mapped to the V3 loop, the difference between the two groups was not caused by these responses. On the other hand, CD4bs-directed responses, despite being lower in overall neutralisation magnitude than the V3-loop responses (Fig. 3.19C), were responsible for at least part of the increased neutralising responses detected in the GLA group. The induction of neutralising CD4bs-specific responses is generally considered a beneficial attribute of an HIV vaccine since the CD4bs is well conserved between isolates and even different clades (Kong and Sattentau, 2012; Schiffner et al., 2013b). However, the increased responses found here were limited to neutralisation-sensitive tier 1 isolates. A possible explanation for this might be a sterically less confined conformation of these isolates compared to more common tier 2 isolates, which might impede access of CD4bs antibodies due to angle-of-approach restrictions (Chen et al., 2009a).

It is surprising how different the results from the two animal experiments presented here were since one showed no effect of cross-linking on immunogenicity whatsoever, whereas the other one showed measurable differences in most assays. Unfortunately, the experiments were too different to determine with certainty the root of this discrepancy. Differences in experimental setup include different animal species, number of animals, viral strains, adjuvants, immunisation schedule and oligomeric properties of the immunogen. The main reason for these extensive differences were administrative rather than designed. In fact, the guinea pig experiment used an experimental setup to assess the cross-linking

approach in the context of a pre-optimised immunisation regimen that was planned to be subsequently tested in macaques. However, the presence of large quantities of monomer and dimer in the UG37 gp140 preparation was worrisome and thus the rabbit immunisations were performed in parallel using strain CN54 gp140 (which is more trimeric than the UG37 preparation) in combination with an adjuvant combination and extended immunisation schedule which was shown to be superior to the standard protocols (data not shown). Considering the number of differences between the studies, it is not possible to identify the cause of the different outcome of the experiments. At the time of the experiments, and even before any results were available, the presence of monomer and dimer in the UG37 preparation was the major concern. However, subsequent results with 'next-generation' trimers have casted doubt whether this was the major issue (see chapters 5 and 8 for a detailed discussion).

Given the striking differences in the peptide array conducted on the rabbit sera, performing a similar analysis on the guinea pig sera might be the easiest way to investigate whether refocusing of antibody responses did occur in the latter study as well. In addition, one should bear in mind that no significant differences in neutralisation were detected in the rabbit group sera after 3 immunisations, which most closely matches the final time-point from the guinea pig study. Increased neutralisation in the rabbit study was only measured after 4 immunisations (at week 24), long after the guinea pig study had been terminated. Therefore, it cannot be ruled out that a similar effect might have taken place if the guinea pigs had received another protein boost. However, differences in CD4bs recognition were already detected after 3 immunisations in the rabbit study – but not in the guinea pig study (data not shown). Given the kinetic of the appearance of differences between groups in the

rabbit study after the third immunisation, it is possible that the adjuvant (PEI) used for the third and fourth injection in this study might have played a role. In addition, animal species can have an effect on the induction of neutralising antibodies. In particular, rodents such as guinea pigs often have very short CDR-H3 regions (Johnson and Wu, 1998), whereas many neutralising HIV-1 antibodies have very long CDR-H3 regions (Breden et al., 2011) thus making guinea pigs a less useful animal model for HIV-1 vaccine trials (Borggren et al., 2013). However, further experiments would be required to understand the mechanism underlying the distinct outcomes of these two studies.

It has been shown in a number of studies that the gp140 glycoproteins used here are not recognised by quaternary specific mAbs such as PG9 or PGT145 (McLellan et al., 2011; Walker et al., 2011b; Klein et al., 2012a). This indicates that the molecules do not display the correct quaternary conformation found on functional Env. Furthermore, aggregates and dimers could be detected even in the CN54 gp140 preparation. A possible way to improve the immunogenicity of cross-linked Env might be the use of better mimics of native trimeric envelope spikes. Furthermore, cross-linking with non-saturating concentrations of glutaraldehyde are expected to lead to stochastic adduct formation. Therefore, other cross-linking agents might be better suitable to preserve the quaternary structure of native Env whilst reducing the binding of non-neutralising mAbs, without altering binding of bNmAbs. In the following chapters, cross-linking improved Env constructs and further optimisation of cross-linking methods are investigated.

In summary, cross-linking of gp140 leads to selective reduction in binding of non-neutralising antibodies whilst maintaining broadly neutralising epitopes. Immunisations

with such fixed immunogens can lead to the induction of more potent NAb responses. Although the observed neutralisation of tier 1 isolates is not in itself novel, the fact that a simple, quick, cheap and safe treatment of gp140 leads to increased stability and improved immunogenicity clearly merits further investigation.

Chapter 4: Chemical cross-linking of membrane-expressed Env

4.1 Introduction

A number of quaternary epitope specific antibodies that are able to bind functional Env trimers expressed on virions or the cell-surface, but do not bind to incorrectly folded forms of Env such as uncleaved trimers or monomeric gp120, have been discovered to date (Walker et al., 2009; Bonsignori et al., 2011; Pejchal et al., 2011; Klein et al., 2012a; Ringe et al., 2013; Falkowska et al., 2014). These antibodies can be separated into the PG9-like bNmAbs including PG9, PG16, PGT145 and CH01, which recognise a glycan-dependent epitope on the V1V2 loop, the 3BC176-like bNmAbs including 3BC176 and 3BC315, which bind to an epitope on the V3 loop that is exposed upon CD4 engagement, and the PGT151-like class of bNmAbs, which bind an epitope spanning both gp120 and gp41 (Walker et al., 2009; Bonsignori et al., 2011; Pejchal et al., 2011; Walker et al., 2011b; Klein et al., 2012a; Ringe et al., 2013; Falkowska et al., 2014). The discovery of these quaternary specific bNmAbs not only helped identify new sites of vulnerability on HIV-1 Env but also provided new tools for the development and characterisation of Env mimetics.

The inability of quaternary specific mAbs to bind most soluble gp140 constructs demonstrates that these gp140s do not display the correct quaternary fold found on functional envelope spikes (Walker et al., 2009; Bonsignori et al., 2011; Pejchal et al., 2011; Walker et al., 2011b; Klein et al., 2012a; Ringe et al., 2013; Falkowska et al., 2014). Thus, during the first years of this thesis, membrane-expressed Env constructs were the only source of correctly folded Env trimers. However, Env complexes are considered to be relatively fragile (recently reviewed in Sattentau, 2014) and thus chemical fixation of the spike might be required to prevent misfolding. As shown in chapter 3, chemical cross-linking might have additional beneficial properties such as preventing the binding of non-

neutralising mAbs and improving the induction of neutralising antibodies *in vivo*. Building on these results, it was hypothesised that in case of correctly folded Env trimers, the exposure of non-neutralising epitopes might be prevented by chemical fixation, thus further increasing the benefits of cross-linking.

In this chapter, the effects of cross-linking of membrane-anchored native Env spikes are investigated. Subsequently, a strategy is devised to use detergent solubilisation of cross-linked Env from the membrane of mammalian cells, followed by immuno-affinity purification using a quaternary epitope specific PG9-like bNmAb, to obtain natively folded Env.

4.2 Results

4.2.1 Cross-linking of cell-surface expressed Env

To test the effects of cross-linking on membrane-expressed Env, transient transfection experiments in HEK-293T cells were performed that analysed mAb recognition of membrane anchored Env with or without cross-linking. However, GLA cross-linking led to the induction of high levels of fluorescence, even in the absence of any antibody staining (Fig. 4.1). Baseline fluorescence increased by over 100-fold in all channels preventing a direct comparison between GLA-treated and unmodified cells. Attempts to decrease the induced fluorescence by using different quenching reagents or chemically reducing the cross-linker after completion of the reaction failed to restore fluorescence to baseline levels (Table 4-1). Thus, analysis of GLA cross-linking effects by flow cytometry was not possible.

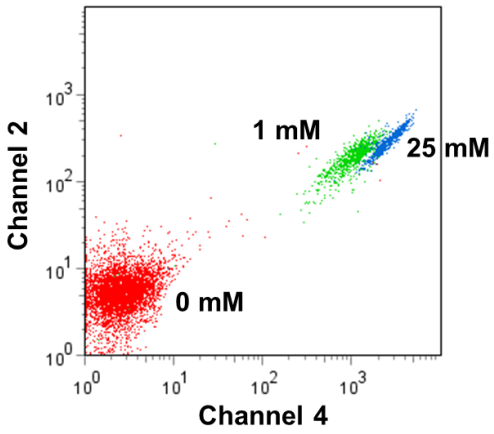

Fig. 4.1: Cross-linking induced fluorescence of HEK-293T cells. Unmodified HEK-293T cells were lifted, cross-linked with the indicated concentrations of GLA and analysed by flow cytometry.

Table 4-1: Mean fluorescence intensity of glutaraldehyde treated cells quenched with different stopping reagents

Substance	-	Glycine	Tris pH 6.8	Trypan blue	$NaBH_4$
0 mM GLA	9.87	10.01	10.48	10.72	9.9
0.1 mM GLA	28.44	54.79	55.68	29.79	21.24
25 mM GLA	100.66	147.61	142.18	106.52	73.47

Since GLA cross-linking was incompatible with flow cytometry, formaldehyde (FA) was used as a cross-linker instead. FA did not affect fluorescence of the cells (compare curves C1 and C2 in Fig. 4.3A). Initially, cross-linking conditions had to be optimised for this cross-linker. Titrations of FA were performed on 293T cells transiently transfected with recombinant Env and the effect on antibody binding was determined by flow cytometry. At a concentration 10 % FA, binding of non-neutralising mAbs 17b (CD4i) and F105 (CD4bs) was almost completely abolished whereas binding of the CD4bs bNmAb VRC01 was mostly preserved (Fig. 4.2). Thus, this FA concentration was chosen for FA cross-linking of cell-surface expressed Env.

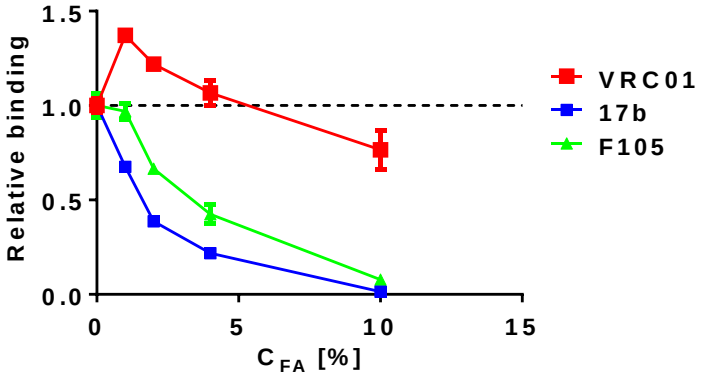

Fig. 4.2: Titration series of formaldehyde. 293T cells were transiently transfected with JRFL Env and cross-linked with the indicated concentrations of FA. Binding of mAbs was assessed by flow cytometry and normalised to the binding of each mAb to unmodified cells.

After finding suitable cross-linking conditions, a larger panel of mAbs was titrated onto cross-linked cells, building on the preliminary results from Fig 4.2. In accordance with the previous results, binding of non-neutralising mAbs 17b and F105 was reduced by over 80 % by fixation (Fig. 4.3). In contrast, binding of three CD4bs bNmAbs was less affected (approx. 20 % reduction for HJ16 and VRC01; Fig. 4.3).

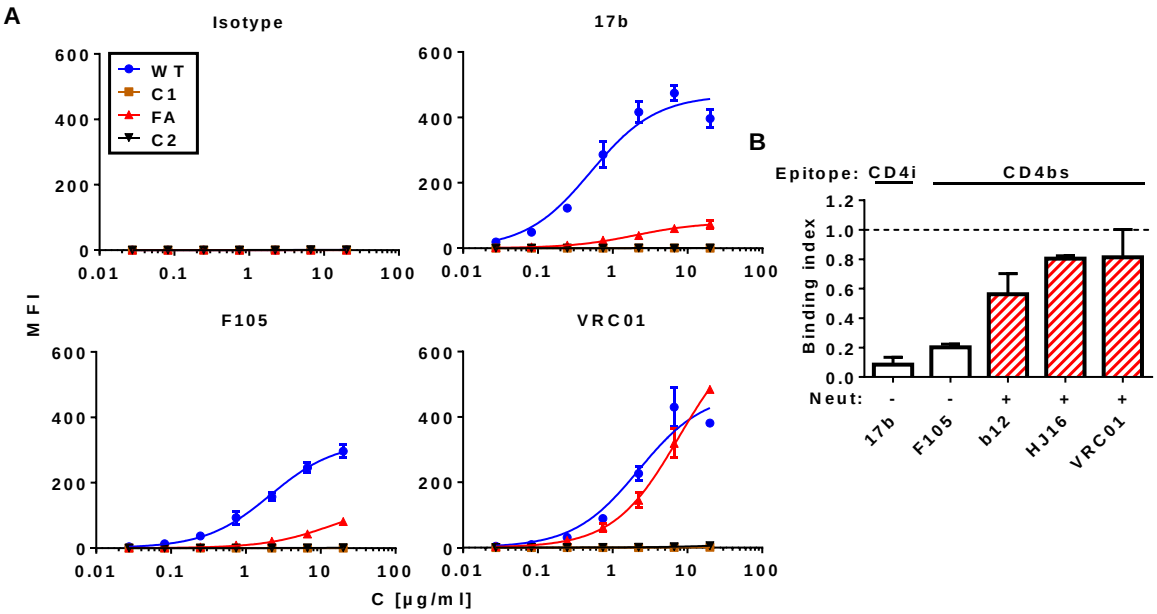

Fig. 4.3: Effects of FA cross-linking on antibody binding. 293T cells were transiently transfected with Env (JRFL SOSIP gp160ΔCT), cross-linked, stained with titration series of the indicated mAbs and analysed by flow cytometry. **A:** Representative binding curves are shown for selected mAbs. Error bars indicate SD of replicate

wells. WT: unmodified Env-expressing cells; FA: Env-expressing cells cross-linked with 10 % FA. C1 and C2: unmodified (C1) or FA-treated (C2) cells expressing negative control protein. **B:** Pooled data are shown for all mAbs tested. Binding indices were calculated as AUC (cross-linked)/AUC (unmodified). Error bars indicate SD of three independent experiments.

The flow cytometry assay described above was not suitable for high throughput analyses. To overcome this issue, a cell-based ELISA (CELISA) assay was adapted from Haim et al. (2009). This had the additional advantage of not relying on fluorescence as a readout, thus allowing the assessment of GLA cross-linking. However, preliminary data showed that the assay was less sensitive than flow cytometry and generated larger errors (compare error bars in Fig. 4.3 and Fig. 4.5). To increase the signal-to-noise ratio, a comparison of expression levels of different Envelope proteins was performed by flow cytometry. The highest binding of polyclonal anti Env probe HIVIG was detected using an Env construct of strain UG37 with the cytoplasmic tail of gp41 truncated (ΔCT; Fig. 4.4). Therefore this strain was selected for future experiments with membrane-expressed Env.

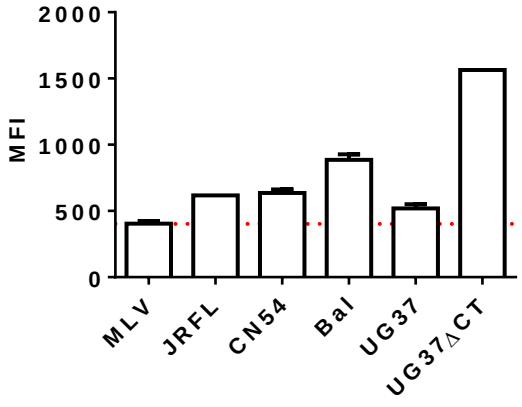

Fig. 4.4: Comparison of expression levels of different *env* genes. HEK-293T cells were transiently transfected with plasmids encoding Env proteins of the indicated HIV-1 strains or negative control murine leukemia virus (MLV). Binding of polyclonal serum HIVIG was detected by flow cytometry.

After finding a highly expressing Env construct, the CELISA method was optimised for detection of cross-linking of Env and under the final conditions showed good agreement with results from FACS (data not shown). Using this assay, GLA cross-linking could be analysed since horseradish peroxidase generated luminescence was used as a read-out rather than fluorescence (Fig. 4.5). In this assay, binding of non-neutralising mAbs 17b and F105 was almost completely abolished by GLA cross-linking. In contrast, binding of all bNmAbs tested was indistinguishable in both GLA cross-linked (red) and unmodified cells (blue) (Fig. 4.5). Importantly, this included the quaternary specific bNmAb PG9 (Fig. 4.5), which only binds to correctly folded functional Env trimers (Walker et al., 2009).

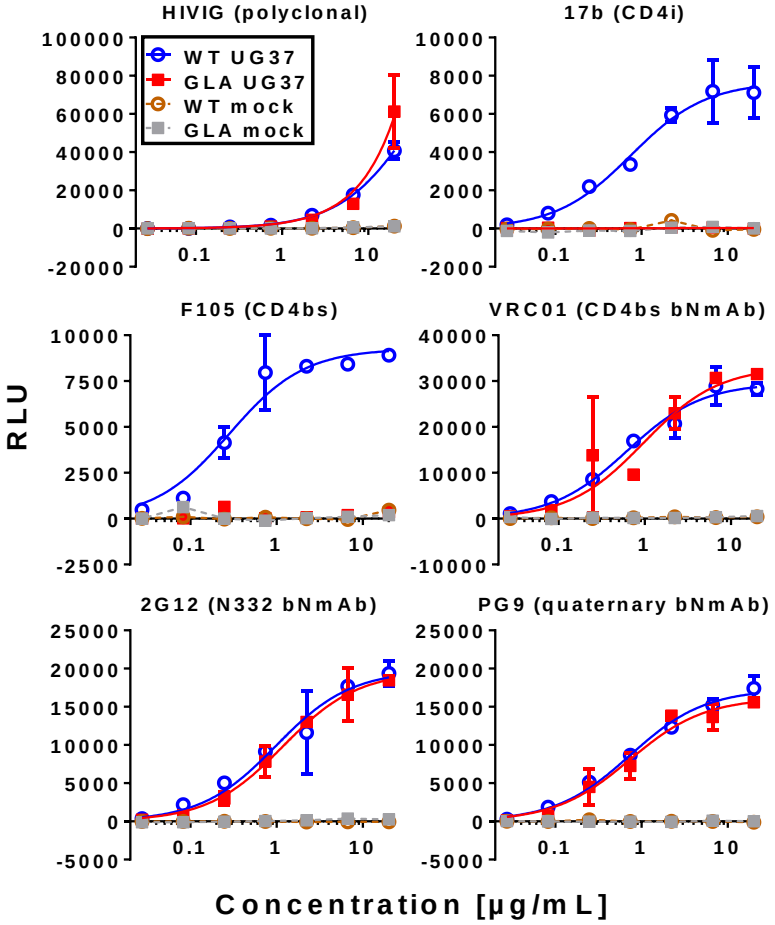

Fig. 4.5: Antigenicity of GLA cross-linked Env. Representative titration series of mAbs (epitopes indicated in brackets) are shown for HEK293-A cells transiently transfected with either UG37 gp160ΔCT or control protein (mock) as indicated. Antibody binding to unmodified (WT) or

cross-linked (GLA) cells was analysed by CELISA. Lines indicate results of the non-linear fit if available. Error bars indicate SD of replicate wells.

In conclusion, cross-linking of Env with either GLA or FA resulted in reduced binding of non-neutralising CD4bs and CD4i mAbs whereas binding of bNmAbs as well as the quaternary structure of the trimer were retained.

4.2.2 **Extraction of Env from the cell membrane**

After establishing the feasibility of cross-linking of membrane-bound envelope spikes, it was hypothesised that purified cross-linked Env might exclusively display neutralising epitopes to the immune system thus leading to the induction of neutralising antibodies. Furthermore, cross-linking might over-come stability problems normally encountered when extracting gp160 from membranes. Therefore, attempts were made to extract the protein from the membrane by detergent solubilisation.

Env was transiently expressed in HEK-293T cells and solubilisation of cross-linked trimer was attempted using the detergent Triton X-100 (Triton). The amount of gp120 extracted from the cells was measured by capture ELISA. In this experiment, very low concentrations of gp120 (< 2.2-2.3 ng/ml) were extracted (Fig. 4.6A). In contrast, concentrations of ~20 ng/ml were achieved in the absence of cross-linking (Fig. 4.6A). Thus, it seems as if cross-linking prevents membrane extraction and therefore conditions were sought that allowed the gentle solubilisation of Env without disturbing the quaternary conformation of the trimer.

In an initial test, two detergents Triton X-100 (Triton) and CHAPS showed the highest amounts of solubilised Env (data not shown). To test the ability of these detergents to solubilise intact Env, they were titrated onto UG37 Env-expressing HEK-293T cells. After a 4 hour incubation (rotating at 4 °C), capture ELISA assays were performed, in which gp120-specific D7324 was used as a capture antibody. The detecting antibody was either the polyclonal antibody HIVIG or gp41 specific mAbs 5F3 and 2F5. Soluble UG37 gp140 was used as a positive control in this assay.

Efficient Env extraction required detergent concentrations of at least the critical micelle concentration (CMC) but further increases of detergent concentrations had only minor effects on protein concentrations in the supernatant (Fig. 4.6B). Using HIVIG as the detection antibody, Triton was able to extract almost twice as much total Env from the membrane compared to CHAPS, suggestive of a higher concentration of gp120 in the supernatant (Fig. 4.6B). However, when capturing with a gp120-specific probe and detecting with gp41-binding mAbs the protein concentrations detected were almost identical between the two detergents. Based on these results, CHAPS-extracted protein seemed to contain larger proportions of intact complexes of gp120 and gp41 and was thus chosen for further experiments.

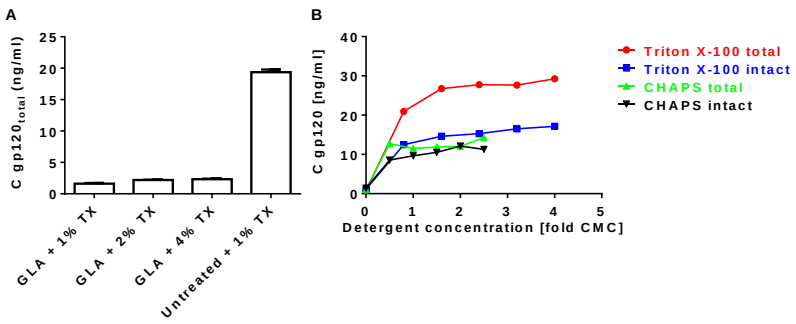

Fig. 4.6: Detergent extraction of Env. UG37 gp160ΔCT was transiently expressed on HEK-293T cells and Env was extracted by incubation with the indicated concentrations of detergents

Triton X-100 (Triton; CMC = 0.2-0.9 mM) or CHAPS (CMC = 6 mM). Concentrations of extracted proteins were measured by capture ELISA using D7324 as the capture mAb. Detection of overall extracted protein (total) was achieved with polyclonal serum (HIVIG), detection of intact Env was achieved using gp41-specific mAbs 5F3 and 2F5. **A:** Cells were cross-linked with GLA before membrane-extraction (GLA) or left untreated. Error bars indicate SD of technical repeats.

After establishing suitable detergent extraction conditions, the feasibility of immuno-affinity purification of solubilised Env was assessed in a small-scale immuno-precipitation experiment. UG37 Env was extracted from transiently transfected HEK-293T cells with CHAPS and subsequently cross-linked with GLA. Immuno-precipitations were performed by incubation with protein A coupled to agarose beads and polyclonal serum (HIVIG), irrelevant control antibody or quaternary conformation specific bNmAb PG9. Bound protein was analysed by Western blot (Fig. 4.7). While the irrelevant control mAb was unable to pull down any detectable Env, several bands were detected in samples precipitated with polyclonal serum or PG9 (Fig. 4.7). Molecular weight analysis indicated an approximate size of ~88 kDa and ~495 kDa for the two most prominent bands in the PG9 precipitated samples. These sizes correlate with the expected sizes for a gp41ΔCT trimer **(**expected size: ~87 kDa) and a gp160 trimer (expected size: ~450 kDa) respectively.

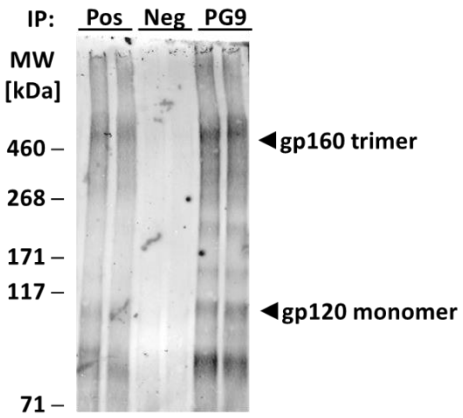

Fig. 4.7: Immuno-precipitation of membrane-extracted Env by quaternary specific bNmAb PG9. UG37 gp160ΔCT was transiently expressed in HEK-293T cells and extracted with 16 mM CHAPS. Clarified supernatants were cross-linked with GLA and incubated with pooled serum from HIV-infected patients (HIVIG; Pos), irrelevant control antibody human anti-human CD8 (Neg) or quaternary conformation specific bNmAb PG9. Antibodies were precipitated with agarose-coupled protein A and precipitates were analysed by Western blot using a mAb cocktail

consisting of HGN194, HR10, HGP68, VRC01, 5F3, 2F5, 4E10 and 2G12. Separate lanes show results from technical repeats.

Taken together, these data show that Env can be extracted from cellular membranes and be enriched by immuno-affinity purification using quaternary specific bNmAbs.

Membrane-protein purification generally leads to relatively low protein concentrations and thus the generation of stable cell lines is usually required to obtain sufficient protein quantities (Chaudhary et al., 2012). Before establishing stable cell lines, suitable Env proteins were selected based on available literature (McLellan et al., 2011). A small panel of Env proteins was selected consisting of strains that were not bound by quaternary specific bNmAb PG16 in a monomeric gp120 format despite a very high neutralisation sensitivity of the corresponding pseudovirus (McLellan et al., 2011).

It is well known that truncation of the cytoplasmic tail of gp160 increases its expression levels (Mao et al., 2012). Thus, stop-codons were introduced into the genes of selected strains by site-directed mutagenesis to generate truncations of gp41 directly after the transmembrane domain. These mutations led to increased expression levels in all strains tested, as expected (data not shown). To test correct folding of the truncated protein, pseudoviruses were generated using each Env both with and without the tail truncation. In each case, the titres of pseudoviruses were very similar for both full-length and tail-truncated Envs, but showed large variations between different strains (data not shown). In addition, neutralisation by a panel of bNmAbs was very similar in the tail truncation mutant (lower panel) compared to the full-length protein (top panel) (Fig. 4.8). Differences in neutralisation were only detected for MPER bNmAb 10E8 which showed a trend towards

increased neutralised against tail-truncated Env. Most importantly, neutralisation by quaternary epitope specific bNmAb PG9 was not affected by the tail truncation (Fig. 4.8).

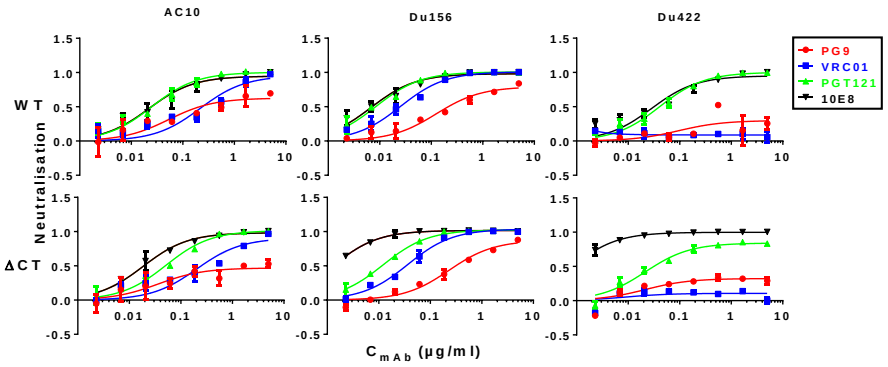

Fig. 4.8: Comparison of the neutralisation sensitivity of full-length and ΔCT Env bearing pseudoviruses. Pseudoviruses were generated bearing full-length (WT) or tail-truncated (ΔCT) Envs. Neutralisation curves from a TZM-bl assay are shown for a panel of bNmAbs. Error bars indicate SD of replicate wells.

Based on these results, strains AC10 (clade B) and Du156 (clade C) were selected and stable cell lines constitutively expressing both WT and ΔCT Envs were established in HEK-293S GnT-I$^{-/-}$ cells (see discussion for choice of cell line). Both AC10 and Du156 were isolated from acutely infected patients approximately 4 weeks after infection. Both strains display all currently known broadly neutralising epitopes and are neutralised by quaternary epitope-specific bNmAb PG16 at IC_{50}s < 0.023 µg/ml whilst the corresponding monomeric gp120 is not being recognised by the same bNmAb (McLellan et al., 2011).

Next, the purification of the extracted protein by lectin affinity chromatography was tested using a GNL column which recognises mannose residues. Supernatant containing extracted Du156 gp160ΔCT was flowed over the column and bound protein was eluted using α-D-mannopyranoside. Analysis by Western blot revealed the presence of Env in the input supernatant and after passing through the GNL column, the Env concentration in the flow

through was reduced by ~70 %. Subsequent elution with α-D-mannopyranoside yielded fractions enriched for Env thus demonstrating successful purification of gp120.

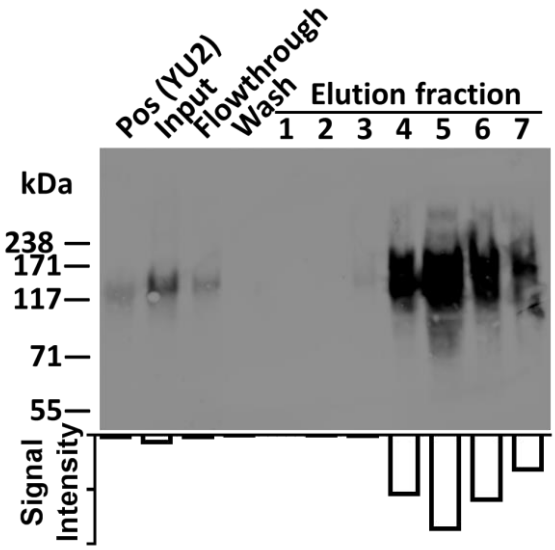

Fig. 4.9: Lectin affinity purification of Du156 gp160ΔCT. Du156 Env was extracted from stably transfected HEK-293S cells. Clarified supernatants (input) were passed through a lectin column, followed by washing and elution with excess α-D-mannopyranoside. Aliquots from the inputs, column flowthrough, washing solution and elution fractions 1-7 were analysed by Western blot using a cocktail of anti Env mAbs. YU2 gp120 was included as a positive control. Signal intensity of DyLight 800 conjugated secondary antibody was quantified on a licor Odyssey fluorescence reader and is shown underneath the graph in arbitrary units.

Antigenicity of the purified Env was tested by SPR. Strong interactions with the quaternary specific bNmAbs PGT145 and 3BC176 and CD4bs mAb F105 were detected (Fig. 4.10). Binding to the CD4bs bNmAb VRC01 was weak but still detectable. Overall these data demonstrate that membrane-extraction and lectin purification of Env yields antigenically intact envelope trimers that are recognised by two different quaternary specific bNmAbs.

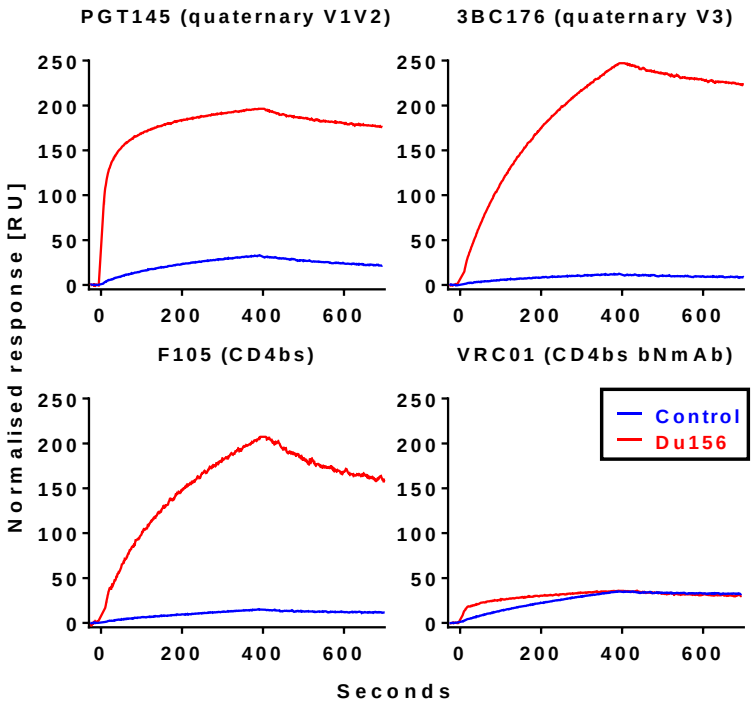

Fig. 4.10: SPR analysis of membrane extracted lectin-purified Du156 Env. Indicated mAbs were captured onto an anti-human IgG-coated SPR chip. Membrane extracted Du156 gp160ΔCT (20-fold diluted fraction 5 from figure Fig. 4.9) was floated over the surface for 400 seconds followed by a 300 second dissociation period. BG505 SOSIP.664 (described in Chapter 5) was used as a positive control.

To assess the purity of the extracted purified membrane protein, protein-containing fractions from the lectin purification were pooled and concentrated under buffer exchange and subjected to reducing, denaturing SDS-PAGE (Fig. 4.11). Coomassie staining showed several bands over a range of different sizes (Fig. 4.11 lane 1). Upon cross-linking of the membrane protein prior to gel electrophoresis, the protein migrated as a single major band of approximately 460 kDa, which is consistent with the expected size of trimeric Env (Fig. 4.11 lane 2). In addition, a smear covering a range of other molecular weights was apparent.

Taken together, these data show that membrane-extracted gp160ΔCT can be purified by lectin affinity chromatography yielding antigenically intact, predominantly trimeric Env.

Following lectin purification, PGT145 affinity purification was performed to remove remaining impurities and select functional Env spikes since PGT145 recognises a quaternary epitope only present on correctly folded Env trimers (Walker et al., 2011b). Unmodified Du156 Env purified in this manner migrated predominantly as a band of approximately 120 kDa as well as a smaller band of ~30 kDa, consistent with monomeric gp120 and gp41 stumps respectively (Fig. 4.11). Surprisingly, a band of ~450 kDa was also visible. Extensive analytical cross-linking (15 mM GLA, 30 min) of the sample yielded predominantly high molecular weight material, migrating at sizes consistent with trimeric Env (~450 kDa) and, to a lesser extent, aggregates thereof.

Standard cross-linking (7.5 mM GLA, 5 min) of lectin-purified Du156 Env followed by PGT145 purification resulted in extraction of predominantly trimeric protein with some monomeric gp120 present in a reducing/denaturing SDS-PAGE analysis (Fig. 4.11). Similar results were obtained using Env from the AC10 strain (Fig. 4.11).

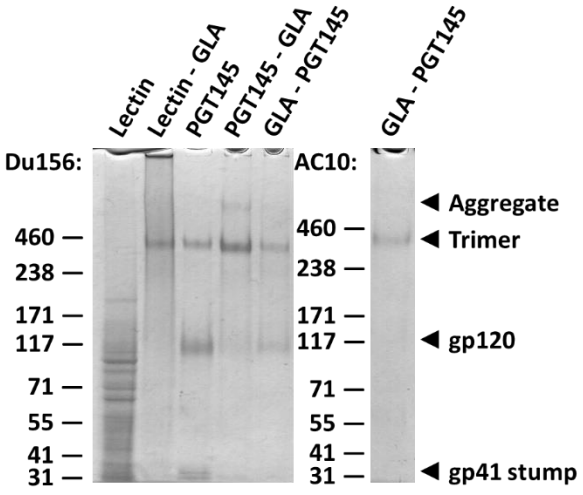

Fig. 4.11: SDS-PAGE analysis of purified gp160ΔCT. Membrane extracted Env was subjected to lectin affinity chromatography and separated by SDS-PAGE without (Lectin) or with analytical GLA fixation (Lectin - GLA). Lectin eluates were further purified using a PGT145 column and fractionated without (PGT145) or with analytical GLA fixation (PGT145 – GLA). Alternatively, standard GLA fixation was performed on lectin purified material prior to PGT145 purification

(GLA – PGT145). SDS-PAGE analysis was performed on all samples from the Du156 strain (left) as well as the final eluates from the AC10 strain (right).

Protein levels recovered from the PGT145 column were very low (50 – 70 µg per litre of cell culture media) allowing only a limited analysis of antigenicity. The largest amounts of protein were obtained for GLA cross-linked Du156 and thus this preparation was analysed by SPR. The GLA-treated next-generation trimer BG505 (described in detail in chapter 5) was used as a control in this experiment (Fig. 4.12). Du156 showed strong binding to the CD4bs bNmAb VRC01, equal to the levels obtained with control trimer BG505. At the same time, binding to the non-neutralising CD4bs mAb F105 was undetectable (Fig. 4.12). Surprisingly, binding to the quaternary specific bNmAb PGT145 was low although this antibody was used for protein purification. However, a strong interaction of Du156 with an independent quaternary bNmAb (3BC176) was detected. In fact, this interaction was much stronger than the binding of 3BC176 to control protein BG505, confirming the correct folding of the Env spike.

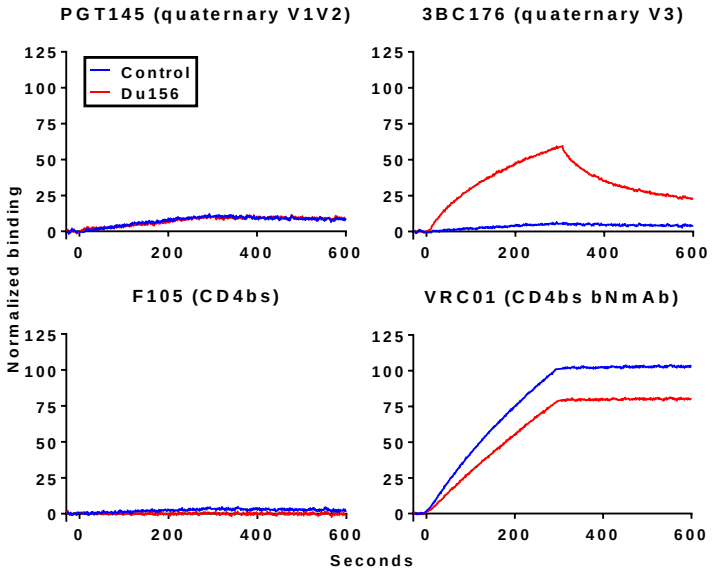

Fig. 4.12: SPR analysis of GLA cross-linked Du156 Env. Indicated mAbs were captured onto an anti-human IgG-coated SPR chip. Equal concentrations of GLA-treated PGT145 purified Du156 or GLA-treated control protein BG505 SOSIP.664 (described in chapter 5) were floated over the

surface for 300 seconds followed by a 300 second dissociation period. Responses were normalised by double referencing followed by normalisation to mAb capture levels.

To directly investigate the folding of the proteins, cryo-EM analysis was performed (Fig. 4.13). In this analysis, all samples investigated showed some correctly folded 'native-like' Env. The highest proportions (30.6 %) of correctly folded trimers were observed for GLA cross-linked Du156 Env. In the absence of cross-linking only 23.6 % native-like trimers were observed for this strain, whilst a larger proportion was monomeric. Yields of correctly folded trimers were lower for strain AC10 (12.2 %). In both cross-linked samples, a large proportion of proteins formed dimers of trimers, consistent with the results from the SDS-PAGE analysis (Fig. 4.11).

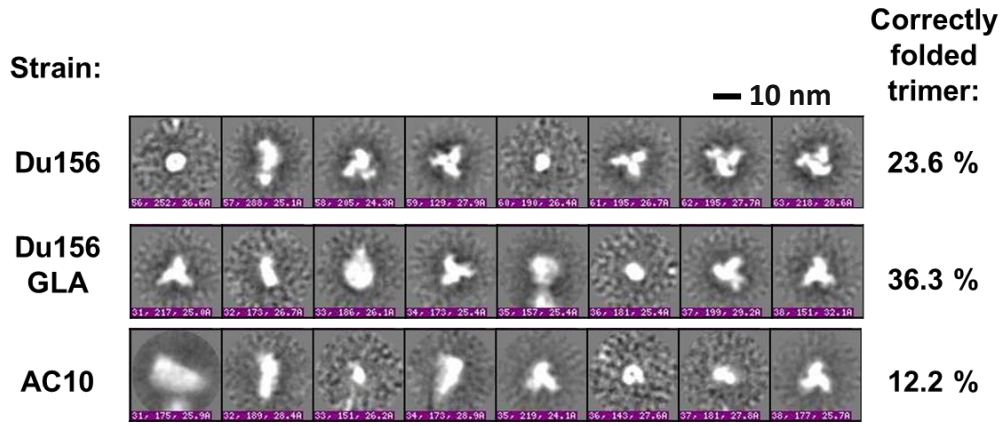

Fig. 4.13: Cryo-EM analysis of membrane-extracted PGT145-purified Env. Representative class averages are shown with the respective proportions of correctly folded 'native-like' Envs indicated.

Taken together, these data show that membrane-expressed Env can be extracted from the membrane and purified without abolishing the quaternary conformation of the protein. Cross-linking followed by purification with a quaternary specific epitope yields predominantly covalently stabilised, trimeric Env that partially retains the correct quaternary conformation of functional Env spikes.

4.3 Discussion

In this chapter, the effects of chemical cross-linking on membrane-bound Env were analysed. Initial experiments showed that the cross-linker GLA was not compatible with analysis by FACS and thus preliminary data were collected using an alternative cross-linker (FA). The data from these experiments showed a selective loss of binding of non-neutralising mAbs whilst binding of all bNmAbs tested was preserved.

After obtaining these encouraging initial results, cell-based ELISAs were adapted to allow the investigation of cross-linking. This assay had two major advantages compared to the previous FACS experiments: it was compatible with GLA cross-linking and allowed a much higher throughput. Experimental compatibility with GLA cross-linking was achieved by using HRP-generated luminescence as a readout rather than fluorescence. The combination of HRP-generated luminescence instead of the colorimetric readouts used in conventional ELISAs also avoided bias of the optical density due to cells or cellular debris, and in combination with modern Western blot reagents can achieve very high sensitivity. The drawbacks of CELISA are a relatively high backgrounds and significant well-to-well variation. However, by using a highly expressing Env protein and a titration series of each mAb, with each concentration tested in triplicate, overall errors were reduced to acceptable levels. A further issue arose when using this assay to compare cross-linked and unmodified cells since the latter tended to be washed out of the wells during the assay procedure. Conditions were optimised to minimise this source of error, by using very gentle buffer conditions (DMEM + 10% FCS for all extended incubation steps) and a very strongly adherent cell line (HEK-293A). The comparable binding curves of the glycan specific bNmAb 2G12 for unmodified and cross-linked cells (Fig. 4.5) as well as microscopic inspection of

the wells at the end of the experiment (data not shown) suggest that these conditions led to equal cell numbers under both conditions.

Using the CELISA assay, GLA cross-linking of Env could be analysed. The final data showed a lack of binding of non-neutralising mAbs to cross-linked Env while binding of bNmAbs was unchanged. In addition, the finding that binding of the quaternary specific bNmAb PG9 was unaffected after cross-linking suggests that cross-linking did not compromise the overall fold of the Env trimer.

Based on these results, it was hypothesised that immunisation with cross-linked native-like trimers might exclusively present neutralising epitopes to the immune system and thus lead to the induction of NAbs. Thus, a strategy was devised to purify correctly folded trimers using a quaternary specific bNmAb such as PG9 or PGT145. Since transfected cells or conventional virus-like particles generally present several copies of Env, immunisation with these would theoretically display both functional and non-functional conformations of Env, the latter containing a range of potentially immunodominant non-neutralising epitopes. Therefore, a strategy using membrane-extraction of Env was designed to separate correctly folded from aberrant forms of Env. In theory, detergent solubilisation should create predominantly monodispersed Env complexes although it cannot be ruled out that other host cell proteins or even additional Env complexes might be embedded in the same detergent micelle as an Env spike.

For any strategy relying on the isolation of Env by quaternary-specific mAbs to succeed, a mAb was required that was able to robustly distinguish between correctly and incorrectly

folded species but does not induce conformational changes. At the time this project was started, three such antibodies were known (PG9, PG16 and PGT145) all of which recognise a glycan-dependent quaternary epitope in the V1V2 loop. It has been suggested that PG9 is less stringent in recognising quaternary conformations than for example PG16 and thus it is not the ideal antibody to extract exclusively correctly folded trimers (McLellan et al., 2011). In some instances, PGT145 is even more dependent on quaternary conformation than PG16, making it an ideal choice for the selection of quaternary structures (Sanders et al., 2013). Little is known about the conformational changes induced by this class of antibodies. However, in the few instances where entropic changes upon the interaction of PG9-like bNmAb with Env have been analysed, little or no changes in entropy have been detected (Julien et al., 2013b; Sanders et al., 2013; Blattner et al., 2014).

The extent to which PG9-like bNmAbs rely on quaternary attributes to bind varies greatly between different strains of HIV-1 (McLellan et al., 2011). Thus, strains were sought that fulfilled the following conditions:

- Very high sensitivity to neutralisation by PG9-like bNmAbs;
- No binding of PG9-like mAbs to gp120;
- Correct formation of all broadly neutralising epitopes;
- High expression levels on transfected cells;
- Transmitted/founder virus or early isolate from acute phase of infection.

Among these requirements, the first two are the most crucial since the isolation of correctly folded Env by PG9-like antibodies can only succeed if these mAbs show a strong preference for the correctly folded trimers over aberrant forms. The expression of all major neutralising epitopes is important during immunisation when these epitopes should be

presented to the immune system. Since purification of membrane proteins in mammalian cells generally produces relatively low yields, the selection of highly expressed strains is important to allow the production of sufficient quantities of protein (Chaudhary et al., 2012). Finally, in case of antigenic differences between acute and chronic viruses, immunisation with transmitted/founder or early acute viruses might induce responses towards more relevant strains than chronic isolates (Liao et al., 2013b).

A search of available literature resulted in the identification of four strains which fulfilled the most crucial of these parameters, namely a high neutralisation sensitivity to PG9-like bNmAbs coupled with undetectable binding of the corresponding monomeric gp120 to PG16 (McLellan et al., 2011). Of these four strains, AC10 and Du156 were neutralised by bNmAbs targeting all common broadly neutralising epitopes and fulfil the three most important conditions. However, neither is a transmitted/founder virus as both were isolated around 4 weeks post infection, thus representing acute infection isolates.

Expression levels of both isolates in a transient transfection system were found to be poor (data not shown). Thus, cytoplasmic tail truncations were performed to increase expression levels (Mao et al., 2012). In addition, truncation of this domain might be beneficial for immunogenicity to avoid the exposure of potentially immunodominant epitopes which are normally intracellular and thus not accessible to antibodies. However, truncated Envs had to be assessed for undesirable side effects caused by this truncation. In a neutralisation assay comparing pseudoviruses bearing full-length and truncated Envs, both function and neutralisation sensitivity seemed to be well preserved. The only notable exception was the gp41 subunit itself which showed a trend towards increased sensitivity to neutralisation. A

possible explanation could be that the cytoplasmic tail might help stabilise the gp41 subunit in a conformation that is more refractory to antibody-based neutralisation. However, since the quaternary structure of the gp120 subunits did not seem to be influenced by these changes, the tail-truncation does not interfere with the overall fold of the envelope spikes.

HEK-293S cells, which have a deletion in the GnT-I locus and thus exclusively express high mannose glycans, were chosen for the expression of Env. The rationale behind this was that PG9 binding has been shown to prefer the smaller Man-5 glycans produced by this cell line. In addition, previous reports had shown increased immunogenicity of gp120s bearing smaller glycans, potentially caused by a better exposure of the CD4bs due to the smaller size of the shielding glycans (Kong et al., 2010).

After establishing the cell type and strain of HIV-1, a purification strategy had to be devised. In order to purify both cross-linked and unmodified proteins, very gentle conditions had to be used. Membrane protein purification often commences with a preparation of cellular membranes by ultracentrifugation, a strategy that has now also been adapted for HIV-1Env (Mao et al., 2012; Mao et al., 2013). However, directly extracting the membrane-protein from whole cells is easier to perform and can lead to higher protein yields (Chaudhary et al., 2012). The potential drawback of lower purity of the final preparation was negligible considering the large number of purification strategies available for HIV-1 Env and the high specificity of bNmAbs.

In order to obtain the highest yields of correctly folded Env, cross-linking should be performed as early in the purification procedure as possible. On the other hand, to be able

to compare cross-linked and unmodified protein, cross-linking should be performed as late as possible. Thus, a compromise was chosen in which Env was solubilised and partially purified before cross-linking. Extraction of correctly folded Env trimers by immunoaffinity chromatography was then performed subsequent to cross-linking to remove any misfolded proteins that might have formed during the cross-linking process. Lectin affinity purification was chosen as the initial purification step since it can be performed under very mild conditions and shows sufficient specificity for Env protein.

A number of detergents were tested in assays examining the solubilisation of Env by capture ELISA. Although detergent Triton showed higher overall solubilisation of gp120, the amounts of gp41 attached to the solubilised gp120 were very similar with the detergent CHAPS. However, it should be noted that the capture ELISA used to determine solubilisation efficiencies was only able to detect gp120-gp41 complexes rather than specifically quantifying intact Env trimers. In fact, mAb D7324, which is the standard antibody for capture ELISAs in our laboratory, should not be able to bind correctly folded Env due to the occlusion of this epitope within the trimer interface. However, subsequent pull-down experiments using PG9 demonstrated the extraction of correctly folded envelope trimers. The detergent CHAPS is commercially available and relatively inexpensive. In addition, it does not contain any primary amines and thus should be compatible with GLA cross-linking.

After optimisation of protein solubilisation and purification steps, mostly trimeric Env protein was obtained that bound well to CD4bs bNmAb VRC01 but not to non-neutralising CD4bs mAb F105. Interestingly, strong binding to F105 was still detected after the lectin purification step. Thus, the lack of binding of this mAb must have occurred as a result of

cross-linking, trimer purification by PGT145 or a combination of the two. Relatively low binding levels of PGT145 to the final product were surprising since PGT145 was used in the purification process. However, the strong binding of quaternary epitope specific bNmAb 3BC176, which recognises an epitope distinct from that of PGT145, demonstrated that correctly folded Env was purified.

Cryo-EM analysis of the purified proteins showed that ~12-30 % formed native-like trimers. This was in agreement with the gel analysis, which had already shown that PGT145-purification was unable to distinguish between trimers and aggregates. The EM-analysis further showed that the aggregates were mostly dimers of trimers that formed surprisingly well folded complexes and thus the numbers of native-like trimers reported here are artificially low. As shown in chapter 5, size exclusion chromatography is able to separate between single trimers and dimers of trimers and thus removing the latter should be relatively straightforward. Alternatively, the lectin-column purification step utilised here might be exchanged for a second quaternary bNmAb purification step such as the recently discovered PGT151. Purification by two quaternary epitope specific mAbs that target independent epitopes might lead to higher proportions of correctly folded Env. In fact, PGT151 has recently been used by another group to purify membrane expressed Env (Blattner et al., 2014).

The biggest challenge faced when purifying membrane expressed Env was the extremely low yields (approximately 50-70 µg final protein) recovered per litre of tissue culture. These low yields prohibited a more comprehensive characterisation of the obtained trimers as well as immunogenicity studies. Low yields may have been caused by low expression of

the protein in the cell lines or denaturation during the solubilisation and purification process. Further optimisation of the purification protocol would be necessary to address the latter point. However, low expression levels might have a specific cause in the case of gp160. Well-developed stable cell lines generally provide much higher expression levels for non-toxic proteins than transient transfections. However, for an unknown reason gp160 is often down-regulated after few passages in stable cell-lines. Since the same is not the case for some gp120 or gp140 constructs (Chung et al., 2014), it seemed possible that stable cell-lines with a tail-truncated Env might not exhibit this phenotype. In addition, for membrane proteins, sorting high-expressing cells from low-expressing cells by FACS is a straightforward method to exclude cells that have down-regulated Env. Nevertheless, indications of down-regulation of the Env constructs used here have been found although no direct comparison between experiments performed at different time-points is possible. Therefore, transient transfections may more reliably produce high protein yields than stable cell lines in this case. Alternatively, inducible cell-lines could be established that might be less susceptible to down-regulation of Env expression.

In conclusion, cross-linking of membrane-bound Env selectively decreases binding of non-neutralising antibodies whilst leaving broadly neutralising epitopes as well as the over-all quaternary conformation intact. The membrane-extraction of intact correctly folded Env trimers developed here produces mostly correctly folded solubilised Env trimers that exclusively display broadly neutralising epitopes thus making them candidates for future immunogenicity trials.

Chapter 5: Chemical cross-linking of next-generation soluble SOSIP gp140

5.1 Introduction

It has been known for some time that soluble Env constructs such as most gp140s do not form the correct quaternary structure adopted by intact membrane-bound Env (Walker et al., 2009; Bonsignori et al., 2011; Pejchal et al., 2011; Walker et al., 2011b; Klein et al., 2012a; Ringe et al., 2013). In the previous chapter, the isolation of membrane-expressed Env was investigated as a method to develop solubilised native Env complexes. However, as discussed in Section 4.3, expression levels were prohibitively low. Recently, a soluble Env construct termed BG505 SOSIP.664 was engineered that almost exclusively binds neutralising antibodies, including quaternary specific bNmAbs such as PGT145 and 3BC176, folds into compact trimers, and can be expressed at reasonable levels in mammalian cell culture (Sanders et al., 2013).

This gp140 is stabilised by the SOSIP set of mutations, including a disulfide bond between gp120 and gp41 plus a mutation which destabilises the post-fusion conformation and therefore helps to maintain the native pre-fusion conformation (Ringe et al., 2013; Sanders et al., 2013). To aid cleavage, an optimised cleavage site is incorporated between gp120 and gp41. In addition, the gp41 subunit is truncated before the MPER (after residue 664 in the HXBC2 numbering system) which leads to increased solubility and prevents aggregation (Klasse et al., 2013). When these mutations (plus the addition of a glycosylation site at position N332 which is required for the purification procedure) are applied to BG505, native-like trimers are formed which are of sufficient quality for crystallisation (Julien et al., 2013a). Interestingly, so far only strain BG505 has formed these native-like compact structures at useful frequencies, whereas other strains still show various levels of aberrant forms of Env (Klasse et al., 2013). Strain BG505 was isolated 6 weeks after a mother-to-

child transmission event and subsequently selected due to its similarity to sequences of strains infecting the donor from whom bNmAbs PG9 and PG16 were isolated (Wu et al., 2006; Hoffenberg et al., 2013). In contrast to most strains, BG505 is bound by PG9 and to a lesser extent PG16 even as monomeric gp120 (Hoffenberg et al., 2013; Sanders et al., 2013). Thus, these two bNmAbs are not quaternary specific for this strain. By contrast, bNmAbs PGT145, CH01, 3BC176 and 3BC315 exert their typical quaternary-preferring phenotype and do not bind monomeric gp120 (Sanders et al., 2013). In general, antibody binding to BG505 SOSIP.664 trimers correlates well with neutralisation of the corresponding pseudovirus (Sanders et al., 2013). However, some non-neutralising V3 loop antibodies are still able to bind the protein with high affinity, indicating room for further improvement of trimer properties (Sanders et al., 2013).

In this chapter, stabilisation of BG505 SOSIP.664 trimers (termed BG505 in this thesis) by chemical cross-linking is optimised *in vitro* and immunogenicity is investigated *in vivo*. Subsequently, methods to further improve the antibody-binding profile of BG505 are explored *in vitro*.

5.2 Results

5.2.1 *In vitro* optimisation of cross-linking of BG505 SOSIP.664 gp140

When the BG505 SOSIP.664 gp140s were discovered in the final year of this project, chemical cross-linking using GLA was tested on these next-generation trimers. After GLA cross-linking of D7324-tagged BG505 using the standard protocol (7.5 mM GLA, 5 min at RT), a capture ELISA was conducted using an extensive panel of antibodies to characterise the effects of cross-linking. Similar to previous results obtained with uncleaved gp140,

binding of non-neutralising antibodies, in particular those targeting the CD4bs (F105 and 15e) and CD4i epitope (17b and X5), were substantially reduced (Fig. 5.1 A and D). b12 binding was also reduced but since it does not neutralise BG505 (Sanders et al., 2013), it is categorised as a non-neutralising antibody for this isolate. In line with the results presented in the previous chapters, binding of neutralising antibodies was generally well preserved (Fig. 5.1 B, C and D). The one exception to this general trend was bNmAb PGT145, which binds to a glycan-dependent quaternary specific epitope in the V1V2 loop (Fig. 5.1 C and D). Surprisingly, the other antibodies targeting this epitope (PG9, PG16 and CH01) were either not affected, or only weakly affected by cross-linking. However, PG9 and PG16 are able to bind BG505 gp120 and thus are not quaternary specific for this isolate (Hoffenberg et al., 2013; Julien et al., 2013b; Sanders et al., 2013). Therefore, CH01 and PGT145 were the only truly quaternary specific antibodies in the test panel and the finding that one of them does not recognise the cross-linked trimer indicates that structural integrity might be at least partially compromised by the cross-linking procedure.

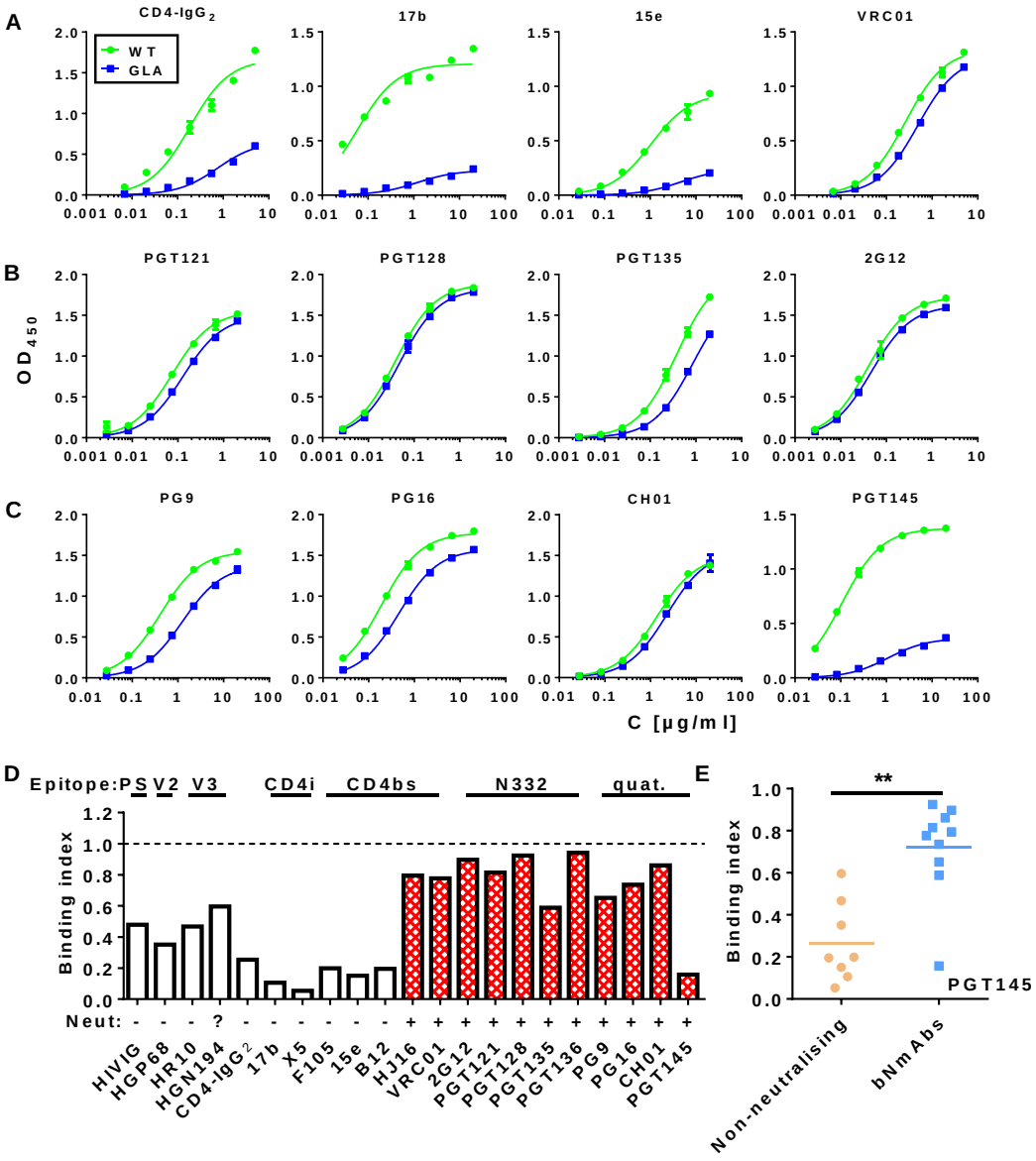

Fig. 5.1: GLA cross-linking of BG505 SOSIP.664. D7324-tagged BG505 gp140 was cross-linked with 7.5 mM GLA and antigenicity was tested by capture ELISA. Example titration curves are shown for CD4bs and CD4i specific mAbs (**A**), N332-glycan specific bNmAbs (**B**) and bNmAbs targeting the quaternary V1V2 epitopes (**C**). D: Binding indices are shown for all antibodies tested. Epitopes are indicated above the bars, neutralisation of homologous pseudovirus (as far as known) is indicated below. E: Binding indices are displayed separated into neutralising and non-neutralising mAbs. ** $p < 0.01$ in a Mann-Whitney test.

To test whether cross-linking induced the loss of binding of quaternary bNmAb PGT145 by disrupting trimer integrity during the cross-linking procedure, GLA-treated BG505 was analysed by cryo-EM. Using this analysis, next generation BG505 gp140 has been shown to consistently form compact symmetrical trimers reminiscent of the mushroom-shaped

complexes formed by membrane-bound Env (Fig. 5.2 and Sanders et al. (2013)). By contrast, uncleaved gp140 such as CN54 gp140 forms irregular shapes consistent with a trimeric gp41 stem from which the three gp120 subunits are 'dangling' off into random directions (Fig. 5.2). Imaging of approximately 5,000 cross-linked BG505 trimers showed that almost half of them (46 %) did not show the compact symmetrical shape found in 100% of unmodified BG505 SOSIP.664 gp140 (Fig. 5.2).

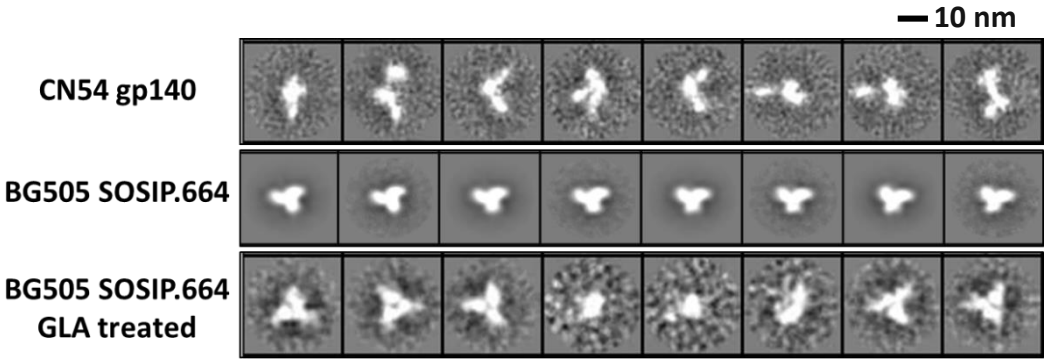

Fig. 5.2: Negative stain cryo-EM analysis of GLA-treated BG505. 2D class averages are shown for a first-generation gp140 (CN54 from Polymun Scientific), the next-generation gp140 BG505 (adapted from Sanders et al. (2013)) and GLA-treated BG505. Smoother projections of unmodified BG505 are due to larger numbers of images used for averaging.

Since antibody PGT145 binding was able to distinguish between correctly and incorrectly folded forms of BG505 an assay was developed utilising this phenomenon to aid in the optimisation of cross-linking of BG505. In this assay, PGT145 binding was measured in parallel by both direct and capture ELISA (Fig. 5.3). In the direct ELISA gp140s were directly coated onto the ELISA leading to mildly denaturing conditions whereas in the capture ELISA an antibody is coated onto the plate that is then used to capture the gp140 from the solution under very gentle conditions. In line with this, quaternary specific bNmAb PGT145 recognised BG505 well in the capture ELISA indicating a general preservation of the quaternary conformation of the glycoprotein during capture (see section 5.3 for a more detailed discussion). Thus, loss of PGT145 binding in the capture assay was used to detect

incorrect quaternary conformations induced by cross-linking. By contrast, direct immobilisation of BG505 gp140 on the ELISA plate led to loss of binding of all quaternary specific mAbs tested (Fig. 5.3 and data not shown) and at the same time allowed the binding of non-neutralising CD4bs mAbs such as F105 (data not shown). bNmAb PG9, which binds an epitope almost identical to PGT145 but is not quaternary specific for isolate BG505, was still able to bind unmodified gp140 in the direct ELISA (Fig. 5.3). GLA cross-linking of BG505 was able to partially restore PGT145 recognition as seen by a PGT145-reactive fraction in the direct ELISA of GLA treated BG505 (Fig. 5.3). As discussed in section 5.3 , binding of PGT145 to cross-linked BG505 in a direct ELISA was thus used to estimate the covalent preservation of the correct quaternary conformation of the trimer.

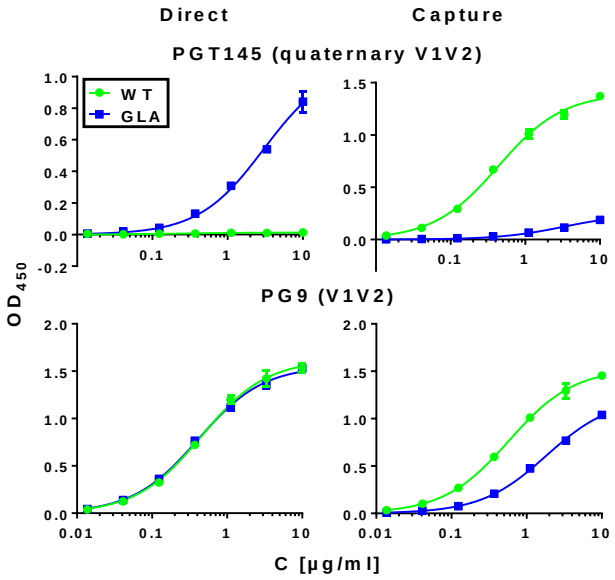

Fig. 5.3: Comparison of direct and capture ELISAs of unmodified and cross-linked BG505. D7324-tagged BG505 was cross-linked with 7.5 mM GLA (blue) or unmodified (green) and analysed in parallel by direct ELISA and D324 capture ELISA using bNmAbs PGT145 and PG9. These bNmAbs recognise almost identical epitopes, although only PGT145 is quaternary specific for isolate BG505.

After developing an assay that indicated the amount of BG505 fixed in the correct conformation, a comprehensive optimisation of cross-linking conditions was conducted. Initially, five different cross-linkers were titrated onto BG505 and the protein was analysed

by direct PGT145 ELISA. In this assay, fixation with low concentrations of cross-linker generally led to low PGT145 binding, indicating insufficient stabilisation of the quaternary conformation (Fig. 5.4). PGT145 signal increased with increasing concentration of the cross-linkers until it peaked and upon further increase of the concentration started to decline again. This decline was interpreted as the result of overt disruption of trimer integrity or prevention of induced fit required for PGT145 engagement. In the simultaneously performed capture ELISA, PGT145 binding decreased with increasing concentration of most cross-linkers, thus confirming the trimer disruption/prevention of induced fit seen in the direct ELISA.

Interestingly, the optimum concentration of cross-linker GLA was very close to 7.5 mM (mean = 7.51 mM in a Gaussian curve fit) thus confirming the results from the optimisation performed on first-generation gp140s in Chapter 3 (Fig. 5.4). The highest peak PGT145 binding values were obtained with the cross-linker combination EDC mixed with NHS (EDC/NHS). Interestingly, this cross-linker forms peptide bonds between carboxy groups and primary amines and thus has a different target site profile compared to all other cross-linkers tested. The second best cross-linker was GLA and therefore, GLA and EDC/NHS were selected for further optimisation.

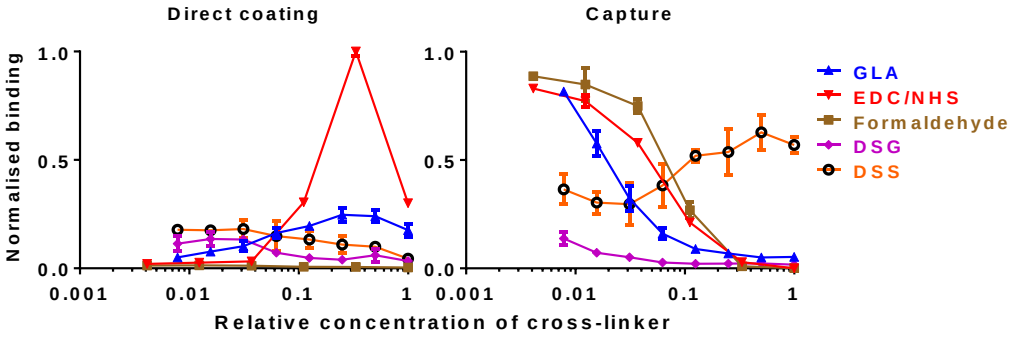

Fig. 5.4: Effect of different cross-linkers upon PGT145 recognition of BG505. D7324-tagged BG505 was cross-linked with the indicated concentrations of cross-linkers and binding of quaternary-epitope specific bNmAb PGT145 was analysed by ELISA using either direct antigen coating (left) or D7324 capture (right). Starting concentration of cross-linkers were 25 mM GLA, 112.5 mM EDC/NHS, 1% formaldehyde, 5 mM DSG and 25 mM DSS.

Based on hypothetical considerations, it seemed possible that a lower concentration of GLA combined with longer reaction times might lead to better preservation of the quaternary structure. Therefore, a time-course ranging from 5 min to 8h was conducted in which GLA was titrated at each time-point (Fig. 5.5A). Unexpectedly, PGT145 showed the highest peak binding at the shortest time tested in the direct ELISA. Further optimisations showed that even shorter reaction times coupled with higher cross-linker concentrations were able to further increase PGT145 binding in this assay (Fig. 5.5C and data not shown). However, in order to further decrease reaction times, the stopping solutions had to be optimised first. Using a colorimetric readout resulting from the reaction of GLA with glycine, a titration of the tris-buffer used to stop the reaction was conducted (Fig. 5.5B). Even when using an extremely high GLA concentration (1.25 M), diluting the reaction 20-fold in 3 M tris (pH 7.4) was able to stop the reaction within 30 seconds. Using these stopping conditions, a time-trial was conducted investigating the cross-linking effects at 500 mM GLA. Cross-linking for 60 seconds with 500 mM GLA followed by quenching by 20-fold dilution in 3 M tris showed a high level of covalent fixation of the quaternary structure of BG505 coupled with robust

reduction in binding of non-neutralising mAbs including F105 and 17b without affecting CD4bs bNmAb VRC01 (Fig. 5.5C). Most importantly, binding of PGT145 was close to its peak under these conditions. Another probe included in this analysis was the quaternary specific bNmAb 3BC176, which binds to an epitope distinct from the PGT145 but nevertheless showed similar trends in this assay.

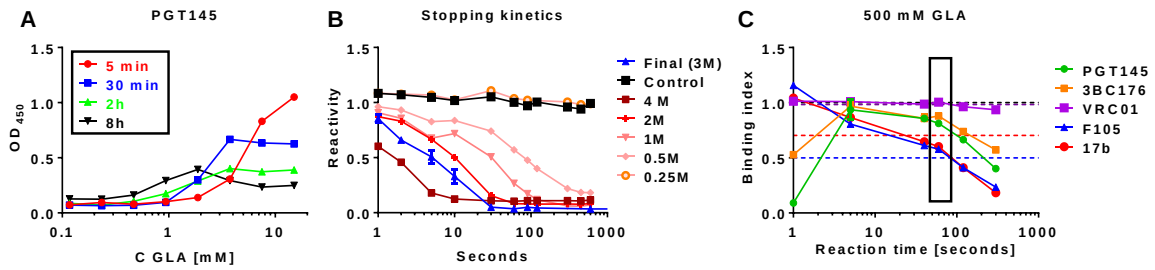

Fig. 5.5: Optimisation of GLA cross-linking of BG505. A: BG505 was cross-linked with titration series of GLA for the indicated times and PGT145 binding was analysed by direct ELISA. **B:** 1.25 M GLA was quenched by diluting it 20-fold in tris (pH 7.4) at the indicated concentrations. After the indicated times, glycine was added to develop a coloured product which was detected by measuring the OD at 320 nm. The final concentration chosen (3M) is indicated in blue. **C:** BG505 was cross-linked with 500 mM GLA for the indicated time periods. Binding of mAbs was measured by direct ELISA. The black box indicates the condition that was chosen as delivering the ideal balance between reduced binding of non-neutralising mAbs F105 and 17b whilst maintaining binding of CD4bs bNmAb VRC01 and quaternary specific bNmAbs PGT145 and 3BC176.

Since EDC/NHS is a two-component cross-linker (composed of EDC and NHS), additional parameters had to be optimised to find ideal cross-linking conditions. The initial test of EDC/NHS cross-linking indicated the requirement of relatively high concentrations of EDC and NHS (Fig. 5.4) and thus optimisation was commenced using the analogue sulfo-NHS (SNHS) instead of NHS due to its better solubility in aqueous solutions (Fig. 5.6A). Independent titration of EDC and SNHS showed a global optimum of PGT145 binding around 1.15 M EDC and 10 mM SNHS in a direct ELISA (Fig. 5.6). A capture ELISA using

D7324 was not possible with this cross-linker since cross-linking led to substantially reduced D7324 biding as shown by direct ELISA, consistent with the presence of four potential modification sites within the tag (Fig. 5.6B).

Considering that 10 mM is within the solubility of NHS, further optimisations were conducted using this simpler alternative. The large quantities of EDC required for efficient cross-linking (1 M) led to the hypothesis that lowering the pH might improve cross-linking since the reaction of EDC with carboxy groups is more efficient at lower pH (Nakajima and Ikada, 1995). Further extensive optimisation showed that cross-linking was slightly more efficient at lower pH (data not shown) and cross-linking efficiency at this lower pH was found to be relatively independent of the NHS concentration (Fig. 5.6 and data not shown). The final conditions chosen were: pre-mixing 2 M EDC with 20 mM NHS in MBS (pH 6.0) followed by addition of the cross-linker to an equal volume of protein (in PBS) for 30 min after which the reaction was quenched with 1 M glycine (pH 7.4) for 10 minutes. This condition was slightly superior to the optimum conditions with SNHS (Fig. 5.6C, black datum).

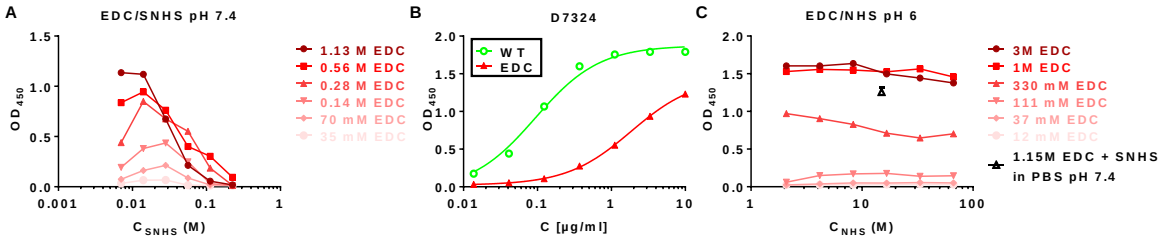

Fig. 5.6: Optimisation of EDC/NHS cross-linking. BG505 was cross-linked with titrating concentrations of both EDC and either Sulfo-NHS (**A**) or NHS (**C**) at pH 7.4 (**A**) or pH 6.0 (**C**) as indicated and PGT145 binding was analysed by direct ELISA. **B:** D7324 binding to D7324-tagged BG505 cross-linked with 1.25 M EDC and 11.25 mM SNHS was tested by direct ELISA.

After optimisation of the cross-linking conditions, antibody binding to cross-linked BG505 was analysed in a comprehensive ELISA screen. A panel of 25 antibodies was titrated onto the cross-linked or unmodified glycoprotein in a direct ELISA (Fig. 5.7 A and B). In parallel, a 2G12 capture ELISA was performed with selected antibodies (Fig. 5.7A). In general, results were relatively similar to those previously obtained under standard GLA cross-linking conditions (Fig. 5.1) including substantially reduced binding of many non-neutralising antibodies such as non-neutralising CD4bs mAbs F105, 15e and b12 as well as CD4i mAbs 17b and X5. Importantly, a large difference to the previous data using "standard conditions" (Fig. 5.1) was observed in the improved binding of quaternary antibody PGT145, in particular in the capture ELISA. Binding of PGT145 was only slightly reduced in contrast to the extensive reduction seen previously (compare Fig. 5.1 and Fig. 5.7). 3BC176 (as well as the closely related bNmAb 3BC315) showed results similar to PGT145 despite recognising a distinct quaternary dependent epitope, thus supporting the results from PGT145. Furthermore, binding of non-neutralising antibodies was significantly more strongly reduced upon cross-linking with either cross-linker than was binding of bNmAbs (Fig. 5.7C). Cross-linking mostly preserved the trimeric organisation of the glycoprotein in a denaturing/reducing SDS-PAGE (Fig. 5.7D). Small amounts of dimer/monomer were visible under these harsh conditions in the GLA-treated but not the EDC-modified sample and the band corresponding to trimeric envelope migrated slightly faster upon EDC treatment compared to GLA, consistent with a more compact fold (Fig. 5.7D).

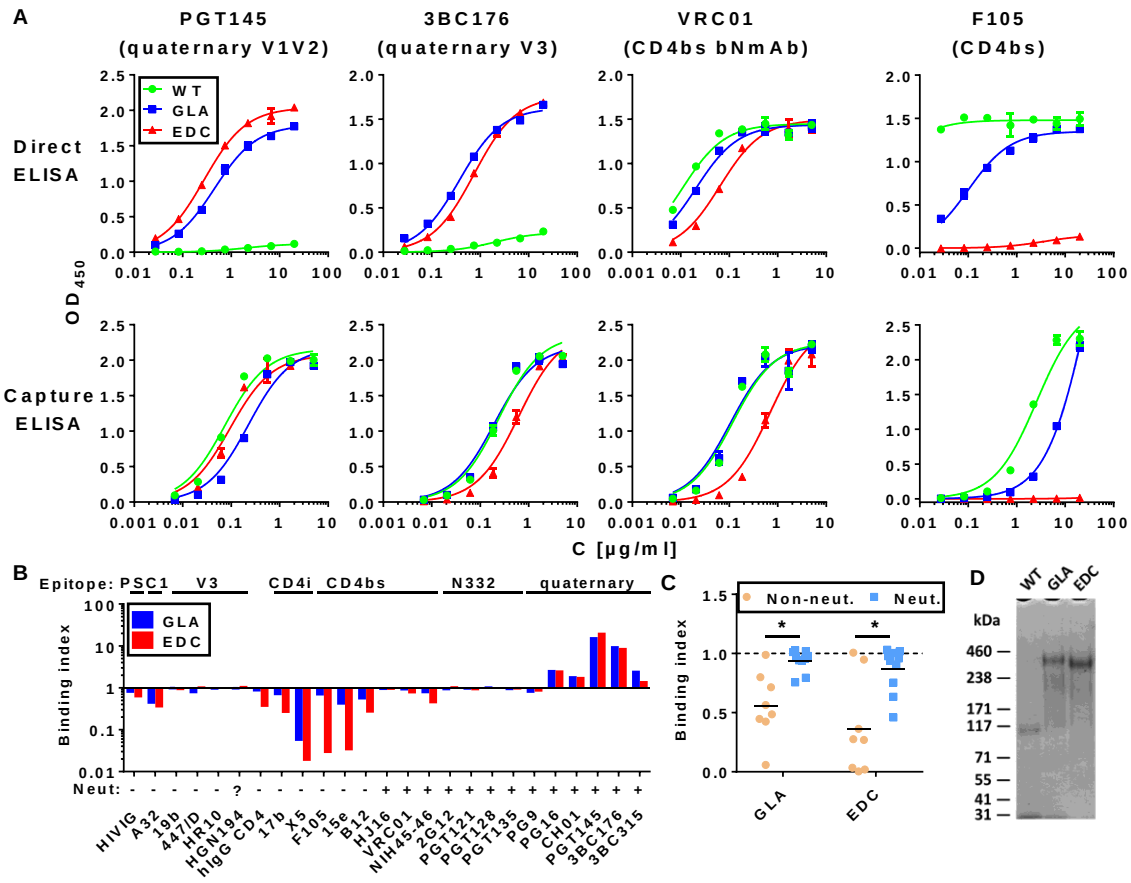

Fig. 5.7: Antigenicity of cross-linked BG505 *in vitro*. A: Representative binding curves of selected mAbs analysed by both direct ELISA and 2G12 capture ELISA. **B:** Binding indices of all antibodies tested in the direct ELISA format are shown as AUC (cross-linked)/AUC (unmodified). Epitopes are indicated above the bars, neutralising antibodies are marked below (as far as known). **C:** Binding indices are shown separated into neutralising and non-neutralising antibodies. Results from a 2G12 capture ELISA were used as far as available (VRC01, F105 and all quaternary specific bNmAbs), whereas all remaining binding indices were determined using the direct ELISA. * $p < 0.05$ in a 1-way ANOVA with Kruskal-Wallis' post-test. **D:** SDS-PAGE analysis of unmodified (WT) or cross-linked BG505.

To further investigate the effects of cross-linking on BG505 antigenicity, antibody binding was tested by SPR analysis. As seen previously (Chapter 3), all differences were more pronounced using this more sensitive assay. In particular, substantial loss of binding of PGT145 was detected against GLA cross-linked gp140 (Fig. 5.8 A and B). Cross-linking with EDC/NHS also led to less PGT145 binding but this was not as pronounced as the effect of GLA cross-linking (Fig. 5.8 A and B). In line with the results from the ELISA, EDC/NHS cross-linking led to stronger reductions in binding of quaternary bNmAb 3BC176 as well as CD4bs

VRC01 when compared to GLA (Fig. 5.8 A and B). In both cases, prevention of induced fit might play a role in these reductions, especially considering that 3BC176 was shown to have a partial CD4-induced phenotype (Klein et al., 2012a). F105 binding was very weak even without cross-linking (<17 RUs), consistent with the lack of binding of non-neutralising antibodies to BG505, but was further decreased upon cross-linking (Fig. 5.8A). Overall, binding of neutralising antibodies was more robustly reduced by cross-linking than binding of bNmAbs (Fig. 5.8C).

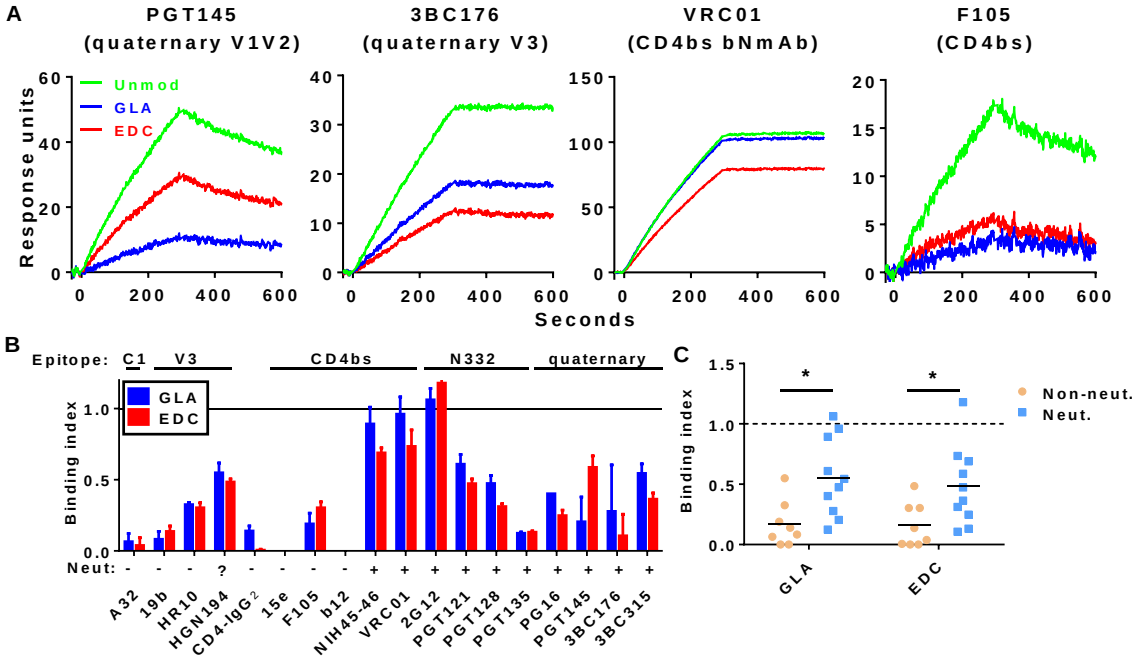

Fig. 5.8: SPR analysis of cross-linked BG505. A: Unmodified or cross-linked BG505 trimers were flowed over SPR chips on which the indicated mAbs had been captured via immobilised anti-human IgG antibodies. Responses were followed for 300 seconds before stopping the injection, followed by a dissociation phase in which buffer was floated over the surface. Responses were normalised to antibody capture levels and double referencing was performed by subtracting signal from a negative control cell (isotype control: human IgG anti human CD8) as well as from a buffer injection. Curves show average responses from two injections. **B:** Binding indices are shown for all mAbs tested. Error bars show SD of two technical repeats. **C:** Binding indices are separated into neutralising and non-neutralising mAbs. * $p < 0.05$ in a 1-way ANOVA with Kruskal-Wallis' post-test.

In conclusion, cross-linking conditions were optimised to better preserve the quaternary fold of BG505 trimers and further increase the existing differential between binding of neutralising and non-neutralising mAbs to BG505.

5.2.2 **Immunogenicity of cross-linked BG505**

After optimising cross-linking of BG505, immunogenicity was tested *in vivo*. BALB/c mice (n=5 per group) were immunised with 10 µg of unmodified or cross-linked (with either GLA or EDC/NHS) BG505. Different adjuvants were used at different time-points starting with 0.5 % Carbopol 971p at week 0, 100 µg PEI at weeks 3, 8 and 12 and protein only at week 16. Serum samples were collected 2 weeks after each immunisation. Immunisation with cross-linked BG505 showed significantly reduced binding antibody endpoint titres against homologous protein after the first and second immunisations when compared to unmodified protein (weeks 2 + 5, Fig. 5.9). However, at the final time-point, titres were statistically indistinguishable between groups. Similar titres were also obtained when cross-linked gp140 was used as the coating antigen (Fig. 5.9B).

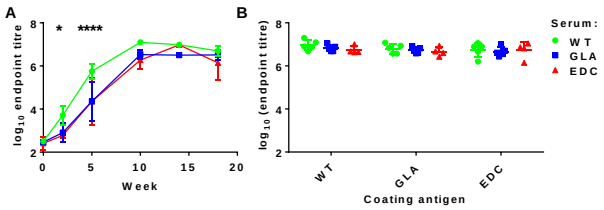

Fig. 5.9: Immunogenicity of cross-linked BG505. BALB/c mice (n = 5 per group) were immunised with unmodified or cross-linked BG505 at weeks 0, 3, 8, 12 and 16 and sera were collected 2 weeks after each injection. **A:** Binding antibody titres against D7324-tagged BG505 were determined by capture ELISA. * $p < 0.05$; *** $p < 0.001$ in a 2-way ANOVA with Dunnett's multiple comparison test. **B:** Direct ELISA endpoint tires against unmodified or cross-linked BG505 are shown for sera from the final bleed (week 18).

To further investigate the epitopes of antibody responses induced by cross-linked BG505, cross-competition analysis was performed using mAbs against six different epitopes. In all

groups the strongest responses were detected against an epitope in the V3 loop (Fig. 5.10A). Furthermore, unmodified BG505 induced weak responses cross-competing with CD4. Responses against the N332, V1V2 and gp120/gp41 epitopes were not higher than those observed with pre-immune sera.

The A32 epitope is occluded in intact Env and thus binding of this mAb to native BG505 is undetectable (Sanders et al., 2013). However, as shown above, direct immobilisation of BG505 leads to a disruption of the quaternary fold of the trimer that exposes several epitopes including the A32 epitope. Therefore, A32 cross-competition was performed in a direct ELISA format. In this assay, unmodified BG505 induced significantly ($p < 0.001$) higher titres of antibodies competing with A32 than the cross-linked trimers (Fig. 5.10).

To further investigate CD4bs responses, binding to CD4bs probes eOD and RSC3 was tested by ELISA. No statistically significant differences between groups were detected in either assay (Fig. 5.10B). Furthermore, although robust binding titres to probe RSC3 were observed, virtually identical responses were detected against the CD4bs knockout control ΔRSC3 leading to RSC3 scores ($\log_{10}$ (RSC3 titre) – $\log_{10}$ (ΔRSC3 titre)) of approximately zero for all animals (Fig. 5.10B).

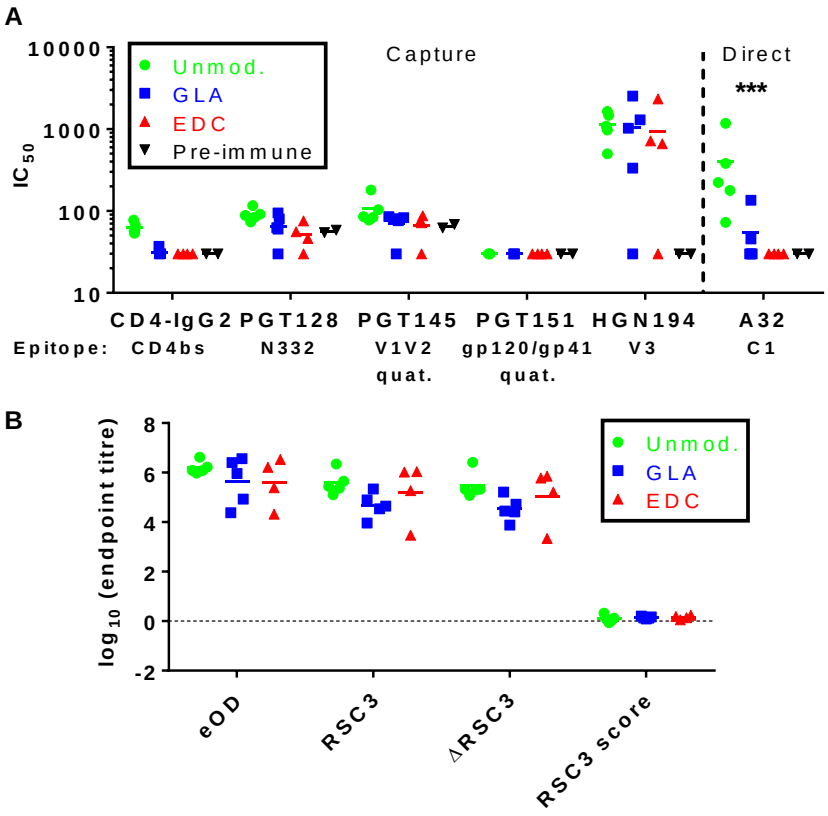

Fig. 5.10: Epitope mapping of sera from BG505-immunised animals. A: Sera from Fig. 5.9 were analysed by cross-competition ELISA using D7324-tagged BG505 immobilised by antibody capture (CD4, PGT128, PGT145, PGT151 and HGN194) or direct coating (A32). **B**: CD4bs responses were detected by direct ELISA using eOD, RSC3 or negative control protein ΔRSC3 as coating antigen. RSC3 scores were calculated by subtracting the log-transformed endpoint titres against ΔRSC3 from the corresponding value for RSC3. *** $p < 0.001$ in a 2-way ANOVA with Dunnett's multiple comparison test.

Taken together, these data show that cross-linking of BG505 leads to delayed induction of antibodies *in vivo* but does not induce strong CD4bs-specific responses.

5.2.3 PGT145 affinity purification of BG505

The *in vitro* characterisation of cross-linked BG505 showed further room for improvement, since binding of quaternary specific bNmAbs was not completely preserved (Fig. 5.7 and Fig. 5.8). Therefore, analogous to the results shown in Chapter 4, PGT145 affinity-

purification was tested as a method to select correctly folded BG505 trimers both before and after cross-linking.

Initially, his-tagged BG505 was transiently expressed in HEK-293A cells. The clarified culture supernatant was then subjected to affinity purification using either a cobalt-affinity purification or immunoaffinity-purification using agarose-immobilised PGT145. After this purification step, oligomerisation of the PGT145-purified material was analysed by gel electrophoresis. However, for unknown reasons, attempts to perform native pages similar to those shown in previous chapters failed to produce clear bands for BG505 (data not shown). Instead, small samples of the material were extensively cross-linked and then separated by conventional SDS-PAGE. In this analysis PGT145-purified BG505 migrated primarily as trimeric protein although some aggregate was still present (Fig. 5.11A). In a subsequent size-exclusion chromatography, his-tag purified BG505 showed several overlapping peaks, consistent with the presence of monomer, dimer, trimer and aggregates (Fig. 5.11B). By contrast, PGT145-purified material only showed two peaks, consistent with the presence of trimer and aggregates but without any monomer or dimer (Fig. 5.11B).

The trimer-containing fractions of each purification were pooled and subsequently analysed by SPR. In general, binding of mAbs was relatively similar between these two preparations (Fig. 5.11C). The most prominent differences were found between all V3 mAbs tested, which bound 55-75 % less to the PGT145-purified glycoprotein.

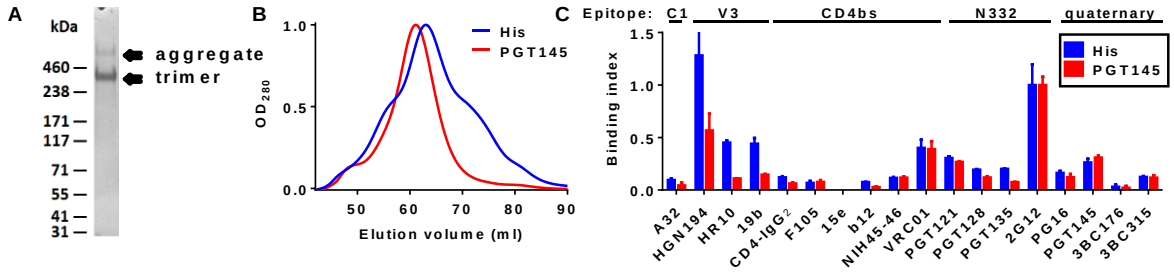

Fig. 5.11: Characterisation of PGT145-purified BG505. A: BG505 was purified from culture supernatant by PGT145 immuno-affinity chromatography, extensively cross-linked and analysed by SDS-PAGE. **B:** Representative size-exclusion chromatography elution profiles are shown for His-tagged BG505 purified by either cobalt-affinity chromatography (His) or PGT145 affinity chromatography (PGT145). **C:** Pooled trimer-containing fractions from each purification method were analysed by SPR. AUC values for each mAb were normalised to mAb immobilisation levels. To normalise for slight differences in protein concentrations, responses were subsequently normalised to result in 2G12 responses corresponding of 1.0. Error bars indicate SD of two technical repeats.

Next, PGT145 purification of cross-linked BG505 was attempted in order to extract only trimers that were still intact after cross-linking. Therefore, BG505 expressed in HEK-293A cells was partially purified from culture supernatants by 2G12 affinity purification and then cross-linked with EDC/NHS, followed by re-purification on a PGT145 immunoaffinity column. The extracted glycoprotein was then analysed by cryo-EM (Fig. 5.12). In this analysis BG505 showed mostly correctly folded trimers (Fig. 5.12 bottom lane). However, a large proportion of the protein was present in form of dimers of trimers. Since this was the only protein analysed by cryo-EM that had not been subjected to size exclusion chromatography, the presence of these dimers of trimers impedes the estimation of correctly folded Env within the trimeric fraction. By contrast with the PGT145 purified material, conventionally purified (2G12 followed by size-exclusion) BG505 only showed 36.3 % or 20.5 % correctly folded trimer after cross-linking with GLA and EDC/NHS respectively (Fig. 5.12). Surprisingly, these values are even lower than those obtained with 7.5 mM “standard” GLA cross-linking. Nevertheless, the fact that the PGT145 purified

material was mostly correctly folded (apart from oligomerisation) shows that this PGT145 affinity chromatography allows the purification of correctly folded trimers.

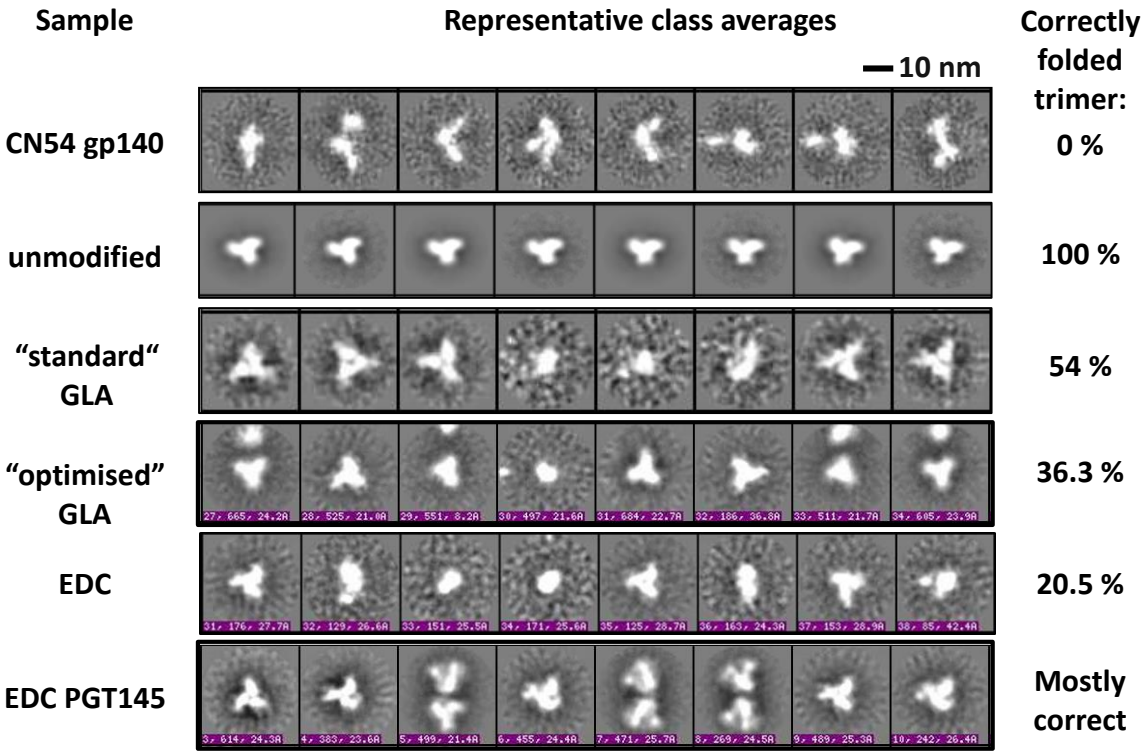

Fig. 5.12: Cryo-EM analysis of cross-linked gp140. 2D class averages are shown for a first-generation gp140 (CN54 from Polymun Scientific), the next-generation gp140 BG505 (adapted from Sanders et al. (2013)) and cross-linked BG505. Cross-linking conditions included were standard GLA cross-linking, optimised GLA cross-linking, EDC/NHS cross-linking and PGT145-purified of EDC/NHS cross-linked BG505 (EDC PGT145). Proportions of native-like trimers are indicated. It should be noted that the PGT145-purified EDC cross-linked sample was the only BG505 sample that was not subjected to size-exclusion chromatography.

To further investigate the properties of PGT145-purified cross-linked BG505, BG505 was expressed in stably transfected HEK-293T cells (Chung et al., 2014) and purified by PGT145 affinity chromatography followed by size exclusion chromatography. GLA cross-linking was performed followed by another round of PGT145 affinity purification. To emphasise the effects of cross-linking and PGT145 re-purification, standard GLA cross-linking conditions (7.5 mM for 5 min at RT) rather than the optimised conditions were chosen for this proof-of-principle experiment. As expected, cross-linking under these conditions led to a robust

reduction of PGT145 binding in a capture ELISA (Fig. 5.13A+B). Re-purification with PGT145 after cross-linking was able to increase binding of PGT145 in both capture and direct ELISAs, confirming successful affinity purification. Effects of PGT145-purification on binding of CD4bs mAbs VRC01 and F105 were minor (Fig. 5.13A+B). However, binding of another quaternary-specific mAb (3BC176) that recognises an independent epitope was increased in a direct ELISA, confirming the purification of correctly folded trimers upon PGT145 affinity chromatography. In accordance with previous results, cross-linking had a significantly greater effect on binding of non-neutralising antibodies compared to bNmAbs (Fig. 5.13C).

Taken together, these data show that PGT145 affinity chromatography is able to selectively extract correctly folded trimer both before and after cross-linking.

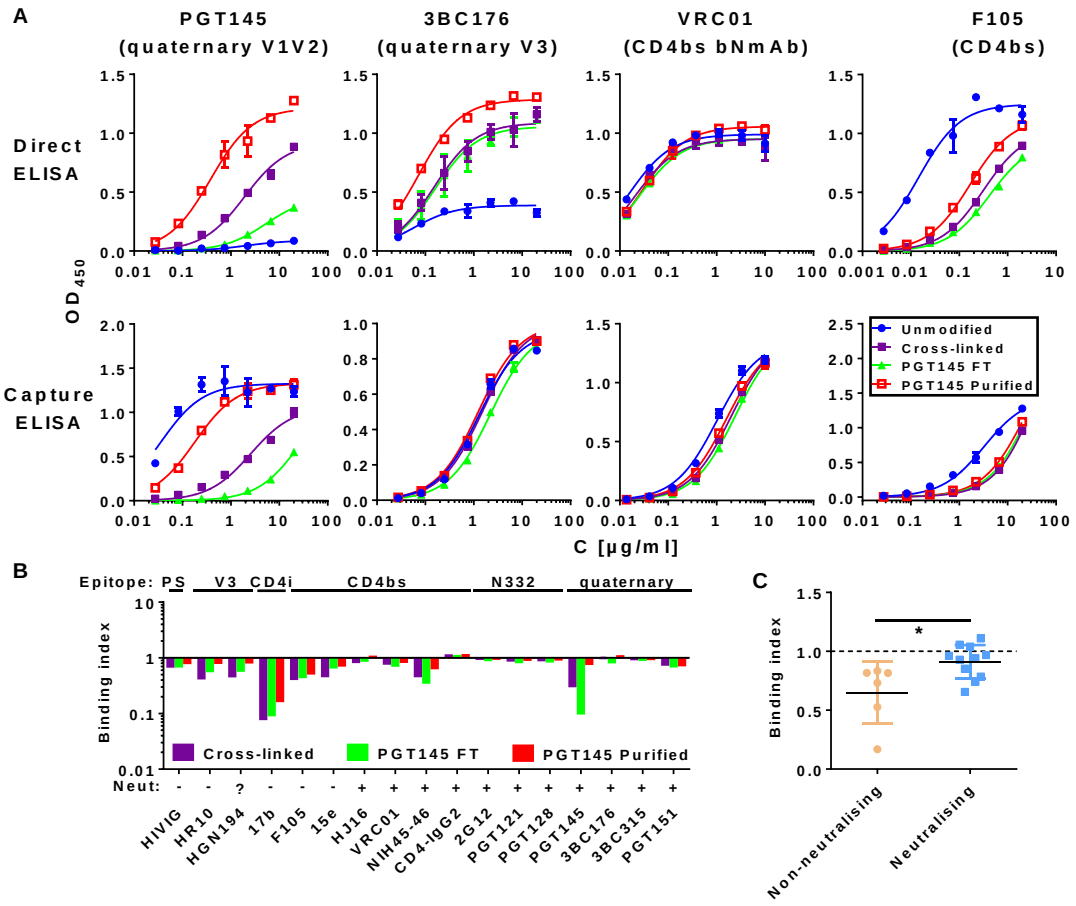

Fig. 5.13: Antigenicity of cross-linked PGT145-repurified BG505 *in vitro*. BG505 was expressed in stably transfected HEK-293T cells and purified by PGT145-affinity purification followed by size-exclusion chromatography (unmodified protein; blue). The protein was cross-linked with GLA using the "standard protocol" (7.5 mM GLA for 5 min at RT; purple) and subjected to another round of PGT145 affinity purification. Both the flow-through (FT; green) and the final eluate (red) from this purification were included in the analysis. **A:** Representative binding curves of selected mAbs analysed by both direct ELISA and 2G12 capture ELISA. **B:** Binding indices of all antibodies tested in the capture ELISA format are shown as AUC (modified)/AUC (unmodified). Epitopes are indicated above the bars, neutralising antibodies are marked below (as far as known). **C:** Binding indices are shown separated into neutralising and non-neutralising antibodies. Results from a 2G12 capture ELISA were used as far as available, whereas data from the direct ELISA were used for HIVIG and CD4-IgG2. * $p < 0.05$ in a Mann-Whitney non-parametric t-test.

5.3 Discussion

In this chapter, cross-linking of next-generation gp140 BG505 was explored. Whilst this glycoprotein folds into compact trimers and binds quaternary-specific but not most non-neutralising antibodies, it is still relatively fragile. For instance, immobilisation on an ELISA

plate is sufficient to abolish binding of quaternary-specific bNmAbs whilst allowing high-affinity binding of non-neutralising antibodies (Fig. 5.3). This phenotype is consistent with a reversion of the structure to conventional first-generation gp140, which forms a trimeric gp41 stalk with three attached intact gp120 molecules that do not fold correctly into the functional compact trimers found on native Env (Ringe et al., 2013). A similar effect was seen upon cross-linking, which partially disrupted trimer integrity. Despite some disruptions, cross-linking was able to stabilise a subpopulation of the trimer sufficiently to retain some binding of quaternary bNmAb PGT145 upon direct ELISA plate coating. Thus, a direct ELISA using PGT145 as the detecting antibody was able to detect the proportion of BG505 covalently cross-linked into the correct conformation.

Based on these results, cross-linking of BG505 was optimised using a direct PGT145 ELISA as readout. Titration of cross-linkers showed that very low concentrations of cross-linkers led to very low signal, presumably due to insufficient stabilisation of the trimer. Increasing concentrations of cross-linker led to increased signal until a peak was reached. Further increasing the concentration of cross-linkers led to reduced signal. This decrease in signal might be due to increased disruption of trimer integrity during the cross-linking process. An alternative explanation might be that cross-linking with higher concentrations prevented any potential induced fit required for high-affinity binding. While cryo-EM analysis is able to directly determine the proportion of correctly folded trimer, it is a relatively low throughput method therefore it was only used to analyse the optimised conditions (Fig. 5.12), whereas the actual optimisation of the cross-linking procedure was performed by direct ELISA with PGT145 binding.

Using this method, GLA and EDC/NHS were found to be the most effective at preserving PGT145 binding in a pre-screen (Fig. 5.4) and subsequently, conditions were further optimised. The cross-linking combination of EDC and NHS has a number of properties distinguishing it from GLA. Firstly, it is a so-called zero-length cross-linker, meaning that no traces of the cross-linker remain on the protein after the reaction is completed (apart from potential addition of the quenching reagent) (Nakajima and Ikada, 1995). Furthermore, it reacts by forming an amide bond between carboxy- and amine groups on the protein (Nakajima and Ikada, 1995). Thus, it has a different modification site profile compared to GLA, restricted to aspartate or glutamate residues in close proximity to amines.

Optimised conditions were found for both GLA and EDC/NHS and in both cases relatively high concentrations showed the optimal preservation of the PGT145 epitope in a direct ELISA. In case of GLA, this is coupled with a relatively short reaction time, consistent with a 'flash-freezing' of the protein. However, a possible drawback of this method is that it might lead to high numbers of lysines with quenched GLA attached with unknown consequences on immunogenicity. In the case of EDC/NHS, only high concentrations of EDC, not of NHS, were required. Potentially, this could indicate a complete utilisation of all carboxy groups which are then either reacted with nearby amines (as found in lysine residues) or revert back to unmodified carboxy groups (Nakajima and Ikada, 1995).

After conditions were optimised, cross-linking was examined by SDS-PAGE as well as by ELISA and SPR. EDC/NHS was better able to prevent trimer disassembly in a reducing/denaturing SDS-PAGE than GLA. This suggests a more extensive fixation induced by this cross-linker, which is further confirmed by the slightly quicker migration of the

trimer through the gel, consistent with a more compact complex (Fig. 5.7C). Both ELISA and SPR showed similar trends in antigenicity although all cross-linking induced effects were more pronounced in the more sensitive SPR analysis. Generally, both cross-linkers showed similar antigenicity profiles upon fixation of BG505 (Fig. 5.7 and Fig. 5.8). Importantly, EDC/NHS retained better PGT145 binding than GLA. On the other hand, 3BC176 binding was better retained upon GLA cross-linking. However, this latter finding might be more influenced by prevention of an induced fit, which could be more of a problem with this mAb than with PGT145 due to its partial CD4 inducible phenotype (Klein et al., 2012a). Another difference between the two cross-linkers is that EDC/NHS treatment induced a small loss of binding of VRC01. This might actually be caused by inhibition of the small induced fit required for VRC01 binding (Wu et al., 2010). Since a comparable pattern was observed with GLA in Chapter 3, this minor decrease might not represent a significant problem for immunisation studies.

After optimisation of the cross-linking conditions, *in vivo* characterisation of the immunogenicity of modified BG505 was performed in mice. Mice have several disadvantages for evaluating antibody responses. Most importantly, they generate antibodies with relatively short CDR-H3 regions compared to humans (Johnson and Wu, 1998), which might be a problem in particular in the case of HIV-1, which tends to induce antibodies with relatively long CDR-H3 regions (Breden et al., 2011). An additional problem is the small amount of serum available for analysis due to the small size of the animals. Finally, pseudovirus neutralisation of mouse sera cannot be reliably determined due to the presence of unknown inhibitory factors (Montefiori, 2005). Nevertheless, epitope mapping

can be performed with murine sera thus giving basic insights into the immunogenicity of a vaccine candidate at relatively low cost.

In vivo, cross-linking of BG505 led to overall reduced immunogenicity, especially early in the immunisation regimen. This might indicate that in the absence of the immunodominant epitopes, which were not exposed upon cross-linking, reduced antibody titres were induced rather than antibody responses being refocused towards other potentially neutralising but immunorecessive areas. If this were the case, it would suggest at least partial denaturation of the unmodified protein *in vivo*, which seems possible considering the relatively conformationally fragile nature of these trimers. This hypothesis is supported by the observation of increased cross-competition of sera from the animals immunised with unmodified BG505 with mAb A32, which binds to the C1 region of the protein and is normally excluded in intact trimers. An alternative explanation for the lower overall antibody responses in the animals receiving cross-linked BG505 might be that T-cell responses were reduced due to the covalent fixation of the protein which might inhibit peptide processing. Lower T-cell help might then have led to lower B-cell responses. This hypothesis could be verified by further investigations into the cellular responses induced by cross-linked BG505.

Epitope mapping showed strong anti-V3 loop responses in all animals. By contrast, limited responses against all other epitopes were detected. In particular, CD4bs responses were completely undetectable in all groups in the RSC3 assay. A possible explanation is that with natively folded Env the CD4bs is so recessed that no responses could be generated towards this region in mice, thus further increasing the immunodominance of the V3 region.

Antibodies to the CD4bs generally require long CDR-H3 regions to contact these epitopes, and such antibodies may not be generated in mice, where antibodies have short CDR-H3 loops (Johnson and Wu, 1998). Immunisations in species with longer CDR-H3 regions such as rabbits or macaques would be required to investigate this.

Since the *in vitro* characterisation showed that even under optimised conditions cross-linked BG505 did not form exclusively native-like compact trimers, extraction of the correct quaternary conformation after cross-linking was attempted to isolate only correctly folded material. In a preliminary experiment with unmodified BG505, PGT145 was able to distinguish between trimers and smaller complexes such as dimers or monomer, as PGT145 affinity purification did not co-purify the lower MW species found in His-tag purified material (Fig). Surprisingly, higher MW oligomers were co-purified, indicating the correct presentation of the PGT145 epitope on these complexes. Therefore, size-exclusion chromatography should be performed in addition to the PGT145 purification step to obtain pure trimer. The antigenicity of PGT145 purified BG505 was relatively similar to unmodified protein, except for anti V3-loop antibodies. Binding of V3-directed mAbs was reduced in PGT145 purified material. It has been shown that V3-loop directed non-neutralising antibodies, including 19b, are able to bind BG505 SOSIP.664 despite not neutralising the corresponding pseudovirus (Sanders et al., 2013). Thus, reduced binding of these V3-loop antibodies to PGT145-purified BG505 indicates that its binding profile might correlate better with its neutralising profile (Sanders et al., 2013) and might suggest that these trimers are more native-like.

Based on these results, a strategy was devised in which BG505 was partially purified, cross-linked and re-purified using PGT145 affinity chromatography. Protein purified by this method was mostly correctly folded although dimers of trimers were still present (Fig. 5.11). To further improve the cross-linking procedure, a size-exclusion step was incorporated. In combination, cross-linking of size-exclusion purified BG505 followed by PGT145 affinity purification led to a partial reversion of the reduced PGT145 binding to the protein upon cross-linking alone. At the same time, binding of an independent quaternary specific bNmAbs (3BC176) was increased, suggesting the purification of correctly folded protein. In this initial trial, the standard GLA cross-linking rather than the optimised conditions were chosen to emphasise the effects on PGT145 binding. Further experiments will attempt to transfer this strategy to EDC/NHS cross-linked material.

Taken together, cross-linking of next-generation trimer BG505 was optimised in this chapter leading to improved preservation of quaternary epitopes even under mildly denaturing conditions.

Chapter 6: Glycan masking using *in situ* polymerisation of sialic acid

6.1 Introduction

Infection with HIV-1 or immunisation with gp120-based antigens generally leads to the induction of strong binding antibody responses but these antibodies mostly target the variable loops or regions within the trimer interface which are occluded in intact virion Env (Gottardo et al., 2013; Schiffner et al., 2013a). The cause of the immunodominance of these non-neutralising epitopes is currently not well understood but the inability to predict and redirect antibody responses towards conserved neutralising epitopes is a major hurdle in the development of vaccines against quickly evolving viruses such as HIV-1 and, to a lesser extent, influenza virus.

Here, a strategy was devised to redirect antibody responses by 'glycan masking' of immunodominant epitopes. It was hypothesised that covalent coupling of immunosilent glycans to immunodominant epitopes might dampen antibody responses towards the masked epitopes and instead redirect antibody responses towards non-masked surfaces. In fact, a large number of pathogens such as *Haemophilus influenzae* use such 'glycan masking' with (poly-) sialic acid of variable chain lengths to escape immune recognition by the host (Vimr et al., 2000; Vimr and Lichtensteiger, 2002; Sato, 2004). Polysialic acid is biodegradable and has non-toxic catabolic products (Gregoriadis et al., 2000; Vimr et al., 2004). In addition, it can theoretically be tailored to have a defined radios and chain length (Brisson et al., 1992). These properties make sialic acid a promising candidate for a glycan masking strategy.

In this chapter, proof-of-principle data of refocusing of antibody responses by glycan masking is presented using the model protein hen egg lysozyme (HEL). Polysialic acid of

different chain lengths were site-specifically coupled to protein surfaces and the effects on antibody-recognition analysed *in vitro*. Subsequently, *in vivo* experiments were conducted to show successful refocusing of antibody responses by glycan masking.

6.2 Results

6.2.1 **Concept**

In collaboration with Benjamin G. Davis and Heiko Schuster from the organic chemistry department of the University of Oxford, a strategy for site-selective addition of polysialic acid chains to target proteins was devised (Fig. 6.1). In a first step, the protein was primed by chemically coupling a lactose residue to primary amines (predominantly the ε-amino group of lysine residues) via IME chemistry (2-imino-2-methoxyethyl-1-thio glycosides) (Lee et al., 1976; Stowell and Lee, 1980; Stowell and Lee, 1982). "Short" α2,8-linked sialic acid (N-Acetylneuraminic acid) chains were then enzymatically attached to the lactose primers *in situ* via α2,3–linkage using the sialyl transferase from *Campylobacter jejuni* (CST-II) (Gilbert et al., 2000). The polysialyl-transferase (PST) from *Neisseria meningitides* was then used to elongate the sialic acid chains to render 'long' α2,8-linked sialic acid chains (Freiberger et al., 2007).

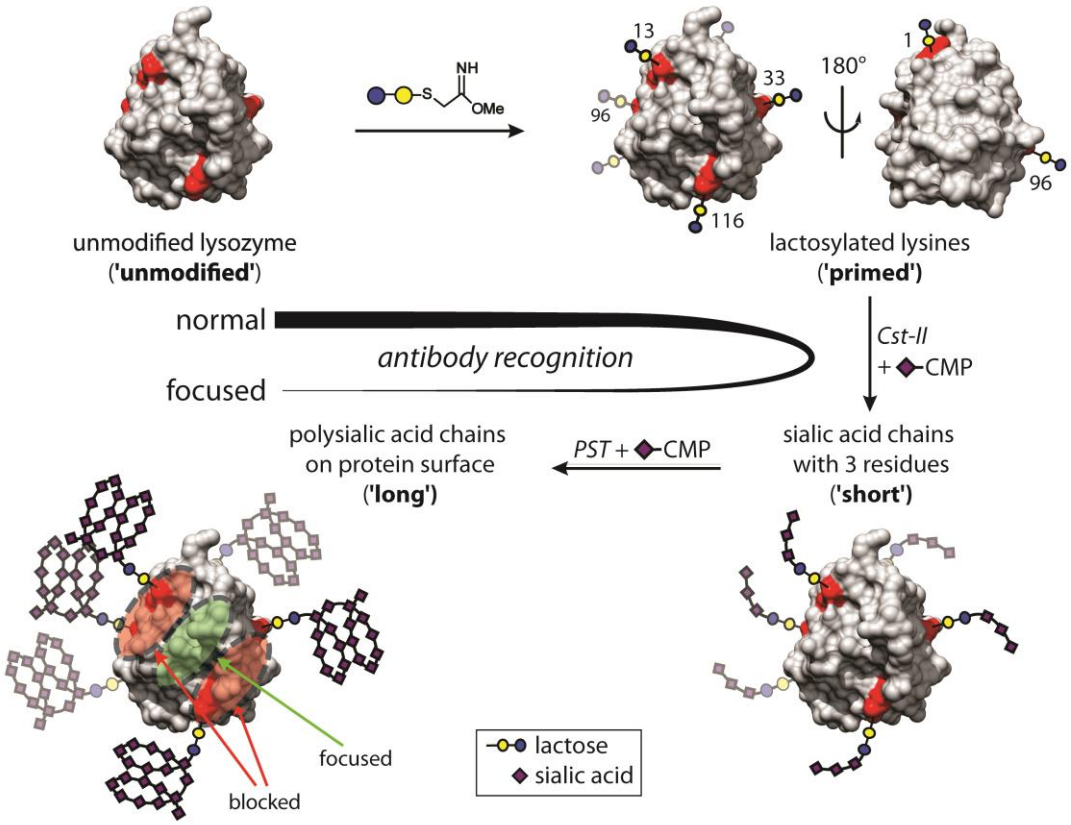

Fig. 6.1: Fig. 1. Approach to on-target sialylation for refocusing of antibody response. General strategy of targeted sialic acid addition to HEL lysines leading to anticipated masking of certain epitopes resulting in focused antibody recognition.

6.2.2 Modification of model protein HEL

The strategy for glycan masking was first tested on model protein HEL, which is compact, globular, and structurally and antigenically well-defined (Davies and Cohen, 1996). Priming by coupling of lactose-residues to HEL lead to a shift in the molecular weight of approximately 1.3 kDa in SDS-PAGE analysis (Fig. 6.2 and Table 6-1). *In situ* sialic acid addition by CST-II renders 'short' chains which showed a further increase in molecular weight by approximately 0.7 kDa. Subsequent polymerisation of 'long' polysialic acid chains by PST yielded a very broad peak in SDS-PAGE analysis consistent with a range of molecular weights. The 'long' samples were stained by an anti-polysialic acid antibody in Western blot analysis (Fig. 6.2B). Control treatment of 'long' samples with neuraminidase reduced the molecular weight (Fig. 6.2A) and abolished detection by anti-polysialic acid antibodies in

the Western blot analysis (Fig. 6.2B). These data indicate that sialic acid chains of different lengths were successfully coupled to primed HEL.

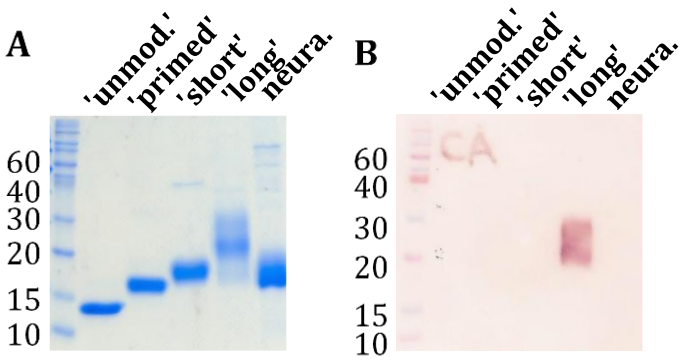

Fig. 6.2: SDS-PAGE analysis of masked HEL. A: Coomassie-stained SDS-page analysis of HEL unmodified and modified by chemical 'priming' and subsequent enzymatic addition of short and long sialic acid chains; 'unmod.' = unmodified HEL; 'primed' = protein modified with a lactose primer motif that can be recognised by subsequent enzymes; 'short' = protein bearing shorter sialic acid chains formed by reaction of primed protein with Cst-II; 'long' = protein bearing longer sialic acid chains formed by reaction with both enzymes Cst-II and PST; neura. = 'long' material after neuraminidase treatment; **B**: Western blot analysis with anti-polysialic acid antibody; CA = colominic acid blotted on membrane as positive control. Experiment performed with H. Schuster.

In order to more precisely measure the molecular weight of the different glycoforms, mass spectrometry was performed using LCT-ESI. In this analysis, primed HEL was almost exclusively detected as a single peak with a molecular mass of 16,688 Da (Fig. 6.3 and Table 6-1) which corresponds to 6 lactose residues coupled per HEL molecule. HEL contains 6 lysine residues which are the primary targets for IME reagents. Normally, the N-terminal α-amine of proteins is also targeted although at a lower efficiency (Lee et al., 1976; Stowell and Lee, 1980; Stowell and Lee, 1982). In the case of HEL, the N-terminal amino-acid is itself a lysine residue which might further reduce the coupling efficiency and thus coupling of 6 lactose residues to the protein was interpreted as 100% coupling efficiency.

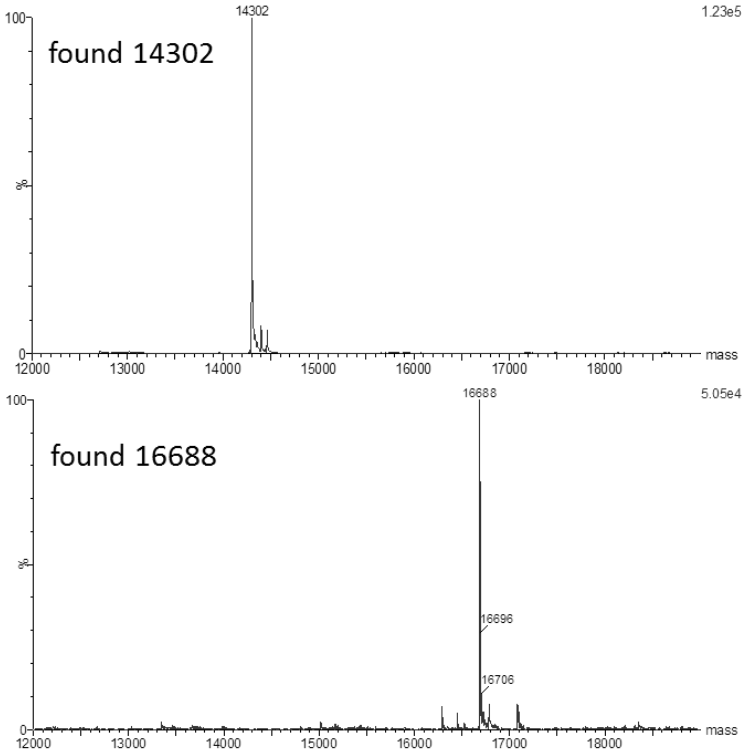

Fig. 6.3: LCT-ESI mass spectrometry analysis of primed HEL. Experimentally found masses for unmodified (top) and primed (bottom) HEL are indicated in Da. The theoretical molecular mass for HEL + 6 lactose residues coupled via IME chemistry is 16,688 Da.

LCT-ESI analysis of 'short' and 'long' samples was not successful and instead MALDI-TOF analysis was performed to analyse the molecular weight of these samples (Fig. 6.4 and Table 6-1). The molecular weight of primed HEL increased by ~1.0 kDa during CST-II mediated sialic acid coupling. This corresponds to the addition of only ~2.5 sialic acid residues per molecule. Subsequent modification of the 'short' sample with PST rendered 'long' chains corresponding to ~16.3 sialic acid molecules per protein with a wide range of molecular weights, equivalent to 1-33 residues.

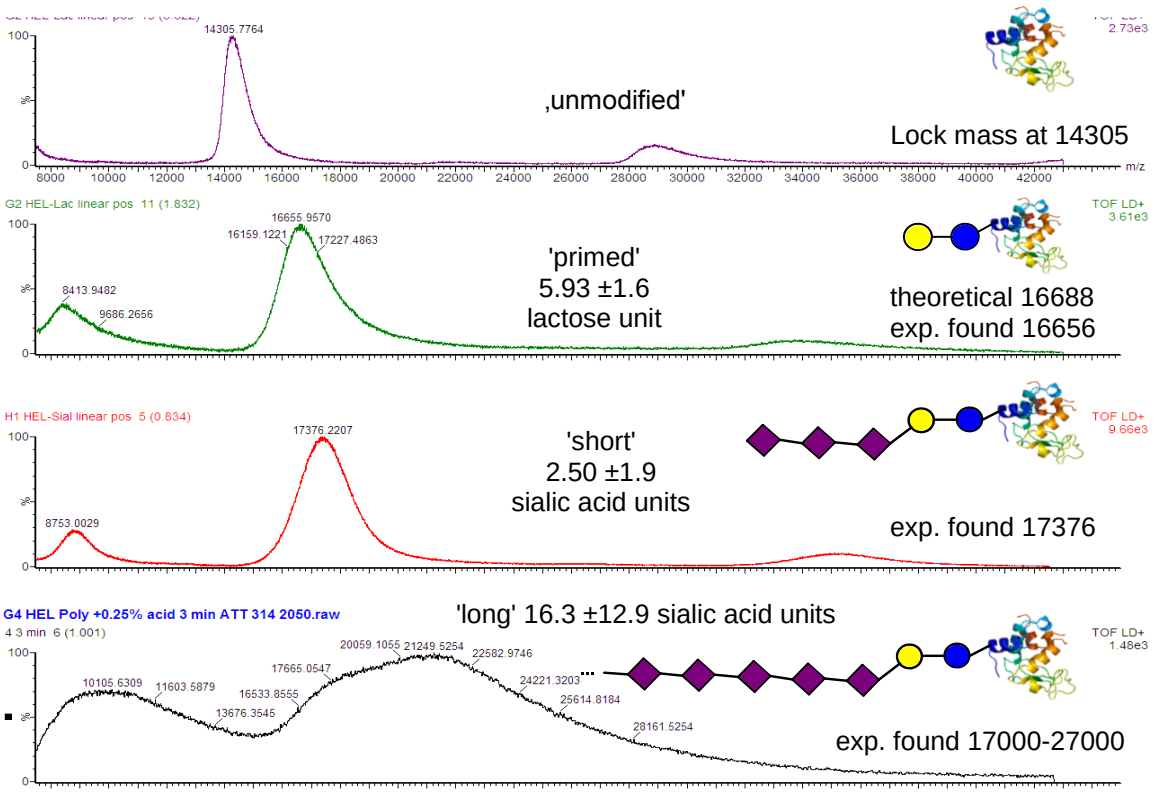

Fig. 6.4: MALDI-TOF spectra of intact proteins. Experimentally found masses as well as the corresponding number of glycan moieties are indicated. Experiment performed by H. Schuster.

Further extensive characterisation of the samples by MS/MS was performed by H. Schuster and confirmed coupling of exactly one lactose residue to each lysine residue within the coverage area (no data was obtained for lysine 96) including the N-terminal lysine residue (data not shown). The presence of sialic acid could only be confirmed for lysines 33 and 116. Chain length analysis showed ~3 and ~11 sialic acid residues per chain for ‘short’ and ‘long’ samples respectively (Table 6-1).

Taken together, these data show that all lysine residues of HEL were modified by lactose via IME chemistry. Enzymatic addition of sialic acid using CST-II only added on average 3 sialic acid residues per protein which were mostly added to a single primed modification site as a chain of 3 residues. The preferential sites for this modification were lysine 34 and

lysine 116. PST elongated these chains to varying degrees leading to chains with an average of 11 sialic acids.

Correct folding of the samples was analysed by circular dichroism analysis. All samples showed signs of secondary structure in this analysis (Fig. 6.5). The difference between 'long' and unmodified samples resembled the published spectrum for polysialic acid. Finally, the enzymatic activity of HEL was tested before and after modification. In this assay, 'primed' HEL was virtually indistinguishable from 'unmodified' enzyme (Table 6-1). 'Short' and 'long' HEL modifications still showed activity although at substantially reduced levels. In conclusion, these data show that modification of HEL retains the overall folding of the protein.

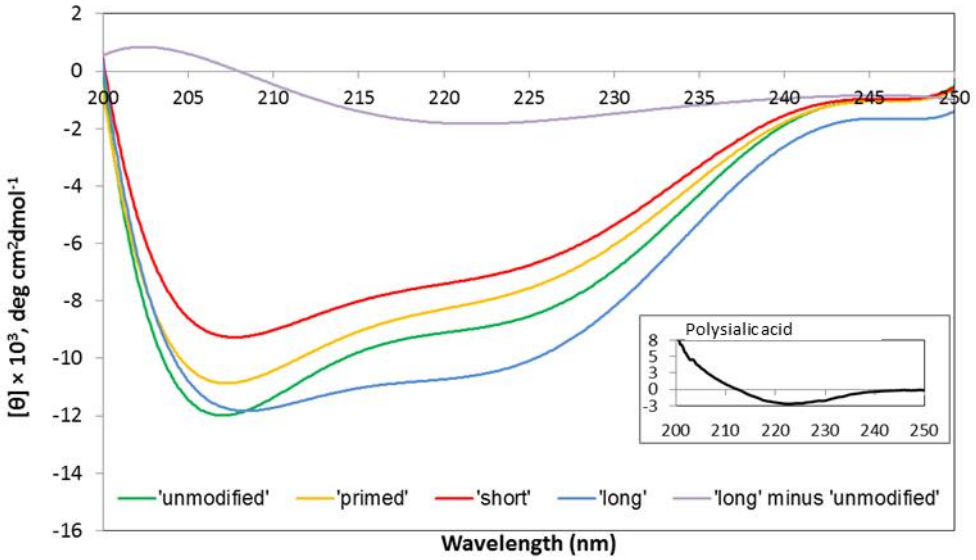

Fig. 6.5: Circular dichroism data of the unmodified and modified lysozyme samples. The small insert shows circular dichroism for commercial polysialic acid. Assay was performed by H. Schuster.

Table 6-1: Summary of analyses performed on masked HEL

	Secondary structure		Gel analysis [kDa]	Mass spectrometry [kDa]		Modification level [residues]			Enzyme Activity [U/ml]
	^{1}H-NMR	CD	SDS-PAGE	LCT-ESI	MALDI-TOF	LCT-ESI	MALDI-TOF	Chain length	EnzChek
unmod.	✓	✓	14.3	14.3	14.3	–	–	–	622.01 ± 0.04
primed	✓	✓	16.6	16.7	16.7	6.00	5.93 ±1.6	–	612 ± 2
short	✓	✓	17.3	–	17.4	–	2.50 ± 1.9	avg. 3	259.0 ± 0.6
long	✓	✓	20.7	–	18.0-25.5	–	16.3±12.9	avg. 11	153 ± 0.9

6.2.3 Antigenicity and immunogenicity of modified HEL

After confirming successful coupling of sialic acid chains to the protein without disrupting its structure or function, the effect of the modifications on antibody recognition were tested *in vitro*. The binding of four different well characterised mAbs (D1.3 (Fischmann et al., 1991) and F10 (Cauerhff et al., 2004)) or camelid Vhh (D2-L29 (De Genst et al., 2006) and cAb-Lys3 (Decanniere et al., 2001)) targeting distinct (though partially overlapping) structurally defined epitopes on the protein was tested. One of these antibodies (D1.3) targets an epitope that contains a modification site (Fig. 6.6A) whereas the other three mAbs bind to epitopes devoid of lysine residues (although lysine residues are in close proximity to all epitopes). SPR analysis showed that with increasing length of the sialic acid chain, the affinity of most mAbs decreased (Fig. 6.6B). Interestingly, the loss of affinity was almost entirely due to decreased on-rates, consistent with steric hindrance of antibody binding, whereas the off-rates remained virtually unchanged (Fig. 6.6B).

In accord with the design of the glycan masking strategy, the loss of binding was epitope-specific ranging from negligible decreases in binding for D2-L29 to almost 20-fold reduced

binding of D1.3 to the 'long' sample. These results correlate with the location of the modification sites since D1.3 binds directly to a lysine residues and is in close proximity to several others whereas the D2-L29 epitope does not interact directly with any lysine residues and the amino groups of the two closest lysine residues are oriented away from the epitope (Fig. 6.6A). Thus, glycan masking leads to predictable site-specific reduction in antibody recognition *in vitro*.

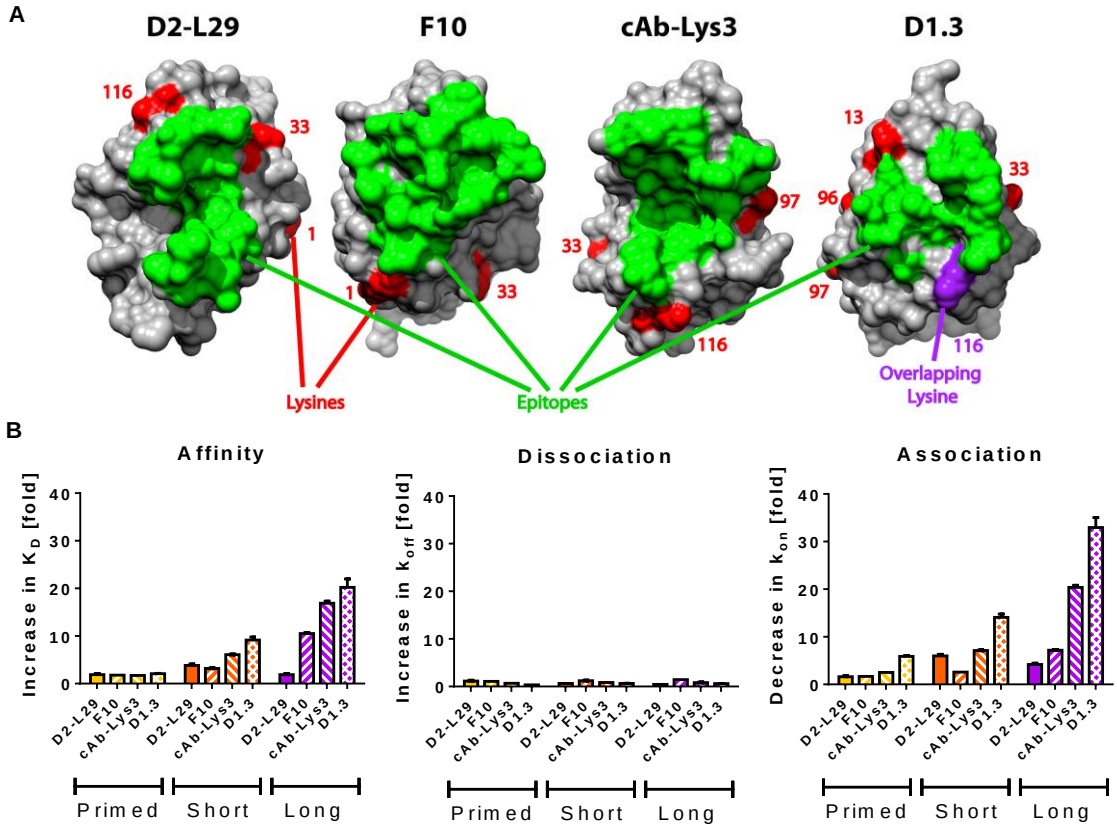

Fig. 6.6: Antigenic properties of modified HEL. A: Epitopes (green) of mAbs and Vhh on HEL (grey), with lysines (red) numbered according to the amino acid sequence of HEL in proximity to the epitopes highlighted. **B:** Modified ligand k_{on}, k_{off} and K_D for modified HEL compared to unmodified protein as determined by SPR.

To test the effect of glycan masking on antibody refocusing *in vivo*, BALB/c mice (n=5 per group) were immunised with the different glycoforms of HEL in carbopol adjuvant. Each animal received 3 immunisations spaced 3 and 4 weeks apart and serum samples were

collected before each immunisation as well as at week 12. Strong serum IgG titres were detected in animals immunised with unmodified protein (Fig. 6.7A). Animals immunised with 'short' or 'long' samples showed somewhat delayed responses compared with unmodified protein but strong responses were detectable after the second immunisation. By contrast, 'primed' samples did not induce strong antibody responses.

To further characterise the binding antibody responses, endpoint titres for sera from the final time point were determined against modified HEL (Fig. 6.7B). Generally antibody titres against these proteins were similar to those observed against unmodified HEL, with similar titres measured for animals receiving unmodified, 'short' or 'long' protein but lower titres for animals immunised with 'primed' antigen. In addition, antibody titres against 'primed' (lactose-modified) unrelated protein HIV-1 gp120 were measured to quantify glycan-specific responses. As expected, animals immunised with unmodified HEL did not develop antibody responses against lactose (Fig. 6.7B). In contrast, varying levels of anti-glycan responses were detected in some but not all of the animals receiving either of the modified immunogens (Fig. 6.7B).

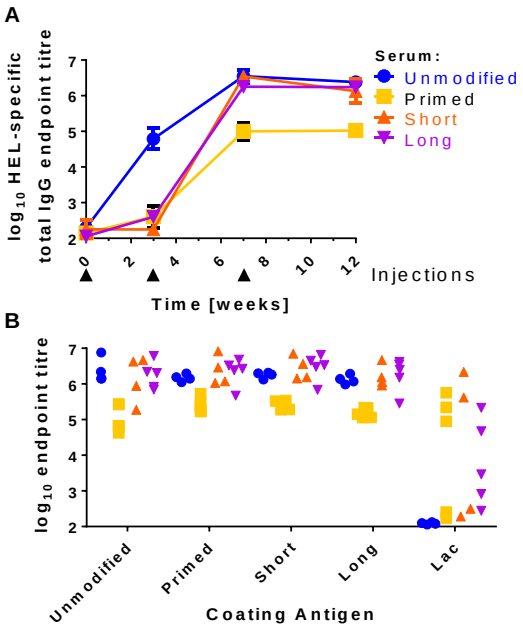

Fig. 6.7: Total HEL-specific IgG response of mice immunised with HEL variants. BALB/c mice (n=5 per group) were immunised with HEL variant at weeks 0, 3 and 7. One animals from the 'short' group had to be prematurely sacrificed due to unrelated illness. **A:** Serum samples of the remaining animals were collected at the indicated time points and total IgG endpoint titres against unmodified HEL were determined by ELISA. **B:** Sera from the final bleed were titrated against the indicated HEL variants ('Unmodified', 'Primed', 'Short' or 'Long') or lactose-modified unrelated protein HIV-1 gp120 (Lac).

To investigate whether glycan masking led to the desired refocusing of antibody responses, epitope mapping was performed by cross-competition ELISA. Since 'primed' HEL did not induce antibody responses, these samples were not included in this analysis. Cross-competition analysis showed that responses towards the masked D1.3 epitope were ~4.3-fold ($p = 0.03$) reduced in the 'short' samples (Fig. 6.8). 'Long' HEL also showed a trend towards lower responses for this epitope although this trend did not reach statistical significance ($p = 0.053$). Thus, glycan masking can dampen antibody responses towards masked epitopes.

By contrast, ~7.5-fold increased antibody responses were detected against the D2-L29 epitope in animals immunised with 'short' samples (p = 0.04). D2-L29 was one of the antibodies targeting an epitope devoid of modification sites and showed the lowest loss in affinity upon glycan modification. Consistent with the affinity measurements, F10 and cAb-Lys3 showed intermediate levels of cross-competition which were not significantly different to those from animals immunised with unmodified samples.

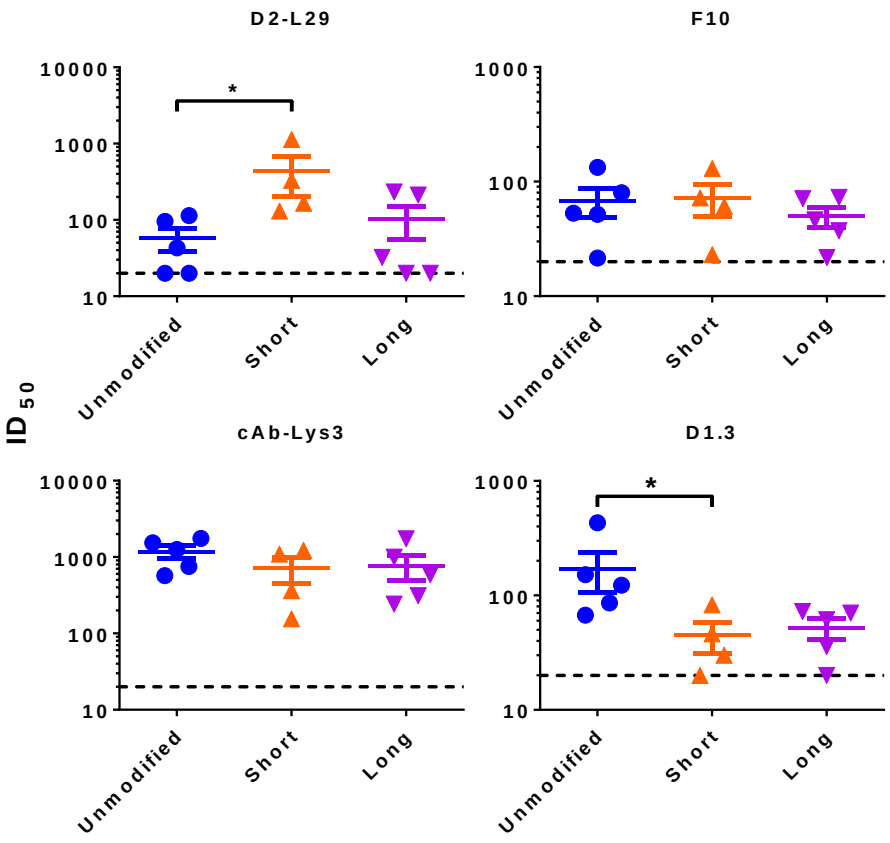

Fig. 6.8: Epitope mapping of sera from immunised mice. Cross-competition with biotinylated HEL-specific antibodies of sera from mice immunised with unmodified or sialic acid-containing HEL was measured by ELISA. Sera from mice immunised with 'primed' HEL were not used for competition analysis since the titres of HEL-specific antibody were too low. * $p < 0.05$ in a one-way ANOVA with Sidak's post-test.

Taken together, these data show that glycan masking can site-specifically lower antibody-recognition which leads to reduced immunogenicity of masked epitopes *in vivo*. Concomitantly, antibody responses towards some epitopes devoid of modification sites

can increase, thus providing proof-of-principle of refocusing of antibody responses by glycan masking.

6.2.4 **Modification of HIV-1 gp120**

After providing proof-of-principle of predictive refocusing of antibody responses by glycan masking on model protein HEL, attempts were made to transfer this strategy to the more relevant glycoprotein gp120. gp120 (strain Bal) was primed with lactose followed by modification with CST-II and PST. Western blot analysis of this glycoprotein showed a shift in molecular weight upon lactose coupling (Fig. 6.9). This shift in molecular weight was approximately 7.3 kDa in size, corresponding to ~18.3 lactose residues (= 57 % coverage). However, subsequent sialic acid with 'short' or 'long' chains yielded only small shifts (< 0.5 kDa) equivalent to 0-1 sialic acid residues (< 5 % coverage). Several attempts to increase the coupling efficiency with increased enzyme or substrate concentrations were unsuccessful (data not shown). Thus, only the lactose primer could quantitatively be added to gp120 protein.

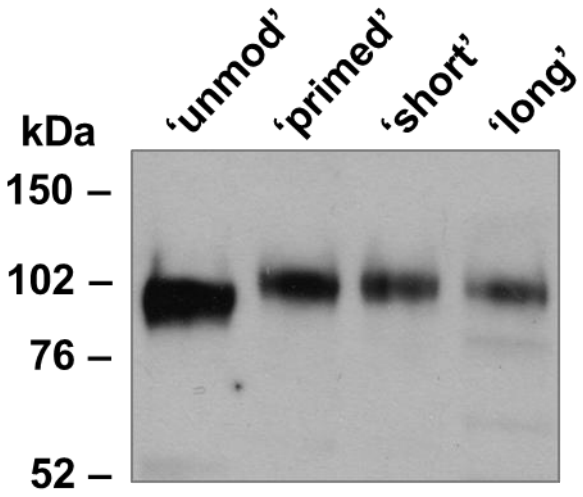

Fig. 6.9: Modification of HIV-1 gp120. HIV-1 gp120 (strain BAL) was modified with lactose (primed) followed by sialic-acid addition by CST-II (short) and PST (long). Proteins were

separated by SDS-PAGE and analysed by Western blot using polyclonal antibody HIVIG for detection.

Since sialic acid addition was unsuccessful, antibody recognition could only be analysed for the lactosylated sample. Therefore, binding of a panel of mAbs to modified gp120 was measured by ELISA (Fig. 6.10). Glycan-specific mAb 2G12 was used as a loading control since this mAb should not be influenced by lactosylation. In fact, binding of 2G12 to unmodified and lactosylated gp120 was comparable (Fig. 6.10A).

The only exclusively protein-based (i.e. not involving glycans) broadly neutralising epitope on gp120 known to date is the CD4bs and therefore binding of CD4bs mAbs including bNmAbs VRC01 and b12 was tested. Substantial reductions in antibody binding to lactosylated gp120 was detected for all CD4bs mAbs tested (Fig. 6.10B). This is consistent with the presence of a modification site within this epitope as well as several additional lysine residues in close proximity (Fig. 6.10B).

Prominent epitopes on gp120 that are common targets of non- or narrowly neutralising antibodies include the variable loops V2 and V3, the latter of which is often immunodominant. HGP68, a mAb targeting the V2 region, showed no difference in binding to unmodified or lactosylated gp120 (Fig. 6.10C). No crystal structure is available defining the precise epitope of this mAb but the epitope has been characterised by peptide array (Corti et al., 2010a). According to these data, the HGP68 mAb binds to a residue which is equivalent to a lysine residue in the BAL sequence. However, this lysine residue is at the very edge of the proposed epitope and peptide-scanning data might not be this precise, in particular since the mapped sequence and the Bal sequence are very different in this region (Fig. 6.10C). Binding of V3-loop specific antibody HR10 was almost completely abolished

upon lactose addition, consistent with the presence of a lysine epitope in the proposed epitope of this mAb. Similarly, binding of CD4i mAb 17b was abolished due to the presence of a lysine residue within this epitope.

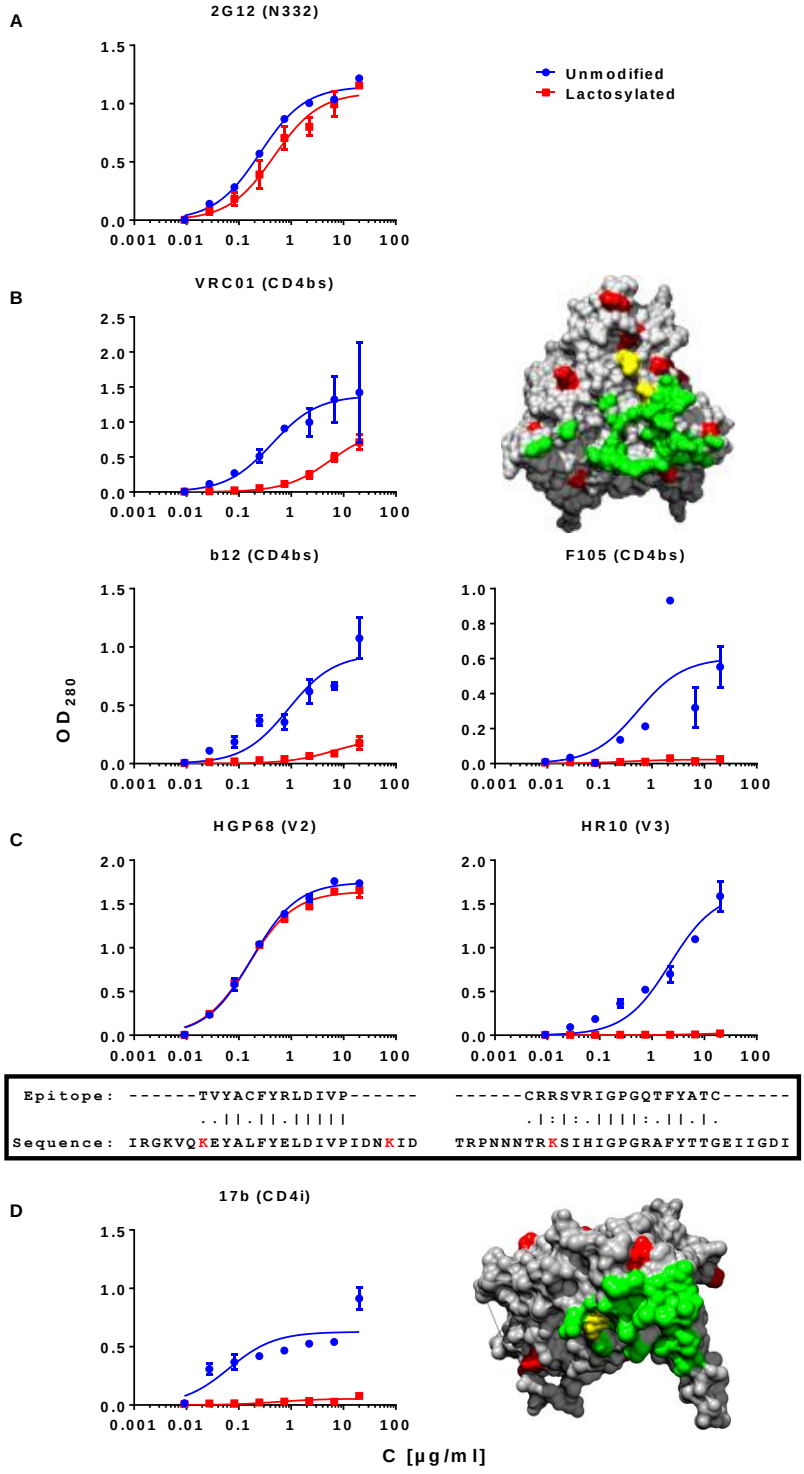

Fig. 6.10: Antigenicity of 'primed' gp120. HIV-1 gp120 (strain Bal) was modified with lactose and antibody recognition was analysed by direct ELISA. Crystal structures are shown where available (green: epitope; red: lysine residue; yellow: lysine residue within epitope). Glycan-

specific mAb 2G12 (A) was used as a loading control. Other epitopes include the CD4bs (B), the variable loops (C) and the CD4i epitope (D). Approximate epitopes for HGP68 and HR10 are indicated based on peptide array data.

Taken together, lactose-coupling to gp120 led to site-specific reductions in antibody binding of mAbs with a confirmed lysine residue within their epitope.

6.3 Discussion

In this chapter, a strategy for refocusing of antibody responses by chemo-enzymatic glycan masking was devised. Given that many viral envelope proteins including HIV-1, influenza A and Hepatitis C are themselves glycoproteins (Julien et al., 2012; Kong et al., 2013a), the easiest method to mask immunodominant epitopes might be by incorporating additional N-linked glycosylation sites. In fact several attempts have been made to use N-linked glycosylation sites for such purposes (Pantophlet et al., 2003; Selvarajah et al., 2005; Selvarajah et al., 2008; Sampath et al., 2013). However, the use of N-linked glycosylation sites has two major drawbacks compared to the chemo-enzymatic approach used here. Firstly, N-linked glycosylation sites can have an impact on folding and processing of the glycoproteins (Daniels et al., 2004). In addition, N-linked glycosylation sites are not utilised in 100% of cases but can be skipped in a stochastic manner (Jones et al., 2005). In a recent analysis of a HIV-1 gp120-based glycoprotein, a particular N-linked glycosylation site was not utilised in ~10% of the glycoproteins (Jardine et al., 2013). Taken together these problems reduce the utility of glycan masking by N-linked glycosylation. Moreover, previous attempts to use N-linked glycosylation sites for glycan masking of HIV-1 gp120 failed to selectively re-direct antibody responses (Pantophlet et al., 2003; Selvarajah et al., 2005).

To circumvent the problems associated with N-linked glycosylation sites, the strategy devised here uses chemo-enzymatic addition of glycans onto fully folded proteins. This chemo-enzymatic approach combines the advantages of control of chain position (using chemistry) with enzymatic chain extension and polymerisation that is highly stereo-, regio- and chemo-selective. By attaching the glycans to already fully folded proteins the impact on folding should be minimised. Furthermore, the IME chemistry chosen for chemically linking the lactose primer to the protein is very selective and does not substantially alter the pKa of the side-chain, thus further reducing the risk of altering the folding of the protein (Lee et al., 1976; Stowell and Lee, 1980; Stowell and Lee, 1982). The addition of the sialic acid was chosen because sialic acid is often found as the capping glycan on naturally occurring glycans including N-linked glycans and is supposedly very immunosilent (Brisson et al., 1992). Finally, using the sequential action of two different enzymes for sialic acid addition allowed control over the length of the attached sialic acid chains which might play an important role in glycan masking.

Chemical coupling of the lactose primer to model protein HEL was highly specific for lysine residues as confirmed by MS/MS analysis. 100% coverage could be achieved although relatively high amounts of glycan were required (250 equivalents per lysine residue), probably due to a competing reaction with water which occurs in aqueous solution, in particular at low but also at physiological pH (Stowell and Lee, 1982). Nevertheless, full coverage was achieved and did not impact folding or function of the protein.

Subsequent enzymatic addition of sialic acid to the lactose primer by CST-II was very inefficient. On average only a single site was utilised per protein and chains of 3 sialic acids

were attached to these sites leading to a coverage of ~14 %. Preferential sites were lysines K33 and K116. The action of enzyme PST elongated these existing chains, leading to average chain lengths of ~11 sialic acid residues, although the length of these chains was quite variable.

In vitro, glycan addition led to site-specific reductions in antibody binding, in particular mAb D1.3 which bound directly to a glycosylation site. It should be noted that D1.3 bound directly to K116 which is one of the two preferential sites for sialic acid addition. The second preferential site, K33, is in very close proximity to this epitope. Reduced binding might either be due to changes in structure of the target protein or might be due to steric hindrance. The finding that reduced affinity was due to reduced on-rates strongly supports the concept of steric hindrance.

In vivo, studies showed very low immunogenicity of the 'primed' protein. This behaviour might be caused by scavenging of D-galactosyl terminal residues by the hepatic asialoglycoprotein receptor (Robinson et al., 2004). However, since the lactose-residues served only as a primer for the sialic acid transferase, this behaviour was not further investigated. By contrast, the 'short' and 'long' sialic acid chains showed slightly delayed immunogenicity that did reach the same levels as unmodified protein after the second immunisation. Anti-glycan responses were detected in some of the animals immunised with modified HEL, but the magnitude of these anti-lactose responses ranged from almost undetectable (~100) to very strong (~10^6) titres in all 3 groups receiving modified protein.

Epitope mapping of the sera from immunised mice showed that glycan masking led to site-specific loss of immunogenicity of lysine-containing epitopes, which was expected due to the steric hindrance of the glycans on B-cell receptors targeting such epitopes. Even more importantly, glycan masking not only reduced the antibody responses to such epitopes but also refocused responses towards non-covered epitopes. This effect might be explained by competition between B cells in the germinal centres (Victora et al., 2010; Natkanski et al., 2013; Gitlin et al., 2014). In the absence of glycan masking, B cells targeting immunodominant epitopes outcompete B cells directed towards sub-dominant epitopes. However, when the dominant epitopes are masked, B cells targeting these epitopes can no longer bind and are removed from germinal centre competition thus allowing previously sub-dominant epitopes to be activated. An alternative explanation might be that of competition for T-cell help (Gitlin et al., 2014), whereby T-cell help is limiting for the activated B cells, meaning that reducing B cell reactivity to otherwise immunodominant epitopes might release T-cell help for B cell targeting previously immunorecessive epitopes. The glycan masking strategy was most successful with short sialic acid chains, whereas longer chains reduced overall reduction in immunogenicity. Therefore, short chains were selected for future studies.

After providing proof-of-principle of antibody refocusing by glycan masking on the model protein HEL, attempts were made to transfer the technique to the more relevant protein HIV-1 gp120. However, coupling efficacy was lower than for model protein HEL. In particular, sialic acid addition by CST-II was virtually undetectable. The reason for the lower activity on gp120 compared to HEL is unclear but it should be noted that even on HEL this step only produced a coverage of ~14%. Given the extensive N-linked glycan shield of

gp120, it is conceivable that access to the short lactose primers was impeded by the much larger N-linked glycans (in this case homogenous Man-5 glycans produced by HEK-293S GnT-I$^{-/-}$ cells). Several attempts to overcome this barrier were unsuccessful and alternative strategies of glycan coupling had to be explored as described in chapter 7. Nevertheless, some important insights could be gained from these experiments. Lactose-priming led to selective alterations in antibody recognition *in vitro*. Unfortunately, binding of antibodies targeting the well-conserved CD4bs was reduced after glycan conjugation, although this was not unexpected due to the presence of lysine residues within the footprint of CD4bs mAbs. Thus, attempts to redirect antibody responses towards this epitope by glycan masking would need to include the remodelling of the lysine residue coverage of the protein.

Taken together, the data presented in this chapter provide proof-of-principle of antibody refocusing by glycan masking. Short sialic acid chains chemo-enzymatically added to the target protein proved most successful in the predictable redirection of antibody responses. Thus, this strategy has the potential to be a useful tool in future vaccine design.

Chapter 7: Glycan masking using 3'-sialyllactose

7.1 Introduction

In the previous chapter, proof-of-principle of antibody refocusing by glycan masking was provided. Site-selective addition of sialic acid chains to model protein HEL led to selective modulation of antibody binding *in vitro* which translated into alterations of antibody responses *in vivo*. The coupling of glycans was performed in a multi-step procedure starting with the chemical addition of a lactose primer to lysine residues followed by enzymatic polymerisation of sialic acid *in situ*. Whereas the first step, the chemical coupling of lactose, provided high coverage of target sites, the following sialic acid addition by CST-II was very inefficient and coupling of sialic acid was undetectable when HIV-1 gp120 was used as the target protein. Here, a new coupling strategy was devised in which the coupling of sialic acid to the lactose primer was performed prior to the established linking of the glycan to the target protein via IME chemistry.

An additional finding in the previous chapter was that short sialic acid chains are better able to redirect antibody responses in the glycan masking strategy than long chains, but lactose on its own is not suitable for masking as it abolishes immunogenicity of the target protein. 3'-sialyllactose (SiaLac), lactose coupled to a single sialic acid, has previously been shown to be very immunosilent (Pan et al., 2005) when chemically coupled to a carrier protein. SiaLac forms the glycan portion of ganglioside GM3 which is found in low concentration on many animal cells (Tsuchida et al., 1987). Since GM3 is highly upregulated in many cancer cells (Yu et al., 2011) it is the target of some cancer-vaccine approaches (Hakomori and Zhang, 1997; Bitton et al., 2002; Yu et al., 2011).

Here, a pre-assembled mono sialic acid reagent SiaLac-IME was developed and tested for its suitability for glycan masking. This construct was then used in site-selective glycan masking of viral glycoprotein antigens from HIV-1 and influenza A.

7.2 Results

7.2.1 *In vitro* assessment of SiaLac for glycan masking

Based on the results obtained in the previous chapter, a revised glycan masking strategy was devised in which SiaLac trisaccharides were pre-assembled and subsequently transferred *en bloc* onto the target molecule via IME chemistry (Fig. 7.1). SiaLac-IME reagents were developed in collaboration with Regis Saliba and Karolis Leonavicus in Benjamin G. Davis' lab. Similar to previous experiments with lactose, full coverage of lysine residues was achieved on model protein HEL as shown by mass spectrometry (Fig. 7.2A).

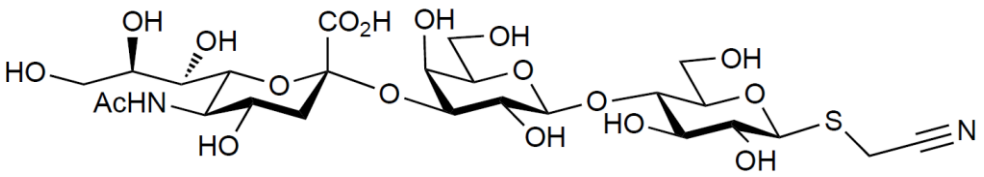

Fig. 7.1: Chemical structure of Sia(α2,3)Lac S-cyanomethyl glycoside used in IME coupling of SiaLac to lysine residues of the target protein.

Similar to the experiments from chapter 6, binding of 4 mAbs targeting distinct epitopes (Fig. 7.2B) on modified HEL was tested. Masking led to up to 5-fold losses in EC_{50} (Fig. 7.2C). In addition, a mutant HEL protein was designed, cloned, expressed, purified and modified with SiaLac that had a new lysine residue introduced into the centre of the F10 epitope (Fig. 7.2B). As expected, introducing this mutation had a major impact (9-fold loss in EC_{50}) on F10 binding upon SiaLac modification whereas the other antibodies were less affected (Fig.

7.2C). Thus, the SiaLac-IME reagent can be coupled to lysine residues with a high efficiency of occupancy and leads to predictable and selective loss of mAb binding to masked epitopes.

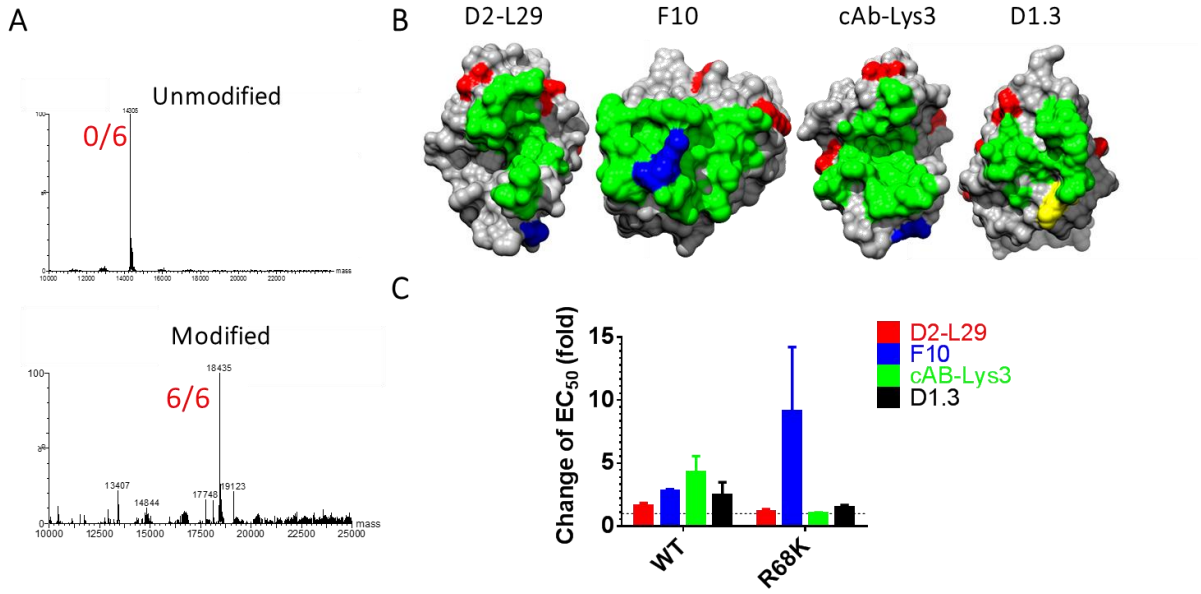

Fig. 7.2: SiaLac modification of HEL. A: LCT-ESI MS of unmodified or SiaLac modified HEL. **B:** Structures of HEL displaying the indicated mAb footprints (green). Red: lysine residues; yellow: lysine residue within epitope; blue: R68K mutation in the mutant protein. **C:** The effect of SiaLac masking is shown as a fold-change according to ELISA analysis.

7.2.2 Development of antigens for SiaLac glycan masking

Since an efficient coupling method of SiaLac was now available, a pipeline was developed in which a series of more relevant antigens were developed that were optimised for glycan masking (Fig. 7.3). Starting with an atomic resolution crystal structure of the target glycoprotein antigen as well as knowledge of broadly neutralising epitopes within the target antigen, lysine mutants were design by a combination of computational modelling and analysis of natural variants found in circulating strains. The mutants should have lysine mutants appropriately spaced across the whole surface area to sterically prevent binding of B cell receptors (in particular to immunodominant epitopes). Only the bNAb epitopes should remain lysine-free thus presenting the only antibody-accessible surface and thus

refocusing antibody responses towards these epitopes. Following computational design, a number of such mutants were assembled by site-directed mutagenesis or gene synthesis. Initially, the corresponding genes were tested for expression and correct folding using small-scale expression, followed by capture ELISA with a panel of conformation-dependent mAbs. If appropriate mutants were found, large-scale expression and purification were performed and the purified proteins modified with SiaLac. The effect of the masking was then analysed *in vitro* using antibodies targeting both 'masked' non-neutralising epitopes and 'unmasked' epitopes. If the antigenicity profile was found to be satisfactory, animal studies were conducted and the effect of glycan masking on antibody refocusing analysed *in vitro*. Based on these results, lysine mutants could then be re-optimised, leading to multiple developmental cycles.

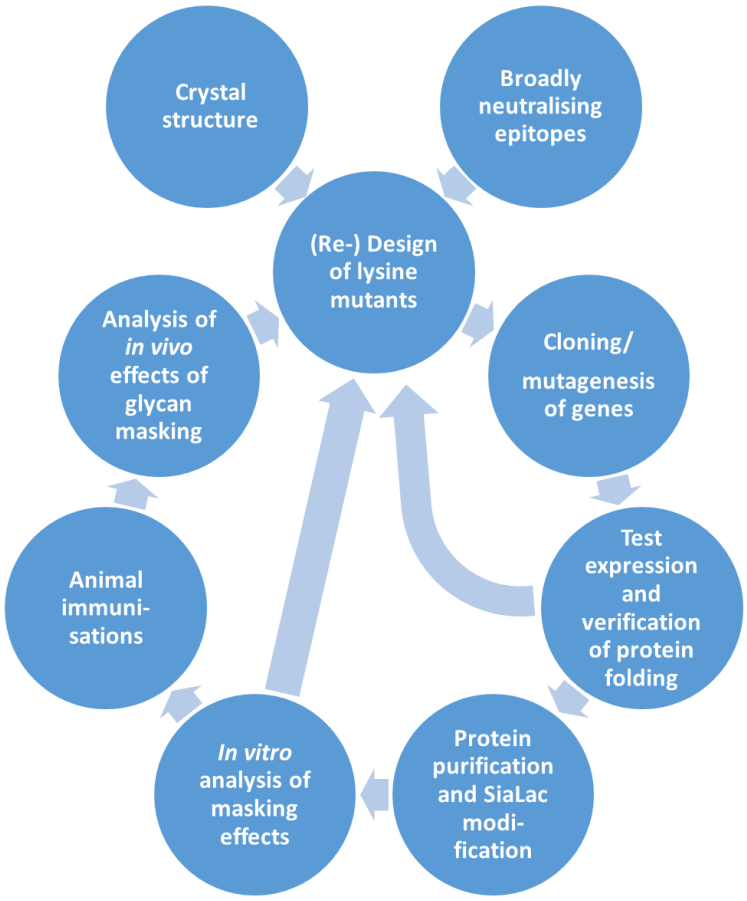

Fig. 7.3: Schematic of the cyclic development of antigens for glycan masking.

This strategy for the development of antigens for glycan masking was transferred to a series of more relevant antigens derived from HIV-1 and influenza surface glycoproteins. Initially, a series of lysine mutants was developed based on a gp120 glycoprotein with the variable loop V2 removed (Δ121-203) but with an intact V3 loop (full sequence in the appendix). The reason for retaining the V3 loop was that it presents a well-characterised immunodominant epitope that allowed the ready investigation of the masking ability of the SiaLac reagent. The final design chosen was based on the HxBc2 viral clone. In addition to this "WT" glycoprotein, a lysine mutant (KM) was designed in which three lysine residues in proximity or overlapping with the CD4bs were mutated to arginine. Mutating these residues aimed at retaining this neutralising epitope available for B-cell recognition upon SiaLac addition, thus focusing antibody responses towards this area. In addition, five additional lysine residues, including R315K in the GPGR motif of the V3 loop), were introduced throughout the remaining protein surface to achieve better coverage and thus immuno-silencing the remaining protein for improved antibody refocusing. Folding of this protein, as well as a series of related designs, was confirmed by binding of conformation-dependent antibodies (Fig. 7.4 and data not shown).

After developing correctly folding gp120 mutants, proteins were expressed in suspension and serum-free-adapted HEK-293S GnT-I$^{-/-}$ cells achieving yields of ~45 mg/l. Proteins were purified, followed by glycan masking with SiaLac. Coupling efficacy was estimated to be close to 100% (26 ± 2 of 25 lysines modified for WT protein, 28 ± 2 of 27 sites modified for KM) as analysed by SDS-PAGE (Fig. 7.4A), and Western blot of de-glycosylated gp120 to eliminate all natural N-linked glycans but leave lysine-adducted SiaLac moieties (not shown).

ELISA analysis showed substantially (~18 and 33 fold higher EC_{50} for WT and KM proteins respectively) reduced antibody recognition of V3-loop-directed antibodies after masking (Fig. 7.4C), consistent with the presence of one and two modification sites within this epitope for WT and KM proteins respectively. Antibodies to the CD4bs showed varying results. Some antibodies including bNmAbs VRC01 and HJ16 were not affected by masking at all, despite the presence of lysine residues within this epitope (Fig. 7.4B). A probable explanation for this behaviour is that the lysine residues are at the very edge of this epitope, which, combined with the flexibility of lysine side chains, might allow the binding of some mAbs with an appropriate binding angle to the masked protein. On the other hand, some weakly or non-neutralising CD4bs mAbs including b12, F105 and 15e bound less to masked protein compared to the unmodified protein as expected (Fig. 7.4C and data not shown). In all cases, this effect was more pronounced in WT protein compared to KM and in fact mAb 15e was only affected in the WT but not the KM protein (not shown).

Based on these results, an improved lysine mutant was designed which had a total of five lysine residues proximal to the CD4bs removed (Fig. 7.4B). Furthermore, a total of eight lysines were added to the protein including three additional lysine residues within the V3 loop bringing the total number of modification sites within this region to five. The addition of these lysine residues to the KM2 protein led to a complete loss of binding of V3-loop mAb HGN194 upon SiaLac masking (Fig. 7.4D and data not shown). By contrast, the removal of additional lysine residues near the CD4bs resulted in complete preservation of all CD4bs mAbs tested.

Taken together, these data show complete masking of gp120-based antigens that led to reduced binding of mAbs targeting weakly or non-neutralising epitopes whilst mostly preserving binding of CD4bs bNmAbs.

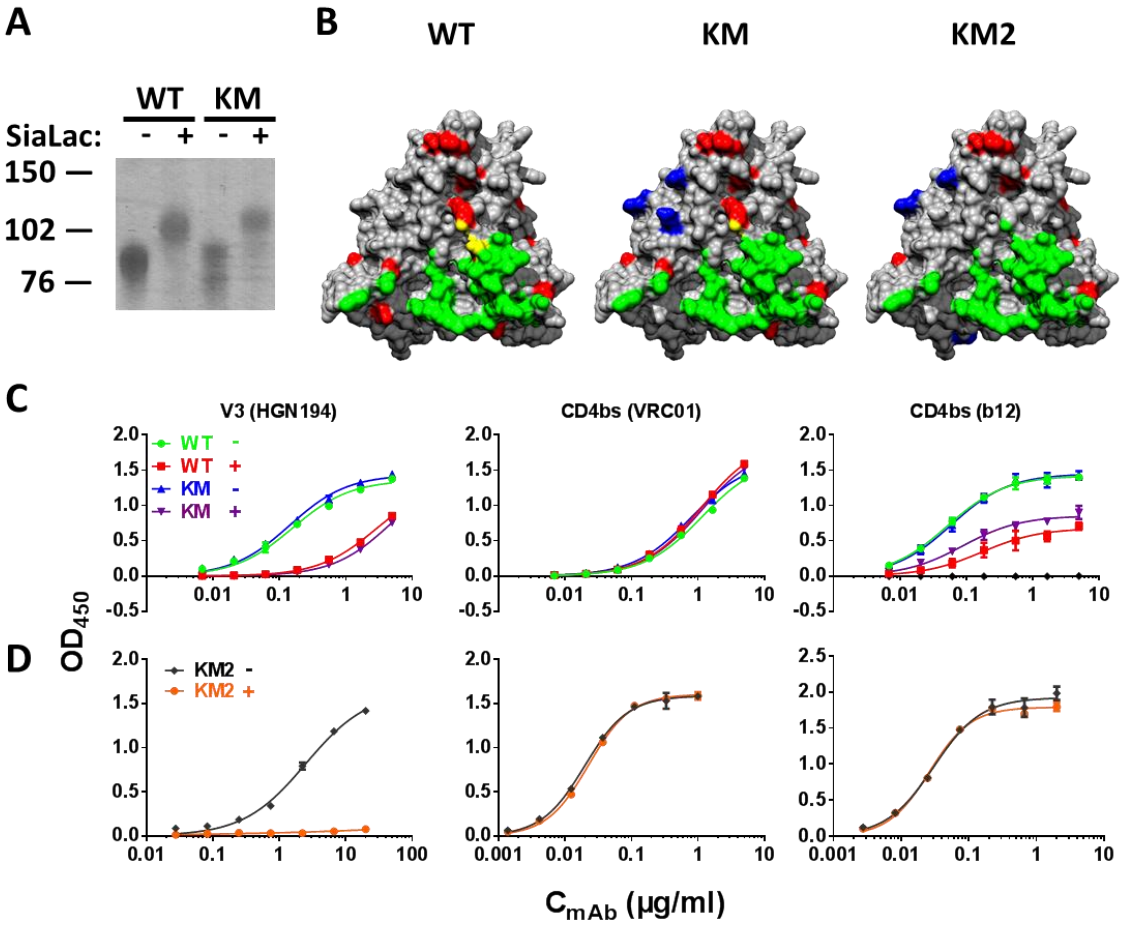

Fig. 7.4: Glycan masking of gp120 lysine mutants. A: SDS-PAGE analysis of SiaLac modified protein. Numbers indicate sizes of the molecular weight marker (in kDa). **B:** Structure of the lysine mutants with the broadly neutralising epitope (VRC01) indicated in green, lysine residues in red, new lysine residues in blue and lysine residues within the epitope in yellow. **C+D:** ELISA analysis of unmodified (-) or SiaLac modified (+) proteins by 3 representative antibodies covering the immunodominant V3 loop and the broadly neutralising CD4bs. Data shown include the wild-type protein (**C**), the first generation lysine mutant (KM, **C**) and the revised lysine mutant (KM2, **D**). Error bars indicate SD of technical repeats. Data in **C** are representative of 3 independent experiments.

The initial gp120 design described above still contained a range of unwanted structures, such as the V3 loop, which could easily be removed. In fact, broadly neutralising CD4bs antibodies of the VRC01 class almost exclusively bind to the outer domain of gp120 and a

number of outer-domain proteins have been designed that stabilise this domain in the absence of the inner domain (Pejchal et al., 2011; Jardine et al., 2013; Joyce et al., 2013). One such protein is eOD-base (engineered outer domain) from the Schief lab (Pejchal et al., 2011; Jardine et al., 2013) and another range of mutations was designed based on this protein. In the final design, three lysine residues were removed from the vicinity of the VRC01 epitope and six additional lysines were introduced to better shield the rest of the protein (see appendix for full sequences).

After confirming correct folding by ELISA using conformation-dependent mAbs (Fig. 7.5C and data not shown), eOD glycoproteins were expressed in suspension-adapted HEK-293S GnT-I$^{-/-}$ cells under serum-free conditions at ~50 mg/L. Purified glycoproteins were modified with SiaLac and analysed by Western blot (Fig. 7.5A). Prior to gel separation, native N-linked glycans were removed by PNGase F treatment to obtain sharper bands and better signal-to-noise due to removal of different glycoforms and smaller over-all protein size respectively. Molecular weight analysis revealed high coverage of ~7.2 out of 7 and ~10.4 out of 10 lysine residues modified for the WT and KM proteins respectively.

Consistent with the molecular design, only few mAbs bound these glycoproteins even in the absence of SiaLac and therefore only a limited analysis of mAb recognition could be performed (data not shown). CD4bs bNmAb VRC01 recognised all four samples (WT and KM each unmodified and masked) equally well in an ELISA indicating no adverse effects of masking (Fig. 7.5C).

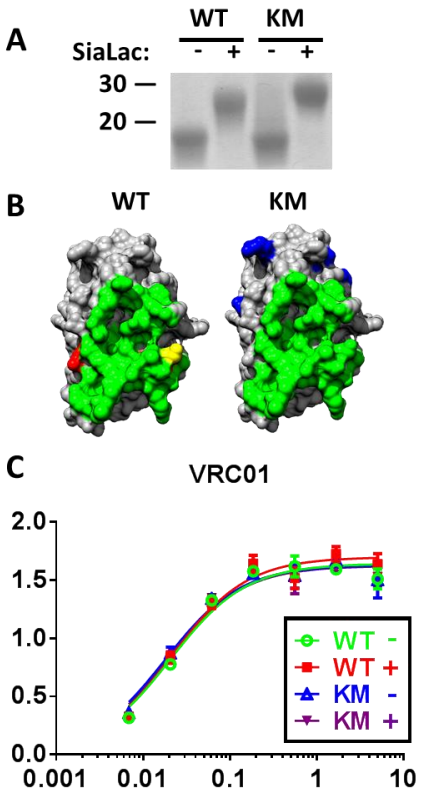

Fig. 7.5: Glycan masking of eOD lysine mutants. A: Western blot analysis of SiaLac modified protein. N-linked glycans were removed prior to gel separation. Numbers indicated sizes of molecular weight marker (in kDa). **B:** Structure of the lysine mutants with the broadly neutralising epitope (VRC01) indicated in green, lysine residues in red, new lysine residues in blue and lysine residues within the epitope in yellow. **C:** ELISA analysis of CD4bs bNmAb VRC01 binding to unmodified (-) or SiaLac modified (+) glycoproteins. Data are representative of 2 independent experiments. Error bars indicate SD of technical repeats.

The glycan masking strategy might in principle be applied to redirect antibody responses for any immunogen if the crystal structure and neutralising epitopes are known. Other candidate infectious diseases for which no universal vaccine is currently available due to the immunodominance of non-neutralising or strain-specific epitopes include influenza virus. The HA glycoprotein is the major target of neutralising antibodies against influenza, but the immunodominant region is the globular head group of HA1, which contains variable overlapping epitopes that elicit strain-specific neutralising antibodies. By contrast, the stalk region comprised of both HA1 and HA2 contains a highly conserved surface containing broadly neutralising antibody epitopes that would, in principle, make an ideal target for

vaccine design. However this stalk region is immunorecessive. Thus, attempts to transfer the glycan masking strategy to the influenza HA glycoprotein, to shift immunodominance from the head to the stem region, were made. Proteins were based on the NC99 ΔRBS glycoprotein from the Nabel lab (Kanekiyo et al., 2013), which contains the extracellular NC99 HA glycoprotein with the cleavage site between HA1 and HA2 removed. The ΔRBS variant was used to avoid problems with HA binding to the terminal sialic acid residue of SiaLac upon masking. Furthermore, this construct contains a trimerisation domain (foldon) and a C-terminal his-tag downstream of a protease cleavage site. Mutants were designed based on this construct. The final KM protein had five lysine residues in the broadly neutralising stalk region removed and a single additional lysine introduced into the head region.

Correct folding was confirmed by binding of a panel of mAbs (Fig. 7.6C and data not shown), and glycoproteins were expressed in serum-free suspension cultures of HEK-293S GnT-I$^{-/-}$ cells. Yields of protein were relatively low with ~1 mg of purified trimeric protein recovered per litre of cell-culture. SiaLac masking was performed and coupling efficiency was analysed by SDS-PAGE and found to be ~31.4 of 33 lysines and ~24 of 29 lysines modified for WT and KM protein respectively (Fig. 7.6A).

ELISA analysis showed complete loss of binding of anti-HA1 head mAb FE17-23 (Corti et al., 2010b) consistent with the large number of lysine residues covering this area (Fig. 7.6 B+C). By contrast, binding of two different anti-stem antibodies was completely preserved (Fig. 7.6 B). Unfortunately, no crystallographic data are available for these mAbs (Corti et al., 2010b) and thus it is not possible to determine whether these mAbs make direct contact

with the lysine proximal to their estimated epitopes. However, the fact that their binding was not modified by addition of SiaLac suggests that any potential contact is not critical for mAb binding.

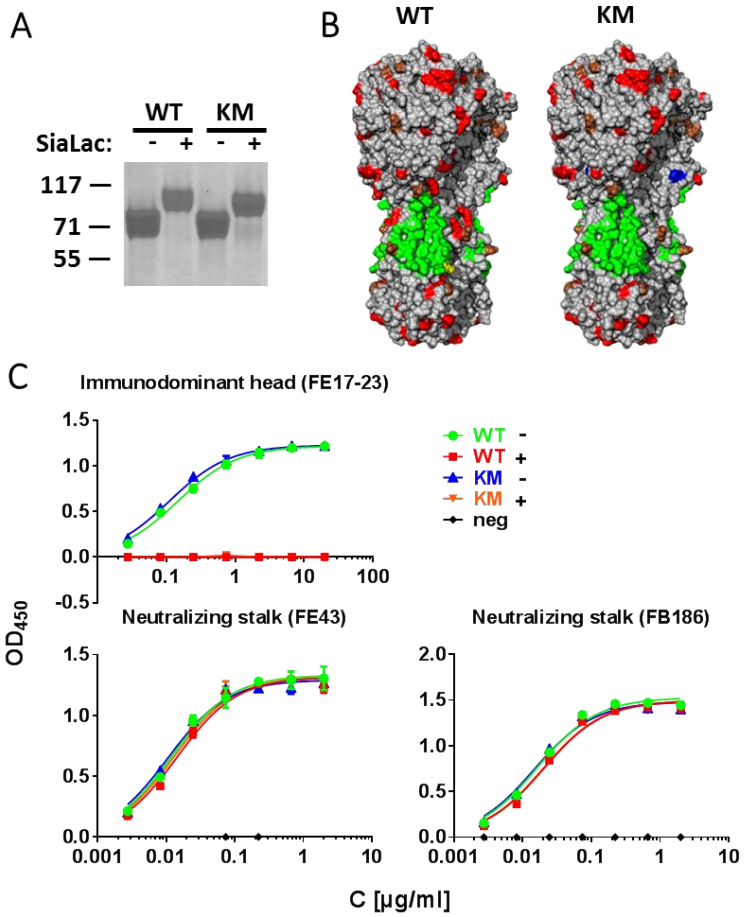

Fig. 7.6: Glycan masking of HA lysine mutants. A: SDS-PAGE analysis of SiaLac modified glycoprotein. Numbers indicated sizes of molecular weight marker (in kDa). **B:** Structure of the lysine mutants with the estimated broadly neutralising epitope indicated in green, N-linked glycosylation sites in brown, lysine residues in red, new lysine residues in blue and lysine residues within the approximate epitope in yellow. **C:** ELISA analysis of unmodified (-) or SiaLac modified (+) proteins. Data are representative of 2 independent experiments. Error bars indicate SD of technical repeats.

Taken together, a number of modified glycoprotein antigens for both HIV-1 and influenza virus were developed that, when modified with SiaLac, present almost exclusively the respective broadly neutralising epitopes.

7.2.3 **Immunogenicity of SiaLac modified immunogens**

After optimising antigens and glycans *in vitro*, immunisations were performed to test the effects of SiaLac glycan masking on antibody refocusing. A trial was conducted in BALB/c mice (n=6 per group) using WT and KM gp120 with or without SiaLac masking (note, KM rather than KM2 was used since at the start of this trial the latter had not yet been developed). The prime was formulated in 0.5 % Carbopol 971p whereas subsequent boosts were formulated in 10 µg MPLA as discussed in section 7.3 .

All antigens induced binding antibody responses to unmodified wt gp120 (Fig. 7.7A). However, the magnitude of these responses showed significant differences between groups ($p < 0.01$ in a 2-way ANOVA with Tukey's post-test). In particular both groups immunised with unmodified protein developed higher binding responses against unmodified gp120 (as measured by ELISA) than the animals immunised with SiaLac modified protein ($p < 0.0001$). In addition, animals immunised with wt gp120 showed higher responses towards the wt probe than animals immunised with the mutant protein ($p = 0.005$ and $p = 0.005$ for unmodified and SiaLac immunised groups respectively). To investigate the bias imposed by the coating antigen, sera from the final time-point were analysed against each of the four different antigens (Fig. 7.7B). Whereas the animals immunised with unmodified gp120 showed relatively similar responses to all four antigens, sera from animals receiving SiaLac proteins showed significantly higher variability ($p = 0.03$ in a Mann-Whitney test) with up to 6000-fold differences between recognition of unmodified and SiaLac modified proteins. Interestingly, the sera from SiaLac immunised animals showed strong IgM responses to SiaLac modified gp120 (but not to unmodified gp120) even at the final time point, indicating incomplete class-switch.

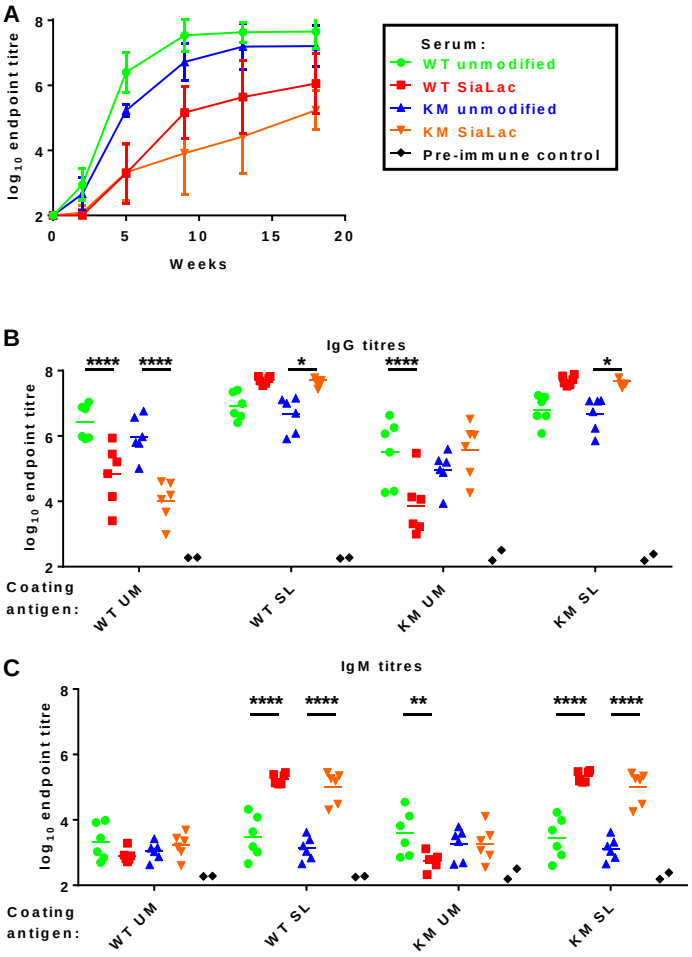

Fig. 7.7: Immunogenicity of SiaLac masked gp120. BALB/c mice (n=6 per group) were immunised with the indicated immunogens formulated in carbopol (prime) or MPLA (boosts) and sera were collected 2 weeks after each immunisation. Endpoint titres were determined by direct ELISA. **A:** Time course of total IgG endpoint titres against unmodified WT protein. **B+C**: Total IgG (**B**) and IgM (**C**) endpoint titres were determined against unmodified (UM) and SiaLac modified (SL) WT and KM proteins for the final time point. Pre-immune pools were included as a control. * $p < 0.05$; ** $p < 0.01$; **** $p < 0.0001$ in a 2-way ANOVA with Tukey's post-test.

The observation that SiaLac-modified gp120 immunised animals recognised SiaLac masked gp120 far better (>1000-fold) than unmodified gp120 suggested that a large proportion of antibodies might either recognise epitopes including SiaLac adducts, or SiaLac on its own. To test whether the latter was the case, responses to an unrelated protein (HEL) unmodified or modified with SiaLac were tested (Fig. 7.8A). No substantial responses were detected at any time point against the unmodified protein. In stark contrast, very strong (endpoint titres $>10^7$) were detected against SiaLac modified HEL in both groups that were

immunised with SiaLac proteins whereas no such responses were detected in the animals receiving unmodified protein indicating strong anti-SiaLac responses. The responses arose very early and were already detectable 2 weeks after the prime and plateaued after the first boost. To further investigate the specificity of these anti-glycan responses, additional glycans were coupled to HEL and endpoint titres against these glycans were determined (Fig. 7.8B). The two additional glycans tested were lactose, which compared to SiaLac is missing the apical sialic acid residue, and SiaGal, which lacks the basal glucose. Responses against these glycans were significantly ($p < 0.0001$ and $p = 0.01$ for lactose and SiaGal respectively in a 1-way ANOVA with Dunn's post-test) lower (3.5 and 4.3 logs for lactose and SiaGal respectively) than those against SiaLac. To rule out involvement of the lysine residue or the IME linker, glycan responses were next analysed in a cross-competition format. In this assay only SiaLac, but none of its individual components (lactose, glucose, galactose and sialic acid) was able to compete with serum binding to HEL-SiaLac (Fig. 7.8C). Taken together these data show a surprisingly strong anti-glycan response induced by SiaLac-modified immunogens, which is highly specific for SiaLac.

To further characterise the antibody responses induced by masked gp120, cross-competition analysis was performed. However, due to the finding that binding antibody titres varied significantly with the target protein, cross-competition against CD4 was performed using all four antigens (WT and KM each unmodified and SiaLac modified) as coating antigen. The amount of cross-competition varied substantially with the coating antigen (Fig. 7.8D). In particular, sera from SiaLac immunised animals only competed with soluble CD4 binding if SiaLac gp120 was used as coating antigen but not with the unmodified antigen. Further epitopes analysed included the V3 loop and the N332 glycan

epitope, although in these cases only unmodified WT protein was used as coating antigen. Responses against the V3 loop were detected in all groups, in particular those without SiaLac masking. No animals showed strong responses against the N332 epitope.

Taken together, these data show the induction of strong anti-SiaLac antibody responses, both IgM and IgG, by both SiaLac-masked gp120-based immunogens. The presence of these antibody responses, particularly of the IgG class, implies T-cell help was available for antibody class switching the antibody-producing B cells. Implications of these strong anti-SiaLac adaptive immune responses are that: i) anti-SiaLac IgG and IgM probably interfere with antibody binding to the gp120 protein surface by binding to the SiaLac adducts and thereby increasing the steric obstruction of the protein surface; ii) they may have impeded the induction of strong gp120 protein-specific responses by scavenging the limited T-cell help available for B-cell maturation.

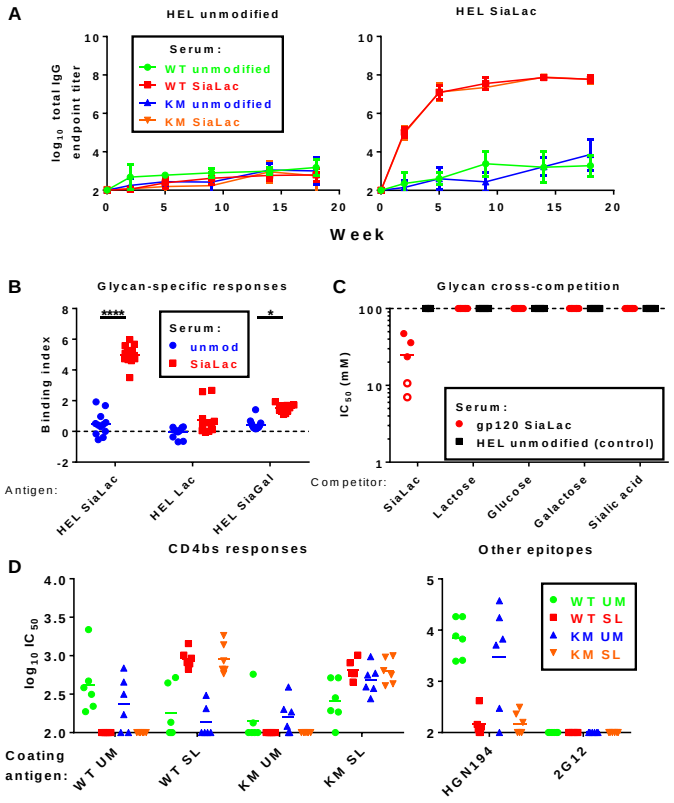

Fig. 7.8: Epitope mapping of SiaLac masked gp120 immunogens. Epitope masking was performed sera described in Fig. 7.7. **A:** Binding total IgG antibody responses against unmodified or SiaLac modified unrelated protein (HEL) was measured for each time point. **B:** Irrelevant protein HEL was modified with SiaLac, lactose alone or SiaGal (lacking the basal galactose) and total IgG binding antibody responses were measured for the final time point. Binding indices were determined by subtracting the corresponding responses against unmodified HEL from those against glycosylated HEL. **C:** Cross-competition of sera from the final bleed against glycans was performed by binding sera to HEL SiaLac at their respective 50% binding concentration in presence of titration series of the indicated glycans. Open circles denote glycans with attached IME linker. **D:** Cross-competition analysis of sera from the final bleed was performed against anti-gp120 probes. CD4bs-specific responses were determined against all four antigens as indicated, HGN194 (V3-loop) and 2G12 (N332 cluster) were only determined against unmodified wildtype gp120. *p < 0.05; **** p < 0.0001 in a 2-way ANOVA with Tukey's post-test.

In parallel to the gp120 immunisations, similar experiments were conducted using HA-based immunogens described above (Fig. 7.6). Overall, results from these immunisations were very similar to those obtained with gp120. Antibody titres induced by SiaLac modified protein measured against unmodified wt protein were up to two $\log_{10}$ lower than those induced by unmodified protein, in particular early in the immunisation regimen (Fig. 7.9A).

However, responses measured against SiaLac modified protein were equal to or even higher than those induced by unmodified protein (Fig. 7.9B).

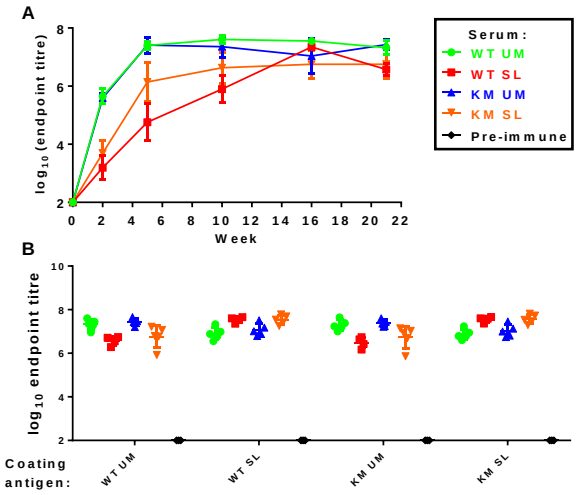

Fig. 7.9: Immunogenicity of SiaLac masked HA. BALB/c mice (n=5 per group) were immunised with the indicated immunogens in carbopol (prime) or MPLA (boosts) and sera were collected 2 weeks after each immunisation. Endpoint titres were determined by direct ELISA. **A:** Time course of total IgG endpoint titres against unmodified WT protein. **B**: Total IgG endpoint titres against unmodified (UM) and SiaLac modified (SL) WT and KM proteins for the final time point. Pre-immune pools were included as a control.

Again, high anti-SiaLac binding antibody responses were detected in an ELISA using glycan-coupled unrelated protein HEL as coating antigen (Fig. 7.10A) whereas no responses were detected against lactose in absence of the sialic acid group. Furthermore, significant responses against SiaGal (lacking the basal glucose compared to SiaLac) were detected although these were still over 100-fold lower than those detected against SiaLac. Since SiaLac is very similar to common terminal groups in N-linked glycans (such as Sialyl-lactosamine, which differs from SiaLac only in the presence of a single N-acetyl group), it was tested whether glycan-specific antibodies would cross-react with N-linked glycans. Responses towards a heavily N-glycosylated unrelated protein (gp120) were measured using both native and deglycosylated protein (Fig. 7.9A). No significant reactivity against N-linked glycans was found in this assay.

Responses directed towards conventional protein-based epitopes were further characterised by standard epitope mapping using unmodified wildtype HA as coating antigen. No competition in the sera from mice immunised with SiaLac-modified HA was detected with either anti-head or anti-stem epitopes (Fig. 7.9B). By contrast, sera from mice immunised with unmodified HA (WT or KM) protein showed responses to both epitopes. Thus, as with the SiaLac-modified gp120 immunised mice, HA-SiaLac-immunised mice may produce globally lower titres of anti-protein antibodies as a result of interference from the immunodominant SiaLac response.

Since the SiaLac-HA immunised animals showed strong responses against SiaLac but not against protein antigens, it was investigated whether glycan-specific antibodies might prevent the induction of anti-stem antibodies by direct competition. Cross-competition of an anti-stem mAb against anti-SiaLac antibodies from sera raised against an unrelated protein (gp120) was analysed by ELISA. In this experiment the anti-SiaLac antibodies were able to out-compete the anti-stem antibody but only if the target protein was SiaLac modified (Fig. 7.9C). Thus anti-SiaLac and anti-stem antibodies directly compete for binding to HA *in vitro* and it cannot be ruled out that competition also exists *in vivo*.

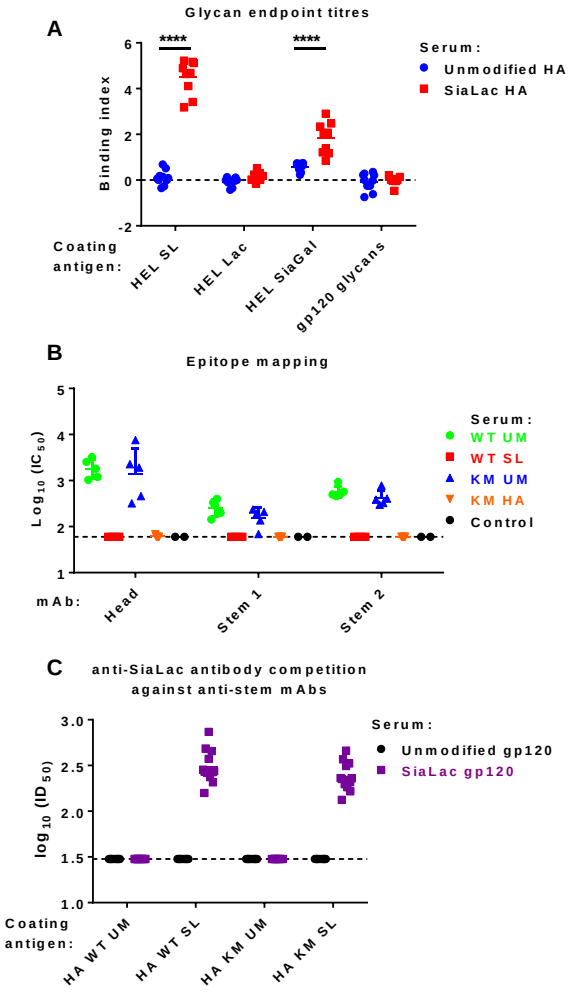

Fig. 7.10: Epitope mapping of SiaLac masked HA immunogens. Epitope mapping was performed on the sera from the experiment described in Fig. 7.9. **A:** Irrelevant protein HEL was modified with SiaLac, lactose alone or SiaGal (lacking the basal galactose compared to SiaLac) and total IgG binding antibody responses were measured for the final time point. In addition, responses were measured against unrelated N-glycosylated protein gp120 before and after deglycosylation. Binding indices were determined by subtracting log-transformed responses against deglycosylated protein from those against glycosylated protein. **** $p < 0.0001$ in a 2-way ANOVA with Tukey's post-test. **B:** Cross-competition analysis of sera from the final bleed was performed against anti-HA probes using unmodified wildtype HA as coating antigen. **C:** Competition of anti-SiaLac antibodies with an anti-stem bNmAb was tested by binding the mAb to the indicated coating HA antigen in presence of a titration series of sera from mice immunised with an unrelated protein (gp120) that was SiaLac modified or left unmodified as indicated (sera from Fig. 7.7).

Due to the surprisingly high magnitude of the anti-SiaLac antibody responses, which is in direct contradiction to previous reports on the immunosilent nature of these glycans (Yu et al., 2011), it was next analysed whether the unusually potent adjuvant combination used here (prime with carbopol 971p, boost with MPLA) was responsible for these strong anti-

glycan responses. Therefore, BALB/c mice (n=3 per group) were immunised with SiaLac modified eOD KM in different adjuvants. Adjuvants included carbopol followed by MPLA, the two FDA approved adjuvants alum and MPLA independently, the novel adjuvant PEI which was developed in our lab (Wegmann et al., 2012; Sheppard et al., 2014), and a no adjuvant group (PBS). A control group receiving unmodified eOD formulated in carbopol (prime) or MPLA (boost) was included. All adjuvant groups induced strong responses to SiaLac as measured by ELISA using SiaLac coupled to the unrelated HEL protein as coating antigen Fig. 7.11. In absence of an adjuvant, SiaLac modified eOD induced substantially lower titres than in presence of adjuvant, although this only reached statistical significance for adjuvants carbopol/MPLA and PEI ($p < 0.05$ in a 1-way ANOVA with Dunn's post-test) due to the small sample size (n=3 per group). No SiaLac-specific responses were detected in control animals immunised with unmodified eOD. Antibody responses against unmodified eOD were low in the animals receiving adjuvanted SiaLac-eOD and undetectable in the PBS group. By contrast, control animals immunised with unmodified eOD showed strong responses against this homologous probe.

Taken together, these data show that high anti-SiaLac antibody responses were induced in the presence of a number of adjuvants, and were therefore independent of the type of adjuvant used.

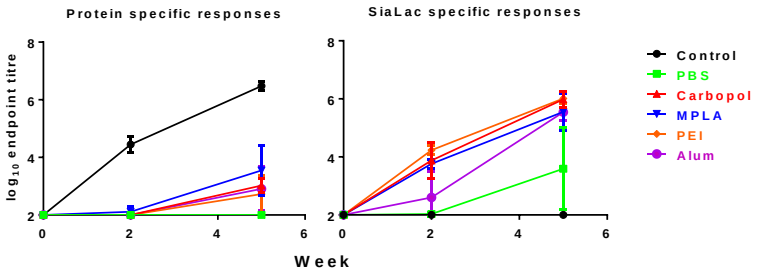

Fig. 7.11: Influence of adjuvant on anti-glycan antibody responses. BALB/c mice (n=3 per group) were immunised twice with 10 µg SiaLac modified eOD formulated in the indicated

adjuvants and sera were collected two weeks after each immunisation. End-point titres against unmodified eOD (protein specific responses) or SiaLac-modified unrelated protein HEL (SiaLac specific responses) were measured by direct ELISA. Due to the high toxicity of carbopol upon repeated immunisations, animals from the carbopol group were primed with carbopol and boosted with MPLA. Control: unmodified eOD formulated in carbopol (prime) or MPLA (boost).

7.3 Discussion

In this chapter, SiaLac-IME was investigated as a candidate reagent for glycan masking. Coupling of fully assembled SiaLac onto the model protein HEL achieved full coverage and loss of antibody binding was achieved as shown by mutation and antigenicity studies.

In parallel to the SiaLac development, several additional antigens were developed for glycan masking. These proteins were resurfaced to contain lysine residues distributed throughout the surface except for the broadly neutralising epitopes, which were depleted of proximal lysines. A conservative approach was chosen for the resurfacing in which most mutations were based on naturally occurring substitutions. This careful approach led to correct folding of all tested lysine mutants including a number of proteins not described in this thesis. The apparent ease of creating such mutants might also be caused by the surface-exposed nature of the mutated residues, which should in theory tolerate a charged amino-acid such as lysine relatively well.

Expression of proteins was performed in suspension-adapted HEK-293S GnT-I$^{-/-}$ cells grown under serum-free conditions in a chemically defined protein free medium. HEK-293S GnT-I$^{-/-}$ cells were chosen since glycans are not processed past the Man-5 stage in these cells thus leading to a relatively homogenous glycan profile (Doores et al., 2010a). In addition, quantification of the sialic acid content is specific for SiaLac in the absence of complex glycans. Yields from high-density suspension culture were very good for gp120 and eOD

based constructs (40-50 mg/l). However, expression levels of large trimeric proteins such as HA (or next-generation gp140 SOSIP proteins described in chapter 5) were low although at least 1 mg of purified trimeric protein was recovered from 1L expression batches which was still higher than levels achieved in adherent cultures (data not shown).

After expressing and purifying the mutant proteins, SiaLac coupling was performed. LCT/ESI Mass spectrometry using standard conditions was not successful in monitoring the coupling for these glycoproteins (data not shown). Instead of optimising custom conditions for monitoring the coupling (for example via MALDI/TOF MS), gel shift was used to analyse the coupling efficiency. This method was chosen despite its much lower accuracy compared to MS as it was well established in the lab. For HIV-based glycoprotein antigens, deglycosylation of N-linked glycans was required prior to gel analysis, yielding sharper bands and improving the signal-to-noise ratio by reducing the overall mass of the target protein. The masses obtained by this method indicated full SiaLac coupling, a finding that was supported by MS analysis of HEL which was always modified in parallel for calibration (data not shown).

Analysis of SiaLac modified proteins in general showed the expected alterations of antibody recognition with substantially reduced binding of mAbs to immunodominant epitopes whilst binding of mAbs to lysine-free neutralising epitopes was retained. In case of gp120, lysine coverage had to be re-optimised to obtain more pronounced discrimination between the effects of these two types of epitopes. In some cases, for example for mAb VRC01, lysine residues at the edge of the epitope were tolerated without an effect on mAb binding upon SiaLac coupling. As previously alluded to, a possible explanation for this finding might

be that the flexible lysine side chain rotates to clear the binding site upon mAb binding thus orienting the SiaLac into a compatible conformation. More analysis with additional glycan mutants or different sizes of glycans would be required to better understand the 'blocking radius' of the glycan.

Immunisations were conducted using a slightly unusual combination of adjuvants, namely carbopol 971p for the prime and MPLA for subsequent boosts. The choice of adjuvant was based on theoretical considerations. It is known that carbopol does not interact directly with gp120 (Krashias et al., 2010) and due to a similar negative charge an interaction with SiaLac is very unlikely. Similarly, MPLA should theoretically not interact with SiaLac. Therefore, the adjuvant effect should in principle not be altered by the presence or absence of SiaLac, and the adjuvant should not modify the presentation of the antigen to the immune system. Both adjuvants are furthermore very potent (data not shown). However, carbopol, especially version 971p, was relatively toxic in mice (data not shown) and thus only a single dose could be administered. Therefore, carbopol was chosen for the prime and MPLA for subsequent boosts.

Immunisation with both HIV-1 gp120 and influenza HA showed very similar results. Immunogenicity against the unmodified protein was drastically reduced in the animals that received SiaLac-masked protein and no refocusing of immune responses towards lysine-free regions was detected. Instead, strong anti-glycan responses were induced in all animals receiving SiaLac modified protein. The anti-SiaLac responses were predominantly class-switched, with only low IgM responses detectable at the final time-point. Although anti-glycan responses are often short-lived IgM-mediated T-cell independent responses,

the responses found here were mostly of an isotype-switched IgG isotype, consistent with the presence of T-cell epitopes on the protein carrier (Liu and Ye, 2012). The large magnitude of the responses found here are surprising since SiaLac modified proteins have previously been shown not to induce strong anti-SiaLac responses (Pan et al., 2005). Differences between the experimental procedures here and those used by Pan et al. include the proteins used, the type of coupling-chemistry and coupling efficiency, the mouse strain, adjuvant and immunisation schedule. Given that the strong anti-glycan responses reported here were achieved with a number of different proteins, the different carrier protein used by Pan et al. is unlikely to play a large role. Pan et al. do not report on their coupling efficiency on a per-lysine basis but they do provide an estimate of 12.4 % (w/w) glycans per total glycoconjugate. Equivalent loading values for the experiments conducted here are slightly though not dramatically higher (16-23% w/w). The strain of mouse used as well as the immunisation schedule might favour the induction of anti-glycan responses in this case since both BALB/c mice and extended immunisation schedules favour stronger responses. Nevertheless, responses detected here seemed to plateau after day 35 (week 5), the same day investigated by Pan et al. despite the latter having received all four immunisations by this time point already. In addition, the amount of glycoconjugate as well as the amount of pure glycan injected was higher in the experiments performed by Pan et al. The type of linker used for coupling of the glycan to the protein might have played a role. The short linker used here might have been sterically more restricted than the long flexible linker used by Pan et al. thus imposing less entropic penalty for B-cell receptor recognition and subsequent antibody binding. Finally, the adjuvant combination used here was quite different from the adjuvant used by Pan et al. (RIBI). Therefore an adjuvant trial was conducted to investigate whether this might have played a role. In this experiment, all

adjuvants induced strong anti-SiaLac responses and thus it is unlikely that the different results are due to differences in the adjuvant system. Taken together, the precise reason for the different results remains unclear. SiaLac, or rather the glycans associated with ganglioside GM3, is upregulated on many cancer cells, in particular melanomas (Tsuchida et al., 1987; Bitton et al., 2002). Therefore, the induction of anti-GM3 is an important goal in cancer-vaccine development (Hakomori and Zhang, 1997; Bitton et al., 2002; Pan et al., 2005; Pejchal et al., 2011; Yu et al., 2011) and the strong anti-SiaLac responses induced here might merit further investigation as a putative cancer vaccine approach.

One effect of the strong anti-SiaLac responses seems to be that refocusing of antibody responses by SiaLac masking was not successful. It was shown that anti-SiaLac antibodies directly outcompeted antibodies directed against the unmodified protein regions, and would be expected to also compete for B-cell recognition of protein surfaces. Nevertheless, additional levels of competition between B cells have been described in the literature, most importantly competition for T-cell help and competition for uptake of antigen presented on follicular dendritic cells (Victora et al., 2010; Natkanski et al., 2013; Gitlin et al., 2014). Which of these mechanisms are involved in the competition observed here, or whether they all play a role, is currently unknown. Thus, although SiaLac coupling was very efficient and *in vitro* masking showed excellent results, it is clear that SiaLac is not a suitable candidate for glycan masking due to its high immunogenicity, and alternative glycans need to be explored for this purpose. Alternatively, prime-boost strategies might be explored in which only the first immunisation is masked with SiaLac whereas subsequent immunisations contain antigens which are either modified with different glycans or remain unmodified. By only receiving a single injection with masked antigen, competition in the

germinal centre might not have completely eliminated B cells targeting the unmasked protein epitopes, thus giving the latter a “head start” compared to masked epitopes which are only available in subsequent immunisations. If this “head start” is enough of an advantage to outcompete otherwise immunodominant epitopes, it should result in a biased B-cell response towards these epitopes in the following immunisations.

Taken together, a cyclic development strategy for glycan masking of experimental vaccine antigens was established that allowed the development of resurfaced mutant proteins with selectively modified immunodominant epitopes *in vitro*. Combined with improved immunosilent glycans this strategy bears potential for future antibody-based vaccine design.

Chapter 8: Discussion

Immunodominance of non-neutralising epitopes is a problem with several pathogens for which no vaccine exists to date. In particular, despite over 30 years of research into HIV-1 vaccine design, no prophylactic vaccine exists due to the immunodominance of non-neutralising or rapidly mutating epitopes (Schiffner et al., 2013b). Predictive refocusing of antibody responses towards neutralising epitopes should in theory overcome this hurdle and is therefore a priority for vaccine development. In this thesis, strategies to refocus antibody responses by chemical modification of vaccine antigens were explored. Two fundamentally different types of chemical modification were investigated, namely cross-linking and glycan masking.

8.1 Chemical cross-linking

Chemical cross-linking showed a selective loss of binding of non-neutralising CD4bs antibodies *in vitro*, an effect that has previously been described by several groups (Sattentau, 1995; Yuan et al., 2006). Here, these findings were extended to include newly discovered broadly neutralising epitopes such as the VRC01 epitope and the quaternary epitope associated with the V1/V2 loop. Interestingly, results for the latter epitope differed depending on the protein analysed. Whereas quaternary-specific bNmAbs do not bind to conventional gp140 as used in chapter 3 (Walker et al., 2009; Walker et al., 2011b; Klein et al., 2012a; Ringe et al., 2013), binding of quaternary specific bNmAbs was analysed in both chapter 4 and 5 with conflicting results. Binding of quaternary specific bNmAb PG9 to membrane-bound Env was not affected by cross-linking whilst a strong loss of binding of quaternary bNmAbs such as PGT145 and 3BC176 was seen upon cross-linking of next-generation SOSIP gp140 (note: PG9 is quaternary-specific for strain UG37 but not BG505 (Hoffenberg et al., 2013; Sanders et al., 2013 and data not shown)). A possible explanation

for this discrepancy might be a difference in the stability of the trimers. The EM data presented have clearly shown that cross-linking can disrupt the correct folding of some BG505 SOSIP gp140 trimers thus providing an immediate explanation for the reduced binding of quaternary-specific bNmAbs. It is therefore possible that membrane-bound Env is more stable than this artificial soluble construct and remains intact during the cross-linking procedure. Cryo-EM analysis of unmodified and cross-linked membrane-bound Env would be required to investigate this hypothesis.

Immunisation with cross-linked first-generation gp140 showed a refocusing of antibody responses. Cross-linked material induced lower antibody responses towards gp41 but increased responses towards the C1, V1V2, V3 and CD4bs epitopes. The CD4bs-specific responses were partially responsible for increased neutralisation of pseudoviruses although these were mostly restricted to neutralisation sensitive tier 1 strains. It was therefore hypothesised that cross-linking of correctly-folded trimers would results in further improved immune responses since these should in theory only present neutralising epitopes. In addition, cross-linking should prevent both the disassembly of Env in solution, which is otherwise prone to dissociate (Moore et al., 1990). Combined with a quaternary-specific purification step, purification of membrane-extracted cross-linked Env was achieved with up to 36% of correctly folded trimer in the final preparation. Further improvements might be achieved by using two quaternary-specific selection steps (rather than one) or by including a size-exclusion step which should remove aggregates still present in the sample. However, glycoprotein yields were prohibitively low and therefore no immunogenicity trials could be conducted.

Due to the low yields of membrane-extracted glycoprotein, efforts were redirected towards cross-linking of correctly folded gp140 SOSIP trimers as soon as these became available. Yields for these glycoproteins were substantially higher (data not shown) and stable cell-lines should further enhance the protein-production capacities (Chung et al., 2014). However, cross-linking partially disrupted the folding of the trimer, and despite extensive re-optimisation of the cross-linking procedure no conditions were found that completely preserved trimer integrity. This might explain why pilot immunisation with cross-linked SOSIP gp140 did not induce increased CD4bs responses as seen in chapter 3. However, other differences include the animal species, the type of cross-linker or cross-linking conditions thus making a direct comparison between these experiments difficult. *In vivo* experiments with PGT145-purified cross-linked SOSIPs will show whether cross-linking has potential for these next-generation trimers.

The benefits of cross-linking go beyond the refocusing of antibody responses. In species expressing compatible CD4 receptors, immunogenicity might be negatively affected by rapid depletion of the trimers by binding to CD4-expressing cells. In addition, CD4-engagement will expose CD4i epitopes leading to the induction of non-neutralising antibodies towards this region. Cross-linking should theoretically avoid both of these problems since binding of CD4 as well as CD4i mAbs is significantly reduced and structural rearrangements are prevented by covalent fixation of the protein. Finally, cross-linked protein may be more resistant to the actions of proteases, extending the half-life of the intact antigen. However this remains to be demonstrated.

Cross-linking under non-saturating conditions, as described here, is generally a stochastic process in which random target groups are covalently connected. In particular, for glutaraldehyde a range of different modifications can theoretically occur since glutaraldehyde itself is prone to form a range of aggregates of varying sizes, thus leading to ill-defined cross-linking distances (Migneault et al., 2004). Furthermore, although primary amines are the preferential target sites, a range of different amino-acids such as tyrosine, tryptophan, phenylalanine, histidine, cysteine, proline, serine, glycine, and arginine can be modified with varying efficiencies (Hopwood et al., 1970; Migneault et al., 2004). These problems can be partially overcome by switching to a cross-linker such as EDC/NHS which has better defined target site compatibility and as a zero-length cross-linker should lead to less variability. Another source of variability is the existence of many conformations of gp120 (Kwong et al., 2002; Yuan et al., 2006) since cross-linking fixes the conformations present at the time of cross-linking (Yuan et al., 2006). To over-come this problem, positive or negative selection with conformation-specific mAbs might be attempted as described in chapters 4 and 5.

Cross-linking of vaccine antigens is a well-tested method with an excellent safety record (Rappuoli, 1994), first having been used in the inactivated polio vaccine and many vaccines afterwards (Melnick, 1978). Although previous vaccine antigens have traditionally been treated with formaldehyde, extensive safety data exists for glutaraldehyde-treated antigens from clinical trials on allergy immunotherapy (Garcia-Selles et al., 2003; Riechelmann et al., 2010; DuBuske et al., 2011). No clinical trials of EDC/NHS cross-linking have been conducted to date, but the low cytotoxicity and the fact that it is a zero-length

cross-linker that does not remain on the target protein suggest that these reagents might be safe to use as well (Park et al., 2002).

Taken together, cross-linking is cheap, safe, inexpensive, increases the stability of the antigen and under certain conditions leads to the induction of slightly elevated neutralising responses *in vivo* thus making it an attractive tool in the future development of HIV-1 Env-based immunogens.

Despite all these advantages of chemical cross-linking, the approach remains relatively difficult to control because cross-linking occurs in a stochastic manner. Transferring this method to the development of vaccine immunogens for other diseases may not be appropriate since conformational masking and subunit instability is probably required for this approach to reach its full potential (Kwong et al., 2002; Yuan et al., 2006; Schiffner et al., 2013a). By contrast, the effects of glycan masking are much better defined since IME chemistry is very specific for primary amines and achieves 100% coverage. Utilisation of secondary modification sites, as they have been described for glutaraldehyde (Hopwood et al., 1970; Migneault et al., 2004), have not been found for IME reagents in MS/MS analysis.

8.2 Glycan masking

The initial approach for glycan masking was a combination of chemically linking a lactose primer to the target protein and enzymatically adding sialic acid chains to these primers *in situ*. This method was tested on model protein HEL where selective loss of antibody binding to masked epitopes was detected *in vitro*. These alterations in antibody recognition *in vitro* translated into differential induction of B-cell responses *in vivo*. Importantly, these

alterations in antibody induction were not restricted to reducing antibody responses towards masked regions but also led to concomitant increases in antibody responses directed towards some non-masked areas. These data support the idea of competition between B cells which can be biased by removing dominant species from the germinal centre reaction. However, despite recent advances in understanding the germinal centre processes (Victora et al., 2010; Natkanski et al., 2013; Gitlin et al., 2014), the competition of B cells in the germinal centre and the resulting immunodominance remain incompletely understood.

Despite the success of the glycan masking strategy on model protein HEL, technical problems prevented the direct transfer of this strategy to more relevant antigens such as HIV-1 gp120. Whereas IME-coupling of the lactose primer to gp120 was still achieved, subsequent *in situ* polymerisation of sialic acid failed, probably due to steric inhibitory effects of the native glycans on gp120 glycoprotein reducing access of the sialyl transferases. Thus, the glycan masking protocol was redesigned to pre-assemble the whole glycan before transferring it to the target protein *en bloc*. At the same time, the sialic acid chain length was changed to include a single sialic acid coupled to the lactose linker. The resulting reagent, SiaLac-IME, could be coupled to all target proteins with high yield although large amounts of reagent were required.

Remodelling the lysine-distribution of a series of viral glycoproteins was achieved resulting in mutants which had lysine residues appropriately spaced throughout the entire surface area except for the broadly neutralising epitopes, which was engineered to be lysine free. Masking of these mutant proteins with SiaLac led to selective loss of binding of non-

neutralising mAbs whilst preserving binding of bNmAbs. Surprisingly, immunisation with these reagents led to the induction of strong anti-SiaLac antibody responses, which appeared to impede the refocusing of antibody responses towards broadly neutralising epitopes not covered in glycans. The magnitude of these responses was surprisingly high considering that anti-glycan antibody responses in general, and anti-SiaLac antibody responses in particular, are supposedly very difficult to induce (Pancera et al., 2010). The question remains why refocusing of antibody responses with oligo-sialic acid was successful whereas mono-sialic acid failed, despite the similar attachment of the sialic acids to the protein via IME-coupled lactose. One possibility is that the longer sialic acid chains were less immunogenic due to the engagement of different siglecs (Varki and Angata, 2006). Another explanation is that the heterologous nature of the *in situ* polymerised sialic acid chains (chain length ranging from 0 to 3 for the 'short' chains) impeded antibody recognition. However, in contrast to the anti-SiaLac responses in chapter 7, anti-lactose responses were not detected in all animals in chapter 6 and the magnitude of such responses was very variable.

In the case of the sialic-acid-capped glycans used here, the observed effects probably exceed simple steric hindrance of B-cell receptor engagement, since sialic acid-containing glycans are recognised by a group of lectins (carbohydrate binding proteins) called siglecs. Many of these glycans have immuno-modulatory functions, which is one of the reasons why they are exploited by a number of pathogens (Khatua et al., 2013). For instance, SiaLac is recognised by siglec-9, an inhibitory siglec that is expressed on a number of immune cells including B cells (Zhang et al., 2000; Rapoport et al., 2003; Padler-Karavani et al., 2014). However, although this receptor generally has inhibitory functions, no data exist on the

effects of siglec-9 signalling in B cells and varying effects have been reported for this receptor in other cell types depending on additional extraneous signals (Varki and Angata, 2006). Another layer of complexity is added by the finding that SiaLac is expressed on the HIV-1 virion (in form of ganglioside GM3) and is suggested to be required for DC-mediated dissemination of virions (Puryear et al., 2012; Puryear et al., 2013). Thus, anti-SiaLac antibodies might bind to HIV-1 virions and reduce viral dissemination via DC-mediated infectious synapses.

Nevertheless, since glycan masking led to refocusing of antibody responses in the HEL model system, this strategy bears potential for future vaccine design. Most importantly, further improvements in the glycans are required for this method to work. Good candidates include sialic acid based reagents similar to those analysed in chapter 6 (Sia_3Lac). Other options include replacing lactose with N-acetyl-lactosamine (LacNAc) resulting in SiaLacNAc, which is commonly found in complex glycans. A recent study performed glycan arrays on 38 naïve macaques measuring both IgG and IgM responses against a total of over 200 glycans which were mostly coupled to carrier proteins such as BSA (Campbell et al., 2013). In this dataset, 24% and 42% of naïve animals responded to SiaLac with IgM and IgG respectively (Fig. 8.1). Responses against lactose were even higher with all animals showing both IgM and IgG responses. Replacing lactose with lactosamine (resulting in LacNAc and SiaLacNAc) led to lower numbers of responding animals with 13% and 3% for IgM and IgG respectively. Even lower responses were detected against high mannose glycans such as Man-5, Man-9 and Man-3, the latter of which might be more suitable for a glycan masking strategy due to its smaller size. Therefore, it should be possible to find a suitable immunosilent glycan that is sufficiently small to allow very specific modulation of antibody

responses, yet large enough to present enough steric hindrance to provide robust shielding of the underlying epitope.

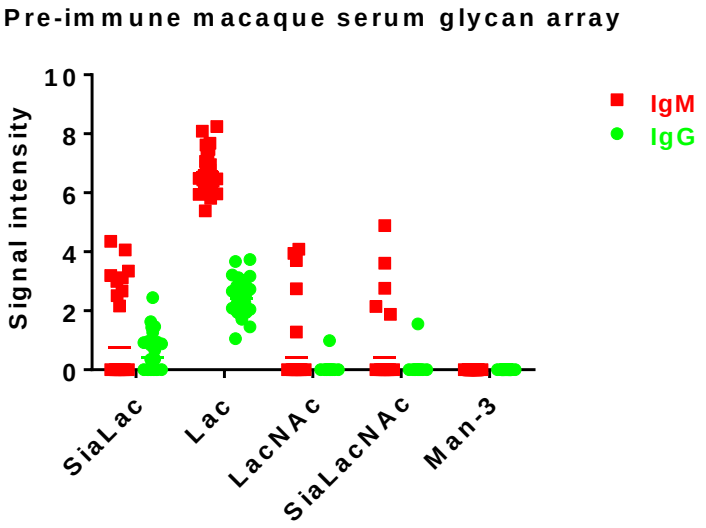

Fig. 8.1: Prevalence of selected anti-glycan antibody responses in naive macaques according to Campbell et al. (2013). Data from supplementary file 2 from Campbell et al. (2013) was analysed by subtracting the negative control protein (without glycan) from the values for proteins with linked glycans. Data shown are both IgM and IgG responses from pre-immune sera of all 38 macaques.

Despite these problems, the cyclic strategy for the development of antigens for glycan masking bears potential for vaccine antigen design. In combination with an improved immunosilent glycan, this strategy might be a valuable tool for future vaccine research. However, even if such an immunosilent glycan were found, glycan-masking of HIV-1 immunogens might not, on its own, be sufficient to induce bNAbs against gp160 due to the additional immune-evasion mechanisms of Env (see section 1.3.3). In fact, glycan masking of the gp120 immunogens presented in this thesis would be expected to mostly induce non-neutralising CD4bs antibodies since no mechanisms were included to prevent the induction of antibodies not being able to bind native Env due to angle-of-approach restrictions. In addition, the germline versions of all bNmAbs found to date do not bind

most Envs and glycan masking on its own would not be expected to suffice to overcome this hurdle (Hoot et al., 2013; McGuire et al., 2014). Thus, additional strategies would be required for the induction of HIV-1 neutralising antibodies. In contrast, soluble influenza HA based proteins, such as the ones developed in this thesis, are generally considered to be natively folded and it has been shown that germline reverted versions of anti-stem bNmAbs against influenza virus do bind to such soluble constructs in the context of membrane-expressed B-cell receptors (Ekiert et al., 2009; Lingwood et al., 2012). Therefore, glycan masking might more easily be applied to influenza compared to HIV-1.

8.3 Future perspectives

Current vaccination strategies for HIV-1 aiming to induce bNAbs are heading towards multi-stage vaccination regimens. A prominent example for such a strategy is the germline-targeted outer domain construct from the Schief lab, which has at its centrepiece a highly engineered outer domain protein, which has been mutated to strongly bind to germline versions of the VRC01 class of bNmAbs (Jardine et al., 2013). Although no *in vivo* data on such strategies have been published to date, which might be due to the lack of a suitable animal system encoding compatible germline genes, these types of proteins have been shown to activate engineered B cells *in vitro* (Jardine et al., 2013; McGuire et al., 2013). Priming of the appropriate immune responses with such an epitope-focused construct could then be followed by other constructs such as native-like trimeric gp140s including BG505 (Sanders et al., 2013), although intermediate steps might be required to guide affinity maturation from the activated germline antibodies towards fully matured bNAbs recognising and neutralising native Env (Jardine et al., 2013). On their own, native-like constructs such as BG505 would be predicted to induce NAbs since binding to the protein

correlates with neutralisation (Sanders et al., 2013). However, without prior priming of bNAb germlines, the resulting antibody responses might be strain-specific and mostly targeted towards immunodominant regions within the variable loops. In the context of a multi-stage epitope-focused vaccination strategy, glycan masking might be a valuable tool to aid focusing the antibody response towards the correct epitope during the early stages, in particular if epitopes are grafted onto artificial backbones from unrelated proteins (Azoitei et al., 2011; Azoitei et al., 2012; Correia et al., 2014; Zhou et al., 2014). The later stages of such a strategy would then require very close mimics of native Env such as BG505 SOSIP.664 trimers (Sanders et al., 2013). During these later stages, cross-linking might be beneficial to stabilise the correct quaternary conformation. In principle, it shouldn't matter whether such strategies are derived from engineered antigens or are recapitulations of the antigens observed during naturally occurring development of bNAbs in infected patients (Liao et al., 2013a; Doria-Rose et al., 2014).

Scaffolded immunogen design might be best suited for CD4bs mAbs where the required germline is abundant (Arnaout et al., 2011; Jardine et al., 2013). In contrast, for many glycan-specific bNmAbs, the abundance of naïve B cells with a compatible B-cell receptor might be much lower due to the long CDR-H3 loops required for these bNmAbs. For example, in a longitudinal study of the development of a PG9-like bNmAb, the germline B-cell receptor had a CDR-H3 length of 35 AA (facilitated by non-templated insertions of >30 nucleotide on each side of the D gene) (Doria-Rose et al., 2014), which is much longer than typically observed CDR-H3 lengths in human B-cell receptors (Johnson and Wu, 1998). Thus, even if a suitable immunogen were developed that allowed the triggering of affinity maturation of these antibodies towards bNAbs, the low abundance of B cells with

compatible B-cell receptors might impede the development of these bNAbs in a large proportion of the population. Insertions (as well as deletions) can occur in B-cell receptors during affinity maturation and these so-called indels appear to be particularly prevalent with HIV-1 bNmAbs (Kepler et al., 2014). Therefore improved adjuvants or immunisation schedules might be required to induce glycan-directed NAbs with such long CDR-H3 regions.

In conclusion, two fundamentally different types of chemical modifications were tested for their ability to refocus antibodies towards neutralising epitopes in this thesis. Both chemical cross-linking and glycan masking were able to redirect antibody responses *in vivo*. Thus, the data presented here highlight the potential of chemical modification of vaccine adjuvants for improved immunogenicity and illustrate their potential for future vaccine design.

Bibliography

Agrawal-Gamse, C., Luallen, R. J., Liu, B., Fu, H., Lee, F. H., Geng, Y. & Doms, R. W. (2011). 'Yeast-elicited cross-reactive antibodies to HIV Env glycans efficiently neutralize virions expressing exclusively high-mannose N-linked glycans'. *J Virol,* 85**,** 470-80.

Allaway, G. P., Davis-Bruno, K. L., Beaudry, G. A., Garcia, E. B., Wong, E. L., Ryder, A. M., Hasel, K. W., Gauduin, M. C., Koup, R. A., Mcdougal, J. S. & Et Al. (1995). 'Expression and characterization of CD4-IgG2, a novel heterotetramer that neutralizes primary HIV type 1 isolates'. *AIDS Res Hum Retroviruses,* 11**,** 533-9.

An, H. J., Gip, P., Kim, J., Wu, S., Park, K. W., Mcvaugh, C. T., Schaffer, D. V., Bertozzi, C. R. & Lebrilla, C. B. (2012). 'Extensive determination of glycan heterogeneity reveals an unusual abundance of high mannose glycans in enriched plasma membranes of human embryonic stem cells'. *Mol Cell Proteomics,* 11**,** M111 010660.

Aricescu, A. R., Lu, W. & Jones, E. Y. (2006). 'A time- and cost-efficient system for high-level protein production in mammalian cells'. *Acta Crystallogr D Biol Crystallogr,* 62**,** 1243-50.

Arnaout, R., Lee, W., Cahill, P., Honan, T., Sparrow, T., Weiand, M., Nusbaum, C., Rajewsky, K. & Koralov, S. B. (2011). 'High-resolution description of antibody heavy-chain repertoires in humans'. *PLoS One,* 6**,** e22365.

Astronomo, R. D., Kaltgrad, E., Udit, A. K., Wang, S. K., Doores, K. J., Huang, C. Y., Pantophlet, R., Paulson, J. C., Wong, C. H., Finn, M. G. & Burton, D. R. (2010). 'Defining Criteria for Oligomannose Immunogens for HIV Using Icosahedral Virus Capsid Scaffolds'. *Chemistry & Biology,* 17**,** 357-370.

Astronomo, R. D., Lee, H. K., Scanlan, C. N., Pantophlet, R., Huang, C. Y., Wilson, I. A., Blixt, O., Dwek, R. A., Wong, C. H. & Burton, D. R. (2008). 'A glycoconjugate antigen based on the recognition motif of a broadly neutralizing human immunodeficiency virus antibody, 2G12, is immunogenic but elicits antibodies unable to bind to the self glycans of gp120'. *Journal of Virology,* 82**,** 6359-6368.

Azoitei, M. L., Ban, Y. E., Julien, J. P., Bryson, S., Schroeter, A., Kalyuzhniy, O., Porter, J. R., Adachi, Y., Baker, D., Pai, E. F. & Schief, W. R. (2012). 'Computational design of high-affinity epitope scaffolds by backbone grafting of a linear epitope'. *J Mol Biol,* 415**,** 175-92.

Azoitei, M. L., Correia, B. E., Ban, Y. E., Carrico, C., Kalyuzhniy, O., Chen, L., Schroeter, A., Huang, P. S., Mclellan, J. S., Kwong, P. D., Baker, D., Strong, R. K. & Schief, W. R. (2011). 'Computation-guided backbone grafting of a discontinuous motif onto a protein scaffold'. *Science,* 334**,** 373-6.

Barouch, D. H., Whitney, J. B., Moldt, B., Klein, F., Oliveira, T. Y., Liu, J., Stephenson, K. E., Chang, H. W., Shekhar, K., Gupta, S., Nkolola, J. P., Seaman, M. S., Smith, K. M., Borducchi, E. N., Cabral, C., Smith, J. Y., Blackmore, S., Sanisetty, S., Perry, J. R., Beck, M., Lewis, M. G., Rinaldi, W., Chakraborty, A. K., Poignard, P., Nussenzweig, M. C. & Burton, D. R. (2013). 'Therapeutic efficacy of potent neutralizing HIV-1-specific monoclonal antibodies in SHIV-infected rhesus monkeys'. *Nature,* 503**,** 224-8.

Bartesaghi, A., Merk, A., Borgnia, M. J., Milne, J. L. & Subramaniam, S. (2013). 'Prefusion structure of trimeric HIV-1 envelope glycoprotein determined by cryo-electron microscopy'. *Nat Struct Mol Biol,* 20**,** 1352-7.

Baum, L. L., Cassutt, K. J., Knigge, K., Khattri, R., Margolick, J., Rinaldo, C., Kleeberger, C. A., Nishanian, P., Henrard, D. R. & Phair, J. (1996). 'HIV-1 gp120-specific antibody-dependent cell-mediated cytotoxicity correlates with rate of disease progression'. *Journal of immunology,* 157**,** 2168-73.

Berg, J. M. T. J. L. S. L. 2012. *Biochemistry,* Basingstoke, W.H. Freeman.

Binley, J. M., Wrin, T., Korber, B., Zwick, M. B., Wang, M., Chappey, C., Stiegler, G., Kunert, R., Zolla-Pazner, S., Katinger, H., Petropoulos, C. J. & Burton, D. R. (2004). 'Comprehensive cross-clade neutralization analysis of a panel of anti-human immunodeficiency virus type 1 monoclonal antibodies'. *J Virol,* 78**,** 13232-52.

Bitton, R. J., Guthmann, M. D., Gabri, M. R., Carnero, A. J., Alonso, D. F., Fainboim, L. & Gomez, D. E. (2002). 'Cancer vaccines: an update with special focus on ganglioside antigens'. *Oncol Rep,* 9**,** 267-76.

Blattner, C., Lee, J. H., Sliepen, K., Derking, R., Falkowska, E., De La Pena, A. T., Cupo, A., Julien, J. P., Van Gils, M., Lee, P. S., Peng, W., Paulson, J. C., Poignard, P., Burton, D. R., Moore, J. P., Sanders, R. W., Wilson, I. A. & Ward, A. B. (2014). 'Structural Delineation of a Quaternary, Cleavage-Dependent Epitope at the gp41-gp120 Interface on Intact HIV-1 Env Trimers'. *Immunity,* 40**,** 669-80.

Blumenthal, R., Durell, S. & Viard, M. (2012). 'HIV entry and envelope glycoprotein-mediated fusion'. *J Biol Chem,* 287**,** 40841-9.

Bobardt, M. D., Chatterji, U., Selvarajah, S., Van Der Schueren, B., David, G., Kahn, B. & Gallay, P. A. (2007). 'Cell-free human immunodeficiency virus type 1 transcytosis through primary genital epithelial cells'. *J Virol,* 81**,** 395-405.

Bonsignori, M., Hwang, K. K., Chen, X., Tsao, C. Y., Morris, L., Gray, E., Marshall, D. J., Crump, J. A., Kapiga, S. H., Sam, N. E., Sinangil, F., Pancera, M., Yongping, Y., Zhang, B., Zhu, J., Kwong, P. D., O'dell, S., Mascola, J. R., Wu, L., Nabel, G. J., Phogat, S., Seaman, M. S., Whitesides, J. F., Moody, M. A., Kelsoe, G., Yang, X., Sodroski, J., Shaw, G. M., Montefiori, D. C., Kepler, T. B., Tomaras, G. D., Alam, S. M., Liao, H. X. & Haynes, B. F. (2011). 'Analysis of a clonal lineage of HIV-1 envelope V2/V3 conformational epitope-specific broadly neutralizing antibodies and their inferred unmutated common ancestors'. *J Virol,* 85**,** 9998-10009.

Borggren, M., Vinner, L., Andresen, B., Grevstad, B., Repits, J., Melchers, M., Elvang, T., Sanders, R., Martinon, F., Dereuddre-Bosquet, N., Bowles, E., Stewart-Jones, G., Biswas, P., Scarlatti, G., Jansson, M., Heyndrickx, L., Grand, R. & Fomsgaard, A. (2013). 'Optimization of HIV-1 Envelope DNA Vaccine Candidates within Three Different Animal Models, Guinea Pigs, Rabbits and Cynomolgus Macaques'. *Vaccines,* 1**,** 305-327.

Borrow, P., Lewicki, H., Hahn, B. H., Shaw, G. M. & Oldstone, M. B. (1994). 'Virus-specific CD8+ cytotoxic T-lymphocyte activity associated with control of viremia in primary human immunodeficiency virus type 1 infection'. *J Virol,* 68**,** 6103-10.

Bournazos, S., Klein, F., Pietzsch, J., Seaman, M. S., Nussenzweig, M. C. & Ravetch, J. V. (2014). 'Broadly Neutralizing Anti-HIV-1 Antibodies Require Fc Effector Functions for In Vivo Activity'. *Cell,* 158**,** 1243-53.

Brasseur, R., Vandenbranden, M., Cornet, B., Burny, A. & Ruysschaert, J. M. (1990). 'Orientation into the lipid bilayer of an asymmetric amphipathic helical peptide located at the N-terminus of viral fusion proteins'. *Biochim Biophys Acta,* 1029**,** 267-73.

Breden, F., Lepik, C., Longo, N. S., Montero, M., Lipsky, P. E. & Scott, J. K. (2011). 'Comparison of antibody repertoires produced by HIV-1 infection, other chronic and acute infections, and systemic autoimmune disease'. *PLoS One,* 6**,** e16857.

Brisson, J. R., Baumann, H., Imberty, A., Perez, S. & Jennings, H. J. (1992). 'Helical Epitope of the Group-B Meningococcal Alpha(2-8)-Linked Sialic-Acid Polysaccharide'. *Biochemistry,* 31**,** 4996-5004.

Buchacher, A., Predl, R., Strutzenberger, K., Steinfellner, W., Trkola, A., Purtscher, M., Gruber, G., Tauer, C., Steindl, F., Jungbauer, A. & Et Al. (1994). 'Generation of human monoclonal antibodies against HIV-1 proteins; electrofusion and Epstein-Barr virus transformation for peripheral blood lymphocyte immortalization'. *AIDS Res Hum Retroviruses,* 10**,** 359-69.

Burton, D. R., Barbas, C. F., 3rd, Persson, M. A., Koenig, S., Chanock, R. M. & Lerner, R. A. (1991). 'A large array of human monoclonal antibodies to type 1 human immunodeficiency virus from combinatorial libraries of asymptomatic seropositive individuals'. *Proc Natl Acad Sci U S A,* 88**,** 10134-7.

Burton, D. R., Hessell, A. J., Keele, B. F., Klasse, P. J., Ketas, T. A., Moldt, B., Dunlop, D. C., Poignard, P., Doyle, L. A., Cavacini, L., Veazey, R. S. & Moore, J. P. (2011). 'Limited or no protection by weakly or nonneutralizing antibodies against vaginal SHIV challenge of macaques compared with a strongly neutralizing antibody'. *Proc Natl Acad Sci U S A,* 108**,** 11181-6.

Burton, D. R., Pyati, J., Koduri, R., Sharp, S. J., Thornton, G. B., Parren, P. W., Sawyer, L. S., Hendry, R. M., Dunlop, N., Nara, P. L. & Et Al. (1994). 'Efficient neutralization of primary isolates of HIV-1 by a recombinant human monoclonal antibody'. *Science,* 266**,** 1024-7.

Calarese, D. A., Scanlan, C. N., Zwick, M. B., Deechongkit, S., Mimura, Y., Kunert, R., Zhu, P., Wormald, M. R., Stanfield, R. L., Roux, K. H., Kelly, J. W., Rudd, P. M., Dwek, R. A., Katinger, H., Burton, D. R. & Wilson, I. A. (2003). 'Antibody domain exchange is an immunological solution to carbohydrate cluster recognition'. *Science,* 300**,** 2065-71.

Campbell, C. T., Llewellyn, S. R., Damberg, T., Morgan, I. L., Robert-Guroff, M. & Gildersleeve, J. C. (2013). 'High-throughput profiling of anti-glycan humoral responses to SIV vaccination and challenge'. *PLoS One,* 8**,** e75302.

Campbell, M. G., Cheng, A., Brilot, A. F., Moeller, A., Lyumkis, D., Veesler, D., Pan, J., Harrison, S. C., Potter, C. S., Carragher, B. & Grigorieff, N. (2012). 'Movies of ice-embedded particles enhance resolution in electron cryo-microscopy'. *Structure,* 20**,** 1823-8.

Cauerhff, A., Goldbaum, F. A. & Braden, B. C. (2004). 'Structural mechanism for affinity maturation of an anti-lysozyme antibody'. *Proc Natl Acad Sci U S A,* 101**,** 3539-44.

Chaudhary, S., Pak, J. E., Gruswitz, F., Sharma, V. & Stroud, R. M. (2012). 'Overexpressing human membrane proteins in stably transfected and clonal human embryonic kidney 293S cells'. *Nat Protoc,* 7**,** 453-66.

Chaudhury, S., Lyskov, S. & Gray, J. J. (2010). 'PyRosetta: a script-based interface for implementing molecular modeling algorithms using Rosetta'. *Bioinformatics,* 26**,** 689-691.

Chen, L., Kwon, Y. D., Zhou, T., Wu, X., O'dell, S., Cavacini, L., Hessell, A. J., Pancera, M., Tang, M., Xu, L., Yang, Z. Y., Zhang, M. Y., Arthos, J., Burton, D. R., Dimitrov, D. S., Nabel, G. J., Posner, M. R., Sodroski, J., Wyatt, R., Mascola, J. R. & Kwong, P. D. (2009a). 'Structural basis of immune evasion at the site of CD4 attachment on HIV-1 gp120'. *Science,* 326**,** 1123-7.

Chen, L., Kwon, Y. D., Zhou, T. Q., Wu, X. L., O'dell, S., Cavacini, L., Hessell, A. J., Pancera, M., Tang, M., Xu, L., Yang, Z. Y., Zhang, M. Y., Arthos, J., Burton, D. R., Dimitrov, D. S., Nabel, G. J., Posner, M. R., Sodroski, J., Wyatt, R., Mascola, J. R. & Kwong, P. D. (2009b). 'Structural Basis of Immune Evasion at the Site of CD4 Attachment on HIV-1 gp120'. *Science,* 326**,** 1123-1127.

Chung, A. W., Isitman, G., Navis, M., Kramski, M., Center, R. J., Kent, S. J. & Stratov, I. (2011). 'Immune escape from HIV-specific antibody-dependent cellular cytotoxicity (ADCC) pressure'. *Proceedings of the National Academy of Sciences of the United States of America,* 108**,** 7505-10.

Chung, N. P., Matthews, K., Kim, H. J., Ketas, T. J., Golabek, M., De Los Reyes, K., Korzun, J., Yasmeen, A., Sanders, R. W., Klasse, P. J., Wilson, I. A., Ward, A. B., Marozsan, A. J., Moore, J. P. & Cupo, A. (2014). 'Stable 293 T and CHO cell lines expressing cleaved, stable HIV-1 envelope glycoprotein trimers for structural and vaccine studies'. *Retrovirology,* 11**,** 33.

Connor, R. I. & Ho, D. D. (1994). 'Human immunodeficiency virus type 1 variants with increased replicative capacity develop during the asymptomatic stage before disease progression'. *J Virol,* 68**,** 4400-8.

Correia, B. E., Bates, J. T., Loomis, R. J., Baneyx, G., Carrico, C., Jardine, J. G., Rupert, P., Correnti, C., Kalyuzhniy, O., Vittal, V., Connell, M. J., Stevens, E., Schroeter, A., Chen, M., Macpherson, S., Serra, A. M., Adachi, Y., Holmes, M. A., Li, Y., Klevit, R. E., Graham, B. S., Wyatt, R. T., Baker, D., Strong, R. K., Crowe, J. E., Jr., Johnson, P. R. & Schief, W. R. (2014). 'Proof of principle for epitope-focused vaccine design'. *Nature,* 507**,** 201-6.

Corti, D., Langedijk, J. P., Hinz, A., Seaman, M. S., Vanzetta, F., Fernandez-Rodriguez, B. M., Silacci, C., Pinna, D., Jarrossay, D., Balla-Jhagjhoorsingh, S., Willems, B., Zekveld, M. J., Dreja, H., O'sullivan, E., Pade, C., Orkin, C., Jeffs, S. A., Montefiori, D. C., Davis, D., Weissenhorn, W., Mcknight, A., Heeney, J. L., Sallusto, F., Sattentau, Q. J., Weiss, R. A. & Lanzavecchia, A. (2010a). 'Analysis of memory B cell responses and isolation of novel monoclonal antibodies with neutralizing breadth from HIV-1-infected individuals'. *PLoS One,* 5**,** e8805.

Corti, D., Suguitan, A. L., Jr., Pinna, D., Silacci, C., Fernandez-Rodriguez, B. M., Vanzetta, F., Santos, C., Luke, C. J., Torres-Velez, F. J., Temperton, N. J., Weiss, R. A., Sallusto, F., Subbarao, K. & Lanzavecchia, A. (2010b). 'Heterosubtypic neutralizing antibodies are produced by individuals immunized with a seasonal influenza vaccine'. *J Clin Invest,* 120**,** 1663-73.

Crooks, E. T., Tong, T., Osawa, K. & Binley, J. M. (2011). 'Enzyme digests eliminate nonfunctional Env from HIV-1 particle surfaces, leaving native Env trimers intact and viral infectivity unaffected'. *J Virol,* 85**,** 5825-39.

Dalgleish, A. G., Beverley, P. C., Clapham, P. R., Crawford, D. H., Greaves, M. F. & Weiss, R. A. (1984). 'The CD4 (T4) antigen is an essential component of the receptor for the AIDS retrovirus'. *Nature,* 312**,** 763-7.

Daniels, R., Svedine, S. & Hebert, D. N. (2004). 'N-linked carbohydrates act as lumenal maturation and quality control protein tags'. *Cell Biochem Biophys,* 41**,** 113-38.

Davies, D. R. & Cohen, G. H. (1996). 'Interactions of protein antigens with antibodies'. *Proc Natl Acad Sci U S A,* 93**,** 7-12.

De Genst, E., Silence, K., Decanniere, K., Conrath, K., Loris, R., Kinne, J., Muyldermans, S. & Wyns, L. (2006). 'Molecular basis for the preferential cleft recognition by dromedary

heavy-chain antibodies'. *Proceedings of the National Academy of Sciences of the United States of America,* 103**,** 4586-91.

Decanniere, K., Transue, T. R., Desmyter, A., Maes, D., Muyldermans, S. & Wyns, L. (2001). 'Degenerate interfaces in antigen-antibody complexes'. *J Mol Biol,* 313**,** 473-8.

Deng, H., Liu, R., Ellmeier, W., Choe, S., Unutmaz, D., Burkhart, M., Di Marzio, P., Marmon, S., Sutton, R. E., Hill, C. M., Davis, C. B., Peiper, S. C., Schall, T. J., Littman, D. R. & Landau, N. R. (1996). 'Identification of a major co-receptor for primary isolates of HIV-1'. *Nature,* 381**,** 661-6.

Diskin, R., Klein, F., Horwitz, J. A., Halper-Stromberg, A., Sather, D. N., Marcovecchio, P. M., Lee, T., West, A. P., Jr., Gao, H., Seaman, M. S., Stamatatos, L., Nussenzweig, M. C. & Bjorkman, P. J. (2013). 'Restricting HIV-1 pathways for escape using rationally designed anti-HIV-1 antibodies'. *J Exp Med,* 210**,** 1235-49.

Diskin, R., Scheid, J. F., Marcovecchio, P. M., West, A. P., Jr., Klein, F., Gao, H., Gnanapragasam, P. N., Abadir, A., Seaman, M. S., Nussenzweig, M. C. & Bjorkman, P. J. (2011). 'Increasing the potency and breadth of an HIV antibody by using structure-based rational design'. *Science,* 334**,** 1289-93.

Doores, K. J., Bonomelli, C., Harvey, D. J., Vasiljevic, S., Dwek, R. A., Burton, D. R., Crispin, M. & Scanlan, C. N. (2010a). 'Envelope glycans of immunodeficiency virions are almost entirely oligomannose antigens'. *Proc Natl Acad Sci U S A,* 107**,** 13800-5.

Doores, K. J., Fulton, Z., Hong, V., Patel, M. K., Scanlan, C. N., Wormald, M. R., Finn, M. G., Burton, D. R., Wilson, I. A. & Davis, B. G. (2010b). 'A nonself sugar mimic of the HIV glycan shield shows enhanced antigenicity'. *Proceedings of the National Academy of Sciences of the United States of America,* 107**,** 17107-17112.

Doores, K. J., Fulton, Z., Huber, M., Wilson, I. A. & Burton, D. R. (2010c). 'Antibody 2G12 recognizes di-mannose equivalently in domain- and nondomain-exchanged forms but only binds the HIV-1 glycan shield if domain exchanged'. *J Virol,* 84**,** 10690-9.

Doria-Rose, N. A., Klein, R. M., Manion, M. M., O'dell, S., Phogat, A., Chakrabarti, B., Hallahan, C. W., Migueles, S. A., Wrammert, J., Ahmed, R., Nason, M., Wyatt, R. T., Mascola, J. R. & Connors, M. (2009). 'Frequency and phenotype of human immunodeficiency virus envelope-specific B cells from patients with broadly cross-neutralizing antibodies'. *J Virol,* 83**,** 188-99.

Doria-Rose, N. A., Schramm, C. A., Gorman, J., Moore, P. L., Bhiman, J. N., Dekosky, B. J., Ernandes, M. J., Georgiev, I. S., Kim, H. J., Pancera, M., Staupe, R. P., Altae-Tran, H. R., Bailer, R. T., Crooks, E. T., Cupo, A., Druz, A., Garrett, N. J., Hoi, K. H., Kong, R., Louder, M. K., Longo, N. S., Mckee, K., Nonyane, M., O'dell, S., Roark, R. S., Rudicell, R. S., Schmidt, S. D., Sheward, D. J., Soto, C., Wibmer, C. K., Yang, Y., Zhang, Z., Nisc Comparative, S., Mullikin, J. C., Binley, J. M., Sanders, R. W., Wilson, I. A., Moore, J. P., Ward, A. B., Georgiou, G., Williamson, C., Abdool Karim, S. S., Morris, L., Kwong, P. D., Shapiro, L. & Mascola, J. R. (2014). 'Developmental pathway for potent V1V2-directed HIV-neutralizing antibodies'. *Nature*.

Dragic, T., Litwin, V., Allaway, G. P., Martin, S. R., Huang, Y., Nagashima, K. A., Cayanan, C., Maddon, P. J., Koup, R. A., Moore, J. P. & Paxton, W. A. (1996). 'HIV-1 entry into CD4+ cells is mediated by the chemokine receptor CC-CKR-5'. *Nature,* 381**,** 667-73.

Dubay, J. W., Roberts, S. J., Brody, B. & Hunter, E. (1992). 'Mutations in the leucine zipper of the human immunodeficiency virus type 1 transmembrane glycoprotein affect fusion and infectivity'. *J Virol,* 66**,** 4748-56.

Dubuske, L. M., Frew, A. J., Horak, F., Keith, P. K., Corrigan, C. J., Aberer, W., Holdich, T. & Von Weikersthal-Drachenberg, K. J. (2011). 'Ultrashort-specific immunotherapy

successfully treats seasonal allergic rhinoconjunctivitis to grass pollen'. *Allergy Asthma Proc,* 32**,** 239-47.

Duncan, C. J., Russell, R. A. & Sattentau, Q. J. (2013). 'High multiplicity HIV-1 cell-to-cell transmission from macrophages to CD4+ T cells limits antiretroviral efficacy'. *AIDS,* 27**,** 2201-6.

Dunlop, D. C., Bonomelli, C., Mansab, F., Vasiljevic, S., Doores, K. J., Wormald, M. R., Palma, A. S., Feizi, T., Harvey, D. J., Dwek, R. A., Crispin, M. & Scanlan, C. N. (2010). 'Polysaccharide mimicry of the epitope of the broadly neutralizing anti-HIV antibody, 2G12, induces enhanced antibody responses to self oligomannose glycans'. *Glycobiology,* 20**,** 812-23.

Ekiert, D. C., Bhabha, G., Elsliger, M. A., Friesen, R. H., Jongeneelen, M., Throsby, M., Goudsmit, J. & Wilson, I. A. (2009). 'Antibody recognition of a highly conserved influenza virus epitope'. *Science,* 324**,** 246-51.

Euler, Z., Van Gils, M. J., Bunnik, E. M., Phung, P., Schweighardt, B., Wrin, T. & Schuitemaker, H. (2010). 'Cross-reactive neutralizing humoral immunity does not protect from HIV type 1 disease progression'. *J Infect Dis,* 201**,** 1045-53.

Falkowska, E., Le, K. M., Ramos, A., Doores, K. J., Lee, J. H., Blattner, C., Ramirez, A., Derking, R., Van Gils, M. J., Liang, C. H., Mcbride, R., Von Bredow, B., Shivatare, S. S., Wu, C. Y., Chan-Hui, P. Y., Liu, Y., Feizi, T., Zwick, M. B., Koff, W. C., Seaman, M. S., Swiderek, K., Moore, J. P., Evans, D., Paulson, J. C., Wong, C. H., Ward, A. B., Wilson, I. A., Sanders, R. W., Poignard, P. & Burton, D. R. (2014). 'Broadly neutralizing HIV antibodies define a glycan-dependent epitope on the prefusion conformation of gp41 on cleaved envelope trimers'. *Immunity,* 40**,** 657-68.

Fields, B. N., Knipe, D. M. & Howley, P. M. 2007. *Fields virology,* Philadelphia, Wolters Kluwer Health/Lippincott Williams & Wilkins.

Fischer, M. J. (2010). 'Amine coupling through EDC/NHS: a practical approach'. *Methods Mol Biol,* 627**,** 55-73.

Fischmann, T. O., Bentley, G. A., Bhat, T. N., Boulot, G., Mariuzza, R. A., Phillips, S. E., Tello, D. & Poljak, R. J. (1991). 'Crystallographic refinement of the three-dimensional structure of the FabD1.3-lysozyme complex at 2.5-A resolution'. *J Biol Chem,* 266**,** 12915-20.

Freiberger, F., Claus, H., Gunzel, A., Oltmann-Norden, I., Vionnet, J., Muhlenhoff, M., Vogel, U., Vann, W. F., Gerardy-Schahn, R. & Stummeyer, K. (2007). 'Biochemical characterization of a Neisseria meningitidis polysialyltransferase reveals novel functional motifs in bacterial sialyltransferases'. *Mol Microbiol,* 65**,** 1258-75.

Frost, S. D., Wrin, T., Smith, D. M., Kosakovsky Pond, S. L., Liu, Y., Paxinos, E., Chappey, C., Galovich, J., Beauchaine, J., Petropoulos, C. J., Little, S. J. & Richman, D. D. (2005). 'Neutralizing antibody responses drive the evolution of human immunodeficiency virus type 1 envelope during recent HIV infection'. *Proc Natl Acad Sci U S A,* 102**,** 18514-9.

Garcia-Selles, J., Pascual, A., Funes, E., Pagan, J. A., Lopez, J. D., Negro, J. M. & Hernandez, J. (2003). 'Clinical efficacy and safety of a depigmented and glutaraldehyde polymerized therapeutic vaccine of Parietaria judaica'. *Allergol Immunopathol (Madr),* 31**,** 63-9.

Gilbert, M., Brisson, J. R., Karwaski, M. F., Michniewicz, J., Cunningham, A. M., Wu, Y., Young, N. M. & Wakarchuk, W. W. (2000). 'Biosynthesis of ganglioside mimics in Campylobacter jejuni OH4384. Identification of the glycosyltransferase genes,

enzymatic synthesis of model compounds, and characterization of nanomole amounts by 600-mhz (1)h and (13)c NMR analysis'. *J Biol Chem,* 275**,** 3896-906.

Gitlin, A. D., Shulman, Z. & Nussenzweig, M. C. (2014). 'Clonal selection in the germinal centre by regulated proliferation and hypermutation'. *Nature,* 509**,** 637-40.

Gorry, P. R., Taylor, J., Holm, G. H., Mehle, A., Morgan, T., Cayabyab, M., Farzan, M., Wang, H., Bell, J. E., Kunstman, K., Moore, J. P., Wolinsky, S. M. & Gabuzda, D. (2002). 'Increased CCR5 affinity and reduced CCR5/CD4 dependence of a neurovirulent primary human immunodeficiency virus type 1 isolate'. *J Virol,* 76**,** 6277-92.

Gottardo, R., Bailer, R. T., Korber, B. T., Gnanakaran, S., Phillips, J., Shen, X., Tomaras, G. D., Turk, E., Imholte, G., Eckler, L., Wenschuh, H., Zerweck, J., Greene, K., Gao, H., Berman, P. W., Francis, D., Sinangil, F., Lee, C., Nitayaphan, S., Rerks-Ngarm, S., Kaewkungwal, J., Pitisuttithum, P., Tartaglia, J., Robb, M. L., Michael, N. L., Kim, J. H., Zolla-Pazner, S., Haynes, B. F., Mascola, J. R., Self, S., Gilbert, P. & Montefiori, D. C. (2013). 'Plasma IgG to linear epitopes in the V2 and V3 regions of HIV-1 gp120 correlate with a reduced risk of infection in the RV144 vaccine efficacy trial'. *PLoS One,* 8**,** e75665.

Gray, R. H., Wawer, M. J., Brookmeyer, R., Sewankambo, N. K., Serwadda, D., Wabwire-Mangen, F., Lutalo, T., Li, X., Vancott, T., Quinn, T. C. & Rakai Project, T. (2001). 'Probability of HIV-1 transmission per coital act in monogamous, heterosexual, HIV-1-discordant couples in Rakai, Uganda'. *Lancet,* 357**,** 1149-53.

Gregoriadis, G., Fernandes, A., Mital, M. & Mccormack, B. (2000). 'Polysialic acids: potential in improving the stability and pharmacokinetics of proteins and other therapeutics'. *Cellular and Molecular Life Sciences,* 57**,** 1964-1969.

Guan, Y., Pazgier, M., Sajadi, M. M., Kamin-Lewis, R., Al-Darmarki, S., Flinko, R., Lovo, E., Wu, X., Robinson, J. E., Seaman, M. S., Fouts, T. R., Gallo, R. C., Devico, A. L. & Lewis, G. K. (2013). 'Diverse specificity and effector function among human antibodies to HIV-1 envelope glycoprotein epitopes exposed by CD4 binding'. *Proceedings of the National Academy of Sciences of the United States of America,* 110**,** E69-78.

Haase, A. T. (2011). 'Early events in sexual transmission of HIV and SIV and opportunities for interventions'. *Annu Rev Med,* 62**,** 127-39.

Haim, H., Si, Z., Madani, N., Wang, L., Courter, J. R., Princiotto, A., Kassa, A., Degrace, M., Mcgee-Estrada, K., Mefford, M., Gabuzda, D., Smith, A. B., 3rd & Sodroski, J. (2009). 'Soluble CD4 and CD4-mimetic compounds inhibit HIV-1 infection by induction of a short-lived activated state'. *PLoS Pathog,* 5**,** e1000360.

Hakomori, S. & Zhang, Y. (1997). 'Glycosphingolipid antigens and cancer therapy'. *Chem Biol,* 4**,** 97-104.

Hallenberger, S., Bosch, V., Angliker, H., Shaw, E., Klenk, H. D. & Garten, W. (1992). 'Inhibition of furin-mediated cleavage activation of HIV-1 glycoprotein gp160'. *Nature,* 360**,** 358-61.

Harris, A., Borgnia, M. J., Shi, D., Bartesaghi, A., He, H., Pejchal, R., Kang, Y. K., Depetris, R., Marozsan, A. J., Sanders, R. W., Klasse, P. J., Milne, J. L., Wilson, I. A., Olson, W. C., Moore, J. P. & Subramaniam, S. (2011). 'Trimeric HIV-1 glycoprotein gp140 immunogens and native HIV-1 envelope glycoproteins display the same closed and open quaternary molecular architectures'. *Proc Natl Acad Sci U S A,* 108**,** 11440-5.

Haynes, B. F., Fleming, J., St Clair, E. W., Katinger, H., Stiegler, G., Kunert, R., Robinson, J., Scearce, R. M., Plonk, K., Staats, H. F., Ortel, T. L., Liao, H. X. & Alam, S. M. (2005). 'Cardiolipin polyspecific autoreactivity in two broadly neutralizing HIV-1 antibodies'. *Science,* 308**,** 1906-8.

Haynes, B. F., Gilbert, P. B., Mcelrath, M. J., Zolla-Pazner, S., Tomaras, G. D., Alam, S. M., Evans, D. T., Montefiori, D. C., Karnasuta, C., Sutthent, R., Liao, H. X., Devico, A. L., Lewis, G. K., Williams, C., Pinter, A., Fong, Y., Janes, H., Decamp, A., Huang, Y., Rao, M., Billings, E., Karasavvas, N., Robb, M. L., Ngauy, V., De Souza, M. S., Paris, R., Ferrari, G., Bailer, R. T., Soderberg, K. A., Andrews, C., Berman, P. W., Frahm, N., De Rosa, S. C., Alpert, M. D., Yates, N. L., Shen, X., Koup, R. A., Pitisuttithum, P., Kaewkungwal, J., Nitayaphan, S., Rerks-Ngarm, S., Michael, N. L. & Kim, J. H. (2012a). 'Immune-correlates analysis of an HIV-1 vaccine efficacy trial'. *N Engl J Med,* 366**,** 1275-86.

Haynes, B. F., Gilbert, P. B., Mcelrath, M. J., Zolla-Pazner, S., Tomaras, G. D., Alam, S. M., Evans, D. T., Montefiori, D. C., Karnasuta, C., Sutthent, R., Liao, H. X., Devico, A. L., Lewis, G. K., Williams, C., Pinter, A., Fong, Y., Janes, H., Decamp, A., Huang, Y., Rao, M., Billings, E., Karasavvas, N., Robb, M. L., Ngauy, V., De Souza, M. S., Paris, R., Ferrari, G., Bailer, R. T., Soderberg, K. A., Andrews, C., Berman, P. W., Frahm, N., De Rosa, S. C., Alpert, M. D., Yates, N. L., Shen, X., Koup, R. A., Pitisuttithum, P., Kaewkungwal, J., Nitayaphan, S., Rerks-Ngarm, S., Michael, N. L. & Kim, J. H. (2012b). 'Immune-correlates analysis of an HIV-1 vaccine efficacy trial'. *The New England journal of medicine,* 366**,** 1275-86.

Hessell, A. J., Hangartner, L., Hunter, M., Havenith, C. E. G., Beurskens, F. J., Bakker, J. M., Lanigan, C. M. S., Landucci, G., Forthal, D. N., Parren, P., Marx, P. A. & Burton, D. R. (2007). 'Fc receptor but not complement binding is important in antibody protection against HIV'. *Nature,* 449**,** 101-U75.

Hessell, A. J., Poignard, P., Hunter, M., Hangartner, L., Tehrani, D. M., Bleeker, W. K., Parren, P. W., Marx, P. A. & Burton, D. R. (2009a). 'Effective, low-titer antibody protection against low-dose repeated mucosal SHIV challenge in macaques'. *Nat Med,* 15**,** 951-4.

Hessell, A. J., Poignard, P., Hunter, M., Hangartner, L., Tehrani, D. M., Bleeker, W. K., Parren, P. W., Marx, P. A. & Burton, D. R. (2009b). 'Effective, low-titer antibody protection against low-dose repeated mucosal SHIV challenge in macaques'. *Nature medicine,* 15**,** 951-4.

Hessell, A. J., Rakasz, E. G., Poignard, P., Hangartner, L., Landucci, G., Forthal, D. N., Koff, W. C., Watkins, D. I. & Burton, D. R. (2009c). 'Broadly neutralizing human anti-HIV antibody 2G12 is effective in protection against mucosal SHIV challenge even at low serum neutralizing titers'. *PLoS Pathog,* 5**,** e1000433.

Hessell, A. J., Rakasz, E. G., Tehrani, D. M., Huber, M., Weisgrau, K. L., Landucci, G., Forthal, D. N., Koff, W. C., Poignard, P., Watkins, D. I. & Burton, D. R. (2010). 'Broadly neutralizing monoclonal antibodies 2F5 and 4E10 directed against the human immunodeficiency virus type 1 gp41 membrane-proximal external region protect against mucosal challenge by simian-human immunodeficiency virus SHIVBa-L'. *J Virol,* 84**,** 1302-13.

Ho, D. D., Mckeating, J. A., Li, X. L., Moudgil, T., Daar, E. S., Sun, N. C. & Robinson, J. E. (1991). 'Conformational epitope on gp120 important in CD4 binding and human immunodeficiency virus type 1 neutralization identified by a human monoclonal antibody'. *J Virol,* 65**,** 489-93.

Hoffenberg, S., Powell, R., Carpov, A., Wagner, D., Wilson, A., Kosakovsky Pond, S., Lindsay, R., Arendt, H., Destefano, J., Phogat, S., Poignard, P., Fling, S. P., Simek, M., Labranche, C., Montefiori, D., Wrin, T., Phung, P., Burton, D., Koff, W., King, C. R., Parks, C. L. & Caulfield, M. J. (2013). 'Identification of an HIV-1 clade A envelope that

exhibits broad antigenicity and neutralization sensitivity and elicits antibodies targeting three distinct epitopes'. *J Virol,* 87**,** 5372-83.

Hoot, S., Mcguire, A. T., Cohen, K. W., Strong, R. K., Hangartner, L., Klein, F., Diskin, R., Scheid, J. F., Sather, D. N., Burton, D. R. & Stamatatos, L. (2013). 'Recombinant HIV envelope proteins fail to engage germline versions of anti-CD4bs bNAbs'. *PLoS Pathog,* 9**,** e1003106.

Hopwood, D., Callen, C. R. & Mccabe, M. (1970). 'The reactions between glutaraldehyde and various proteins. An investigation of their kinetics'. *Histochem J,* 2**,** 137-50.

Horwitz, J. A., Halper-Stromberg, A., Mouquet, H., Gitlin, A. D., Tretiakova, A., Eisenreich, T. R., Malbec, M., Gravemann, S., Billerbeck, E., Dorner, M., Buning, H., Schwartz, O., Knops, E., Kaiser, R., Seaman, M. S., Wilson, J. M., Rice, C. M., Ploss, A., Bjorkman, P. J., Klein, F. & Nussenzweig, M. C. (2013). 'HIV-1 suppression and durable control by combining single broadly neutralizing antibodies and antiretroviral drugs in humanized mice'. *Proc Natl Acad Sci U S A,* 110**,** 16538-43.

Hraber, P., Seaman, M. S., Bailer, R. T., Mascola, J. R., Montefiori, D. C. & Korber, B. T. (2014). 'Prevalence of broadly neutralizing antibody responses during chronic HIV-1 infection'. *AIDS,* 28**,** 163-9.

Hu, G., Liu, J., Taylor, K. A. & Roux, K. H. (2010). 'Structural Comparison of HIV-1 Envelope Spikes with and without the V1/V2 Loop'. *J Virol*.

Huang, C. C., Tang, M., Zhang, M. Y., Majeed, S., Montabana, E., Stanfield, R. L., Dimitrov, D. S., Korber, B., Sodroski, J., Wilson, I. A., Wyatt, R. & Kwong, P. D. (2005). 'Structure of a V3-containing HIV-1 gp120 core'. *Science,* 310**,** 1025-8.

Huang, J., Kang, B. H., Pancera, M., Lee, J. H., Tong, T., Feng, Y., Georgiev, I. S., Chuang, G. Y., Druz, A., Doria-Rose, N. A., Laub, L., Sliepen, K., Van Gils, M. J., De La Pena, A. T., Derking, R., Klasse, P. J., Migueles, S. A., Bailer, R. T., Alam, M., Pugach, P., Haynes, B. F., Wyatt, R. T., Sanders, R. W., Binley, J. M., Ward, A. B., Mascola, J. R., Kwong, P. D. & Connors, M. (2014). 'Broad and potent HIV-1 neutralization by a human antibody that binds the gp41-gp120 interface'. *Nature*.

Huang, J., Ofek, G., Laub, L., Louder, M. K., Doria-Rose, N. A., Longo, N. S., Imamichi, H., Bailer, R. T., Chakrabarti, B., Sharma, S. K., Alam, S. M., Wang, T., Yang, Y., Zhang, B., Migueles, S. A., Wyatt, R., Haynes, B. F., Kwong, P. D., Mascola, J. R. & Connors, M. (2012). 'Broad and potent neutralization of HIV-1 by a gp41-specific human antibody'. *Nature,* 491**,** 406-12.

Huang, Y., Gilbert, P. B., Montefiori, D. C. & Self, S. G. (2009). 'Simultaneous Evaluation of the Magnitude and Breadth of a Left and Right Censored Multivariate Response, with Application to HIV Vaccine Development'. *Stat Biopharm Res,* 1**,** 81-91.

Huber, M., Fischer, M., Misselwitz, B., Manrique, A., Kuster, H., Niederost, B., Weber, R., Von Wyl, V., Gunthard, H. F. & Trkola, A. (2006). 'Complement lysis activity in autologous plasma is associated with lower viral loads during the acute phase of HIV-1 infection'. *PLoS Med,* 3**,** e441.

Jardine, J., Julien, J. P., Menis, S., Ota, T., Kalyuzhniy, O., Mcguire, A., Sok, D., Huang, P. S., Macpherson, S., Jones, M., Nieusma, T., Mathison, J., Baker, D., Ward, A. B., Burton, D. R., Stamatatos, L., Nemazee, D., Wilson, I. A. & Schief, W. R. (2013). 'Rational HIV immunogen design to target specific germline B cell receptors'. *Science,* 340**,** 711-6.

Johnson, G. & Wu, T. T. (1998). 'Preferred CDRH3 lengths for antibodies with defined specificities'. *Int Immunol,* 10**,** 1801-5.

Jolly, C., Welsch, S., Michor, S. & Sattentau, Q. J. (2011). 'The regulated secretory pathway in CD4(+) T cells contributes to human immunodeficiency virus type-1 cell-to-cell spread at the virological synapse'. *PLoS Pathog,* 7**,** e1002226.

Jones, J., Krag, S. S. & Betenbaugh, M. J. (2005). 'Controlling N-linked glycan site occupancy'. *Biochim Biophys Acta,* 1726**,** 121-37.

Joyce, M. G., Kanekiyo, M., Xu, L., Biertumpfel, C., Boyington, J. C., Moquin, S., Shi, W., Wu, X., Yang, Y., Yang, Z. Y., Zhang, B., Zheng, A., Zhou, T., Zhu, J., Mascola, J. R., Kwong, P. D. & Nabel, G. J. (2013). 'Outer domain of HIV-1 gp120: antigenic optimization, structural malleability, and crystal structure with antibody VRC-PG04'. *J Virol,* 87**,** 2294-306.

Julien, J. P., Cupo, A., Sok, D., Stanfield, R. L., Lyumkis, D., Deller, M. C., Klasse, P. J., Burton, D. R., Sanders, R. W., Moore, J. P., Ward, A. B. & Wilson, I. A. (2013a). 'Crystal structure of a soluble cleaved HIV-1 envelope trimer'. *Science,* 342**,** 1477-83.

Julien, J. P., Lee, J. H., Cupo, A., Murin, C. D., Derking, R., Hoffenberg, S., Caulfield, M. J., King, C. R., Marozsan, A. J., Klasse, P. J., Sanders, R. W., Moore, J. P., Wilson, I. A. & Ward, A. B. (2013b). 'Asymmetric recognition of the HIV-1 trimer by broadly neutralizing antibody PG9'. *Proc Natl Acad Sci U S A,* 110**,** 4351-6.

Julien, J. P., Lee, P. S. & Wilson, I. A. (2012). 'Structural insights into key sites of vulnerability on HIV-1 Env and influenza HA'. *Immunol Rev,* 250**,** 180-98.

Jung, D., Giallourakis, C., Mostoslavsky, R. & Alt, F. W. (2006). 'Mechanism and control of V(D)J recombination at the immunoglobulin heavy chain locus'. *Annu Rev Immunol,* 24**,** 541-70.

Kanekiyo, M., Wei, C. J., Yassine, H. M., Mctamney, P. M., Boyington, J. C., Whittle, J. R., Rao, S. S., Kong, W. P., Wang, L. & Nabel, G. J. (2013). 'Self-assembling influenza nanoparticle vaccines elicit broadly neutralizing H1N1 antibodies'. *Nature,* 499**,** 102-6.

Karasavvas, N., Billings, E., Rao, M., Williams, C., Zolla-Pazner, S., Bailer, R. T., Koup, R. A., Madnote, S., Arworn, D., Shen, X., Tomaras, G. D., Currier, J. R., Jiang, M., Magaret, C., Andrews, C., Gottardo, R., Gilbert, P., Cardozo, T. J., Rerks-Ngarm, S., Nitayaphan, S., Pitisuttithum, P., Kaewkungwal, J., Paris, R., Greene, K., Gao, H., Gurunathan, S., Tartaglia, J., Sinangil, F., Korber, B. T., Montefiori, D. C., Mascola, J. R., Robb, M. L., Haynes, B. F., Ngauy, V., Michael, N. L., Kim, J. H., De Souza, M. S. & Collaboration, M. T. (2012). 'The Thai Phase III HIV Type 1 Vaccine trial (RV144) regimen induces antibodies that target conserved regions within the V2 loop of gp120'. *AIDS Res Hum Retroviruses,* 28**,** 1444-57.

Katoh, K., Asimenos, G. & Toh, H. (2009). 'Multiple alignment of DNA sequences with MAFFT'. *Methods Mol Biol,* 537**,** 39-64.

Kawahara, J., Ohmori, T., Ohkubo, T., Hattori, S. & Kawamura, M. (1992). 'The structure of glutaraldehyde in aqueous solution determined by ultraviolet absorption and light scattering'. *Anal Biochem,* 201**,** 94-8.

Kepler, T. B., Liao, H. X., Alam, S. M., Bhaskarabhatla, R., Zhang, R., Yandava, C., Stewart, S., Anasti, K., Kelsoe, G., Parks, R., Lloyd, K. E., Stolarchuk, C., Pritchett, J., Solomon, E., Friberg, E., Morris, L., Karim, S. S., Cohen, M. S., Walter, E., Moody, M. A., Wu, X., Altae-Tran, H. R., Georgiev, I. S., Kwong, P. D., Boyd, S. D., Fire, A. Z., Mascola, J. R. & Haynes, B. F. (2014). 'Immunoglobulin Gene Insertions and Deletions in the Affinity Maturation of HIV-1 Broadly Reactive Neutralizing Antibodies'. *Cell Host Microbe,* 16**,** 304-13.

Khatua, B., Roy, S. & Mandal, C. (2013). 'Sialic acids siglec interaction: a unique strategy to circumvent innate immune response by pathogens'. *Indian J Med Res,* 138**,** 648-62.

Kilmarx, P. H. (2009). 'Global epidemiology of HIV'. *Curr Opin HIV AIDS,* 4**,** 240-6.

Klasse, P. J. (2007). 'Modeling how many envelope glycoprotein trimers per virion participate in human immunodeficiency virus infectivity and its neutralization by antibody'. *Virology,* 369**,** 245-62.

Klasse, P. J., Depetris, R. S., Pejchal, R., Julien, J. P., Khayat, R., Lee, J. H., Marozsan, A. J., Cupo, A., Cocco, N., Korzun, J., Yasmeen, A., Ward, A. B., Wilson, I. A., Sanders, R. W. & Moore, J. P. (2013). 'Influences on trimerization and aggregation of soluble, cleaved HIV-1 SOSIP envelope glycoprotein'. *J Virol,* 87**,** 9873-85.

Klatzmann, D., Champagne, E., Chamaret, S., Gruest, J., Guetard, D., Hercend, T., Gluckman, J. C. & Montagnier, L. (1984). 'T-lymphocyte T4 molecule behaves as the receptor for human retrovirus LAV'. *Nature,* 312**,** 767-8.

Klein, F., Gaebler, C., Mouquet, H., Sather, D. N., Lehmann, C., Scheid, J. F., Kraft, Z., Liu, Y., Pietzsch, J., Hurley, A., Poignard, P., Feizi, T., Morris, L., Walker, B. D., Fatkenheuer, G., Seaman, M. S., Stamatatos, L. & Nussenzweig, M. C. (2012a). 'Broad neutralization by a combination of antibodies recognizing the CD4 binding site and a new conformational epitope on the HIV-1 envelope protein'. *J Exp Med,* 209**,** 1469-79.

Klein, F., Halper-Stromberg, A., Horwitz, J. A., Gruell, H., Scheid, J. F., Bournazos, S., Mouquet, H., Spatz, L. A., Diskin, R., Abadir, A., Zang, T., Dorner, M., Billerbeck, E., Labitt, R. N., Gaebler, C., Marcovecchio, P. M., Incesu, R. B., Eisenreich, T. R., Bieniasz, P. D., Seaman, M. S., Bjorkman, P. J., Ravetch, J. V., Ploss, A. & Nussenzweig, M. C. (2012b). 'HIV therapy by a combination of broadly neutralizing antibodies in humanized mice'. *Nature,* 492**,** 118-22.

Kong, L., Giang, E., Nieusma, T., Kadam, R. U., Cogburn, K. E., Hua, Y., Dai, X., Stanfield, R. L., Burton, D. R., Ward, A. B., Wilson, I. A. & Law, M. (2013a). 'Hepatitis C virus E2 envelope glycoprotein core structure'. *Science,* 342**,** 1090-4.

Kong, L., Lee, J. H., Doores, K. J., Murin, C. D., Julien, J. P., Mcbride, R., Liu, Y., Marozsan, A., Cupo, A., Klasse, P. J., Hoffenberg, S., Caulfield, M., King, C. R., Hua, Y., Le, K. M., Khayat, R., Deller, M. C., Clayton, T., Tien, H., Feizi, T., Sanders, R. W., Paulson, J. C., Moore, J. P., Stanfield, R. L., Burton, D. R., Ward, A. B. & Wilson, I. A. (2013b). 'Supersite of immune vulnerability on the glycosylated face of HIV-1 envelope glycoprotein gp120'. *Nat Struct Mol Biol,* 20**,** 796-803.

Kong, L. & Sattentau, Q. J. (2012). 'Antigenicity and Immunogenicity in HIV-1 Antibody-Based Vaccine Design'. *J AIDS Clin Res,* S8**,** 3.

Kong, L., Sheppard, N. C., Stewart-Jones, G. B., Robson, C. L., Chen, H., Xu, X., Krashias, G., Bonomelli, C., Scanlan, C. N., Kwong, P. D., Jeffs, S. A., Jones, I. M. & Sattentau, Q. J. (2010). 'Expression-system-dependent modulation of HIV-1 envelope glycoprotein antigenicity and immunogenicity'. *J Mol Biol,* 403**,** 131-47.

Krashias, G., Simon, A. K., Wegmann, F., Kok, W. L., Ho, L. P., Stevens, D., Skehel, J., Heeney, J. L., Moghaddam, A. E. & Sattentau, Q. J. (2010). 'Potent adaptive immune responses induced against HIV-1 gp140 and influenza virus HA by a polyanionic carbomer'. *Vaccine,* 28**,** 2482-9.

Kulp, D. W. & Schief, W. R. (2013). 'Advances in structure-based vaccine design'. *Curr Opin Virol,* 3**,** 322-31.

Kwong, P. D., Doyle, M. L., Casper, D. J., Cicala, C., Leavitt, S. A., Majeed, S., Steenbeke, T. D., Venturi, M., Chaiken, I., Fung, M., Katinger, H., Parren, P. W., Robinson, J., Van

Ryk, D., Wang, L., Burton, D. R., Freire, E., Wyatt, R., Sodroski, J., Hendrickson, W. A. & Arthos, J. (2002). 'HIV-1 evades antibody-mediated neutralization through conformational masking of receptor-binding sites'. *Nature,* 420**,** 678-82.

Kwong, P. D., Wyatt, R., Robinson, J., Sweet, R. W., Sodroski, J. & Hendrickson, W. A. (1998). 'Structure of an HIV gp120 envelope glycoprotein in complex with the CD4 receptor and a neutralizing human antibody'. *Nature,* 393**,** 648-59.

Labrijn, A. F., Poignard, P., Raja, A., Zwick, M. B., Delgado, K., Franti, M., Binley, J., Vivona, V., Grundner, C., Huang, C. C., Venturi, M., Petropoulos, C. J., Wrin, T., Dimitrov, D. S., Robinson, J., Kwong, P. D., Wyatt, R. T., Sodroski, J. & Burton, D. R. (2003). 'Access of antibody molecules to the conserved coreceptor binding site on glycoprotein gp120 is sterically restricted on primary human immunodeficiency virus type 1'. *J Virol,* 77**,** 10557-65.

Lai, R. P., Seaman, M. S., Tonks, P., Wegmann, F., Seilly, D. J., Frost, S. D., Labranche, C. C., Montefiori, D. C., Dey, A. K., Srivastava, I. K., Sattentau, Q., Barnett, S. W. & Heeney, J. L. (2012). 'Mixed adjuvant formulations reveal a new combination that elicit antibody response comparable to Freund's adjuvants'. *PLoS One,* 7**,** e35083.

Lavine, C. L., Lao, S., Montefiori, D. C., Haynes, B. F., Sodroski, J. G., Yang, X. Z. & Immunol, N. C. H. a. V. (2012). 'High-Mannose Glycan-Dependent Epitopes Are Frequently Targeted in Broad Neutralizing Antibody Responses during Human Immunodeficiency Virus Type 1 Infection'. *Journal of Virology,* 86**,** 2153-2164.

Lederman, M. M., Jump, R., Pilch-Cooper, H. A., Root, M. & Sieg, S. F. (2008). 'Topical application of entry inhibitors as "virustats" to prevent sexual transmission of HIV infection'. *Retrovirology,* 5**,** 116.

Lee, Y. C., Stowell, C. P. & Krantz, M. J. (1976). '2-Imino-2-methoxyethyl 1-thioglycosides: new reagents for attaching sugars to proteins'. *Biochemistry,* 15**,** 3956-63.

Leonard, C. K., Spellman, M. W., Riddle, L., Harris, R. J., Thomas, J. N. & Gregory, T. J. (1990). 'Assignment of intrachain disulfide bonds and characterization of potential glycosylation sites of the type 1 recombinant human immunodeficiency virus envelope glycoprotein (gp120) expressed in Chinese hamster ovary cells'. *J Biol Chem,* 265**,** 10373-82.

Lever, A. M. & Jeang, K. T. (2006). 'Replication of human immunodeficiency virus type 1 from entry to exit'. *Int J Hematol,* 84**,** 23-30.

Li, M., Gao, F., Mascola, J. R., Stamatatos, L., Polonis, V. R., Koutsoukos, M., Voss, G., Goepfert, P., Gilbert, P., Greene, K. M., Bilska, M., Kothe, D. L., Salazar-Gonzalez, J. F., Wei, X., Decker, J. M., Hahn, B. H. & Montefiori, D. C. (2005). 'Human immunodeficiency virus type 1 env clones from acute and early subtype B infections for standardized assessments of vaccine-elicited neutralizing antibodies'. *J Virol,* 79**,** 10108-25.

Liao, H. X., Lynch, R., Zhou, T., Gao, F., Alam, S. M., Boyd, S. D., Fire, A. Z., Roskin, K. M., Schramm, C. A., Zhang, Z., Zhu, J., Shapiro, L., Program, N. C. S., Mullikin, J. C., Gnanakaran, S., Hraber, P., Wiehe, K., Kelsoe, G., Yang, G., Xia, S. M., Montefiori, D. C., Parks, R., Lloyd, K. E., Scearce, R. M., Soderberg, K. A., Cohen, M., Kamanga, G., Louder, M. K., Tran, L. M., Chen, Y., Cai, F., Chen, S., Moquin, S., Du, X., Joyce, M. G., Srivatsan, S., Zhang, B., Zheng, A., Shaw, G. M., Hahn, B. H., Kepler, T. B., Korber, B. T., Kwong, P. D., Mascola, J. R. & Haynes, B. F. (2013a). 'Co-evolution of a broadly neutralizing HIV-1 antibody and founder virus'. *Nature,* 496**,** 469-76.

Liao, H. X., Tsao, C. Y., Alam, S. M., Muldoon, M., Vandergrift, N., Ma, B. J., Lu, X., Sutherland, L. L., Scearce, R. M., Bowman, C., Parks, R., Chen, H., Blinn, J. H.,

Lapedes, A., Watson, S., Xia, S. M., Foulger, A., Hahn, B. H., Shaw, G. M., Swanstrom, R., Montefiori, D. C., Gao, F., Haynes, B. F. & Korber, B. (2013b). 'Antigenicity and immunogenicity of transmitted/founder, consensus, and chronic envelope glycoproteins of human immunodeficiency virus type 1'. *J Virol,* 87**,** 4185-201.

Lingwood, D., Mctamney, P. M., Yassine, H. M., Whittle, J. R., Guo, X., Boyington, J. C., Wei, C. J. & Nabel, G. J. (2012). 'Structural and genetic basis for development of broadly neutralizing influenza antibodies'. *Nature,* 489**,** 566-70.

Liu, C. C. & Ye, X. S. (2012). 'Carbohydrate-based cancer vaccines: target cancer with sugar bullets'. *Glycoconj J,* 29**,** 259-71.

Liu, J., Bartesaghi, A., Borgnia, M. J., Sapiro, G. & Subramaniam, S. (2008). 'Molecular architecture of native HIV-1 gp120 trimers'. *Nature,* 455**,** 109-13.

Liu, R., Paxton, W. A., Choe, S., Ceradini, D., Martin, S. R., Horuk, R., Macdonald, M. E., Stuhlmann, H., Koup, R. A. & Landau, N. R. (1996). 'Homozygous defect in HIV-1 coreceptor accounts for resistance of some multiply-exposed individuals to HIV-1 infection'. *Cell,* 86**,** 367-77.

Liu, Y. J., Joshua, D. E., Williams, G. T., Smith, C. A., Gordon, J. & Maclennan, I. C. M. (1989). 'Mechanism of Antigen-Driven Selection in Germinal-Centers'. *Nature,* 342**,** 929-931.

Luallen, R. J., Lin, J., Fu, H., Cai, K. K., Agrawal, C., Mboudjeka, I., Lee, F. H., Montefiori, D., Smith, D. F., Doms, R. W. & Geng, Y. (2008). 'An engineered Saccharomyces cerevisiae strain binds the broadly neutralizing human immunodeficiency virus type 1 antibody 2G12 and elicits mannose-specific gp120-binding antibodies'. *J Virol,* 82**,** 6447-57.

Lyumkis, D., Julien, J. P., De Val, N., Cupo, A., Potter, C. S., Klasse, P. J., Burton, D. R., Sanders, R. W., Moore, J. P., Carragher, B., Wilson, I. A. & Ward, A. B. (2013). 'Cryo-EM structure of a fully glycosylated soluble cleaved HIV-1 envelope trimer'. *Science,* 342**,** 1484-90.

Madhavi, V., Kent, S. J. & Stratov, I. (2012). 'HIV-specific antibody-dependent cellular cytotoxicity: a novel vaccine modality'. *Expert Rev Clin Immunol,* 8**,** 767-74.

Magnus, C., Rusert, P., Bonhoeffer, S., Trkola, A. & Regoes, R. R. (2009). 'Estimating the stoichiometry of human immunodeficiency virus entry'. *J Virol,* 83**,** 1523-31.

Mao, Y., Wang, L., Gu, C., Herschhorn, A., Desormeaux, A., Finzi, A., Xiang, S. H. & Sodroski, J. G. (2013). 'Molecular architecture of the uncleaved HIV-1 envelope glycoprotein trimer'. *Proc Natl Acad Sci U S A,* 110**,** 12438-43.

Mao, Y., Wang, L., Gu, C., Herschhorn, A., Xiang, S. H., Haim, H., Yang, X. & Sodroski, J. (2012). 'Subunit organization of the membrane-bound HIV-1 envelope glycoprotein trimer'. *Nat Struct Mol Biol,* 19**,** 893-9.

Mascola, J. R., Stiegler, G., Vancott, T. C., Katinger, H., Carpenter, C. B., Hanson, C. E., Beary, H., Hayes, D., Frankel, S. S., Birx, D. L. & Lewis, M. G. (2000). 'Protection of macaques against vaginal transmission of a pathogenic HIV-1/SIV chimeric virus by passive infusion of neutralizing antibodies'. *Nat Med,* 6**,** 207-10.

Mattson, G., Conklin, E., Desai, S., Nielander, G., Savage, M. D. & Morgensen, S. (1993). 'A practical approach to crosslinking'. *Mol Biol Rep,* 17**,** 167-83.

Mccoy, L. E., Quigley, A. F., Strokappe, N. M., Bulmer-Thomas, B., Seaman, M. S., Mortier, D., Rutten, L., Chander, N., Edwards, C. J., Ketteler, R., Davis, D., Verrips, T. & Weiss, R. A. (2012). 'Potent and broad neutralization of HIV-1 by a llama antibody elicited by immunization'. *J Exp Med,* 209**,** 1091-103.

Mcguire, A. T., Glenn, J. A., Lippy, A. & Stamatatos, L. (2014). 'Diverse recombinant HIV-1 Envs fail to activate B cells expressing the germline B cell receptors of the broadly neutralizing anti-HIV-1 antibodies PG9 and 447-52D'. *J Virol,* 88**,** 2645-57.

Mcguire, A. T., Hoot, S., Dreyer, A. M., Lippy, A., Stuart, A., Cohen, K. W., Jardine, J., Menis, S., Scheid, J. F., West, A. P., Schief, W. R. & Stamatatos, L. (2013). 'Engineering HIV envelope protein to activate germline B cell receptors of broadly neutralizing anti-CD4 binding site antibodies'. *J Exp Med,* 210**,** 655-63.

Mclellan, J. S., Chen, M., Joyce, M. G., Sastry, M., Stewart-Jones, G. B., Yang, Y., Zhang, B., Chen, L., Srivatsan, S., Zheng, A., Zhou, T., Graepel, K. W., Kumar, A., Moin, S., Boyington, J. C., Chuang, G. Y., Soto, C., Baxa, U., Bakker, A. Q., Spits, H., Beaumont, T., Zheng, Z., Xia, N., Ko, S. Y., Todd, J. P., Rao, S., Graham, B. S. & Kwong, P. D. (2013). 'Structure-based design of a fusion glycoprotein vaccine for respiratory syncytial virus'. *Science,* 342**,** 592-8.

Mclellan, J. S., Pancera, M., Carrico, C., Gorman, J., Julien, J. P., Khayat, R., Louder, R., Pejchal, R., Sastry, M., Dai, K., O'dell, S., Patel, N., Shahzad-Ul-Hussan, S., Yang, Y., Zhang, B., Zhou, T., Zhu, J., Boyington, J. C., Chuang, G. Y., Diwanji, D., Georgiev, I., Kwon, Y. D., Lee, D., Louder, M. K., Moquin, S., Schmidt, S. D., Yang, Z. Y., Bonsignori, M., Crump, J. A., Kapiga, S. H., Sam, N. E., Haynes, B. F., Burton, D. R., Koff, W. C., Walker, L. M., Phogat, S., Wyatt, R., Orwenyo, J., Wang, L. X., Arthos, J., Bewley, C. A., Mascola, J. R., Nabel, G. J., Schief, W. R., Ward, A. B., Wilson, I. A. & Kwong, P. D. (2011). 'Structure of HIV-1 gp120 V1/V2 domain with broadly neutralizing antibody PG9'. *Nature,* 480**,** 336-43.

Melnick, J. L. (1978). 'Advantages and disadvantages of killed and live poliomyelitis vaccines'. *Bull World Health Organ,* 56**,** 21-38.

Migneault, I., Dartiguenave, C., Bertrand, M. J. & Waldron, K. C. (2004). 'Glutaraldehyde: behavior in aqueous solution, reaction with proteins, and application to enzyme crosslinking'. *Biotechniques,* 37**,** 790-6, 798-802.

Miller, C. J., Li, Q., Abel, K., Kim, E. Y., Ma, Z. M., Wietgrefe, S., La Franco-Scheuch, L., Compton, L., Duan, L., Shore, M. D., Zupancic, M., Busch, M., Carlis, J., Wolinsky, S. & Haase, A. T. (2005). 'Propagation and dissemination of infection after vaginal transmission of simian immunodeficiency virus'. *J Virol,* 79**,** 9217-27.

Moldt, B., Rakasz, E. G., Schultz, N., Chan-Hui, P. Y., Swiderek, K., Weisgrau, K. L., Piaskowski, S. M., Bergman, Z., Watkins, D. I., Poignard, P. & Burton, D. R. (2012). 'Highly potent HIV-specific antibody neutralization in vitro translates into effective protection against mucosal SHIV challenge in vivo'. *Proc Natl Acad Sci U S A,* 109**,** 18921-5.

Montefiori, D. C. (2005). 'Evaluating neutralizing antibodies against HIV, SIV, and SHIV in luciferase reporter gene assays'. *Curr Protoc Immunol,* Chapter 12**,** Unit 12 11.

Moore, J. P., Mckeating, J. A., Weiss, R. A. & Sattentau, Q. J. (1990). 'Dissociation of gp120 from HIV-1 virions induced by soluble CD4'. *Science,* 250**,** 1139-42.

Moore, J. P. & Sodroski, J. (1996). 'Antibody cross-competition analysis of the human immunodeficiency virus type 1 gp120 exterior envelope glycoprotein'. *J Virol,* 70**,** 1863-72.

Moore, J. P., Thali, M., Jameson, B. A., Vignaux, F., Lewis, G. K., Poon, S. W., Charles, M., Fung, M. S., Sun, B., Durda, P. J. & Et Al. (1993). 'Immunochemical analysis of the gp120 surface glycoprotein of human immunodeficiency virus type 1: probing the structure of the C4 and V4 domains and the interaction of the C4 domain with the V3 loop'. *J Virol,* 67**,** 4785-96.

Moore, P. L., Crooks, E. T., Porter, L., Zhu, P., Cayanan, C. S., Grise, H., Corcoran, P., Zwick, M. B., Franti, M., Morris, L., Roux, K. H., Burton, D. R. & Binley, J. M. (2006). 'Nature of nonfunctional envelope proteins on the surface of human immunodeficiency virus type 1'. *J Virol,* 80**,** 2515-28.

Moremen, K. W., Tiemeyer, M. & Nairn, A. V. (2012). 'Vertebrate protein glycosylation: diversity, synthesis and function'. *Nat Rev Mol Cell Biol,* 13**,** 448-62.

Moulard, M., Phogat, S. K., Shu, Y., Labrijn, A. F., Xiao, X., Binley, J. M., Zhang, M. Y., Sidorov, I. A., Broder, C. C., Robinson, J., Parren, P. W., Burton, D. R. & Dimitrov, D. S. (2002). 'Broadly cross-reactive HIV-1-neutralizing human monoclonal Fab selected for binding to gp120-CD4-CCR5 complexes'. *Proc Natl Acad Sci U S A,* 99**,** 6913-8.

Nakajima, N. & Ikada, Y. (1995). 'Mechanism of amide formation by carbodiimide for bioconjugation in aqueous media'. *Bioconjug Chem,* 6**,** 123-30.

Natkanski, E., Lee, W. Y., Mistry, B., Casal, A., Molloy, J. E. & Tolar, P. (2013). 'B cells use mechanical energy to discriminate antigen affinities'. *Science,* 340**,** 1587-90.

Padler-Karavani, V., Hurtado-Ziola, N., Chang, Y. C., Sonnenburg, J. L., Ronaghy, A., Yu, H., Verhagen, A., Nizet, V., Chen, X., Varki, N., Varki, A. & Angata, T. (2014). 'Rapid evolution of binding specificities and expression patterns of inhibitory CD33-related Siglecs in primates'. *FASEB J,* 28**,** 1280-93.

Paiardini, M., Pandrea, I., Apetrei, C. & Silvestri, G. (2009). 'Lessons learned from the natural hosts of HIV-related viruses'. *Annu Rev Med,* 60**,** 485-95.

Pan, Y., Chefalo, P., Nagy, N., Harding, C. & Guo, Z. (2005). 'Synthesis and immunological properties of N-modified GM3 antigens as therapeutic cancer vaccines'. *J Med Chem,* 48**,** 875-83.

Pancera, M., Majeed, S., Ban, Y. E., Chen, L., Huang, C. C., Kong, L., Kwon, Y. D., Stuckey, J., Zhou, T., Robinson, J. E., Schief, W. R., Sodroski, J., Wyatt, R. & Kwong, P. D. (2010). 'Structure of HIV-1 gp120 with gp41-interactive region reveals layered envelope architecture and basis of conformational mobility'. *Proc Natl Acad Sci U S A,* 107**,** 1166-71.

Pantophlet, R., Wilson, I. A. & Burton, D. R. (2003). 'Hyperglycosylated mutants of human immunodeficiency virus (HIV) type 1 monomeric gp120 as novel antigens for HIV vaccine design'. *J Virol,* 77**,** 5889-901.

Park, S. N., Park, J. C., Kim, H. O., Song, M. J. & Suh, H. (2002). 'Characterization of porous collagen/hyaluronic acid scaffold modified by 1-ethyl-3-(3-dimethylaminopropyl)carbodiimide cross-linking'. *Biomaterials,* 23**,** 1205-12.

Pejchal, R., Doores, K. J., Walker, L. M., Khayat, R., Huang, P. S., Wang, S. K., Stanfield, R. L., Julien, J. P., Ramos, A., Crispin, M., Depetris, R., Katpally, U., Marozsan, A., Cupo, A., Maloveste, S., Liu, Y., Mcbride, R., Ito, Y., Sanders, R. W., Ogohara, C., Paulson, J. C., Feizi, T., Scanlan, C. N., Wong, C. H., Moore, J. P., Olson, W. C., Ward, A. B., Poignard, P., Schief, W. R., Burton, D. R. & Wilson, I. A. (2011). 'A potent and broad neutralizing antibody recognizes and penetrates the HIV glycan shield'. *Science,* 334**,** 1097-103.

Phillips, A. N., Lee, C. A., Elford, J., Janossy, G., Timms, A., Bofill, M. & Kernoff, P. B. (1991). 'Serial CD4 lymphocyte counts and development of AIDS'. *Lancet,* 337**,** 389-92.

Piantadosi, A., Panteleeff, D., Blish, C. A., Baeten, J. M., Jaoko, W., Mcclelland, R. S. & Overbaugh, J. (2009). 'Breadth of neutralizing antibody response to human immunodeficiency virus type 1 is affected by factors early in infection but does not influence disease progression'. *J Virol,* 83**,** 10269-74.

Pope, M. & Haase, A. T. (2003). 'Transmission, acute HIV-1 infection and the quest for strategies to prevent infection'. *Nat Med,* 9**,** 847-52.

Posner, M. R., Hideshima, T., Cannon, T., Mukherjee, M., Mayer, K. H. & Byrn, R. A. (1991). 'An IgG human monoclonal antibody that reacts with HIV-1/GP120, inhibits virus binding to cells, and neutralizes infection'. *J Immunol,* 146**,** 4325-32.

Puryear, W. B., Akiyama, H., Geer, S. D., Ramirez, N. P., Yu, X., Reinhard, B. M. & Gummuluru, S. (2013). 'Interferon-inducible mechanism of dendritic cell-mediated HIV-1 dissemination is dependent on Siglec-1/CD169'. *PLoS Pathog,* 9**,** e1003291.

Puryear, W. B., Yu, X., Ramirez, N. P., Reinhard, B. M. & Gummuluru, S. (2012). 'HIV-1 incorporation of host-cell-derived glycosphingolipid GM3 allows for capture by mature dendritic cells'. *Proc Natl Acad Sci U S A,* 109**,** 7475-80.

Qin, Y., Banasik, M., Kim, S., Penn-Nicholson, A., Habte, H. H., Labranche, C., Montefiori, D. C., Wang, C. & Cho, M. W. (2014). 'Eliciting neutralizing antibodies with gp120 outer domain constructs based on M-group consensus sequence'. *Virology,* 462-463**,** 363-76.

Rapoport, E., Mikhalyov, I., Zhang, J., Crocker, P. & Bovin, N. (2003). 'Ganglioside binding pattern of CD33-related siglecs'. *Bioorg Med Chem Lett,* 13**,** 675-8.

Rappuoli, R. (1994). 'Toxin inactivation and antigen stabilization: two different uses of formaldehyde'. *Vaccine,* 12**,** 579-81.

Reeves, P. J., Callewaert, N., Contreras, R. & Khorana, H. G. (2002). 'Structure and function in rhodopsin: high-level expression of rhodopsin with restricted and homogeneous N-glycosylation by a tetracycline-inducible N-acetylglucosaminyltransferase I-negative HEK293S stable mammalian cell line'. *Proc Natl Acad Sci U S A,* 99**,** 13419-24.

Rerks-Ngarm, S., Pitisuttithum, P., Nitayaphan, S., Kaewkungwal, J., Chiu, J., Paris, R., Premsri, N., Namwat, C., De Souza, M., Adams, E., Benenson, M., Gurunathan, S., Tartaglia, J., Mcneil, J. G., Francis, D. P., Stablein, D., Birx, D. L., Chunsuttiwat, S., Khamboonruang, C., Thongcharoen, P., Robb, M. L., Michael, N. L., Kunasol, P. & Kim, J. H. (2009). 'Vaccination with ALVAC and AIDSVAX to prevent HIV-1 infection in Thailand'. *N Engl J Med,* 361**,** 2209-20.

Richman, D. D. & Bozzette, S. A. (1994). 'The impact of the syncytium-inducing phenotype of human immunodeficiency virus on disease progression'. *J Infect Dis,* 169**,** 968-74.

Richman, D. D., Wrin, T., Little, S. J. & Petropoulos, C. J. (2003). 'Rapid evolution of the neutralizing antibody response to HIV type 1 infection'. *Proc Natl Acad Sci U S A,* 100**,** 4144-9.

Riechelmann, H., Schmutzhard, J., Van Der Werf, J. F., Distler, A. & Kleinjans, H. A. (2010). 'Efficacy and safety of a glutaraldehyde-modified house dust mite extract in allergic rhinitis'. *Am J Rhinol Allergy,* 24**,** e104-9.

Ringe, R. P., Sanders, R. W., Yasmeen, A., Kim, H. J., Lee, J. H., Cupo, A., Korzun, J., Derking, R., Van Montfort, T., Julien, J. P., Wilson, I. A., Klasse, P. J., Ward, A. B. & Moore, J. P. (2013). 'Cleavage strongly influences whether soluble HIV-1 envelope glycoprotein trimers adopt a native-like conformation'. *Proc Natl Acad Sci U S A,* 110**,** 18256-61.

Robinson, M. A., Charlton, S. T., Garnier, P., Wang, X.-T., Davis, S. S., Perkins, A. C., Frier, M., Duncan, R., Savage, T. J., Wyatt, D. A., Watson, S. A. & Davis, B. G. (2004). 'LEAPT: Lectin-directed enzyme-activated prodrug therapy'. *Proceedings of the National Academy of Sciences of the United States of America,* 101**,** 14527-14532.

Rolland, M., Edlefsen, P. T., Larsen, B. B., Tovanabutra, S., Sanders-Buell, E., Hertz, T., Decamp, A. C., Carrico, C., Menis, S., Magaret, C. A., Ahmed, H., Juraska, M., Chen, L., Konopa, P., Nariya, S., Stoddard, J. N., Wong, K., Zhao, H., Deng, W., Maust, B. S.,

Bose, M., Howell, S., Bates, A., Lazzaro, M., O'sullivan, A., Lei, E., Bradfield, A., Ibitamuno, G., Assawadarachai, V., O'connell, R. J., Desouza, M. S., Nitayaphan, S., Rerks-Ngarm, S., Robb, M. L., Mclellan, J. S., Georgiev, I., Kwong, P. D., Carlson, J. M., Michael, N. L., Schief, W. R., Gilbert, P. B., Mullins, J. I. & Kim, J. H. (2012). 'Increased HIV-1 vaccine efficacy against viruses with genetic signatures in Env V2'. *Nature,* 490**,** 417-20.

Rothenberg, R. B., Scarlett, M., Del Rio, C., Reznik, D. & O'daniels, C. (1998). 'Oral transmission of HIV'. *AIDS,* 12**,** 2095-105.

Rudicell, R. S., Kwon, Y. D., Ko, S. Y., Pegu, A., Louder, M. K., Georgiev, I. S., Wu, X., Zhu, J., Boyington, J. C., Chen, X., Shi, W., Yang, Z. Y., Doria-Rose, N. A., Mckee, K., O'dell, S., Schmidt, S. D., Chuang, G. Y., Druz, A., Soto, C., Yang, Y., Zhang, B., Zhou, T., Todd, J. P., Lloyd, K. E., Eudailey, J., Roberts, K. E., Donald, B. R., Bailer, R. T., Ledgerwood, J., Program, N. C. S., Mullikin, J. C., Shapiro, L., Koup, R. A., Graham, B. S., Nason, M. C., Connors, M., Haynes, B. F., Rao, S. S., Roederer, M., Kwong, P. D., Mascola, J. R. & Nabel, G. J. (2014). 'Enhanced potency of a broadly neutralizing HIV-1 antibody in vitro improves protection against lentiviral infection in vivo'. *J Virol*.

Salk, J. E., Krech, U., Youngner, J. S., Bennett, B. L., Lewis, L. J. & Bazeley, P. L. (1954). 'Formaldehyde treatment and safety testing of experimental poliomyelitis vaccines'. *Am J Public Health Nations Health,* 44**,** 563-70.

Sampath, S., Carrico, C., Janes, J., Gurumoorthy, S., Gibson, C., Melcher, M., Chitnis, C. E., Wang, R., Schief, W. R. & Smith, J. D. (2013). 'Glycan masking of Plasmodium vivax Duffy Binding Protein for probing protein binding function and vaccine development'. *PLoS Pathog,* 9**,** e1003420.

Sanders, R. W., Derking, R., Cupo, A., Julien, J. P., Yasmeen, A., De Val, N., Kim, H. J., Blattner, C., De La Pena, A. T., Korzun, J., Golabek, M., De Los Reyes, K., Ketas, T. J., Van Gils, M. J., King, C. R., Wilson, I. A., Ward, A. B., Klasse, P. J. & Moore, J. P. (2013). 'A next-generation cleaved, soluble HIV-1 Env Trimer, BG505 SOSIP.664 gp140, expresses multiple epitopes for broadly neutralizing but not non-neutralizing antibodies'. *PLoS Pathog,* 9**,** e1003618.

Sanders, R. W., Venturi, M., Schiffner, L., Kalyanaraman, R., Katinger, H., Lloyd, K. O., Kwong, P. D. & Moore, J. P. (2002a). 'The mannose-dependent epitope for neutralizing antibody 2G12 on human immunodeficiency virus type 1 glycoprotein gp120'. *J Virol,* 76**,** 7293-305.

Sanders, R. W., Vesanen, M., Schuelke, N., Master, A., Schiffner, L., Kalyanaraman, R., Paluch, M., Berkhout, B., Maddon, P. J., Olson, W. C., Lu, M. & Moore, J. P. (2002b). 'Stabilization of the soluble, cleaved, trimeric form of the envelope glycoprotein complex of human immunodeficiency virus type 1'. *J Virol,* 76**,** 8875-89.

Sarzotti-Kelsoe, M., Daniell, X., Todd, C. A., Bilska, M., Martelli, A., Labranche, C., Perez, L. G., Ochsenbauer, C., Kappes, J. C., Rountree, W., Denny, T. N. & Montefiori, D. C. (2014). 'Optimization and validation of a neutralizing antibody assay for HIV-1 in A3R5 cells'. *J Immunol Methods*.

Sather, D. N., Armann, J., Ching, L. K., Mavrantoni, A., Sellhorn, G., Caldwell, Z., Yu, X., Wood, B., Self, S., Kalams, S. & Stamatatos, L. (2009). 'Factors associated with the development of cross-reactive neutralizing antibodies during human immunodeficiency virus type 1 infection'. *J Virol,* 83**,** 757-69.

Sato, C. (2004). 'Chain length diversity of sialic acids and its biological significance'. *Trends in Glycoscience and Glycotechnology,* 16**,** 331-344.

Sattentau, Q. J. (1995). 'Conservation of HIV-1 gp120 neutralizing epitopes after formalin inactivation'. *AIDS,* 9**,** 1383-5.

Sattentau, Q. J. (2014). 'Immunogen design to focus the B-cell repertoire'. *Curr Opin HIV AIDS*.

Scanlan, C. N., Pantophlet, R., Wormald, M. R., Ollmann Saphire, E., Stanfield, R., Wilson, I. A., Katinger, H., Dwek, R. A., Rudd, P. M. & Burton, D. R. (2002). 'The broadly neutralizing anti-human immunodeficiency virus type 1 antibody 2G12 recognizes a cluster of alpha1-->2 mannose residues on the outer face of gp120'. *J Virol,* 76**,** 7306-21.

Scharf, L., Scheid, J. F., Lee, J. H., West, A. P., Jr., Chen, C., Gao, H., Gnanapragasam, P. N., Mares, R., Seaman, M. S., Ward, A. B., Nussenzweig, M. C. & Bjorkman, P. J. (2014). 'Antibody 8ANC195 reveals a site of broad vulnerability on the HIV-1 envelope spike'. *Cell Rep,* 7**,** 785-95.

Scheid, J. F., Mouquet, H., Ueberheide, B., Diskin, R., Klein, F., Oliveira, T. Y., Pietzsch, J., Fenyo, D., Abadir, A., Velinzon, K., Hurley, A., Myung, S., Boulad, F., Poignard, P., Burton, D. R., Pereyra, F., Ho, D. D., Walker, B. D., Seaman, M. S., Bjorkman, P. J., Chait, B. T. & Nussenzweig, M. C. (2011). 'Sequence and structural convergence of broad and potent HIV antibodies that mimic CD4 binding'. *Science,* 333**,** 1633-7.

Schief, W. R., Ban, Y. E. & Stamatatos, L. (2009). 'Challenges for structure-based HIV vaccine design'. *Curr Opin HIV AIDS,* 4**,** 431-40.

Schiffner, T., Kong, L., Duncan, C. J., Back, J. W., Benschop, J. J., Shen, X., Huang, P. S., Stewart-Jones, G. B., Destefano, J., Seaman, M. S., Tomaras, G. D., Montefiori, D. C., Schief, W. R. & Sattentau, Q. J. (2013a). 'Immune focusing and enhanced neutralization induced by HIV-1 gp140 chemical cross-linking'. *J Virol,* 87**,** 10163-72.

Schiffner, T., Sattentau, Q. J. & Dorrell, L. (2013b). 'Development of prophylactic vaccines against HIV-1'. *Retrovirology,* 10**,** 72.

Schiffner, T., Sattentau, Q. J. & Duncan, C. J. (2013c). 'Cell-to-cell spread of HIV-1 and evasion of neutralizing antibodies'. *Vaccine,* 31**,** 5789-97.

Schulke, N., Vesanen, M. S., Sanders, R. W., Zhu, P., Lu, M., Anselma, D. J., Villa, A. R., Parren, P. W., Binley, J. M., Roux, K. H., Maddon, P. J., Moore, J. P. & Olson, W. C. (2002). 'Oligomeric and conformational properties of a proteolytically mature, disulfide-stabilized human immunodeficiency virus type 1 gp140 envelope glycoprotein'. *J Virol,* 76**,** 7760-76.

Selvarajah, S., Puffer, B., Pantophlet, R., Law, M., Doms, R. W. & Burton, D. R. (2005). 'Comparing antigenicity and immunogenicity of engineered gp120'. *J Virol,* 79**,** 12148-63.

Selvarajah, S., Puffer, B. A., Lee, F. H., Zhu, P., Li, Y., Wyatt, R., Roux, K. H., Doms, R. W. & Burton, D. R. (2008). 'Focused dampening of antibody response to the immunodominant variable loops by engineered soluble gp140'. *AIDS Res Hum Retroviruses,* 24**,** 301-14.

Shattock, R. J. & Moore, J. P. (2003). 'Inhibiting sexual transmission of HIV-1 infection'. *Nat Rev Microbiol,* 1**,** 25-34.

Sheppard, N. C., Brinckmann, S. A., Gartlan, K. H., Puthia, M., Svanborg, C., Krashias, G., Eisenbarth, S. C., Flavell, R. A., Sattentau, Q. J. & Wegmann, F. (2014). 'Polyethyleneimine is a potent systemic adjuvant for glycoprotein antigens'. *Int Immunol*.

Shih, T. A., Meffre, E., Roederer, M. & Nussenzweig, M. C. (2002). 'Role of BCR affinity in T cell dependent antibody responses in vivo'. *Nat Immunol,* 3**,** 570-5.

Shingai, M., Donau, O. K., Plishka, R. J., Buckler-White, A., Mascola, J. R., Nabel, G. J., Nason, M. C., Montefiori, D., Moldt, B., Poignard, P., Diskin, R., Bjorkman, P. J., Eckhaus, M. A., Klein, F., Mouquet, H., Cetrulo Lorenzi, J. C., Gazumyan, A., Burton, D. R., Nussenzweig, M. C., Martin, M. A. & Nishimura, Y. (2014). 'Passive transfer of modest titers of potent and broadly neutralizing anti-HIV monoclonal antibodies block SHIV infection in macaques'. *J Exp Med*.

Shingai, M., Nishimura, Y., Klein, F., Mouquet, H., Donau, O. K., Plishka, R., Buckler-White, A., Seaman, M., Piatak, M., Jr., Lifson, J. D., Dimitrov, D. S., Nussenzweig, M. C. & Martin, M. A. (2013). 'Antibody-mediated immunotherapy of macaques chronically infected with SHIV suppresses viraemia'. *Nature,* 503**,** 277-80.

Sierra, S., Kupfer, B. & Kaiser, R. (2005). 'Basics of the virology of HIV-1 and its replication'. *J Clin Virol,* 34**,** 233-44.

Sigal, A., Kim, J. T., Balazs, A. B., Dekel, E., Mayo, A., Milo, R. & Baltimore, D. (2011). 'Cell-to-cell spread of HIV permits ongoing replication despite antiretroviral therapy'. *Nature,* 477**,** 95-8.

Simek, M. D., Rida, W., Priddy, F. H., Pung, P., Carrow, E., Laufer, D. S., Lehrman, J. K., Boaz, M., Tarragona-Fiol, T., Miiro, G., Birungi, J., Pozniak, A., Mcphee, D. A., Manigart, O., Karita, E., Inwoley, A., Jaoko, W., Dehovitz, J., Bekker, L. G., Pitisuttithum, P., Paris, R., Walker, L. M., Poignard, P., Wrin, T., Fast, P. E., Burton, D. R. & Koff, W. C. (2009). 'Human immunodeficiency virus type 1 elite neutralizers: individuals with broad and potent neutralizing activity identified by using a high-throughput neutralization assay together with an analytical selection algorithm'. *J Virol,* 83**,** 7337-48.

Smalls-Mantey, A., Connors, M. & Sattentau, Q. J. (2013). 'Comparative efficiency of HIV-1-infected T cell killing by NK cells, monocytes and neutrophils'. *PLoS One,* 8**,** e74858.

Smalls-Mantey, A., Doria-Rose, N., Klein, R., Patamawenu, A., Migueles, S. A., Ko, S. Y., Hallahan, C. W., Wong, H., Liu, B., You, L., Scheid, J., Kappes, J. C., Ochsenbauer, C., Nabel, G. J., Mascola, J. R. & Connors, M. (2012). 'Antibody-dependent cellular cytotoxicity against primary HIV-infected CD4+ T cells is directly associated with the magnitude of surface IgG binding'. *Journal of virology,* 86**,** 8672-80.

Stiehm, E. R., Mofenson, L., Zolla-Pazner, S., Jackson, B., Martin, N. L. & Ammann, A. J. (1995). 'Summary of the workshop on passive immunotherapy in the prevention and treatment of HIV infection. The Passive Antibody Workshop Participants'. *Clin Immunol Immunopathol,* 75**,** 84-93.

Stowell, C. P. & Lee, Y. C. (1980). 'Preparation of some new neoglycoproteins by amidination of bovine serum albumin using 2-imino-2-methoxyethyl 1-thioglycosides'. *Biochemistry,* 19**,** 4899-904.

Stowell, C. P. & Lee, Y. C. (1982). 'Preparation of neoglycoproteins using 2-imino-2-methoxyethyl 1-thioglycosides'. *Methods Enzymol,* 83**,** 278-88.

Sullivan, N., Sun, Y., Sattentau, Q., Thali, M., Wu, D., Denisova, G., Gershoni, J., Robinson, J., Moore, J. & Sodroski, J. (1998). 'CD4-Induced conformational changes in the human immunodeficiency virus type 1 gp120 glycoprotein: consequences for virus entry and neutralization'. *J Virol,* 72**,** 4694-703.

Sun, Z. Y., Oh, K. J., Kim, M., Yu, J., Brusic, V., Song, L., Qiao, Z., Wang, J. H., Wagner, G. & Reinherz, E. L. (2008). 'HIV-1 broadly neutralizing antibody extracts its epitope from a kinked gp41 ectodomain region on the viral membrane'. *Immunity,* 28**,** 52-63.

Tersmette, M., Gruters, R. A., De Wolf, F., De Goede, R. E., Lange, J. M., Schellekens, P. T., Goudsmit, J., Huisman, H. G. & Miedema, F. (1989). 'Evidence for a role of virulent human immunodeficiency virus (HIV) variants in the pathogenesis of acquired

immunodeficiency syndrome: studies on sequential HIV isolates'. *J Virol,* 63**,** 2118-25.

Thali, M., Moore, J. P., Furman, C., Charles, M., Ho, D. D., Robinson, J. & Sodroski, J. (1993). 'Characterization of conserved human immunodeficiency virus type 1 gp120 neutralization epitopes exposed upon gp120-CD4 binding'. *J Virol,* 67**,** 3978-88.

Titanji, B. K., Aasa-Chapman, M., Pillay, D. & Jolly, C. (2013). 'Protease inhibitors effectively block cell-to-cell spread of HIV-1 between T cells'. *Retrovirology,* 10**,** 161.

Tomaras, G. D., Ferrari, G., Shen, X., Alam, S. M., Liao, H. X., Pollara, J., Bonsignori, M., Moody, M. A., Fong, Y., Chen, X., Poling, B., Nicholson, C. O., Zhang, R., Lu, X., Parks, R., Kaewkungwal, J., Nitayaphan, S., Pitisuttithum, P., Rerks-Ngarm, S., Gilbert, P. B., Kim, J. H., Michael, N. L., Montefiori, D. C. & Haynes, B. F. (2013). 'Vaccine-induced plasma IgA specific for the C1 region of the HIV-1 envelope blocks binding and effector function of IgG'. *Proceedings of the National Academy of Sciences of the United States of America,* 110**,** 9019-24.

Tong, T., Crooks, E. T., Osawa, K. & Binley, J. M. (2012). 'HIV-1 virus-like particles bearing pure env trimers expose neutralizing epitopes but occlude nonneutralizing epitopes'. *J Virol,* 86**,** 3574-87.

Tsuchida, T., Saxton, R. E., Morton, D. L. & Irie, R. F. (1987). 'Gangliosides of human melanoma'. *J Natl Cancer Inst,* 78**,** 45-54.

Unaids (2013). 'UNAIDS report on the global aids epidemic 2013'.

Van Gils, M. J., Euler, Z., Schweighardt, B., Wrin, T. & Schuitemaker, H. (2009). 'Prevalence of cross-reactive HIV-1-neutralizing activity in HIV-1-infected patients with rapid or slow disease progression'. *Aids,* 23**,** 2405-14.

Varki, A. & Angata, T. (2006). 'Siglecs--the major subfamily of I-type lectins'. *Glycobiology,* 16**,** 1R-27R.

Verkoczy, L., Diaz, M., Holl, T. M., Ouyang, Y. B., Bouton-Verville, H., Alam, S. M., Liao, H. X., Kelsoe, G. & Haynes, B. F. (2010). 'Autoreactivity in an HIV-1 broadly reactive neutralizing antibody variable region heavy chain induces immunologic tolerance'. *Proc Natl Acad Sci U S A,* 107**,** 181-6.

Victora, G. D. & Nussenzweig, M. C. (2012). 'Germinal centers'. *Annu Rev Immunol,* 30**,** 429-57.

Victora, G. D., Schwickert, T. A., Fooksman, D. R., Kamphorst, A. O., Meyer-Hermann, M., Dustin, M. L. & Nussenzweig, M. C. (2010). 'Germinal center dynamics revealed by multiphoton microscopy with a photoactivatable fluorescent reporter'. *Cell,* 143**,** 592-605.

Vimr, E. & Lichtensteiger, C. (2002). 'To sialylate, or not to sialylate: that is the question'. *Trends Microbiol,* 10**,** 254-257.

Vimr, E., Lichtensteiger, C. & Steenbergen, S. (2000). 'Sialic acid metabolism's dual function in Haemophilus influenzae'. *Mol Microbiol,* 36**,** 1113-23.

Vimr, E. R., Kalivoda, K. A., Deszo, E. L. & Steenbergen, S. M. (2004). 'Diversity of microbial sialic acid metabolism'. *Microbiology and Molecular Biology Reviews,* 68**,** 132-+.

Vittinghoff, E., Douglas, J., Judson, F., Mckirnan, D., Macqueen, K. & Buchbinder, S. P. (1999). 'Per-contact risk of human immunodeficiency virus transmission between male sexual partners'. *Am J Epidemiol,* 150**,** 306-11.

Walker, L. M., Huber, M., Doores, K. J., Falkowska, E., Pejchal, R., Julien, J. P., Wang, S. K., Ramos, A., Chan-Hui, P. Y., Moyle, M., Mitcham, J. L., Hammond, P. W., Olsen, O. A., Phung, P., Fling, S., Wong, C. H., Phogat, S., Wrin, T., Simek, M. D., Koff, W. C.,

Wilson, I. A., Burton, D. R. & Poignard, P. (2011a). 'Broad neutralization coverage of HIV by multiple highly potent antibodies'. *Nature,* 477**,** 466-70.

Walker, L. M., Huber, M., Doores, K. J., Falkowska, E., Pejchal, R., Julien, J. P., Wang, S. K., Ramos, A., Chan-Hui, P. Y., Moyle, M., Mitcham, J. L., Hammond, P. W., Olsen, O. A., Phung, P., Fling, S., Wong, C. H., Phogat, S., Wrin, T., Simek, M. D., Protocol, G. P. I., Koff, W. C., Wilson, I. A., Burton, D. R. & Poignard, P. (2011b). 'Broad neutralization coverage of HIV by multiple highly potent antibodies'. *Nature,* 477**,** 466-70.

Walker, L. M., Phogat, S. K., Chan-Hui, P. Y., Wagner, D., Phung, P., Goss, J. L., Wrin, T., Simek, M. D., Fling, S., Mitcham, J. L., Lehrman, J. K., Priddy, F. H., Olsen, O. A., Frey, S. M., Hammond, P. W., Kaminsky, S., Zamb, T., Moyle, M., Koff, W. C., Poignard, P. & Burton, D. R. (2009). 'Broad and potent neutralizing antibodies from an African donor reveal a new HIV-1 vaccine target'. *Science,* 326**,** 285-9.

Walker, L. M., Sok, D., Nishimura, Y., Donau, O., Sadjadpour, R., Gautam, R., Shingai, M., Pejchal, R., Ramos, A., Simek, M. D., Geng, Y., Wilson, I. A., Poignard, P., Martin, M. A. & Burton, D. R. (2011c). 'Rapid development of glycan-specific, broad, and potent anti-HIV-1 gp120 neutralizing antibodies in an R5 SIV/HIV chimeric virus infected macaque'. *Proc Natl Acad Sci U S A,* 108**,** 20125-9.

Wegmann, F., Gartlan, K. H., Harandi, A. M., Brinckmann, S. A., Coccia, M., Hillson, W. R., Kok, W. L., Cole, S., Ho, L. P., Lambe, T., Puthia, M., Svanborg, C., Scherer, E. M., Krashias, G., Williams, A., Blattman, J. N., Greenberg, P. D., Flavell, R. A., Moghaddam, A. E., Sheppard, N. C. & Sattentau, Q. J. (2012). 'Polyethyleneimine is a potent mucosal adjuvant for viral glycoprotein antigens'. *Nature Biotechnology,* 30**,** 883-U116.

Wei, X., Decker, J. M., Wang, S., Hui, H., Kappes, J. C., Wu, X., Salazar-Gonzalez, J. F., Salazar, M. G., Kilby, J. M., Saag, M. S., Komarova, N. L., Nowak, M. A., Hahn, B. H., Kwong, P. D. & Shaw, G. M. (2003). 'Antibody neutralization and escape by HIV-1'. *Nature,* 422**,** 307-12.

White, T. A., Bartesaghi, A., Borgnia, M. J., Meyerson, J. R., De La Cruz, M. J., Bess, J. W., Nandwani, R., Hoxie, J. A., Lifson, J. D., Milne, J. L. & Subramaniam, S. (2010). 'Molecular architectures of trimeric SIV and HIV-1 envelope glycoproteins on intact viruses: strain-dependent variation in quaternary structure'. *PLoS Pathog,* 6**,** e1001249.

Whitney, J. B., Hill, A. L., Sanisetty, S., Penaloza-Macmaster, P., Liu, J., Shetty, M., Parenteau, L., Cabral, C., Shields, J., Blackmore, S., Smith, J. Y., Brinkman, A. L., Peter, L. E., Mathew, S. I., Smith, K. M., Borducchi, E. N., Rosenbloom, D. I., Lewis, M. G., Hattersley, J., Li, B., Hesselgesser, J., Geleziunas, R., Robb, M. L., Kim, J. H., Michael, N. L. & Barouch, D. H. (2014). 'Rapid seeding of the viral reservoir prior to SIV viraemia in rhesus monkeys'. *Nature,* 512**,** 74-7.

Wibmer, C. K., Bhiman, J. N., Gray, E. S., Tumba, N., Abdool Karim, S. S., Williamson, C., Morris, L. & Moore, P. L. (2013). 'Viral escape from HIV-1 neutralizing antibodies drives increased plasma neutralization breadth through sequential recognition of multiple epitopes and immunotypes'. *PLoS Pathog,* 9**,** e1003738.

Wikipedia. 2014. *HIV* [Online]. Available: http://en.wikipedia.org/wiki/HIV [Accessed 10.04.2014.

Wilkins, M. R., Gasteiger, E., Bairoch, A., Sanchez, J. C., Williams, K. L., Appel, R. D. & Hochstrasser, D. F. (1999). 'Protein identification and analysis tools in the ExPASy server'. *Methods Mol Biol,* 112**,** 531-52.

Wu, L., Gerard, N. P., Wyatt, R., Choe, H., Parolin, C., Ruffing, N., Borsetti, A., Cardoso, A. A., Desjardin, E., Newman, W., Gerard, C. & Sodroski, J. (1996). 'CD4-induced interaction of primary HIV-1 gp120 glycoproteins with the chemokine receptor CCR-5'. *Nature,* 384**,** 179-83.

Wu, S., Avila-Sakar, A., Kim, J., Booth, D. S., Greenberg, C. H., Rossi, A., Liao, M., Li, X., Alian, A., Griner, S. L., Juge, N., Yu, Y., Mergel, C. M., Chaparro-Riggers, J., Strop, P., Tampe, R., Edwards, R. H., Stroud, R. M., Craik, C. S. & Cheng, Y. (2012). 'Fabs enable single particle cryoEM studies of small proteins'. *Structure,* 20**,** 582-92.

Wu, X., Parast, A. B., Richardson, B. A., Nduati, R., John-Stewart, G., Mbori-Ngacha, D., Rainwater, S. M. & Overbaugh, J. (2006). 'Neutralization escape variants of human immunodeficiency virus type 1 are transmitted from mother to infant'. *J Virol,* 80**,** 835-44.

Wu, X., Yang, Z. Y., Li, Y., Hogerkorp, C. M., Schief, W. R., Seaman, M. S., Zhou, T., Schmidt, S. D., Wu, L., Xu, L., Longo, N. S., Mckee, K., O'dell, S., Louder, M. K., Wycuff, D. L., Feng, Y., Nason, M., Doria-Rose, N., Connors, M., Kwong, P. D., Roederer, M., Wyatt, R. T., Nabel, G. J. & Mascola, J. R. (2010). 'Rational design of envelope identifies broadly neutralizing human monoclonal antibodies to HIV-1'. *Science,* 329**,** 856-61.

Wyatt, R., Kwong, P. D., Desjardins, E., Sweet, R. W., Robinson, J., Hendrickson, W. A. & Sodroski, J. G. (1998). 'The antigenic structure of the HIV gp120 envelope glycoprotein'. *Nature,* 393**,** 705-11.

Xiao, X., Chen, W., Feng, Y., Zhu, Z., Prabakaran, P., Wang, Y., Zhang, M. Y., Longo, N. S. & Dimitrov, D. S. (2009). 'Germline-like predecessors of broadly neutralizing antibodies lack measurable binding to HIV-1 envelope glycoproteins: implications for evasion of immune responses and design of vaccine immunogens'. *Biochem Biophys Res Commun,* 390**,** 404-9.

Yang, X., Kurteva, S., Ren, X., Lee, S. & Sodroski, J. (2005). 'Stoichiometry of envelope glycoprotein trimers in the entry of human immunodeficiency virus type 1'. *J Virol,* 79**,** 12132-47.

Yang, X., Kurteva, S., Ren, X., Lee, S. & Sodroski, J. (2006). 'Subunit stoichiometry of human immunodeficiency virus type 1 envelope glycoprotein trimers during virus entry into host cells'. *J Virol,* 80**,** 4388-95.

Yates, N. L., Liao, H. X., Fong, Y., Decamp, A., Vandergrift, N. A., Williams, W. T., Alam, S. M., Ferrari, G., Yang, Z. Y., Seaton, K. E., Berman, P. W., Alpert, M. D., Evans, D. T., O'connell, R. J., Francis, D., Sinangil, F., Lee, C., Nitayaphan, S., Rerks-Ngarm, S., Kaewkungwal, J., Pitisuttithum, P., Tartaglia, J., Pinter, A., Zolla-Pazner, S., Gilbert, P. B., Nabel, G. J., Michael, N. L., Kim, J. H., Montefiori, D. C., Haynes, B. F. & Tomaras, G. D. (2014). 'Vaccine-Induced Env V1-V2 IgG3 Correlates with Lower HIV-1 Infection Risk and Declines Soon After Vaccination'. *Sci Transl Med,* 6**,** 228ra39.

Yu, S., Wang, Q., Zhang, J., Wu, Q. & Guo, Z. (2011). 'Synthesis and Evaluation of Protein Conjugates of GM3 Derivatives Carrying Modified Sialic Acids as Highly Immunogenic Cancer Vaccine Candidates'. *Medchemcomm,* 2**,** 524-530.

Yuan, W., Bazick, J. & Sodroski, J. (2006). 'Characterization of the multiple conformational States of free monomeric and trimeric human immunodeficiency virus envelope glycoproteins after fixation by cross-linker'. *J Virol,* 80**,** 6725-37.

Zanetti, G., Briggs, J. A., Grunewald, K., Sattentau, Q. J. & Fuller, S. D. (2006). 'Cryo-electron tomographic structure of an immunodeficiency virus envelope complex in situ'. *PLoS Pathog,* 2**,** e83.

Zhang, J. Q., Nicoll, G., Jones, C. & Crocker, P. R. (2000). 'Siglec-9, a novel sialic acid binding member of the immunoglobulin superfamily expressed broadly on human blood leukocytes'. *J Biol Chem,* 275**,** 22121-6.

Zhou, T., Zhu, J., Yang, Y., Gorman, J., Ofek, G., Srivatsan, S., Druz, A., Lees, C. R., Lu, G., Soto, C., Stuckey, J., Burton, D. R., Koff, W. C., Connors, M. & Kwong, P. D. (2014). 'Transplanting supersites of HIV-1 vulnerability'. *PLoS One,* 9**,** e99881.

Zhou, T. Q., Georgiev, I., Wu, X. L., Yang, Z. Y., Dai, K. F., Finzi, A., Kwon, Y. D., Scheid, J. F., Shi, W., Xu, L., Yang, Y. P., Zhu, J. A., Nussenzweig, M. C., Sodroski, J., Shapiro, L., Nabel, G. J., Mascola, J. R. & Kwong, P. D. (2010). 'Structural Basis for Broad and Potent Neutralization of HIV-1 by Antibody VRC01'. *Science,* 329**,** 811-817.

Zolla-Pazner, S., Decamp, A. C., Cardozo, T., Karasavvas, N., Gottardo, R., Williams, C., Morris, D. E., Tomaras, G., Rao, M., Billings, E., Berman, P., Shen, X., Andrews, C., O'connell, R. J., Ngauy, V., Nitayaphan, S., De Souza, M., Korber, B., Koup, R., Bailer, R. T., Mascola, J. R., Pinter, A., Montefiori, D., Haynes, B. F., Robb, M. L., Rerks-Ngarm, S., Michael, N. L., Gilbert, P. B. & Kim, J. H. (2013). 'Analysis of V2 antibody responses induced in vaccinees in the ALVAC/AIDSVAX HIV-1 vaccine efficacy trial'. *PLoS One,* 8**,** e53629.

Appendix

A.i. Supplementary tables

Table A. 1: List of anti-HIV-1 Env mAbs used in this thesis

mAb	Epitope	bNmAb	Comment	Source	Ref
10E8	MPER	+		Expressed	(Huang et al., 2012)
15e	CD4bs	-		IAVI NAC	(Ho et al., 1991)
17b	CD4i	-		IAVI NAC	(Thali et al., 1993)
2F5	MPER	+	autoreactive	IAVI NAC	(Buchacher et al., 1994)
2G12	N332	+	Glycan binding only	Expressed	(Buchacher et al., 1994)
3BC176	V3/CD4i	+	quaternary	Expressed	(Klein et al., 2012a)
3BC315	V3/CD4i	+	quaternary	Expressed	(Klein et al., 2012a)
4E10	MPER	+	autoreactive	IAVI NAC	(Buchacher et al., 1994)
5F3	gp41 HR1	-		Polymun	(Buchacher et al., 1994)
A32	C1	-		IAVI NAC	(Moore et al., 1993)
b12	CD4bs	+		IAVI NAC	(Burton et al., 1991)
b6	CD4bs	-		IAVI NAC	(Burton et al., 1991)
CD4-IgG$_2$	CD4bs	+	tetrameric	NIH Aids reagent	(Allaway et al., 1995)
F105	CD4bs	-		NIH Aids reagent	(Posner et al., 1991)
HGN194	V3	+/-		D. Corti	(Corti et al., 2010a)
HGP68	V2	-		D. Corti	(Corti et al., 2010a)
HIVIG	Polyclonal	-		NIH Aids reagent	(Stiehm et al., 1995)
HJ16	CD4bs	+		D. Corti	(Corti et al., 2010a)
HR10	V3	-		D. Corti	(Corti et al., 2010a)
NIH45-46	CD4bs	+		Expressed	(Scheid et al., 2011)
PG16	V1V2	+	quaternary	IAVI NAC	(Walker et al., 2009)
PG9	V1V2	+	quaternary	IAVI NAC	(Walker et al., 2009)
PGT121	N332	+		IAVI NAC	(Walker et al., 2011b)
PGT128	N332	+		IAVI NAC	(Walker et al., 2011b)
PGT135	N332	+		IAVI NAC	(Walker et al., 2011b)
PGT145	V1V2	+	quaternary	Expressed	(Walker et al., 2011b)
PGT151	gp41-gp120 interface	+		Expressed	(Falkowska et al., 2014)
VRC01	CD4bs	+		Expressed	(Wu et al., 2010)
X5	CD4i	-		IAVI NAC	(Moulard et al., 2002)

A.ii. Protein sequences

Below are protein sequences of the mutants design in this thesis. Newly introduced lysine residues are indicated in blue, removed lysines in red, the V3-loop is underscored and "↓" denotes the predicted cleavage site after the leader sequence.

A.ii.1. HWT

MDAMKRGLCCVLLLCGAVFVSP↓SQEIHARFRRGARSGNSTEKLWVTVYYGVPVWKEATTTLFCAS
DAKAYDTEVHNVWATHACVPTDPNPQEVVLVNVTENFNMWKNDMVEQMHEDIISLWDQSLKPC
VACPKVSFEPIPIHYCAPAGFAILKCNNKTFNGTGPCTNVSTVQCTHGIRPVVSTQLLLNGSLAEEEVVI
RSVNFTDNAKTIIVQLNTSVEINCTRPNNNTRKRIRIQRGPGRAFVTIGKIGNMRQAHCNISRAKWNN
TLKQIASKLREQFGNNKTIIFKQSSGGDPEIVTHSFNCGGEFFYCNSTQLFNSTWFNSTWSTEGSNNTE
GSDTITLPCRIKQIINMWQKVGKAMYAPPISGQIRCSSNITGLLLTRDGGNSNNESEIFRPGGGDMRD
NWRSELYKYKVVKIEPLGVAPTKAKRRVVQREKRLEKHHHHHH-

A.ii.2. HKM

MDAMKRGLCCVLLLCGAVFVSP↓SQEIHARFRRGARSGNSTEKLWVTVYYGVPVWKEATTKLFCAS
DAKAYDTEVHNVWATKACVPTDPKPQEVVLVNVTENFNMWKNDMVEQMHKDIISLWDQSLKPC
VACPKVSFEPIPIHYCAPAGFAILKCNNKTFNGTGPCTNVSTVQCTHGIRPVVSTQLLLNGSLAEEEVVI
RSVNFTDNARTIIVQLNTSVEINCTRPNNNTRKRIRIQRGPGKAFVTIGKIGNMRQAHCNISRAKWNN
TLKQIASKLREQFGNNKTIIFKQSSGGDPEIVTHSFNCGGEFFYCNSTQLFNSTWFNSTWSTEGSNNTE
GSDTITLPCRIRQIINMWQKVGRAMYAPPISGQIRCSSNITGLLLTRDGGNSNNESEIFRPGGGDMRD
NWRSELYKYKVVKIEPLGVAPTKAKRRVVQREKRLEKHHHHHH-

A.ii.3. HKM2

MDAMKRGLCCVLLLCGAVFVSP↓SQEIHARFRRGARSGNSTEKLWVTVYYGVPVWKEATTKLFCAS

DAKAYDTEVHNVWATKACVPTDPKPQEVVLVNVTENFNMWENDMVEQMHEDIISLWDQSLKPCV

ACPKVSFEPIPIHYCAPAGFAILKCNNKTFNGTGPCTNVSTVQCTHGIRPVVSTQLLLNGSLAEEEVVIR

SVDFTDNARTIIVQLNTSVEINCTRPNNNTRKRIRIKRGPGKAFVKIGKIGNMRKAHCNISRAKWNNTL

KQIASKLREQFGNNKTIIFAQSSGGDPEIVTHSFNCGGEFFYCNSTQLFNSTWFNSTWSTEGSNNTEG

SDTITLPCRIRQIINMWQEVGRAMYAPPISGKIRCSSNITGLLLTRDGGNSNNESEIFRPGGGDMRDN

WRSELYKYKVVKIEPLGVAPTKAKRRVVQREKRLEKHHHHHH-

A.ii.4. eOD_base

MGILPSPGMPALLSLVSLLSVLLMGCVA↓ETGDTITLPCRPAPPPHCSSNITGLILTRDGGNSNDESEIF

RPGGGDMRDIARCQIAGTVVSSQLLLNGSLAEEEVVIRSVDFTDNAKSICVQLNTSVEINCTGAGHCNI

SRAKWNNTLKQIASKLREQFGNNKTIIFKQSSGGDPEIVTHWFNCGGEFFYCNSTQLFNSTWFNSTW

SGTKHHHHHH--

A.ii.5. eOD_KM

MGILPSPGMPALLSLVSLLSVLLMGCVA↓ETGDTITLPCKPAPPPKCSSNITGLILTRDGGNSNDESEIF

RPGGGDMRDIARCQIAGKVVSSQLLLNGSLAKEEVVIRSVDFTDNARSICVQLNTSVEINCTGAGHCN

ISRAKWNNTLKQIASKLREQFGNRTIIFAQSSGGDPEIVTHWFKCGGEFFYCNSTKLFNSTWFNSTWS

GTKHHHHHH--

A.ii.6. NC99_WT

MKAKLLVLLCTFTATYA↓DTICIGYHANNSTDTVDTVLEKNVTVTHSVNLLEDSHNGKLCLLKGIAPLQ

LGNCSVAGWILGNPECELLISKESWSYIVETPNPENGTCYPGYFADYEELREQLSSVSSFERFEIFPKESS

WPNHTVTGVSASCSHNGKSSFYRNLLWLTGKNGLYPNLSKSYVNNKEKEVLVLWGVHHPPNIGNQR

ALYHTENAYVSVVSSHYSRRFTPEIAKRPKVRDQEGRINYYWTLLEPGDTIIFEANGNLIAPWYAFALSR

GFGSGIITSNAPMDECDAKCQTPQGAINSSLPFQNVHPVTIGECPKYVRSAKLRMVTGLRNIPQRETR

GLFGAIAGFIEGGWTGMVDGWYGYHHQNEQGSGYAADQKSTQNAINGITNKVNSVIEKMNTQFT

AVGKEFNKLERRMENLNKKVDDGFLDIWTYNAELLVLLENERTLDFHDSNVKNLYEKVKSQLKNNAK

EIGNGCFEFYHKCNNECMESVKNGTYDYPKYSEESKLNREKIDSGRLVPRGSPGSGYIPEAPRDGQAY

VRKDGEWVLLSTFLGHHHHHH--

A.ii.7. NC99_KM

MKAKLLVLLCTFTATYA↓DTICIGYHANNSTDTVDTVLERNVTVTHSVNLLEDSHNGKLCLLKGIAPLQ

LGNCSVAGWILGNPECELLISKESWSYIVETPNPENGTCYPGYFADYEELREQLSSVSSFERFEIFPKESS

WPNHTVTGVSASCSHNGKSSFYRNLLWLTGKNGLYPNLSKSYVNNKEKEVLVLWGVHHPPNIGNQT

ALYHTENAYVSVVSSHYSRRFTPEIAKRPKVRDQEGRINYYWTLLEPGDTIIFEANGNLIAPWYAFALSR

GFGSGIITSNAPMDECDARCQTPKGAINSSLPFQNVHPVTIGECPRYVRSAKLRMVTGLRNIPQRETR

GLFGAIAGFIEGGWTGMVDGWYGYHHQNEQGSGYAADQRSTQNAINGITNKVNSVIEKMNTQFT

AVGKEFNKLERRMENLNKKVDDGFLDIWTYNAELLVLLENERTLDFHDSNVKNLYERVKSQLKNNAK

EIGNGCFEFYHKCNNECMESVKNGTYDYPKYSEESKLNREKIDSGRLVPRGSPGSGYIPEAPRDGQAY

VRKDGEWVLLSTFLGHHHHHH--